INVESTIGATION OF SUBMERGED TROMMEL SCREEN

By

CJ Laker

Thesis presented in partial fulfilment

of the requirements for the degree

of

MASTER OF ENGINEERING

(MINERAL PROCESSING ENGINEERING)

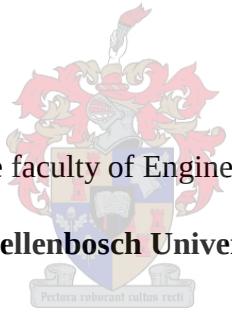

In the faculty of Engineering

at Stellenbosch University

Supervisor:

Prof. Guven Akdogan

Co-Supervisor:

Prof. Steven Bradshaw

April 2022

DECLARATION

By submitting this thesis electronically, I declare that the entirety of the work contained therein is my own, original work, that I am the sole author thereof (save to the extent explicitly otherwise stated), that reproduction and publication thereof by Stellenbosch University will not infringe any third party rights and that I have not previously in its entirety or in part submitted it for obtaining any qualification.

Date: *April 2022*

OPSOMMING

Draaisiwwe word ondersoek as ’n alternatief tot drein en afspoel vibrerende skerms vir die doel van digte medium herwinning. Ysterերts en sikloon 40 geatomiseerde ferrosilikon is gebruik om skermdoeltreffendheid op onderdompelde wasdraaisiwwe te toets. Hierdie draaisiwwe bestaan uit twee tipes kamers, een vir medium dreinering en twee onderdompelde waskamers om aanklewende medium te was.

Die doeltreffendheid van die dreinkamer is geëvalueer met oorvloei eienskappe soos voginhoud, FeSi-inhoud en oorgedraagde FeSi, deur medium relatiewe digtheid (RD) te varieer tussen 2.7 en 3.6. Die resultate is vergelyk met vorige studies van vibrerende drein- en afspoelskerms deur Kabondo (2018). Die toetswerk is uitgevoer op twee aparte draaisifontwerpe, Onderdompelde DMS Draaisif (Mk1) en Draaisif Mk2. As gevolg van ontwerpbeperkinge in die ontwerp van Mk1, was daar groot onsekerheid in die resultate van die eerste ondersoek. Mk1 se doeltreffendheid was egter hoogs belowend in vergelyking met vibrerende dreinskerms. Persentasie vog in die oorvloei van Mk1 het ’n maksimum van 3.60% by ’n medium RD van 3.6, terwyl vibrerende skerm-resultate tussen 10.29% en 27.91% by laer medium RDe onder 2.3 gestrek het. %FeSi in die oorvloei van die dreinkamer van Mk1 het tussen 11.05% en 18.76% gestrek terwyl vibrerende skerms tussen 9.71% en 36.01% gestrek het. Oorgedraagde %FeSi op Mk1 het ’n maksimum van 4.96% bereik terwyl die vibrerende skerm tussen 3.12% en 10.46% gestrek het. Buiten ’n kompeterende dreinering van draaisif Mk1, het lottoetse uitgevoer in die onderdompelde waskamers van Mk1, gekombineer met banktoetse vir onderdompelde was en afspoel, tot die gevolg gelei dat die mees effektiewe wasmetode beweging van partikels binne ’n onderdompelde bad was. Doeltreffendheid vir onderdompelde was het tussen 84.82% tot 99.7% gestrek, in vergelyking met 74.24% vir afspoel van medium.

Dit is geregverdig om ’n nuwe toetsdraaisif te ontwerp, Mk2, uit wat geleer is van die eerste veldtog. Die tweede draaisif (Mk2) is ontwerp met nege verskillende ondervloei uitstromings. Vir die eerste keer in oop literatuur, het Mk2 insig verskaf oor materiaalverspreiding en gebruikte skermarea van ’n draaisif deur hierdie uitstromings te evalueer. Dit is gevind dat 98% van dreinering plaasvind deur die middel en in die rigting van die rotasie van die draaisif.

Die werk op draaisif Mk2 is uitgevoer by soortgelyke bedryfskondisies as Mk1. Die resultate van Mk2 het hoër herhaalbaarheid en statistiese beduidendheid gehad. Vertroue in

die resultate is verskaf en daar is tot die gevolgtrekking gekom dat draaisiwwe ’n kompeterende alternatief tot vibrerende dreinering- en afspoelskerms is.

Toekomstige werk sal toetswerk insluit op alle oorblywende bedryfsparameters om ’n volledige verstaan te ontwikkel van hoe hierdie parameters die bedryf van draaisiwwe beïnvloed.

ABSTRACT

Trommels are investigated as an alternative to drain and rinse vibrating screens for the purpose of dense medium recovery. Iron ore and cyclone 40 atomized ferrosilicon were used to test screen performance on a submerged washing trommel. This trommel consists of two types of chambers, one for medium drainage and two submerged wash chambers to wash adhering medium.

The performance of the drain chamber was evaluated with overflow properties such as moisture content, FeSi content and FeSi carryover, by varying medium relative density (RD) between 2.7 and 3.6. The results were compared to past studies on a vibrating drain and rinse screen by Kabondo (2018). The test work was performed on two separate trommel designs, Submerged DMS Trommel (Mk1) and Trommel Mk2. Due to design limitations in the design of Mk1, there was great uncertainty in the results from the first investigation. Mk1's performance was however highly promising compared to vibrating drain screens. Percentage moisture in the overflow of Mk1 had a maximum of 3.60 % at a medium RD of 3.6, while vibrating screen results ranged between 10.29 % and 27.91 % at lower medium RDs below 2.3. % FeSi in the overflow of the drain chamber of Mk1 ranged between 11.05 % and 18.76 %, while the vibrating screen ranged between 9.71 % and 36.01 %. % FeSi carryover on Mk1 reached a maximum of 4.96 % while the vibrating screen ranged between 3.12 % and 10.46 %. In addition to competitive drainage of trommel Mk1, batch tests performed in the submerged wash chambers of Mk1, combined with bench tests for submerged washing and rinsing, concluded that the most effective washing method was motion of particles within a submerged bath. Efficiency for submerged washing ranged from 84.82 % to 99.7 %, compared to 74.24 % for rinsing of medium.

It was justified to design a new test trommel, Mk2, from the learnings of the first campaign. The second trommel (Mk2) was designed with nine different underflow discharges. For the first time in open literature, trommel Mk2 provided insight into material distribution and utilised screen area of a trommel by evaluating these discharges. It was found that 98 % of drainage occurs through the middle and towards the direction of rotation of the trommel.

The work on trommel Mk2 was performed at similar operating conditions as Mk1. The results of Mk2 had higher repeatability and statistical significance. Confidence was provided in the results and it was concluded that trommels is a competitive alternative to vibrating drain and rinse screens.

Future work will include test work on all remaining operating parameters to develop a complete understanding how these parameters govern the operation of trommels.

ACKNOWLEDGEMENTS

Thanks to my parents, Chris and Anette Laker, for their unconditional love, support and being the parents that most people can only dream of having.

Thanks to Prof. Akdogan for excellent mentorship and selecting me for this post-graduate project.

Special thanks to Prof. Akdogan, Prof. Dorfling and Dr. Snyders for recognising my ability and for believing in me when no one else did.

Thank you to Prof. Bradshaw for the time and effort put into reviewing my report.

Thanks to everyone who forms part of my support structure; friends and family, for helping me through challenging times.

Special thanks to Dr. Jurisch for his exceptional friendship and setting an unfaultable example for me to follow.

Thanks to Multotec Manufacturing Pty Ltd. for providing me with the opportunity and resources required to complete this project.

Special thanks to Mr. Pieters for exceptional mentorship at Multotec Manufacturing.

TABLE OF CONTENTS

LIST OF FIGURES

LIST OF TABLES

NOMENCLATURE

Abbreviation	Description
Mk1	Mark 1 (First Submerged DMS Trommel design)
Mk2	Mark 2 (Second, improved Test Trommel design)
FeSi	Ferrosilicon
DMS	Dense medium separation
DMC	Dense medium circuit
PSD	Particle size distribution
RD	Relative density

Symbol	Description	Unit of measurement (if applicable)
A	Length of a rectangular aperture	mm
a	Width of an aperture	mm
C	Fraction of water to the undersize	Dimensionless (fraction)
d	Mean particle size	micron
g	Gravitational acceleration	m/s^2
L	Screen length	m
p	Probability of passing of a particle	Dimensionless
Q	Ratio of aperture area to total screen area	Dimensionless
r	Drum radius	m
V	Total particle velocity in screen	m/s

Symbol	Description	Unit of measurement (if applicable)
d_{25}	Particle size with 25% probability of reporting to overflow	micron
D_{50}	Cut size	micron
d_{50}	Corrected cut size	micron
d_{75}	Particle size with 75% probability of reporting to overflow	micron
E_{25}	Fraction of d_{25} particle size reporting to overflow	Dimensionless (fraction)
E_{75}	Fraction of d_{75} particle size reporting to overflow	Dimensionless (fraction)
E_{Oi}	Efficiency of recovery of particle size (i) to oversize stream	Dimensionless (fraction)
E_{OC}	Corrected recovery to oversize	%
f_m	Mass fraction of medium particles in feed stream	Dimensionless (fraction)
M_f	Mass flowrate of solids in the feed stream	t/hr
M_o	Mass flowrate of solids to the oversize stream	t/hr
n_n	Total number of impingements of particle on screen surface	Dimensionless
n_r	Rotational velocity of screen	RPM
O_m	Mass fraction of medium particles in oversize stream	Dimensionless

		(fraction)
V_x	Horizontal component of particle velocity in screen	m/s
V_y	Vertical component of particle velocity in screen	m/s
x_0	Minimum particle size in a distribution	micron
x_m	Maximum particle size in a distribution	micron
$\dot{x_0}$	Horizontal particle location in screen	Coordinate
$\dot{z_0}$	Vertical particle location in screen	Coordinate
%OA	Percentage open area	%
$f(x_1)$	Number fraction of particles with diameter of x_1	Dimensionless (fraction)

Symbol	**Description**	**Unit of measurement (if applicable)**
α_a	Angle of location of point on a rotating screen	Degrees
α_s	Separation sharpness	1/micron (gradient of partition curve)
β	Angle of inclination of drum screen	rad
θ	Angle describing particle motion	Degrees
$\ddot{\theta}$	Particle acceleration	m/s^2
η	Viscosity	Centipoise
μ	Particle coefficient of friction	Dimensionless
ω	Rotational velocity	rad/s

1. INTRODUCTION

1.1. Background and project significance

Dense medium separation is a common process in the mining industry. The loss of medium forms a large portion of the operational cost of a dense medium circuit. Although there are many possible sources of medium losses in a dense medium plant, it is estimated that up to 80% of media losses occur on the drain and rinse vibrating screens as a result of medium adhesion to the sinks product of a dense medium cyclone (Napier-Munn, et al., 1995). The high capacity of these processes implies that even marginal improvement in efficiency of medium recovery result in significant decrease in operational cost. Therefore it is of great interest to investigate possible alternatives to the drain and rinse vibrating screen that are typically utilized in the industry today.

It has been well established in the industry of dense medium separation, that washing water overcomes the adhesive forces between ferrosilicon (FeSi) and ore particles. As such, practically all dense medium circuits use spray water to recover medium that adheres to ore particles in drain and rinse screens, preventing it to be drained from the slurry (Bevilacqua & Ferrara, 1994), (Bosman, 2014), (Kabondo, 2018), (Marsh, 1945), (Napier-Munn & Scott, 1990), (Napier-Munn, et al., 1995), (Sripriya, et al., 2003), (Sripriya, et al., 2006). Multotec Manufacturing Pty Ltd. and its partners developed a concept of submerged washing, as an alternative to rinsing ore with medium adhering to it. Submersion of these particles overcomes the adhesive forces between them. Submersion is however not possible in the context of a vibrating screen, because the drag forces associated with such intense vibration under water would be immense.

Trommels are well known for their versatility and after being used for over four centuries in the mining industry (Alter, et al., 1981), have demanded the recognition in the field as a competitive screening unit under most circumstances. Trommels have many advantages over vibrating screens, some of which relate to the lower mechanical stress, wear and power requirement associated with a rotating drum as opposed to a vibrating deck (Wills & Napier-Munn, 2006). These advantages are specifically appealing in the context of submerged screening, because a rotational motion in a submerged bath is much less straining on the motors that drive the motion of the screen.

1.2. Submerged test trommel 1 (Mk 1)

A collaborative effort between Multotec Manufacturing Pty Ltd. and its partners accomplished the design and manufacturing of a new type of trommel called the submerged

trommel. This trommel was developed as a test unit for further investigation of the concept of submerged washing and to determine the viability of using a trommel as an alternative to a vibrating drain and rinse screens. The equipment drawing is provided in Appendix A for context.

The submerged trommel (Mk1) consists of numerous sections that are intended to fulfil two different purposes in sequence. The first chamber is intended as a drain chamber, where the majority of medium is drained from the dense medium cyclone product stream (sinks or floats) and recovered to the correct medium sump. The subsequent chambers are submerged under water, intended to recover the adhered medium that was lost to the overflow of the drain chamber.

1.2.1. Project objectives: Submerged test trommel 1 (Mk 1)

The objectives of the first study on the submerged test trommel (Mk1) are summarised:

- Determine operating limits for the test trommel screen and identify design improvements required to make the screen more efficient.
- Determine the media recovery performance of test trommel (Mk1).
- Compare performance of test trommel (Mk1) from this study to that of a vibrating drain and rinse screen from the study performed by Kabondo (2018).
- Assess using various performance criteria if trommel screens are a viable alternative to vibrating drain screens.
- Determine viability of submerged washing as an alternative to rinse washing.

1.3. Improved drain test trommel 2 (Mk2)

The study on the submerged test trommel (Mk1) created the desire to further investigate trommels as an alternative to drain and rinse vibrating screens. The results from the study on the submerged test trommel (Mk1) indicated that trommels are indeed promising as an alternative to vibrating drain and rinse screens. Unfortunately, the design shortcomings of the submerged test trommel (Mk1) did not render it suitable for accurate test work that represents steady state operation. This introduced a large extent of uncertainty to the results that were obtained on the submerged test trommel (Mk1). As such, it was desired to redesign the trommel (Mk2) to repeat the tests that were performed on the first submerged test trommel (Mk1) to provide statistical significance to the results that were obtained.

Past studies on trommels have developed models to describe particle movement in trommels. These models typically use a geometric approach to predict particle motion and the probability of particles passing through the apertures of a trommel (Alter, et al., 1981), (Gaudin, 1939), (Mellmann, 2001), (Stessel & Kranc, 1992), (Stessel & Cole, 1996). Due to

the immense complexity of particle motion in a rotating drum, particularly incorporating inter-particle interactions, predictive models are typically accompanied by a fair degree of uncertainty. The large degree of variation between different applications and materials of trommel operation introduces the desire to produce empirical test data that provides insight into the inner workings of a trommel. So far, all known studies on test trommels have had only a single overflow discharge and a single underflow discharge. It is believed that performing test work while sampling multiple underflows at different locations under the trommel (Mk2) will provide insight into material motion and distribution inside of a trommel. This data will add great value to the field of knowledge by enabling the verification of models, whether it is mathematically derived probability models of particles passing through apertures or models developed by discreet element method (DEM) coupled with computational fluid dynamics (CFD).

1.3.1. Project objectives: Improved Test Trommel (Mk2)

The objectives of the second study on the second iteration of the test trommel (Mk2) are summarised:

- Design new test trommel (Mk2) to overcome limitations of the submerged test trommel (Mk1).
- Repeat tests performed on test trommel (Mk1) to verify or disprove results of first study.
- Further investigate viability of trommels as an alternative to vibrating drain screens.
- Investigate material distribution and drainage rate as a function of location in the trommel (Mk2).

2. LITERATURE REVIEW

2.1. Dense medium circuits

Dense medium circuits are designed to separate valuable minerals from gangue materials after the ore exits the comminution circuit for liberation. The separation is based on the difference in density between the minerals of interest and the rest. Typically the valuable minerals are heavier than the gangue materials. This separation is accomplished with a dense medium cyclone. Dense medium, such as ferrosilicon and magnetite, is used in the slurry to exploit the difference in density between the valuable and gangue minerals and their likeliness to sink or float from the suspension. The slurry is pumped into the cyclone, where heavier minerals sink and are collected by the apex. Lighter minerals float and are caught by the vortex finder. Due to the geometrical design of the cyclone, the floats exit the top of the unit while the sinks exit the bottom of the unit (Bosman, 2014), (Sripriya, et al., 2003), (Sripriya, et al., 2006).

Studies by Bosman (2014), Noble and Luttrell (2015) revealed that magnetite is only a suitable medium in systems with a separation density below 2000 kg/m^3. Higher densities than that require a heavier medium such as ferrosilicon.

It is well known in the DMS industry that the heavy medium and the ore particles adhere to each other. This is undesirable because the heavy medium is expensive. Ideally the heavy medium must be recycled for long term use. Plenty of research has been completed on the topic of medium recovery in the dense medium circuit (Bevilacqua & Ferrara, 1994), (Bosman, 2014), (Collins, et al., 1974), (Kabondo, 2018), (Marsh, 1945), (Napier-Munn & Scott, 1990), (Napier-Munn, et al., 1995), (Sripriya, et al., 2003), (Sripriya, et al., 2006). The standard circuit for heavy medium recovery is illustrated in Figure 1.

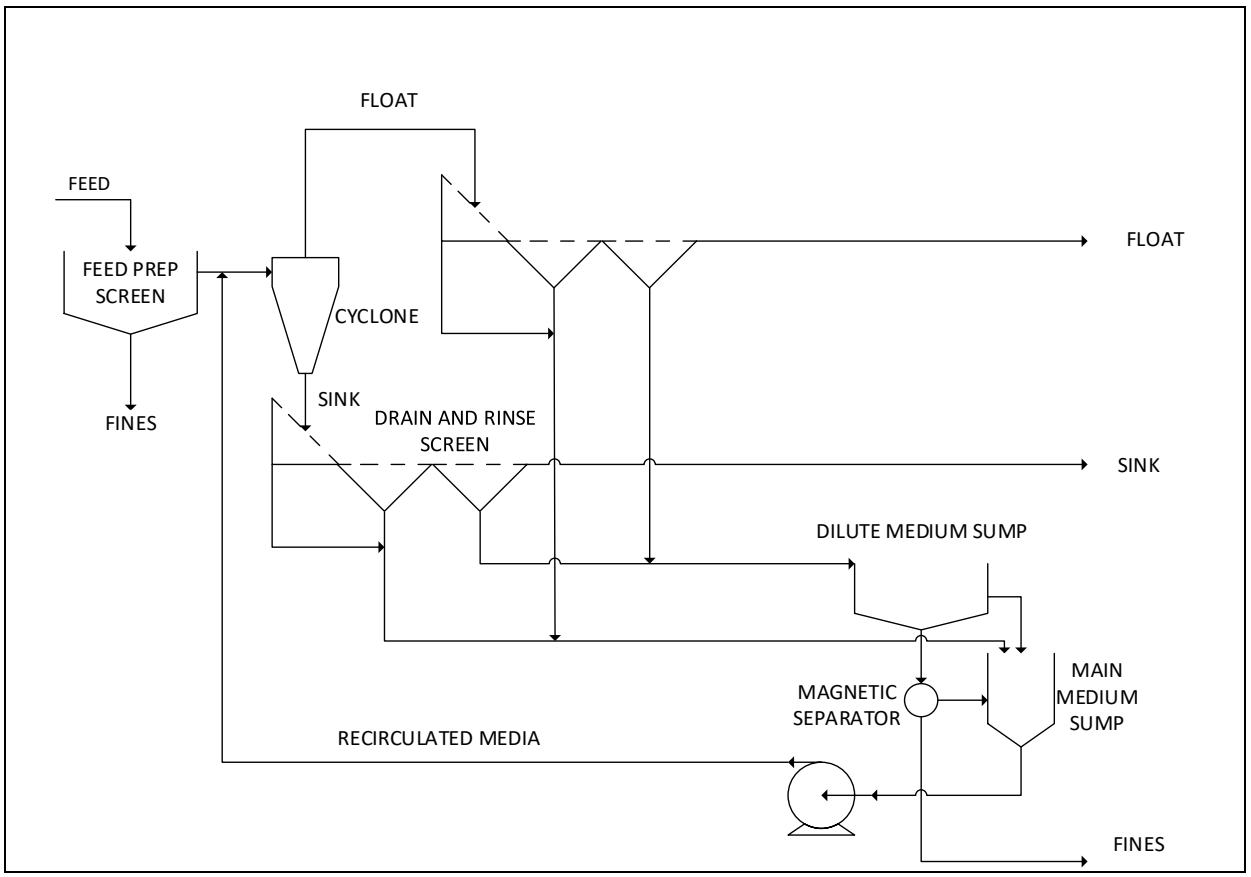

Figure 1. Simplified process flow diagram for dense medium circuit to recover dense medium.

It is typical in the DMS industry to use drain and rinse vibrating screens because they are effective and versatile. There are various drain and rinse screen designs, but it is generally accepted that horizontal screens with an angle between low (10^o) and a slight reverse angle (-5^o) with a linear motion is optimal for ensuring screening efficiency (Wills & Napier-Munn, 2006), (Liu, 2009), (Sullivan, 2013). The linear motion is preferred over elliptical motion because it delivers higher G-forces, which relate to reduced screen blinding (Burke & Craig, 2005).

The purpose of this study is however an investigation of the viability of replacing the drain and rinse vibrating screens in the industry with a new type of submerged trommel screen. More specifically, the operating parameters at which the submerged trommel screen will be tested will be similar to a previous study on a vibrating screen to enable direct comparison of the results. The absence of high G-forces in a gradually rotating trommel screen increases the probability of screen blinding in the trommel (Wills & Napier-Munn, 2006). However these tests refer to traditional trommel screens, not a submerged trommel screen like the one that is investigated in this study. The difference between traditional trommel screens and the submerged trommel screen is, as the name suggests, the submersion of the screen and its

contents under water. The submersion affects the interaction between particles and also the forces acting upon particles during rotation of the trommel, as the particles settle through water as opposed to tumbling through air.

In typical dense medium circuits, the sink and float from the cyclone are screened with vibrating drain and rinse screens. Prior to the vibrating screens there are often sieve bends, which serves as a rough screening before the slurry is fed to the vibrating drain section of the screen. This is to decrease the size of the vibrating screen. For trommel screens with an equivalent total screen area as a vibrating screen, the effective screening area of the trommel is lower than the flat surface vibrating screen. This is because a fraction of the screen area is facing upward or sideward due to its circular shape, resulting in that fraction of the total screen area not being utilised at any given time. The industry standard, set by Multotec Manufacturing Pty Ltd. is that approximately one third of the total screen area of a trommel is being utilised at a time. It is therefore apparent that sieve bends will also likely be required if the vibrating screens are replaced with trommel screens in the industry. The medium that is drained to the underflow is recycled to the circuit feed via a medium sump. The oversize stream exits the draining section and enters the rinse section of the screen. Here the medium is washed from the ore particles with water sprayers. The underflow of this section of the screen is too dilute to recycle directly and it is typically contaminated by undesirable fines that form slimes in the circuit. Previous studies have concluded that the presence of the slimes constructively affect medium stability but has a negative impact on the viscosity (Grobler, et al., 2002). Separation in the cyclone and on the screen is hindered by high viscosity medium. Therefore the medium is separated from the undesired fines by magnetic separation and thereafter the medium containing liquid is then thickened before being recycled to the circuit feed via a separate sump. The undesired fines are bled from the system.

2.1.1. Ferrosilicon selection

Ferrosilicon suspensions have non-Newtonian rheological characteristics. Under the right conditions, these suspensions are stable, but stability can become an issue if the conditions are not selected properly. Studies on the relationship between medium viscosity and medium RD have been performed and are available in literature (Collins, et al., 1974). The results are plotted in Figure 2.

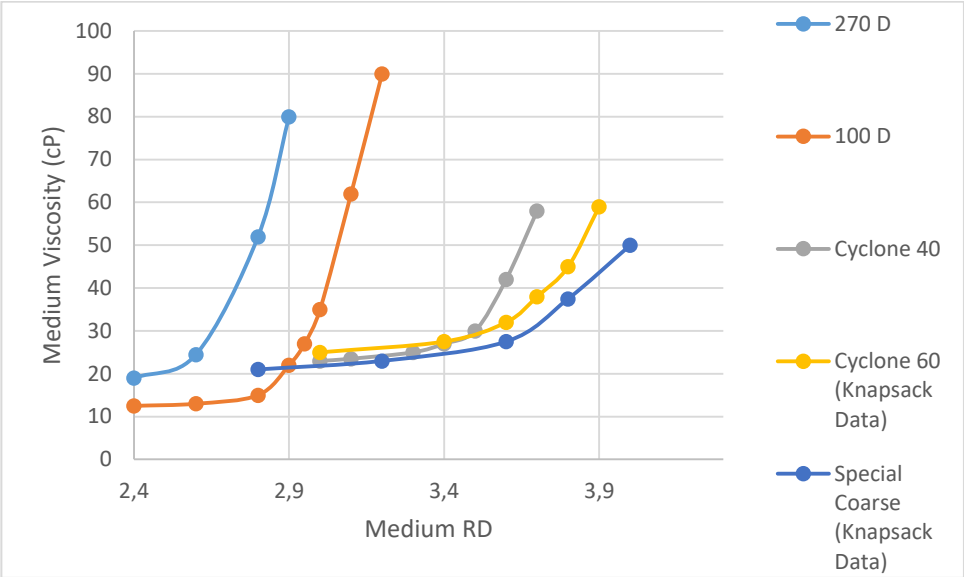

Figure 2. Medium viscosity as a function of medium RD for various ferrosilicon types (adapted from Collins, et al. (1974)

Figure 2 indicates that there is typically a small increase in medium viscosity with an increase in medium RD in the lower RD range. A critical point exists, beyond which further increase in medium RD results in a sudden and steep increase in medium viscosity. The high medium viscosity has detrimental effects on both cyclone and screen operation. It is desirable to operate below the critical point. Atomized ferrosilicon has significantly higher critical points than milled ferrosilicon and is therefore better suited for processes that operate at a high RD above 2.9, as illustrated in Figure 2 (Collins, et al., 1974).

2.1.2. Medium losses in the dense medium circuit

Although the conservation of medium is an important aspect of optimising the circuit, extreme difficulty accompanies the process of pinpointing exactly where medium is lost by mass balances of medium over the circuit. A multitude of factors contributes to the loss of medium (Sripriya, et al., 2006), (Napier-Munn, et al., 1995):

- Excessive fresh medium addition to the cyclone;
- Inefficiencies in the magnetic separation;
- Inefficiencies in rinsing of cyclone products on the screen;
- Housekeeping;
- Ore porosity;
- Adhesive forces between ore and media;
- Corrosion and abrasion due to exposure to mechanical strain or corrosive environments.

It is estimated that approximately 80% of medium losses occur on the drain and rinse vibrating screens (Napier-Munn, et al., 1995).

High momentary fluctuations in the circuit, as well as the difficulty of quantifying medium degradation, contribute to the difficulty of performing an accurate medium balance over the DMC.

2.1.3. Medium adhesion

One factor that plays a major role in the recovery of dense medium and the loss thereof, is medium adhesion. Medium adhesion refers to the extent to which dense medium adheres to coarser ore particles due to attractive forces between the two types of particles.

Past studies have found that adhesion loss is increased by the following factors:

- Increase in screen loading;
- Increase in operating density.

An increase in medium RD, particularly in the higher medium density regions where there is a steep increase in medium viscosity, decreases the drainage characteristics of the medium and leads to excessive medium losses (Napier-Munn, et al., 1995).

2.2. Screening

A screen is typically a surface that has multiple holes or apertures, used to separate fractions of a composite stream mechanically. The screen is used as an obstruction for passing of materials of a specific particle size. The aperture size of the screen is usually selected so that some of the smaller particles (undersize) are able to pass through the apertures, while others are too large (oversize) and are therefore retained on the screen surface. In this way, the particles are classified by size. In the screening process, particles collide multiple times with the screen surface by means of shaking, vibration or rotation. In order to ensure sufficient screening efficiency, it is required to use a large enough screen area to guarantee that the particles are granted enough opportunity to pass through the apertures (Napier-Munn, et al., 1999). Each collision has a probability for undersize particles to pass through the screen aperture and report to the undersize discharge. There are various different types of screening for different applications. The most common types of screening include (Dong & Yu, 2009):

1. Classification, grading or sizing; this type of screening is applied to classify material with a wide particle size distribution into narrower particle size range fractions. Screens with decreasing aperture sizes are used in series to classify the feed materials.
2. De-sliming; this type of screening is applied to remove certain fine particles (<500 micron) classified as slimes, from coarser ore particles.

3. Medium recovery; heavy medium such as ferrosilicon and magnetite used for dense medium separation are separated from coarser ore particles in order to recover the medium.
4. Scalping; in cases where the desired particle sizes are in the lower range, this type of screening is applied to remove the coarser particles from the stream.
5. Dewatering; finally this type of screening is used when there is excess water with the particles and need to be removed.

Although vibrating screens have been the focus in the mineral processing industry due to their versatility (Gupta & Yan, 2006), the engineering industry is always striving towards improvement and optimization.

For screening that utilizes a flat screen surface, for example vibrating screens, undersize particles pass through the screen apertures, but oversize particles are retained on the screen. A bed of oversize particles is formed on the screen. This bed of coarser particles affects the screening as they obstruct the screen apertures. Smaller particles have to pass through the coarser material bed to reach the screen surface before passing through the apertures. This is called material stratification. This phenomenon was found to have a fundamental effect on screening rate and various studies has been performed to quantify the effects of operating parameters on stratification and ultimately the screening rate (Hudson & Jansen, 1969), (Soldinger, 1999), (Ferrera, et al., 1988), (Feller, 1976), (Standish, et al., 1986), (Sabusanghe, et al., 1989), (Trumic & Magdalinovic, 2011).

2.2.1. Screening fundamentals

Industrial sizing is used to separate particles based on their size. Sizing is typically appropriate in the size range between 40 micron and 300 mm. Screening can be performed on a dry or wet basis. Dry screening is limited to a minimum particle size of approximately 5 mm, while wet screening is possible at much lower particle sizes of 250 micron. The difference between screening and classification is that classification is appropriate for smaller particle sizes (under 250 micron). This type of separation needs larger screen areas and it is not economically viable to have a large throughput (Wills & Napier-Munn, 2006).

In the context of dense medium separation, wet screening is appropriate. The solids are in suspension and typically at high relative densities.

2.2.1.1. Screen performance

Two main factors define the performance of a screen. The first is the screen capacity or screening rate and the second is the screening efficiency (Gupta & Yan, 2006). Screen

efficiency and capacity are typically inversely proportional, which means that neither of the parameters can be maximised without a cost in the other.

The screen capacity relates to the feed flow rate at which the unit can operate. The capacity is related directly to the screen area. Capacity factors are used to describe the various feed material properties and screen operating conditions.

2.2.1.1.1. Screen efficiency

In the ideal screening scenario, all particles that are smaller than the screen aperture size will pass through the screen, while all the particles greater than the aperture size will not. In reality this is not the case. With enough time and opportunities to contact the screen in different orientations, all undersized particles should eventually pass through the screen. However, the demand for high throughput limits the time that a particle spends on the screen. This in turn limits the efficiency that is achievable (Gupta & Yan, 2006). The screen efficiency is therefore defined as the screen's ability to place particles of a certain size from the feed, in the correct stream (underflow or overflow) by using the appropriate screen aperture size. The fraction of the particles in that size range in the feed that reports to either the underflow or the overflow streams are typically illustrated with efficiency or partition curves. A mass balance of materials in a particular size range over the separation unit is used to determine the fractions of that material that reports to the underflow or overflow stream. In the context of medium recovery, all medium particles are undersized and should report to the underflow stream of the screen, while ore particles are retained on the screen and report to the overflow. Thereby separation of medium from ore is accomplished. The efficiency of a medium recovery screen can therefore be quantified by the carryover of medium to the overflow stream. The % medium carryover is calculated as the fraction of medium fed to the screen that reports to the overflow stream as a result of medium adhesion to the ore particles, and is calculated with Equation 1:

$$\%Medium\ carryover = \left(\frac{O_m M_o}{f_m M_f}\right) \qquad \text{[Equation 1]}$$

Where M_o is the mass flowrate to the oversize stream, O_m is the mass fraction of medium particles in the oversize stream, M_f is the mass flowrate of the feed and f_m is the mass fraction of medium particles in the feed.

Some parameters that affect screening efficiency include (Napier-Munn, et al., 1999):

- Moisture content;
- Near-size material;
- Particle shape;
- Density.

These parameters will be discussed in more detail later on in the literature review.

2.2.1.1.1.1. Water bypass to oversize stream

In the case of ideal separation, all the water and undersize particles would drain through the screen apertures into the underflow. Water that bypasses the screen and report to the overflow is therefore an indication of inefficient operation and can be used to quantify the efficiency. In the context of wet screening, an increase in water bypass typically leads to an increase in fines carryover to the overflow (Rogers & Brame, 1985), (Napier-Munn, et al., 1999).

2.3. Trommel screens

Trommel screens are extremely versatile and have been used in the mineral processing industry for more than four centuries (Alter, et al., 1981). A trommel screen, also known as a rotary drum screen, consists of a cylinder shaped screen media, as illustrated in Figure 3.

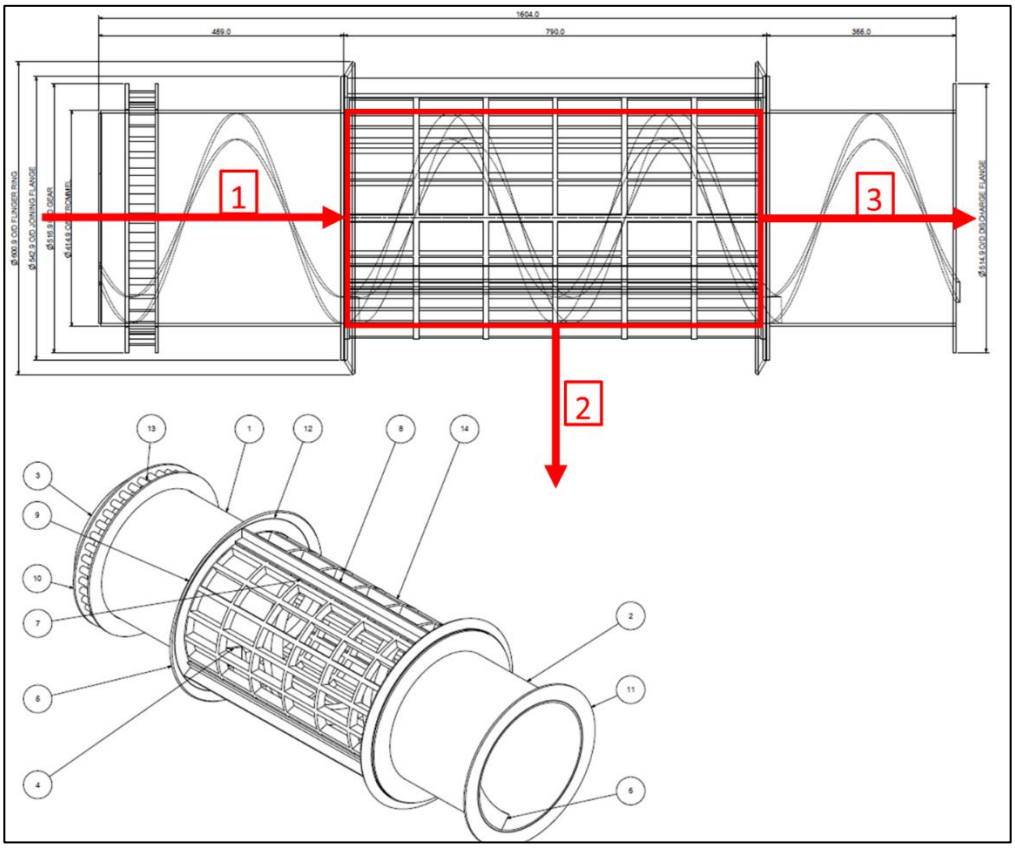

Figure 3. Equipment drawing of a trommel screen (Mk2) with its feed and underflow and overflow discharges.

Material is fed into the cylindrical screen from the feed end (stream 1). Trommels can be either self-driven or bolt-on. Self-driven trommels are rotated with an electrical or hydraulic motor. Bolt-on trommels are, as the name suggests, bolted onto a mill for the purpose of removing scats and oversized particles from the process stream (Wills & Napier-Munn, 2006). The screen media is selected to facilitate separation, where undersized particles pass through the apertures to the underflow (stream 2), while oversized particles are retained in the screen and are transported along the length, to report to the overflow (stream 3).

2.3.1. Particle motion

In a rotating drum or trommel screen, the motion of the particles are unique from other types of screens. The particle motion inside of the screen will be described in this section.

2.3.1.1. Particle motion mechanisms

Different rotational velocities result in different particle motion mechanisms in the drum. The mechanisms are slumping or cascading, cataracting and centrifuging by increasing rotational velocity. The illustrations indicate the peak height that the particles remain adjacent to the drum wall (Stessel & Kranc, 1992).

2.3.1.1.1. Slumping or cascading motion

The particles rotate with the drum, but are not carried high up on the drum wall before sliding or tumbling back to the bottom of the drum by the free surface. Only small particles (filter granules) near the trommel body are screened and this results in a low screening efficiency (Stessel & Kranc, 1992).

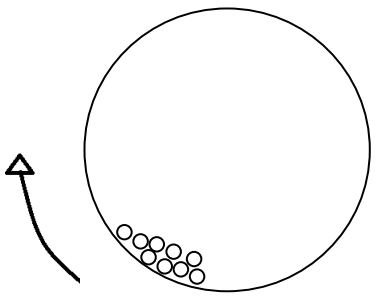

Figure 4. Slumping or cascading motion

The factors that govern the slumping motion in a trommel, are: (Chen, et al., 2010), (Mellmann, 2001)

- Rotation speed;
- Particle size;
- Cylinder diameter.

2.3.1.1.2. Cataracting motion

With higher rotational velocity, the particles remain adjacent to the drum wall to a greater height. The particles detach from the wall closer to the top of the drum. As a result of the Brazil nut effect, the larger granules segregate near the inner core while smaller granules stay near the screen surface. Therefore smaller filter granules pass through the screen. Higher screening efficiency is accomplished due to turbulent flow of particles (Vesilind & Rimer, 1981).

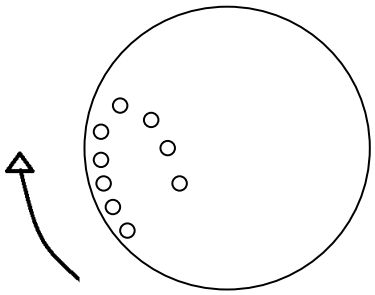

Figure 5. Cataracting motion

For dry screening, it is desirable to operate a trommel at a cataracting motion. Studies by Alter, et al. (1980) focus only on the geometry of the motion, for example the locations of departure, together with impact angle. Other studies by Glaub et al. (1982) go further to incorporate the force balance on a particle at the moment of departure, leading to velocity vectors describing their trajectory through the trommel. These vectors are described by [Equation 2] and [Equation 3], after numerous simplifications.

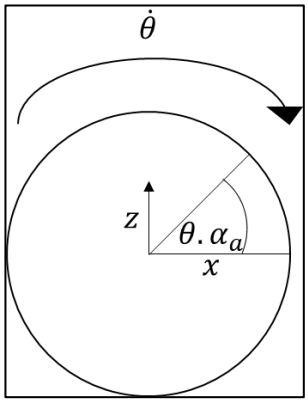

Figure 6. Graphical illustration of parameters that describe particle motion in a trommel.

Where α_a is the angle of location of a point on the screen, and θ is the angle describing particle motion. Then:

$$\dot{\theta}R\cos\alpha_a = \dot{z}_0 \quad \text{[Equation 2]}$$

$$\dot{\theta}R\sin\alpha_a = \dot{x}_0 \quad \text{[Equation 3]}$$

Where z and x are the vertical and horizontal location of the particles, respectively. The subscript 0 indicates the moment of departure from the screen surface (Glaub, et al., 1982).

2.3.1.1.3. Centrifuging motion

At high enough rotational velocities the particles remain adjacent to the drum wall because the centrifugal force is always greater than the gravitational force on the particles. Screening efficiency decreases.

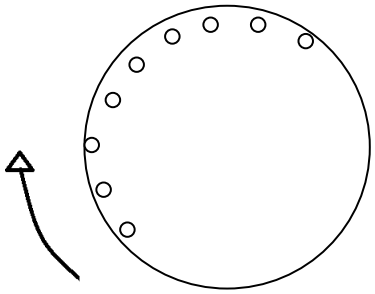

Figure 7. Centrifuging motion.

The models for particle motion, residence time and special screening rate for trommel screens are important to know, in order to be able to understand the trommel, however it might be too complex to attempt to model the particle motion inside of the screens. The trommel screen does not allow opening of the screen during operation and it is difficult to measure or track the motion of particles inside of the screen while it is rotating under high slurry flow rates. The objective of this project is to comment on the viability of replacing vibrating drain and rinse screens with the submerged trommel screen. To accomplish this, one must produce results that are comparable to that produced on the vibrating screen. Therefore the separation efficiency and parameters of interest will be selected to correspond with the vibrating screen, not to attempt to model particle motion inside of the trommel.

2.3.1.2. Particle velocity and screening

In the sections where the particle size is smaller than the aperture size, the particle velocity (V) can be separated into a horizontal (V_x), vertical (V_y) and axial components. Past studies have found that in the absence of scrolls, the axial velocity is mostly driven by the screen inclination angle (Stessel & Kranc, 1992). Generally the trommel inclination angle is small (between 0 ^{o} and 5 ^{o}), which justifies the omission of the axial velocity component in various studies (Alter, et al., 1981), (Glaub, et al., 1982). The angle between the particle velocity and the vertical component is denoted by Θ.

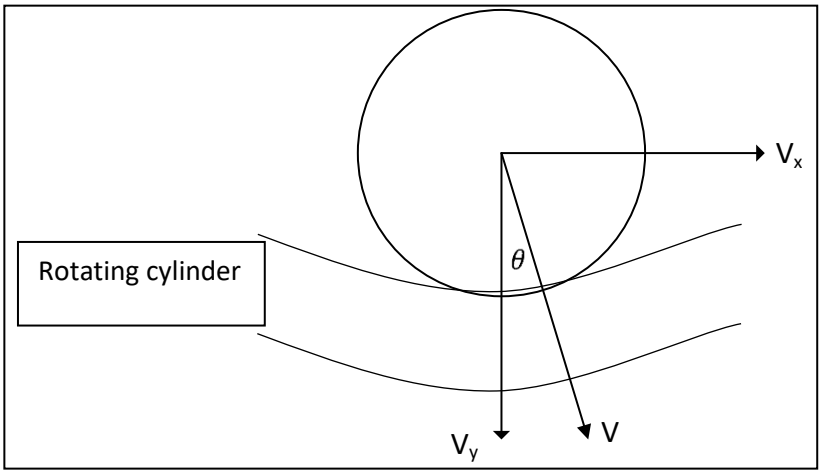

Figure 8. Graphical illustration of velocity components of a particle in a rotating cylinder.

The vertical and horizontal components are calculated as follows:

$$V_y = V\cos\theta \qquad \text{[Equation 4]}$$

$$V_x = V\sin\theta \qquad \text{[Equation 5]}$$

When the vertical velocity component is greater than the horizontal component, the particle escapes through the aperture. If the horizontal component is greater than the vertical component, the particle remains within the drum. The larger particles remain inside of the drum until the aperture is larger than the particle diameter, at which point that particle will behave the same as explained here (Chen, et al., 2010).

2.3.2. Parameters describing trommel performance

As with most screens, the main parameters that describe the performance of a trommel screen are:

- Screening rate;

The screening rate refers to the capacity of the screen and indicates the throughput that the screen can deliver (Napier-Munn, et al., 1999), (Wills & Napier-Munn, 2006).

- Screening efficiency.

The screening efficiency refers to the sharpness of separation. This parameter is dependent on the application and design specification of the screen (Rogers & Brame, 1985), (Napier-Munn, et al., 1999), (Wills & Napier-Munn, 2006).

2.3.3. Trommel models to describe operation

Although trommel screens are one of the oldest screening devices, very little information is available about design and sizing of trommels for specific applications. Due to the complexity

of the process, a great deal of trommel designs have been based on empirical data (Stessel & Kranc, 1992). Some studies have been conducted to develop models for design and sizing of trommels (Stessel & Kranc, 1992), (Stessel & Cole, 1996), (Alter, et al., 1981), (Gaudin, 1939). There is a desire to improve the understanding of the inner workings of a trommel by gathering empirical data that will provide insight into material distribution inside of the trommel during operation.

2.3.4. Operating parameters affecting screen performance

A number of operating parameters impact the performance of any screen, including static screens, vibrating screens and trommels. These parameters include feed flow rate, screen inclination angle, number and size of screen apertures, percent open area of screen media, feed characteristics such as PSD and particle shape and feed density (Gupta & Yan, 2006), (Wills & Napier-Munn, 2006), (Napier-Munn, et al., 1999), (Feller, 1976). These parameters of interest will be discussed first. Other operating parameters that affect the screen performance of rotating drum screens specifically, include drum size and rotational velocity (Alter, et al., 1981), (Stessel & Kranc, 1992), (Stessel & Cole, 1996), (Chen, et al., 2010). These parameters will be discussed thereafter.

2.3.4.1. Feed flow rate

Increasing the feed rate to a screen typically increases the screening rate and throughput of a screen, however increasing the feed flow rate of material beyond the screen capacity causes the screening efficiency to decrease (Orrino & Khakhar, 2000). This is because the feed rate directly impacts the material depth and residence time of material on the screen. Increasing the feed flow rate beyond the capacity of the screen causes the excess of feed to bypass the screen and fine materials flow straight to the overflow, or in the context of a multi-stage trommel screen, are carried over to the next chamber in the trommel screen. Increasing the feed rate will only have a desired outcome to a certain maximum point, after which the screening efficiency plummets with further increase in feed rate (Burke & Craig, 2005).

2.3.4.2. Feed PSD and particle shape

Since screening is a mechanical process that separates solids based on particle size, therefore the material size distribution has an impact impact on the performance of a screen. Three different particle size ranges are typically referred to, namely fine, near size and coarse. The fractions of these size ranges greatly affect screening (Soldinger, 1999), (Standish, et al., 1986). Depending on the application, different size fractions will have different interactions with various sizes and shapes of apertures. Furthermore, the stratification of undersized

particles to the screen surface is a prerequisite to separation (Soldinger, 1999). According to Soldinger (1999), high quantities of fines (above 30%) often interfere with stratification of near sized particles. Particles in the near size range are the most difficult to screen, because they tend to block the screen apertures (Wills & Napier-Munn, 2006). Wills & Napier-Munn (2006) state that elongated particles are difficult to screen due to the fact that these particles have to assume the correct orientation to pass through the apertures.

2.3.4.3. Feed slurry relative density / solids concentration

Feed slurry density and solids concentration are important factors that have a great effect on screening performance. Typically, dry screening is appropriate for 4 mm undersize, but high frequency screening can be applied to as low as 45 microns. Wet screening is effective down to 250 microns (Wills & Napier-Munn, 2006). This is because the water provides a mechanism for transport of fine solids through the screen media (Valine, et al., 2009). If there is insufficient water to transport the fines from the ore particles into the underflow, the fines are retained in the particle bed and is carried over to the screen overflow (Guerreiro, et al., 2015). The solids concentration of a slurry also has a direct impact on the viscosity of the slurry. The maximum solids concentration that is appropriate for a specific application, depends on the materials used. High viscosity typically results in decreased drainage characteristics (Collins, et al., 1974).

2.3.4.4. Material friability

Considering the great impact that feed PSD has on the separation efficiency, material friability will have an effect on the screening. Friability is breaking or erosion of particles in the system. As the particles degrade or decrease in size, they behave differently and can affect the system, for example by blinding a screen aperture after decreasing in size and then getting stuck (Govender & Van Dyk, 2003). Other materials may get crushed or ground into much smaller particles that can then easily pass through screen apertures that would have been too large without particle breakage.

2.3.4.5. Material flowability

This property refers to the rheology of a slurry. The viscosity and settling stability of the material has a great impact on the system. A change in stability of a slurry will result in different settling of particles. A change in particle settling will have a significant impact on the screening process. A change in viscosity has a great impact on the manner in which the slurry flows over the screens. Stability and viscosity of the slurry is mostly affected by the factors listed below: (Boylu et al. 2004; Napier-Munn & Scott 1990; Luckham & Ukeje

1999; Poletto & Joseph. 1995; Mangesana et al. 2008; Olhero & Ferreira 2004; Amiri et al. 2010; Alturki et al. 2013)

- Presence of ore slimes;
- Shear rate accumulation;
- Oxidation and degradation of medium;
- Disintegration and shape of medium;
- Solid concentration.

2.3.4.6. Screen inclination angle

Screen inclination angle refers to the angle from the horizontal that a screen is installed at. In the context of flat deck horizontal screens, it is common to elevate the feed end of the screen, however in some cases the discharge end of the screen can also be elevated. The biggest effect of lifting the feed end of the screen is that the particle velocity over the screen surface increases. This allows quicker stratification of finer particles to the screen surface (Sawant, et al., 2016). Due to the inclination angle of a flat deck screen in combination with the particle movement on the screen surface, the particles see a smaller aperture than the actual size of the aperture (Wills & Napier-Munn, 2006).

Trommels are typically designed on a small angle to horizontal (between 0 ^{o} and 5 ^{o}) to promote material flow along the length of the trommel (Wills & Napier-Munn, 2006). This decreases material residence time in the trommel. A study that investigated inclination angle on trommels has found that an increase in inclination angle increased the screening efficiency, but after a certain point it also became detrimental to the screening efficiency (Chen, et al., 2010). This was explained by the relative velocities of the particles. Recall that the particle velocity (V) can be separated into a horizontal (V_x), vertical (V_y) and axial components, as illustrated in Figure 8 in the particle velocity section. At a large enough angle, V_x is greater than V_y, which implies that the particles roll horizontally over the apertures because they have too much momentum to pass through the aperture. An increase in inclination angle also decreases residence time inside of the screen, which decreases the number of impingements and, in turn, screen efficiency.

The effect of screen incline on the apparent aperture size in a trommel is smaller compared to that of a vibrating screen, because the material moves along the circumference and along the length of the trommel. Increasing inclination angle also increases the production rate by increasing the particle velocity, V. This is at the cost of screening efficiency. Conversely, decreasing the angle results in longer residence times and increasing screening efficiency. On a trommel screen, the effect of inclination angle is however very small and its effect is often

omitted in model development (Alter, et al., 1981), (Stessel & Kranc, 1992), (Glaub, et al., 1982).

2.3.4.7. Aperture size, shape and percent open area

Aperture size and shape is selected based on the specification that is required for the application, which is typically a cut point for separation. The aperture size and shape affects the probability of passing of particles. This function has been developed by a number of academics since its conception by Gaudin (1939). Originally, the function considered the probability of passing of a single particle on a screen surface. Since then, the function has been developed to incorporate the effect of other undersized particles in the vicinity of the particle in question, as well as stratification rates (Ferrera, et al., 1988), (Trumic & Magdalinovic, 2011).

The throughput capacity of a screen is greatly dependent on the percentage open area of the screen media, because it limits the area that the material can pass through. A greater open area implies a greater throughput for this reason (Wills & Napier-Munn, 2006). This implies that the throughput of a screen can be severely limited by a low percentage open area, even if the probability of passing is high.

Percentage open area typically decreases for finer apertures to ensure that the panels remain structurally rigid.

2.3.4.8. Particle friction coefficient

In the context of a trommel, typical models to predict the motion of particles within the trommel incorporate the rise of particles with trommel rotation and the departure trajectory. The acceleration of a particle is expressed with the following [Equation 6]:

$$\ddot{\theta} = \mu\dot{\theta}^2 - \frac{g}{R}(\mu\, sin\theta + cos\theta) \qquad \text{[Equation 6]}$$

Using the same notation as before, where θ is the angle describing particle motion, g is the gravitational acceleration (m/s^2), R is the trommel radius (m). μ is the coefficient of friction of the particle against the surface, either kinetic or static coefficient of friction, depending on if the particle is slipping or not (Stessel & Cole, 1996).

2.3.4.9. Drum size

At constant operating parameters, the size of the screen area of a trommel is directly related to the number of impingements that will occur before the material exits the screen via the oversize discharge (Alter, et al., 1981). The number of impingements, in turn, is directly related to the probability of passing and thereby screening efficiency. Not only does a greater

screen area increase the probability of passing, but also the capacity of the screen (Gupta & Yan, 2006), (Napier-Munn, et al., 1999), (Wills & Napier-Munn, 2006).

2.3.4.10. Rotation velocity

The effect of rotation velocity on the screening efficiency of a trommel is not as obvious. Rotation velocity increases the centrifugal force that the material experience, which could enhance drainage, however the rotation velocity also affects the material motion type in the screen from slumping to cataracting and ultimately centrifuging (Alter, et al., 1981), (Stessel & Cole, 1996), (Stessel & Kranc, 1992), (Chen, et al., 2010). A study by Chen, et al (2010) found that screening efficiency improved with an increase in rotation velocity at low rotation velocities, however a further increase in rotation velocity beyond the critical point reduces the screening efficiency as the material enters a centrifuging motion and the number of impingements is reduced, because the material adheres to the screen surface.

2.3.5. Trommel screen physical design considerations

Based on the application of the trommel screen, there are multiple design considerations that differentiate these screens from each other.

2.3.5.1. Flights, lifter bars and baffles

Some trommels include flights, lifter bars and baffles inside of the rotating drum to manipulate the movement of material inside of the screen (Kelly, 2007) (Zhou, et al., 2016), (Wills & Napier-Munn, 2006). These installations are typically mounted to the inside of the screen and rotate with the screen to influence particle movement, as illustrated in Figure 9.

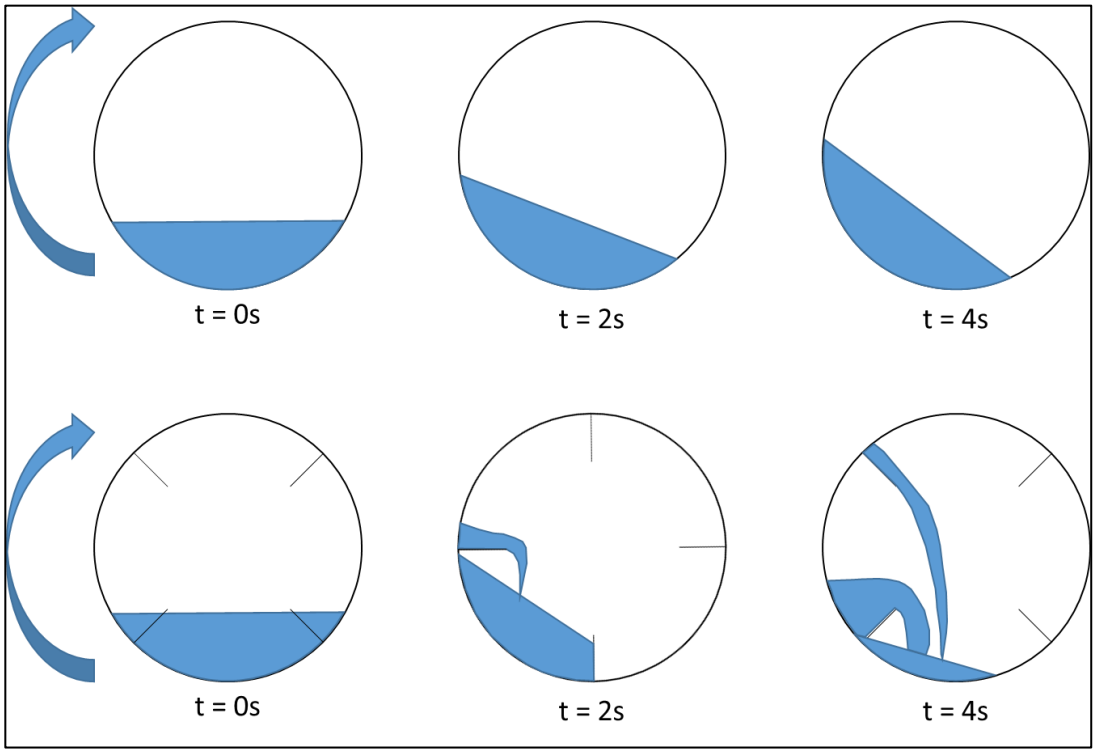

Figure 9. Illustration of the effect of flights and lifter bars on material motion in a rotating drum.

The addition of lifter bars impacts the flow distribution inside of the trommel by lifting the material higher along the circumference of the trommel during rotation, as illustrated in the bottom row of Figure 9.

2.3.5.2. Concentric screens

This design of the trommel screen has multiple layers of screens around each other. The largest aperture size screen is closest to the center, near the rotation axis. Finer particles are able to pass through more screens as they move outward (Wills & Napier-Munn, 2006).

2.3.5.3. Series screen

This trommel screen has a single drum with different screen aperture sizes along the length of the drum. The aperture size increases along the length of the drum so that the finer materials pass first (Wills & Napier-Munn, 2006).

2.3.5.4. Internal screw (scroll) for particle migration

An internal screw is often fitted in the drum. The rotation of the screw forces the movement of particles through the drum from finest to coarsest screen aperture sizes. The internal screw is typically used in drums that is flat or at a low elevation angle below 5^{o} (Wills & Napier-Munn, 2006).

2.3.6. Trommel comparison with vibrating drain and rinse screen

Vibrating screens are typically applied for the purpose of drain and rinse recovery of dense medium (Napier-Munn & Scott, 1990), (Sripriya, et al., 2006), (Sripriya, et al., 2003), (Napier-Munn, et al., 1995).

The submerged trommel screen is a relatively new concept that was developed to investigate its viability as a replacement for the vibrating drain and rinse screens that are currently common in the industry. No evidence has been found in open literature that trommels have been investigated for the purpose of medium drainage in the context of dense medium separation. Trommels have numerous advantages over vibrating screens that make them appealing as an alternative, if the performance is competitive for this application.

Therefore, for the purpose of investigating the trommel screen as an alternative to the vibrating drain and rinse screen, it is of interest to compare the advantages and disadvantages of the two types of screens. The advantages and disadvantages are discussed in the followings.

2.3.6.1. Advantages of trommel screens

Trommel screens are significantly cheaper to manufacture than vibrating screens (Wills & Napier-Munn, 2006). Vibrating screens require a very strong structural integrity of the screen itself, as well as the supporting structures. Furthermore, the motors of a vibrating screen are more complex, expensive and power intensive than the motors required to drive a self-driven trommel.

Rotational motion produces much less noise than vibrating screens, so trommels do not have as much noise pollution as vibrating screens.

Trommel screens tend to last longer than vibrating screens because of the smaller mechanical stress. Trommel screens are also very mechanically robust (Wills & Napier-Munn, 2006).

2.3.6.2. Disadvantages of trommel screens

Trommel screens have a smaller capacity (less material is screened in the same time) because only a fraction of the total screen area is utilised at a time, while vibrating screens utilise the entire screen area continuously (Wills & Napier-Munn, 2006).

Trommel screens are more prone to plugging and blinding, especially when different screen aperture sizes are in series. The vibration in vibrating screens reduces pegging and blinding by shaking the particles out of the screen apertures. The movement in trommel screens are

more gradual, which allows pegged particles to remain inside of the apertures (Wills & Napier-Munn, 2006).

2.4. Literature significance

This section is aimed at summarising the literature review and to explain how the literature guided the study.

2.4.1. Dense medium separation

The literature on dense medium separation allows the selection for operating conditions for the test work, as well as the framework for evaluation of performance of the dense medium trommels. The work that was performed by Kabondo (2018) provides a means to compare the performance of the trommels with that of a horizontal drain and rinse vibrating screen to evaluate the viability of trommels for this application.

2.5. Screening and screen performance

Classic screening fundamentals and separation efficiency applies to dense medium separation, because the recovery of medium by drainage is in essence classification of solids by size. The aperture size for dense medium separation is selected such that all coarse ore particles are retained on the screen, while the fine FeSi is drained with water to the undersize of the screen. Since no ore particles report to the underflow of the dense medium trommels (Mk1 and Mk2), the performance of the screen can be quantified by the fraction of misplacement of fines and water to the overflow. This simplifies the quantification of the performance of the screen by evaluating parameters such as % FeSi in overflow, % FeSi carryover to overflow, % moisture in overflow and drainage rates.

2.6. Trommel operation and particle motion

Open literature describes three main particle motion mechanisms, namely slumping/cascading, cataracting and centrifuging motion. It is known that cascading motion is ideal for dry screening, however little work has been published on the ideal motion for drainage of fines in a wet application on trommels, particularly in applications with a significant bed of oversized particles like in DMS.

Literature identified the most important factors affecting screen performance of trommels as:

- Feed flow rate;
- Feed PSD and particle shape;
- Feed slurry RD or slurry solids concentration;
- Material friability and flowability;

- Screen inclination angle;
- Aperture size, shape and percent open area;
- Particle friction coefficient;
- Drum size;
- Rotation velocity.

Test trommel Mk1 was already designed and manufactured before the start of this project, which means that physical dimensions of the unit were fixed. Literature did however provide insight into parameters that needed to be selected and considered for comparison of the trommel (Mk1) with a vibrating drain and rinse screen. The literature also assists with design considerations of the drain trommel (Mk2).

Models that predict particle motion inside of a trommel are very limited, usually considering only a single particle at a time. These models are typically accompanied by a number of assumptions to simplify the calculations, such as perpendicular collision of particles with the screen surface, no slippage between particles and screen surface, negligible inter-particle interactions and uniform particle shape. The models can be modified to incorporate the PSD and shape of particles, but increases the complexity of the calculations for probability of passing, significantly. In particular applications such as DMS, the predictive models is not expected to be accurate because of a great extent of inter-particle interactions and a significant particle bed on the screen. Furthermore, it is extremely difficult to evaluate the movement of particles during operation of a trommel because of the inaccessibility of the unit.

Literature does not provide a tool to predict material distribution inside of a trommel. The collection of empirical data for various applications seems to be the best method of learning about material distribution inside of trommels. There is a great need in literature for test work that provides insight into material distribution, which in turn relates to throughput in various areas of the trommel. This can be best accomplished by designing a trommel (Mk2) that samples from various locations in the trommel to relate local drainage rate with material distribution on the screen.

3. EXPERIMENTAL SETUP AND DESIGN

3.1. Introduction

This section will discuss the characteristics of the submerged test trommel Mk1, material preparation and characterisation and the experimental procedure for the first test campaign.

3.2. Material selection, preparation and characterisation

Materials were selected to mimic the materials used in the study by Kabondo (2018) in order to allow direct comparison of the results.

3.2.1. Iron ore

The iron ore that was used for this experimental work was acquired from Sishen Mine, located in Kathu. The first step to prepare the material was to sun-dry on a tarpaulin to ensure that all residual moisture was removed. The material was then screened to remove -1.5 mm and +16 mm particle sizes.

The -1.5mm particle sizes were removed because it was desired to retain all ore particles on the screen, while only the medium drained to the underflow. Ore fines have been proven to increase medium viscosity and stability (Bosman, 2014), (Sripriya, et al., 2003), (Marsh, 1945). The -1.5 mm fraction was less than 3% in the study by Kabondo and it was estimated that removal of this fraction would not have a significant impact on overall screen performance.

After isolating the desired particle size range, the material was blended and split into representative samples to perform PSD analysis on the sample. The samples were split into ten smaller samples of 500g using a rotary splitter, after which three repeat PSD analysis tests were performed to confirm iron ore PSD. The particle size distributions obtained, are illustrated in Figure 10. Comparison of the iron ore PSD indicates that the results are repeatable and that the samples are representative.

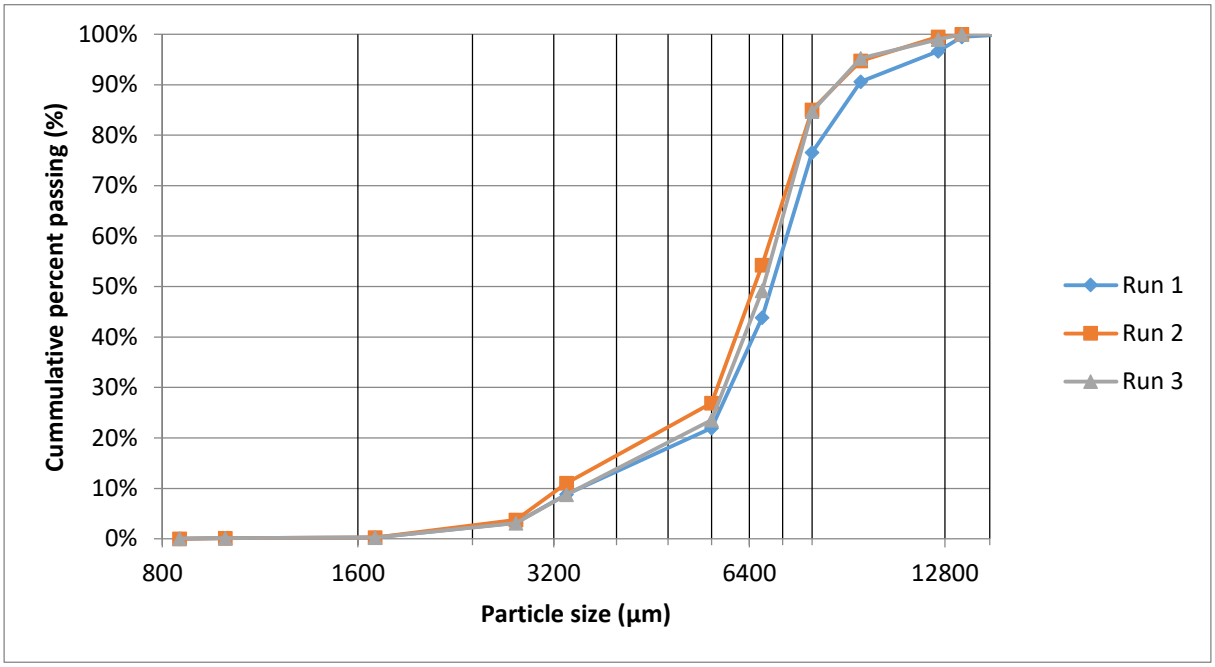

Figure 10. Particle size distribution of iron ore used in the study.

3.2.2. Ferrosilicon

Ferrosilicon was selected such that the viscosity of the medium does not exceed the critical point in the relative density range that would be investigated. The viscosities of various types of ferrosilicon are illustrated in Figure 11.

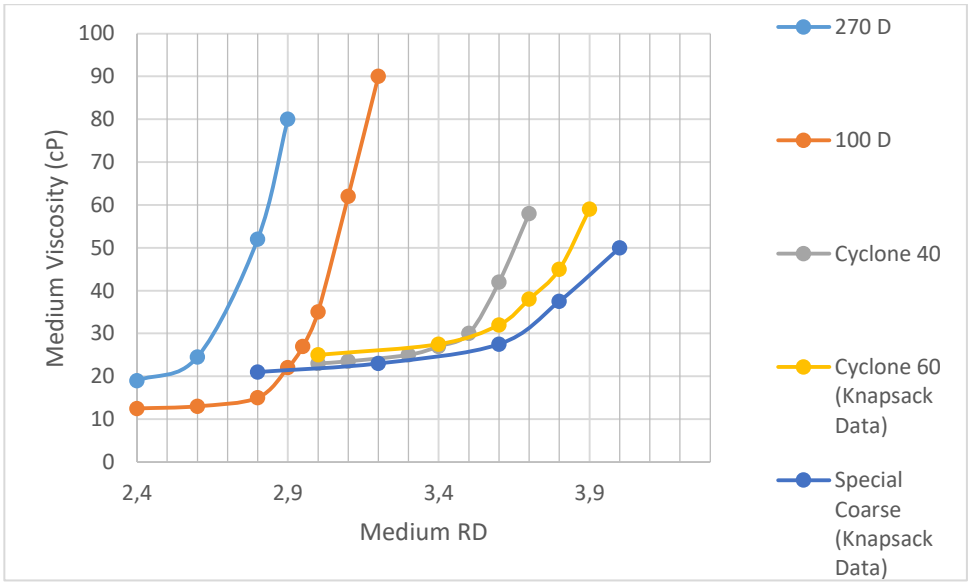

Figure 11. Medium viscosity as a function of medium RD for various ferrosilicon types (adapted from Collins, et al. (1974)

As illustrated in Figure 11, the milled ferrosilicon (270 D and 100 D) spike in viscosity at a relatively low medium RD below 2.8. The next option was Cyclone 40 Atomized FeSi, that has a critical medium RD of approximately 3.5. Therefore Cyclone 40 was selected as the ferrosilicon for this test campaign. As with the iron ore, the material was blended and split

into smaller representative samples of approximately 30 kg. This representative sample was then split into 10 smaller samples using a rotary splitter. The FeSi density was measured with a pycnometer as 7.2 t/m^3. This density was used to perform three repeat PSD analysis tests using a Malvern Mastersizer 3000. The result for the average FeSi PSD is illustrated in Figure 12.

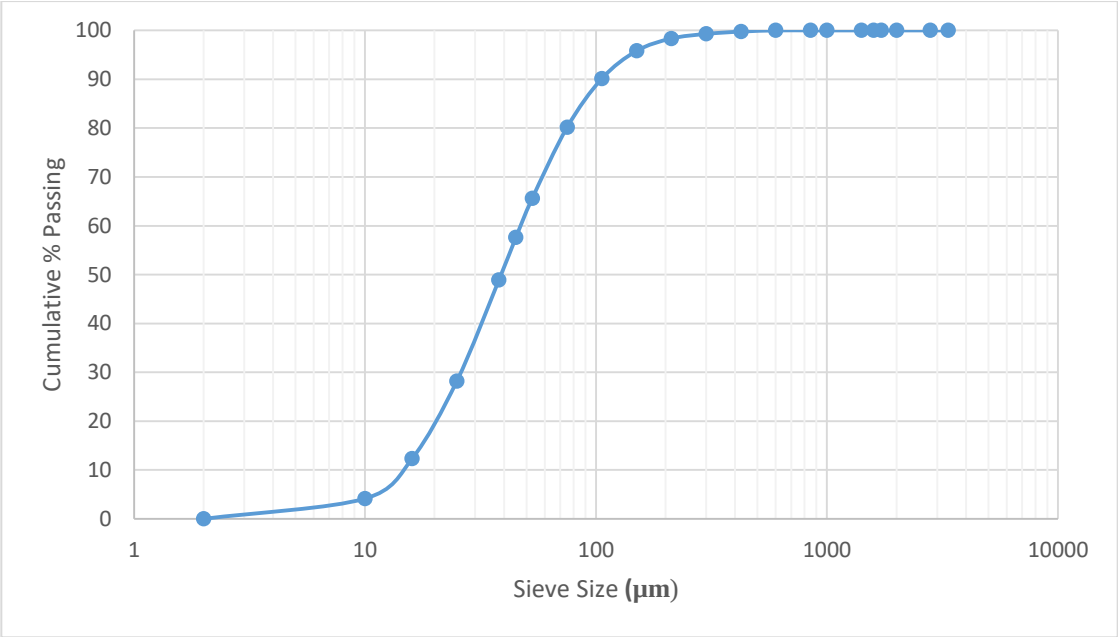

Figure 12. Particle size distribution of Cyclone 40 ferrosilicon used in this study.

The D_{50} of the Cyclone 40 Atomized FeSi was precisely 40 microns. Approximately 90% of particles were smaller than 100 microns.

3.3. Characterisation of equipment

This section consists of a brief equipment description.

3.3.1. Submerged DMS test trommel (Mk1)

The trommel screen (Mk1) consists of four chambers, each containing its own screen. The screens are circular and mounted on a central shaft that extends through all four chambers. The screen diameter of all sections is 0.796 m, with a screen length of 0.63 m. The shaft is driven by a 7.5 kW motor at 24 RPM. Figure 13 is an isometric drawing of the trommel screen. After that follows a photograph of the trommel (Mk1) and the pilot plant in Figure 14.

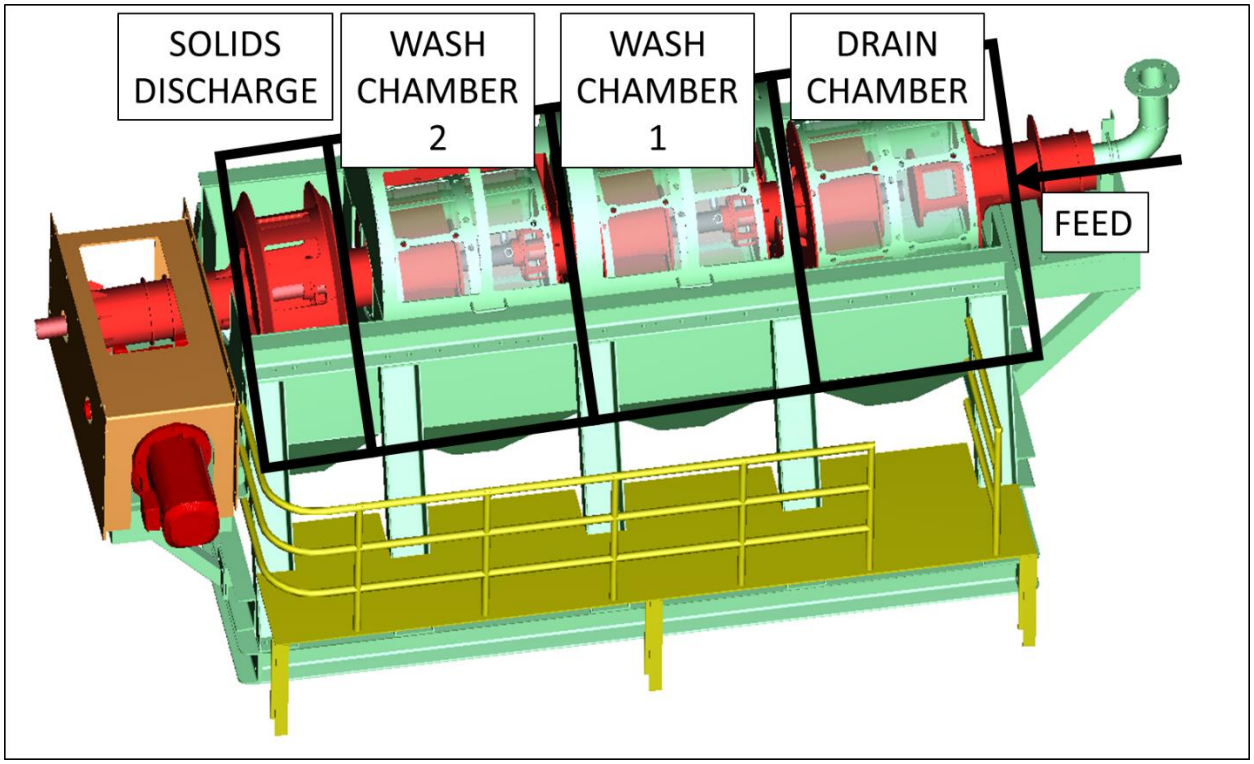

Figure 13. Isometric drawing of Submerged DMS Trommel (Mk1).

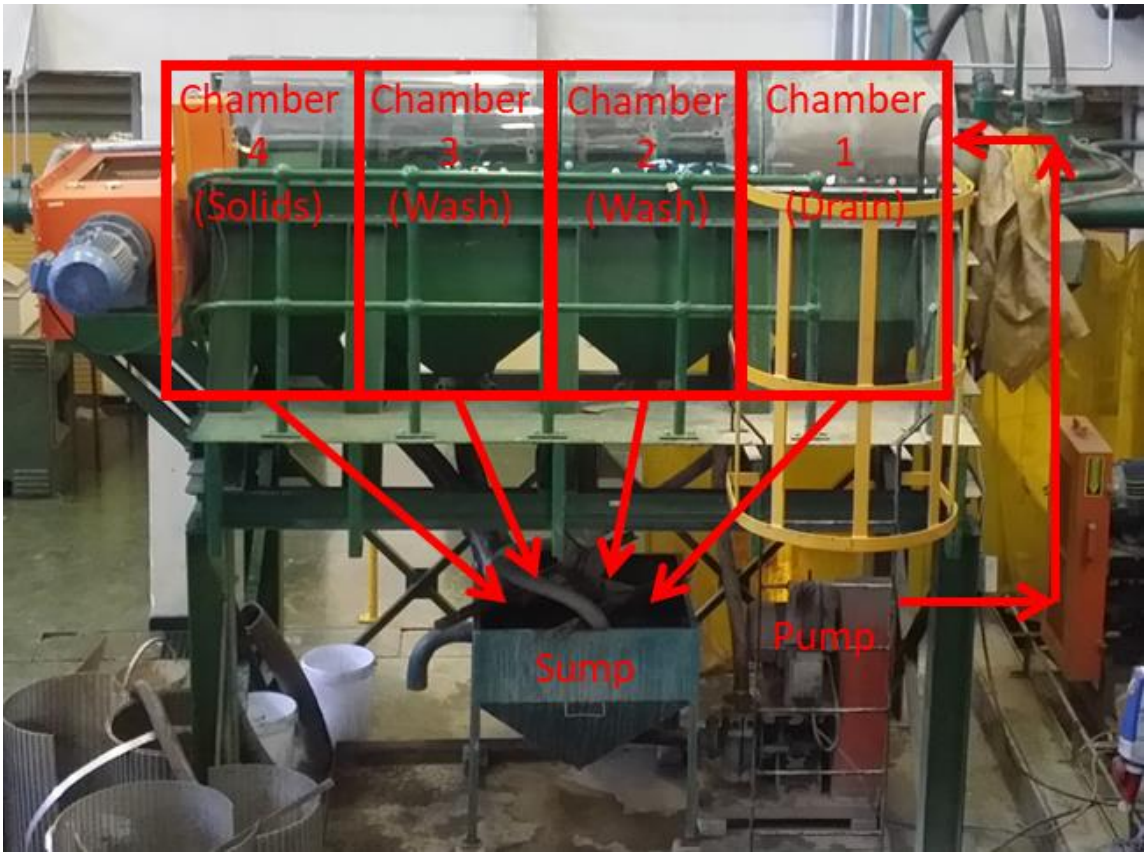

Figure 14. Photograph of experimental setup of Submerged DMS Trommel (Mk1).

The first chamber on the feed side of the trommel (Mk1) is the drain chamber. This chamber has no obstruction for flow that passes the screen apertures to the underflow and drains back into the sump. The slurry enters the chamber inside of the screens that retain larger ore particles while a large portion of the liquid containing fine particles is drained back into the sump. The feed side of the drain chamber, situated inside of the screen bracket, is shown in Figure 15.

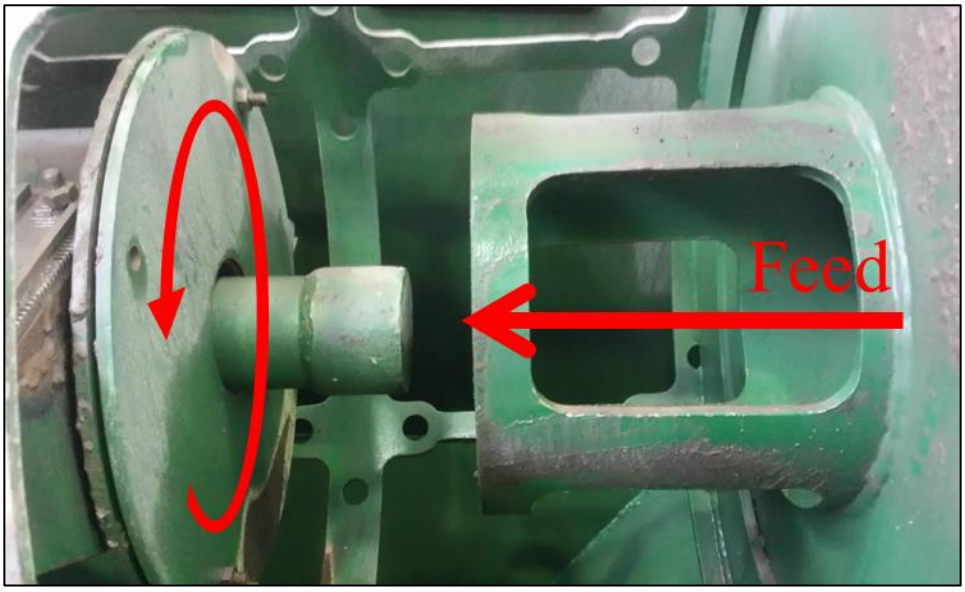

Figure 15. Photograph of feed configuration of Submerged DMS Trommel (Mk1), Drain chamber.

The shaft inside of the screen is designed with paddles to scoop the retained ore particles into an opening in the shaft. The inside of the shaft is designed with scrolls that convey the scooped solids through to the following wash chamber, shown in Figure 16.

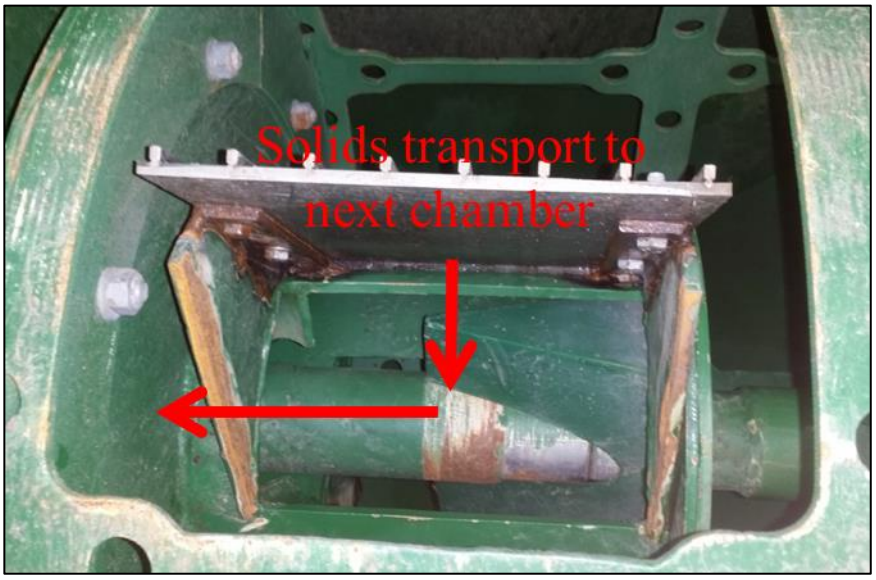

Figure 16. Photograph of solids transport mechanism of Drain chamber (overflow)

The second and third chambers are submerged. The screens are rotating in the middle of the chamber while the bottom of the chamber acts as a water tank that overflows into the sump. These chambers are intended to wash the medium (FeSi or magnetite) from the ore particles. The washing water is sprayed from inside of the screens. The larger ore particles are once again retained within the screens while the fines are able to exit the screens with the water from the water nozzles through overflow slots for the chamber. Both the second and third chambers have individual outlets that return to the sump. Figure 17 shows a photograph of the wash chamber.

Figure 17. Photograph of wash chamber in Submerged DMS Trommel (Mk1).

The screen media that was used is a Linatex® mat, punched with 0.8 mm x 13 mm apertures, with an effective open area of 15.04 %. These screens wrap tightly around the screen brackets shown in the photographs. Figure 18 shows the same chamber (chamber 2) as Figure 17, but with the rubber screen mat wrapped over the screen bracket, as it would look if the chamber is in operation. The mass of the ore inside of the screen is supported by the three screen braces on the sides and in the middle of the screen. Additional measures were taken to close openings on the seam of the mat. Cable ties and wire stiches were implemented to seal the seam of the screen mat and prevent spillage. This is illustrated with Figure 18.

Figure 18. Linatex screen mat secured onto screen bracket.

3.3.1.1. DMS Test Trommel (Mk1) circuit

Figure 19 is a photograph of the support units used to operate Test Trommel Mk1. The sump (number 1) is approximately 250 L square shaped tank with the edges converging to the bottom near the outlet. The flexi pipes (2) on the outlets of the four chambers in the trommel (Mk1) enter the sump from the respective sides. An agitator (3) was installed in the sump in order to prevent solids settling of medium during operation. Finally, the pump (4) was used to circulate medium through the feed pipe (5) to the drain chamber of Test Trommel Mk1.

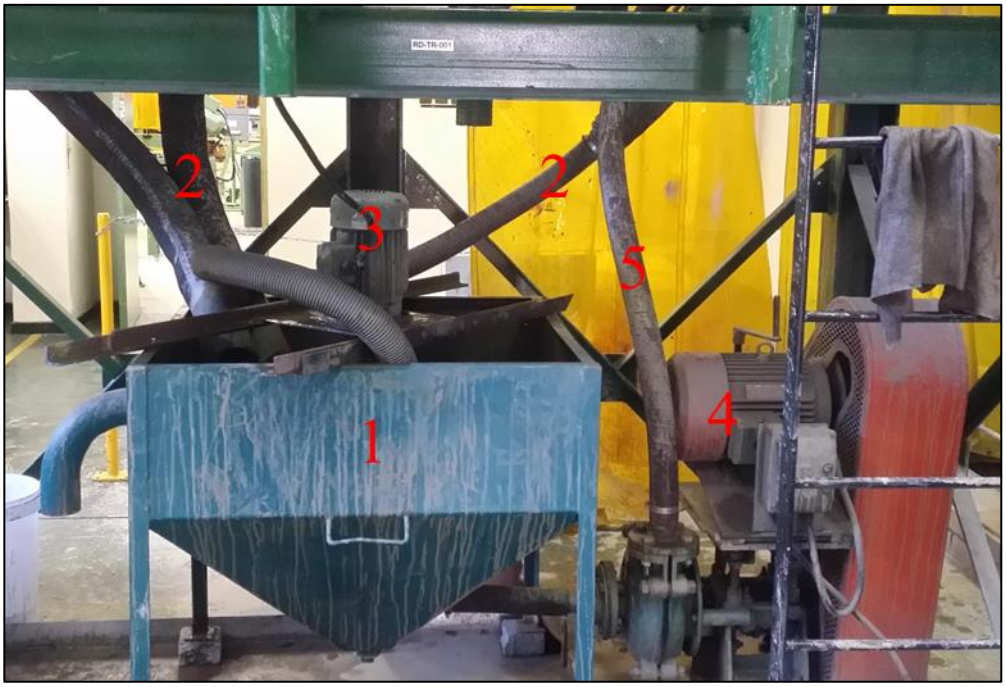

Figure 19. Photograph of support units used to operate Submerged DMS Trommel Mk1.

3.4. Drain chamber mass balance

The drain chamber is of the Submerged DMS test trommel (Mk1) accomplishes the majority of medium drainage, similar to the drain section of a horizontal drain and rinse screen. The

objective is to compare the performance of the drain chamber of the submerged DMS trommel (Mk1) to that of a horizontal drain screen, in terms of % FeSi in the overflow stream, % FeSi carryover, % moisture in the overflow and drainage rate.

The overflow from the drain chamber feeds directly into the submerged chamber. Due to the design of the submerged DMS trommel (Mk1), it was not possible to bypass the wash chambers in order to investigate the drain chamber in isolation. As a result, steady state had to be simulated in the drain chamber.

In order to compare the operating parameters of approximated steady state operation with actual steady state operation, a mass balance is required. In steady state operation of the drain chamber, the medium and water that is drained from the drain chamber would be circulated to the sump and fed back into the drain chamber. The oversized ore particles would be transported to the overflow of the screen and into the sump, where it would be mixed with the rest of the slurry and fed back to the drain chamber. The steady state circuit is illustrated in Figure 20.

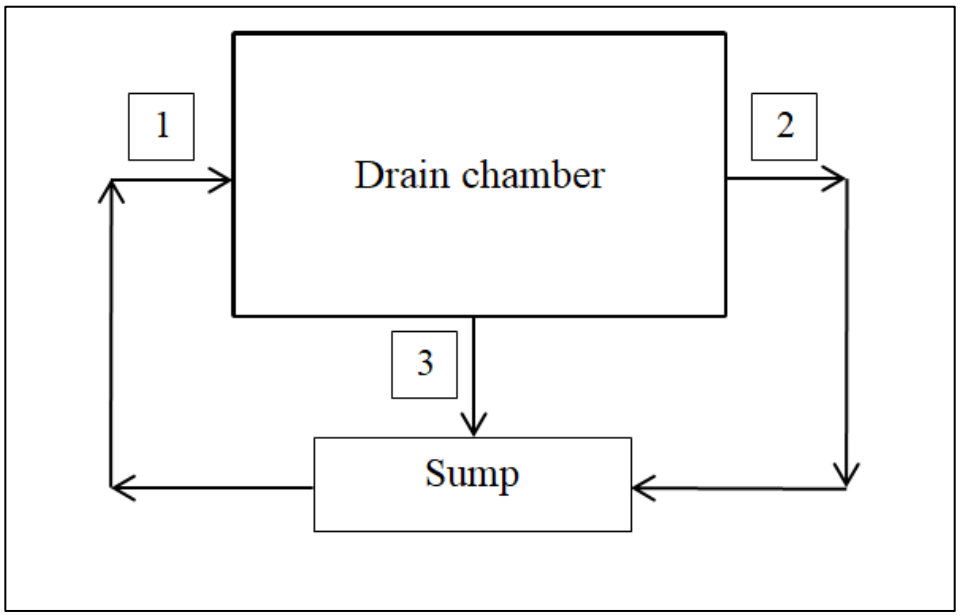

Figure 20. Process flow diagram of drain chamber during steady state operation.

During steady state operation of the circuit, the slurry, consisting of ore, medium and water would be mixed in the sump. Stream 1 would consist of all three these compounds being fed to the drain chamber screen. In the screen, the medium and water would be drained to stream 3, while the coarse ore particles would be retained on the screen and transported to the overflow stream 2. Stream 2 would then be fed to the sump where it would be mixed with the rest of the slurry for re-circulation. During start-up, the ore would accumulate in the drain chamber screen until the overflow stream 2 flow rate started increasing. This would continue

until the overflow stream 2 ore flow rate reaches the rate at which the ore is fed to the screen. Once these two flow rates are equal, steady state would be reached.

The initial strategy to vary feed flow rate and relative density would work in an experimental setup that allows steady state, however the next section will discuss the complications of varying flow rate in an approximated steady state setup. Figure 21 illustrates the break in the circuit that prevents steady state operation in the experimental setup of the submerged test trommel (Mk1).

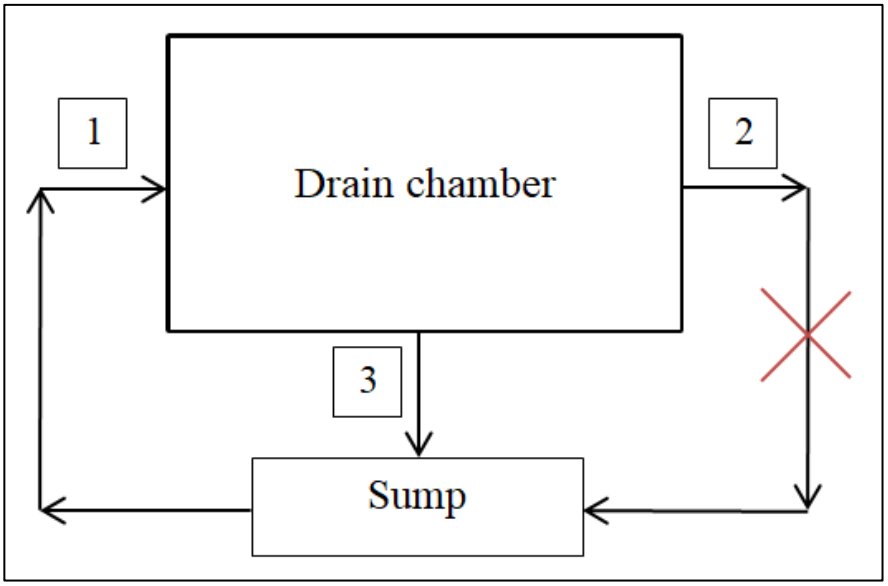

Figure 21. Process flow diagram of drain chamber without the ability to bypass wash chamber.

In this experimental work it was not possible to re-circulate the ore overflow stream to the sump because the equipment was not designed in a way that allowed the wash chamber, after the drain chamber, to be bypassed. All of the ore that was transported from the drain chamber accumulated in the wash chamber. For this reason, only the medium and water is circulated over the ore in the screen. In order to ensure that the maximum, constant ore transport rate could be achieved from the drain chamber, the ore that was loaded in the drain chamber screen had to exceed 40 kg. A smaller ore quantity in the screen would result in a steady decrease in ore transport rate over time, due to the steady decrease in ore quantity in the screen.

Varying the feed flow rate (stream 1) in this setup while keeping the ore quantity in the screen constant, would not have the desired effect of representing a variation in feed flow rate on the typical steady state circuit. In the steady state circuit, varying the feed rate would vary the rate of each component in that stream to the same extent, namely the ore, water and medium. In the context of the approximate steady state setup where the ore is loaded into the screen in

batch, varying the feed flow rate would only vary the water and medium flow rates. In order to keep the ore to medium ratio of the feed consistent, one would have to adjust the ore transport rate to correspond with the ore feed rate that would be appropriate for that particular feed rate. The ore transport rate would have to be adjusted by changing the mass of ore loaded into the screen before the experiment starts. From the test work that was done to relate the ore transport rate to the ore quantity in the screen, discussed in the results section, it was found that the ore transport rate is very difficult to control. In order to mimic a particular steady state, the medium was circulated over the ore in the screen, while the trommel (Mk1) was rotated to expose all ore particles to the medium and to fill the scrolls with ore; to get it to the closest state it could be that represented steady operation. Since the ore transport rate is sensitive to the ore quantity in the screen, the ore transport rate decreases at a significant rate as the ore is being transported from the drain screen. The task of preparing for a run at various ore transport rates by running the tests at various ore quantities in the screen and filling the scrolls with the appropriate ore quantity is a near impossible task. Instead of attempting such a complex procedure, it was decided that it would be more sensible to vary the medium density at a constant flow rate by using the maximum ore transport rate. This procedure at least provides confidence that the ore transport rate is constant at its maximum as long as the ore quantity in the screen exceeds 40 kg.

3.5. Experimental procedure

The submerged DMS trommel (Mk1) consisted of two different types of chambers, namely the drain chamber and the subsequent wash or rinse chambers. Upon delivery, the equipment was not functional and numerous modifications had to be made during the commissioning of the trommel (Mk1) to enable experimental work. These modifications are discussed in detail in Appendix A.

After the modifications discussed in Appendix A, the drain chamber could be operated in a simulated steady state.

Recall that the objectives of the Submerged DMS Trommel (Mk1) study, after completing commissioning of the unit, were:

- Determine operating limits for the test trommel screen and identify design improvements required to make the screen more efficient.
- Determine the media recovery performance of test trommel (Mk1).
- Compare performance of test trommel (Mk1) from this study to that of a vibrating drain and rinse screen from the study performed by Kabondo (2018).
- Assess using various performance criteria if trommel screens are a viable alternative to vibrating drain screens.

- Determine viability of submerged washing as an alternative to rinse washing.

The tests that were performed to achieve these objectives, are discussed in the following sections.

3.5.1. Drain chamber

The first step in the sequence of processes to recover FeSi in the DMS circuit is drainage of the medium, thereby separating the majority of medium from the coarse ore particles. Consequently, the drain chamber is the first chamber in the DMS trommel (Mk1) and naturally the first process that is investigated. The ore transport discharge of the drain chamber is the feed to the first submerged wash chamber, which further promotes the notion to investigate and quantify operation of the drain chamber and then using that data to investigate the submerged chambers.

The first objective of the test work was to determine the operating limits of the Mk1 test trommel. There were two possible limits of operation of the Mk1 test trommel. The first is its drainage capacity and the second is ore transport capacity. As such, the tests were designed to investigate both of these factors. The medium feed to the trommel was increased systematically until pump capacity was reached, which resulted in severe spillage. The unit was modified to be able to handle the high feed, as discussed in Appendix A.

The second step was to investigate ore transport capacity. In order to simulate steady state operation, it had to be ensured that the ore transport could be maintained at a constant rate. It was found that ore transport is a function of ore quantity in the drain chamber screen. Tests were therefore performed to investigate the dependence of ore transport rate on ore quantity in the screen, in order to determine steady state ore transport rate at the maximum rate.

The second main objective of the study is to determine the media recovery performance of the drain section of the trommel. Tests were performed on the drain chamber of the trommel by simulating steady state and circulating medium (FeSi and water) through the drain chamber while loading an ore quantity, that would ensure the maximum ore transport rate, into the drain chamber. Mixing of the medium and ore in the drain chamber was achieved through rotation of the trommel during medium circulation. The parameters that were evaluated to quantify the drain chamber performance were % FeSi in overflow (transported with the ore to the subsequent submerged wash chamber), % FeSi carryover (the fraction of medium fed to the drain chamber that reports to the overflow stream), % moisture in the overflow and medium drainage rate of the drain chamber. These screen performance parameters were then

compared to those achieved in the study by Kabondo (2018) to achieve the third objective of the study.

The step-wise procedures for experimental work on the drain chamber, as well as sample processing procedures for medium only and medium plus ore samples are provided in Appendix B.

3.5.2. Wash chamber tests

The fifth objective of the study on the Submerged DMS test trommel (Mk1) is to investigate the viability of submerged washing. First, submerged washing was tested in the submerged wash chamber of the Submerged DMS test trommel (Mk1).

Similarly to the drain chamber, the wash chambers could not be operated continuously due to the design of the trommel (Mk1). While it was possible to feed the wash chamber from the drain chamber during operation, it would be impossible to quantify the exact mass of medium that entered the wash chamber during operation. While one could collect a relatively dry pulp in the wash chamber after transport from the drain chamber, it was not possible to collect the entire dilute medium in the wash chamber after operation, to sample and quantify the operation of the wash chamber. Instead it was decided that the wash chamber would be operated in batch and loaded with a known quantity of pulp that simulated the discharge from the drain chamber. The pulp was prepared separately and loaded into the wash chamber screen after the wash chamber was filled with clean water to simulate operation. The pulp was loaded into the submerged screen and sampled after various number of screen rotations to quantify the washing of the pulp.

3.5.3. Pulp washing bench tests

Due to the significant limitations of the submerged chamber in the Submerged DMS test trommel (Mk1), it was decided to perform bench tests for submerged washing. The purpose is to perform three types of pulp washing tests under similar conditions, namely:

- Rinse washing (currently applied in industry on horizontal drain and rinse screens);
- Submerged washing of a stationary bed;
- Submerged washing of a settling bed.

The aim of these tests were to compare the efficiency of washing of the pulp using three different washing methods, using a constant water volume, pulp composition, washing time and bed dimensions. Ultimately, the objective of these tests are to determine whether or not submerged washing could be a viable alternative to rinse washing, which is currently utilised

in the industry. This investigation will accomplish the fifth test objective by enabling to conclude whether or not submerged washing is a viable alternative to rinse washing under similar conditions.

3.5.3.1. Rinse bench tests

The first set of bench tests that were performed to recover FeSi from the pulp, was rinse tests. For these tests, a 1mm aperture sieve was loaded with 3.9 kg ore and 20 wt% moist FeSi, which simulated the worst case scenario overflow pulp properties from the drain chamber tests. 3 L of clean water was sprayed uniformly over the pulp bed on the sieve over a period of 16 seconds. The FeSi that was washed from the pulp was collected in a bucket. After the test, the rinsed FeSi in the bucket was filtered, oven dried and weighed according to the medium sample processing procedure in Appendix B. The washed ore that was retained on the sieve, was washed properly and processed according to the sample processing procedure for ore and medium, discussed in Appendix B.

3.5.3.2. Submerged washing bench tests

The second set of bench tests that were performed to recover FeSi from the pulp, was submerged washing tests. For these tests, a 1mm aperture sieve was loaded once again with 3.9 kg ore and 20 wt% moist FeSi. For the submerged washing bench tests, 3 L of clean water was once again used for washing, as with the rinsing bench tests. For these tests, however, the water was inserted into a 5L PVC bucket. The sieve containing the pulp bed was inserted into the bucket, such that the pulp bed was submerged under the water level in the bucket. The bucket was shaken with a linear orbital shaker at three different RPM values (75, 90 and 105) for a duration of 16 seconds. After 16 seconds of shaking was completed, the sieve with ore was removed. The ore was processed according to the procedure in section 0, and the medium that was washed from the ore and collected in the bucket was processed according to section 0. A photo of the submerged ore bed in a 5 L bucket, retained on a 1mm aperture sieve is illustrated in Figure 22.

Figure 22. Photograph of submerged ore bed on sieve for submerged washing bench tests.

3.5.3.3. Submerged washing and settling bench tests

The submerged washing with settling bench tests were close to identical to the submerged washing only bench tests. Instead of loading the entire pulp bed onto the sieve and submerging the sieve and all of the pulp simultaneously, for these tests the empty sieve was inserted and submerged under the water in the bucket. The shaker was switched on at the appropriate RPM (75, 90 and 105). These were the limits of operation of the shaker and was not necessarily intended to mimic rotation of the submerged trommel. The objective was to establish investigate the efficiency of submerged washing and to compare it to rinse washing under controlled conditions (constant water volume, constant washing time, constant pulp properties and constant bed dimensions. During shaking, the pulp was added systematically into the water. Instead of being shaken for 16 seconds while submerged, for these tests the pulp was added into already stirred water over the course of 16 seconds. After all of the pulp was added to the system within 16 seconds, the stirrer was switched off and the sieve was removed from submersion. The two samples (FeSi that was washed from the pulp and collected in the bucket, and retained ore on the sieve), were once again processed according to the appropriate procedures in Appendix B.

4. RESULTS AND DISCUSSIONS: SUBMERGED DMS TROMMEL (Mk1)

4.1. Introduction

This section contains the experimental results that was generated and the discussion thereof. The first set of data was generated with batch operation of the individual chambers of the Submerged DMS Trommel (Mk1). As discussed, these batch tests were designed in such a way that it mimics steady state operation of each chamber.

The experimental work was initiated by characterising the materials. The next step was to characterise the feed to the drain chamber of the screen. The drain chamber is the first in the sequence of continuous operation of the trommel (Mk1) and was therefore the first chamber to be investigated. The results obtained in the drain chamber were used to determine the characteristics of the materials that were loaded in the wash chamber in batch.

Finally the results and discussions of the bench scale tests are included to compare the effectiveness of separation by submerged washing under conditions directly comparable with rinsing separation. The goal with these tests is to gain a better understanding of the concept of submerged washing.

4.2. Equipment calibration

4.2.1. Pump calibration

The pump speed was varied by adjusting the pulley system so that the pulley belt tightens and loosens around the pulleys. Therefore the pump speed is related to the distance between the pulleys. It was necessary to calibrate the pump to determine how the distance on the pump setting translated to volumetric flow rate at various slurry densities. The distance between the plates that are adjusted with the screw lever was measured and used to represent the pump setting. The results for the pump calibration are summarized in Figure 23.

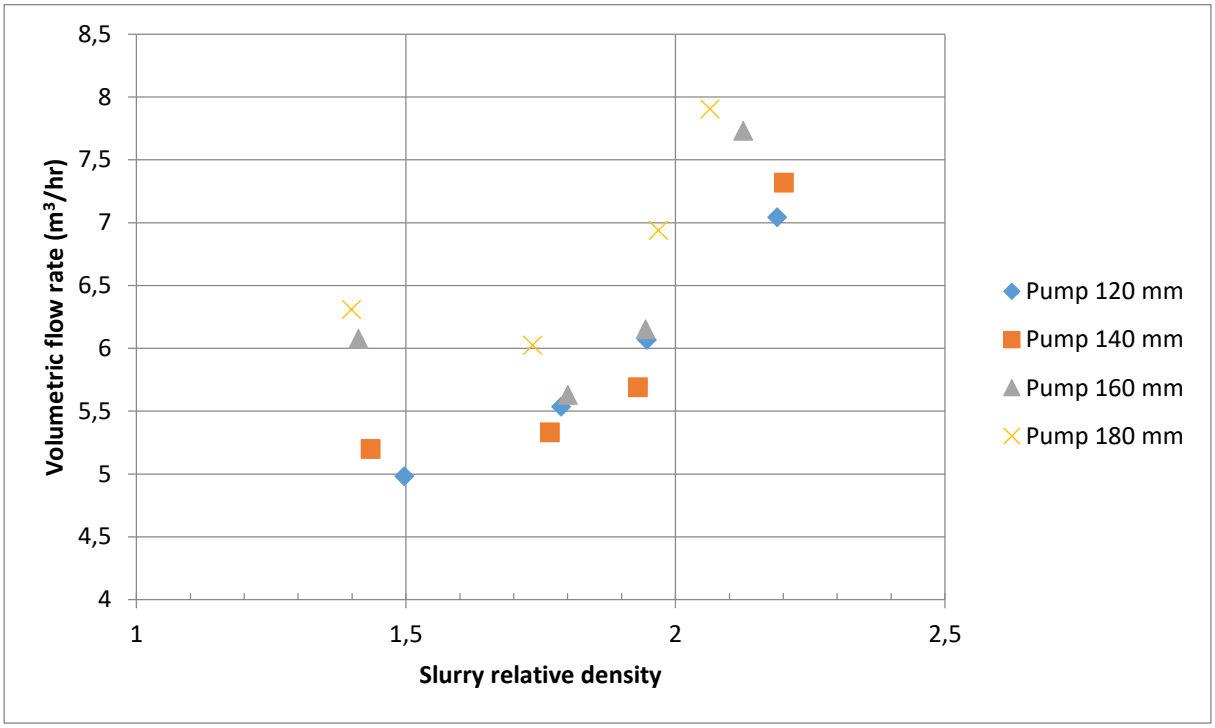

Figure 23. Volumetric flow rate delivered at different pump settings over slurry relative density range 1.4 to 2.4.

The first trend that is apparent from the data is that the volumetric flow rate of the slurry delivered by the pump increases with an increase in distance between the pulleys. At the lowest slurry density of approximately 1.4 kg/L, the volumetric flow rate delivered by the pump increased from 5 m^3/h to 6.3 m^3/h from the minimum to the maximum pump setting of 120 mm to 180 mm, respectively. For the same variation in pump setting at the higher slurry density of approximately 2.1 kg/L, the overall volumetric flow rate for the range of pump settings were higher around 7.5 m^3/h and the increase was slight, from 7 m^3/h to 7.9 m^3/h.

It is shown in the data in Figure 23 that there is some variance in the flow rate delivered by the pump. The systematic increase in pump setting at a given slurry density does not always relate to a corresponding, systematic increase in flow rates. The greatest contributing factor to the variation in pump speed is the instability of the flow pattern inside of the sump. Initially it was assumed that the drain stream from the trommel (Mk1) would provide sufficient agitation in the sump to keep the solids in suspension. However, during sampling of the drain chamber underflow, the flow pattern would be disturbed, and solids would start to settle. This resulted in fluctuation in relative density of the slurry and ultimately affected the volumetric flow rate delivered by the pump.

An agitator was installed to ensure a uniform and constant mixing in the sump. Though effective, the agitator introduced a new complication that the pump would occasionally suck air through the vortex. The slurry volume was increased to 220 L, which is the volume

capacity of the sump, but the pump would still occasionally suck air through the vortex. Ultimately the experimental procedure was adjusted such that the agitator was switched off before the pump was switched on. The tests were conducted shortly after the agitator was switched off before the solids could settle to a significant extent. After the run, the agitator was switched back on to achieve sufficient mixing.

Note that the tests were conducted in batches of constant medium RD, varying pump setting during each batch. This indicates that there is a lot of variance with regards to feed rate dependence on pump setting. The lowest setting of 120 mm is not always the lowest feed rate at a given medium RD. Furthermore, the apparent increase in feed rate with an increase in medium RD is also very unexpected, because an increase in medium RD increases the difficulty to pump the slurry. It was concluded that the method of varying feed rate by adjusting the pulley system of the pump is not correct. Even though there is a change in feed rate with a change in pulley positions, this resulted in unpredictable behaviour of the system. The inability to vary feed rate on the given setup resulted in the decision that the main focus of the test work would rather be to investigate the effect of medium RD on screen performance.

4.3. Drain chamber operation

4.3.1. Introduction

As discussed, steady state operation was unattainable on the first iteration of the trommel (Mk1) design. As such the experimental work was designed to mimic steady state as closely as possible. During typical operation, the slurry that is fed to the trommel (Mk1) consisted of medium and ore. For this experimental work the medium was circulated separately from the ore, while the ore was loaded into the screens prior to the experimental run.

4.3.2. Ore transport rate

The ore transport rate from the drain chamber is related to the quantity of ore in the drain chamber screen. In order to mimic steady state it was necessary to ensure that the ore transport rate from the drain chamber remained constant over the sampling period. Therefore the ore transport rate was investigated for different ore quantities in the screen. The goal was to find the ore quantity in the drain screen that resulted in the maximum ore transport rate from that chamber. This ore quantity would then be used in the investigation of the drain chamber. The results of the ore transport rate are given in Figure 24.

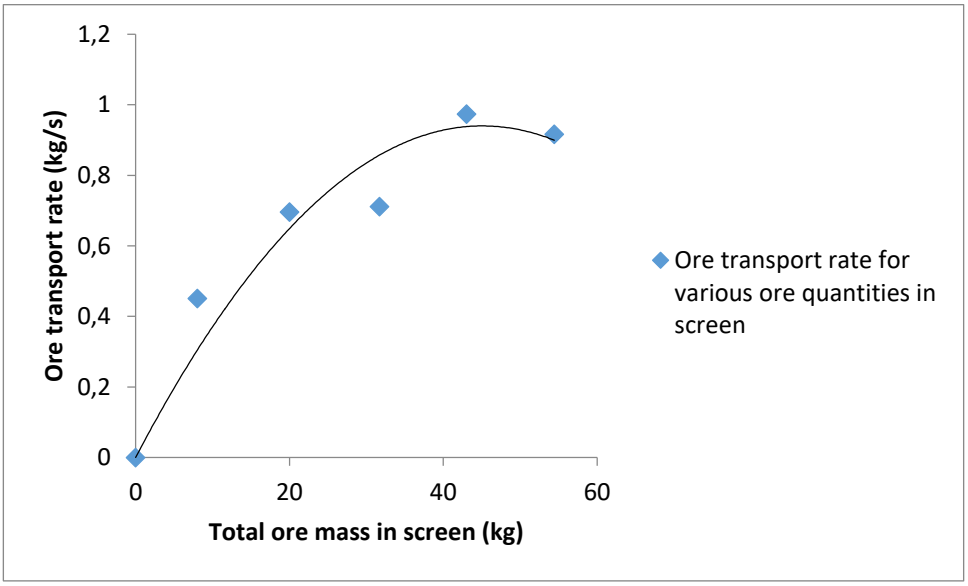

Figure 24.Ore transport rate for various ore quantities in screen.

The data illustrated in Figure 24 shows the increase in ore transport rate with increasing ore mass loaded into the drain screen. The trend starts at the origin because with no ore in the screen, there is no ore to be transported. As the ore quantity in the screen gradually increases, the bed height in the screen also increases and the pedals inside of the screen become more effective at scooping the ore from the screen during rotation. The ore transport rate increases until the transport scrolls fill up completely. At this point, the maximum ore transport rate of approximately 0.97 kg/s is reached when the ore quantity in the screen exceeds 40 kg. After this point the ore transport rate reaches a maximum and fluctuates around a value of approximately 0.95 kg/s. It was not possible to increase the ore loading in the screen beyond 54 kg to show that the ore transport rate plateaus at approximately 0.97 kg/s, because it was not physically possible to secure the screen braces with more than 54 kg of ore inside of the screen.

It is important to note at this point that the ore transport tests were performed with moist ore in the absence of any dense medium. This was done to determine the maximum ore transport rate of the coarse ore particles and its dependence on the ore loading in the screen. These values are specific to the bulk density of the ore. The maximum mass transport rate of a pulp consisting of medium, water and ore will be different from the maximum value found for ore only.

In the context of continuous operation, this data will be relevant during start-up of the equipment. Initially the drain chamber screen will be empty and a slurry consisting of ore, medium and water will be fed to the drain chamber at a constant flow rate. The coarser ore particles that are unable to pass through the screen apertures will gradually start to

accumulate while the finer medium particles and water will drain through the screen apertures and out through the drain chamber outlet. The quantity of ore particles retained in the screen will increase until the ore bed depth increases beyond the point that the ore transport pedals can start scooping the ore from the screen into the transport scrolls. As the ore quantity increases further, the ore transport rate will increase until the mass flow rate of ore into the screen is equal to the transport rate of ore to the wash chamber. At this point, steady state will be reached in the drain chamber.

4.3.3. Effect of relative density on feed rate

As mentioned, it was decided that the pump setting would be kept constant for the investigation of the drain chamber. The flow rate was measured at the various relative densities to determine whether the slurry density had a significant impact on the volumetric flow rate delivered by the pump. The results of the relative density tests are illustrated in Figure 25.

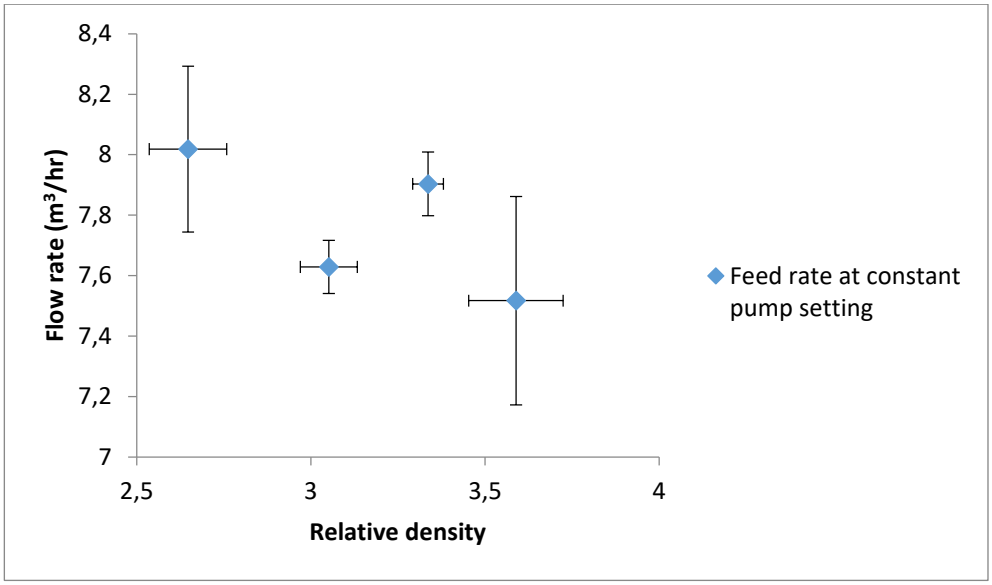

Figure 25. Slurry volumetric flow rate for various medium RD.

Upon first glance it seems that the volumetric flow rate delivered by the pump decreases with an increase in relative density. This could be explained by the fact that the slurry becomes more difficult to pump with increasing density and viscosity. As the resistance to flow increases, the volumetric flow rate decreases. Confidence intervals for this study was calculated by assuming a normal distribution and performing a two-tailed test. The 95% confidence intervals indicate that the apparent decrease in flow rate is not significant with regards to the typical variance between the repeat measurements for each relative density. This implies that the flow rate to the drain chamber should rather be estimated as the same flow rate with variance for the different relative densities.

4.3.4. Repeatability and statistical analysis of drain chamber results

4.3.4.1. Ore transport at single RD of 3.6

For perfect separation in the drain chamber, all of the medium would be drained while clean ore is transported as the overflow product. This is, of course, not the case in real screening and therefore the inefficiency of separation is quantified by the FeSi and water content in the overflow product stream. Each run required approximately two hours for preparation, sample analysis and washing and clean-up procedure after the run. The experimental work was also very physically straining. This combination of circumstances limited the practical number of repeats per run to three.

The first repeatability comparison is that of the approximate maximum ore transport rate, after being dried, from the drain chamber to the rinse chamber at the highest RD value of 3.6. The results for each repeat sample are given in a bar graph, Figure 26.

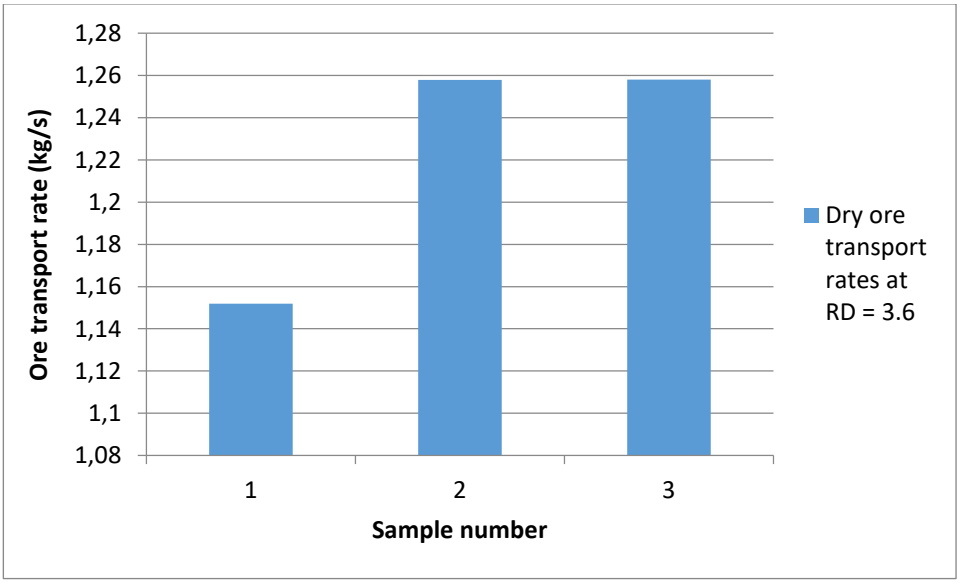

Figure 26. Illustration of sample repeatability for ore transport rate.

As repetitions, these values are expected to be equal for each of the three samples. The first sample was not at maximum ore transport rate with a value of 1.15 kg/s, compared to the higher ore transport rates of 1.26 kg/s for samples two and three. It is suspected that the lower ore transport rate is observed because the ore transport from the drain chamber to the rinse chamber has not reached the desired maximum that could be achieved by full scrolls.

It was estimated that four rotations would be sufficient to fill the scrolls to the point where the maximum ore transport for those operating parameters is reached. As discussed in the ore transport rate analysis, this is not necessarily the scroll capacity, it is just the ore quantity in the scrolls that correspond with the ore transport rate achievable under those conditions.

Analysis of the results indicated that another rotation was required before the first experimental run to fill the scrolls completely. However, the number of rotations also had to be limited to prevent that an excessive quantity of ore is transported from the drain chamber screen. If the ore quantity that was transported from the drain screen was too high, the ore transport rate started decreasing as a function of the lower ore quantity in the drain screen.

4.3.4.2. FeSi carryover rate at single RD of 3.6

The next parameter of interest is the carryover rate of FeSi. Since there is an increase in solids transport rate from sample one to samples two and three, it is also expected that this will be accompanied by an increase in medium carryover. The medium carryover rate is illustrated in Figure 27.

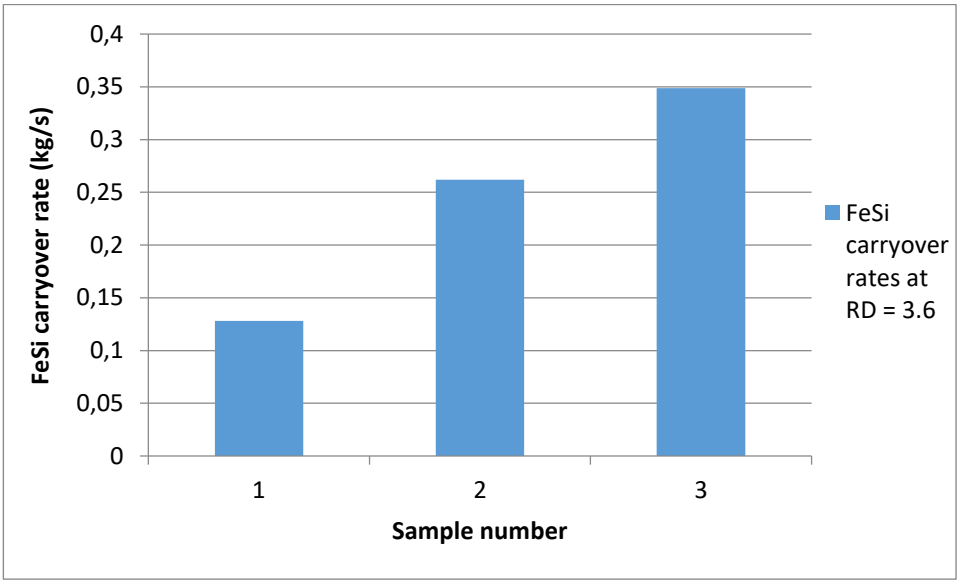

Figure 27. Illustration of sample repeatability for FeSi carryover rate.

There is a significant increase in medium carryover rate from 0.13 kg/s at sample 1, to 0.26 kg/s at sample 2. The medium carryover rate increased by 100% from sample one to sample two. There is a further increase in medium carryover rate from sample two to sample three, which is not a result of an increase in ore transport rate, like it was between samples one and two, because there was no increase in ore transport rate between samples two and three.

For this reason it is of interest to calculate the quantity of FeSi carried over to the wash chamber as a percentage of total mass of material transported to the wash chamber.

4.3.4.3. FeSi content in the solids transport overflow at single RD of 3.6

The calculated FeSi contents in the solids transported via the overflow, are illustrated in Figure 28.

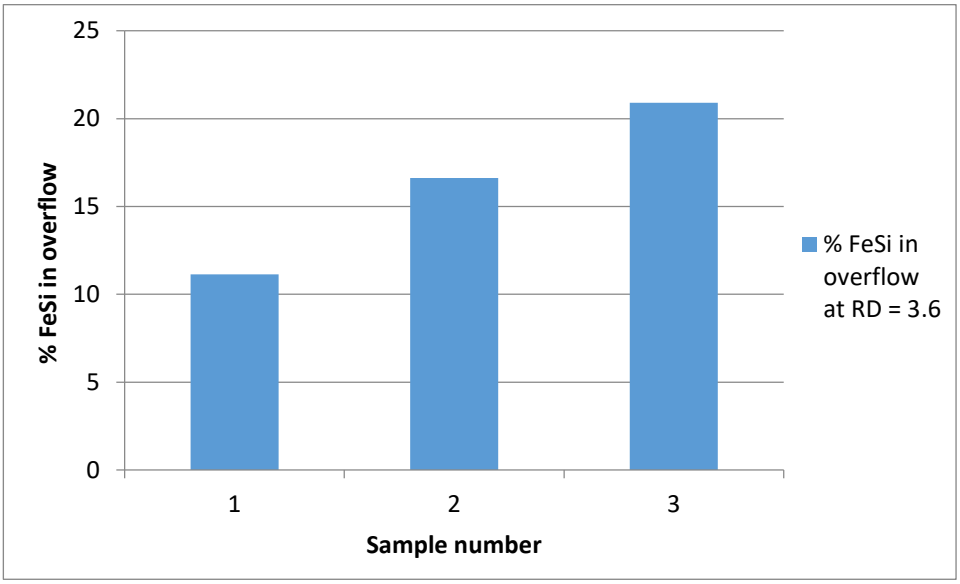

Figure 28. Illustration of sample repeatability for % FeSi in overflow.

The increase in % medium in overflow from sample one to sample three is approximately 50%. This is significantly smaller than the discrepancy of 100% for medium carryover rate in kg/s. If the increase in medium carryover was only a result of the increase in ore transport as the ore transport rate increased to the maximum value, the % medium in the overflow should remain constant. The discrepancy between % medium in the overflow for different samples indicate that the ratio of medium and ore also changed over time between samples. This gradual change seems to slow down between samples 2 and 3, where the increase in % medium in the overflow from sample 2 to sample 3 is only 25.8 %.

This phenomenon in the data reveals that the mixing in the drain chamber is not consistent. This can be expected, considering that the clean ore was loaded into the drain chamber screen and the medium was pumped over it. The ore was dirtied with medium before loading into the drain chamber, but scooping 40 kg of dirty and wet ore at a rate of 500g per scoop, takes approximately 10 minutes to fill the screen. During this time, the medium drains form the bed and the medium to ore ratio changes. The medium also tends to settle closer to the bottom of the bed, resulting in a medium concentration gradient through the bed. Even though the medium at the correct concentration is pumped over the bed and rotated twice before the test begins (to attempt to achieve a uniform distribution of medium over the entire ore bed), it is not sufficient to achieve uniform medium distribution throughout the bed at the highest relative density of 3.6. Furthermore, if the number of rotations for mixing with the medium is increased to achieve better mixing of medium into the ore bed, the quantity of ore that is transported during rotation is also increased, thereby increasing the time required to scoop that ore back into the drain chamber screen. Ultimately that results in a longer duration of

time for the medium to drain through the ore bed and from the ore that is scooped from where it accumulates in the rinse chamber.

In conclusion, the repetitions are not entirely consistent, but attempting to do more runs on a single day was not possible. For this reason, it was decided to exclude the first sample in the series, writing it off for occurring in an onset-period while the system is still reaching its "steady state". The consideration of excluding the first sample in the series will be kept in mind until the rest of the data is analysed and it can be seen in the context of the bigger picture.

4.3.4.4. Ore (dried) transport rate over RD range 2.7 to 3.6

Moving on from comparison of repeats at a single RD value, the next step is to compare the repeats over the entire RD range that was investigated. These results are illustrated in Figure 29.

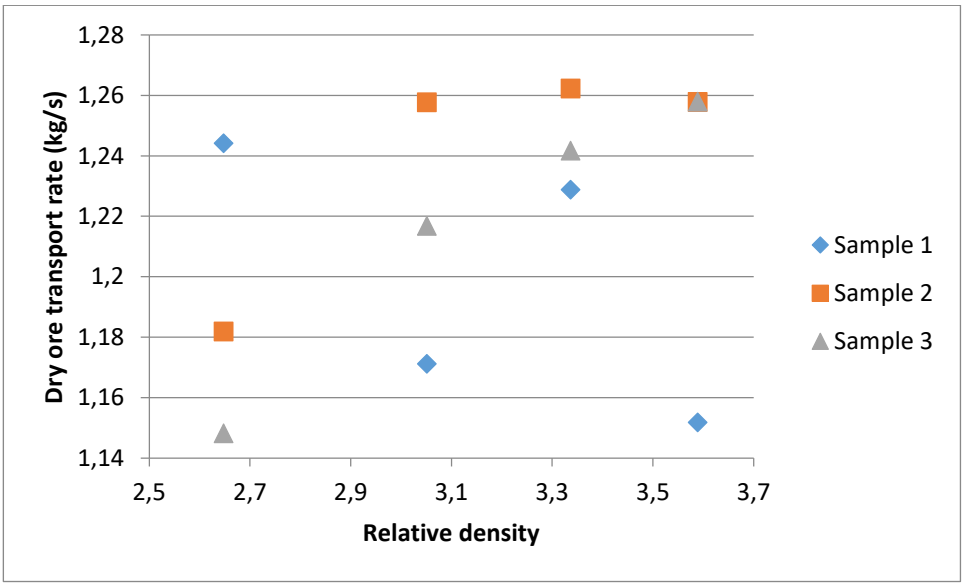

Figure 29. Dry ore transport rate of various repeat samples over medium RD range.

The data in Figure 29 illustrates the transport rate of ore only, determined by collecting the wet pulp samples that were transported to the rinse chamber, washing the ore thoroughly and drying it to calculate the ore (dried) transport rate. The first sample in each batch of tests at constant medium RD do not adhere to the general trends observed for the other samples. At an RD of approximately 3.6, as discussed in the previous section, the ore transport rate of sample 1 (1.15 kg/s) is significantly lower than samples 2 and 3, which were almost equal at a value of 1.26 kg/s. At an RD of 3.3, the transport rate is the closest to the other two samples at 1.23 kg/s. At an RD of 3, the transport rate of 1.17 kg/s is once again significantly lower

than samples 2 and 3, both above 1.2 kg/s. At the lowest RD of 2.7, the ore transport rate of 1.24 kg/s is significantly higher than samples 2 and 3, both of which are below 1.81 kg/s.

The first sample in each series deviates significantly from the rest of the set. After loading the ore bed into the drain chamber screen, the scrolls are empty and the bed shape does not represent the shape of a bed that is formed by slurry that is fed to the screen from the pump at steady state. Increasing the number of rotations to shape the bed and to fill the scrolls was not a practical solution, because the wash chamber was not equipped to support a larger quantity of ore accumulating in the chamber without becoming an obstruction for rotating parts. Furthermore, increasing the number of rotations would result in a significant decrease in ore quantity in the drain screen, which in turn would result in the solids transport being affected. On the other hand, rotating the chamber piece-wise and collecting smaller amounts of ore after being transported and scooping it back into the drain chamber, is too time intensive and is very physically straining for the investigator performing the experiments.

As such, it was decided that the first sample in each set must be discarded due to the fact that the system is still in an onset phase during the first sample. It was also decided that two samples in each set (samples 2 and 3) are assumed to be representative.

4.3.5. Pulp / dirty ore transport compared to clean ore transport

The first set of results that was investigated from operation of the drain chamber is a comparison of the ore transport rate from the drain chamber to the wash chamber during circulation of the medium. The ore transport rate that was achieved during this operation is compared to the maximum ore transport rate that was achieved with clean ore in Figure 30.

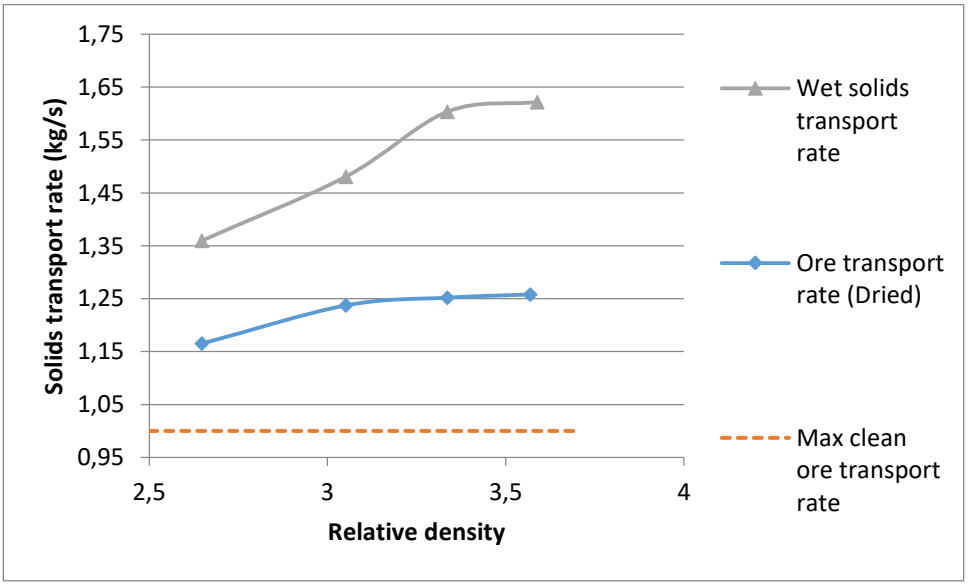

Figure 30. Solids transport rate over medium RD range.

The dotted line at 1 kg/s illustrates the maximum ore transport rate that was achieved with varying moist and clean ore quantity in the screen, as discussed in the previous section. Thereafter, the ore was loaded in the screen and the medium was circulated over the bed while the screen was rotated to expose the entire surface area of the ore to the circulating medium. The two curves at the top of the graph show the data that was produced with rotation of the screen to allow transport of the pulp inside of the drain chamber screen. The grey curve at the top of the graph is the transport rate of the pulp, which is the total solids transport rate of the ore, FeSi and moisture. The wet samples were washed and dried to determine the rate of transport of clean, dry iron ore, which is represented by the blue curve in the middle.

The maximum ore transport rate that could be reached in the absence of medium in the drain chamber was 1 kg/s as discussed in the previous section. After the addition of medium, it is expected that the total solid transport rates increased from 1 kg/s to the range of 1.36 to 1.62 kg/s, as the FeSi that adheres to the ore particles contribute to the total mass transfer rate of wet solids. What is interesting is that the transport rate of the ore only, after washing and drying, also increased to the range of 1.17 kg/s to 1.26 kg/s from the original maximum of 1 kg/s. Although there was a large degree of variance in the data on test trommel Mk1, this increase in ore transport rate from 1 kg/s to 1.17 kg/s at a medium RD of 2.7, exceeded the range of variability. The minimum ore transport rate of a single sample was measured at 1.18 kg/s, which is still significantly higher than the maximum that was measured for clean ore transport rate. The mean dirty pulp transport rate was even higher than that. This result confirms how the presence of medium changes the physical properties of the pulp. With clean ore particles, the particles do not adhere to each other. With the addition of medium, there is not only adhesion between the FeSi and the ore, but also a degree of adhesion between ore and ore with medium as the adhesive. With this adhesion the solids behave more like a unit of pulp than a collection of individual particles. This affects the way that the solids are scooped up by the transport mechanism.

This provides insight in the limiting mechanism for solid transport from the drain chamber to the rinse chamber. If the ore transport scrolls were the limiting factor, it would mean that scroll was physically filled to capacity and the ore transport rate could not be increased by feeding a higher RD slurry to the screen. Therefore the ore transport rate would remain at a maximum value for a given ore mass loaded into the drain chamber screen before the experimental run. The increase in ore transport rate with increase in feed slurry RD implies that the scooping pedals that feed the scrolls is the limiting mechanism for ore transport. An increase in slurry RD leads to a higher pulp density. The ore particles tend to adhere to each

other more at higher pulp densities. The higher pulp density increases the pedals' effectiveness at scooping the material into the scroll openings, hence the increase in ore transport rate. At a lower feed RD, the pulp becomes more difficult to scoop because the ore particles tend to separate and fall from the pedals and through the opening in the shaft without being fed to the scroll. When the particles adhere to each other, a larger portion on the ore particles that are scooped up is effectively fed to transport scroll.

It is apparent that an increase in FeSi quantity also increases the adhesion of the solids and with it, the effectiveness of the scooping mechanism. In addition, the mass of FeSi contributes to the total mass of wet solids that is transported, so increasing the relative density of the slurry also results in an increase in total solids transported by increasing the rate of FeSi transport to the washing chamber.

4.3.6. FeSi carryover to wash chamber

Knowing that the limiting mechanism is the scooping pedals and not the scroll, one would expect an increase in medium carried over to the rinse chamber with an increase in ore transport to the rinse chamber. The data, illustrated in Figure 31, confirms this phenomenon.

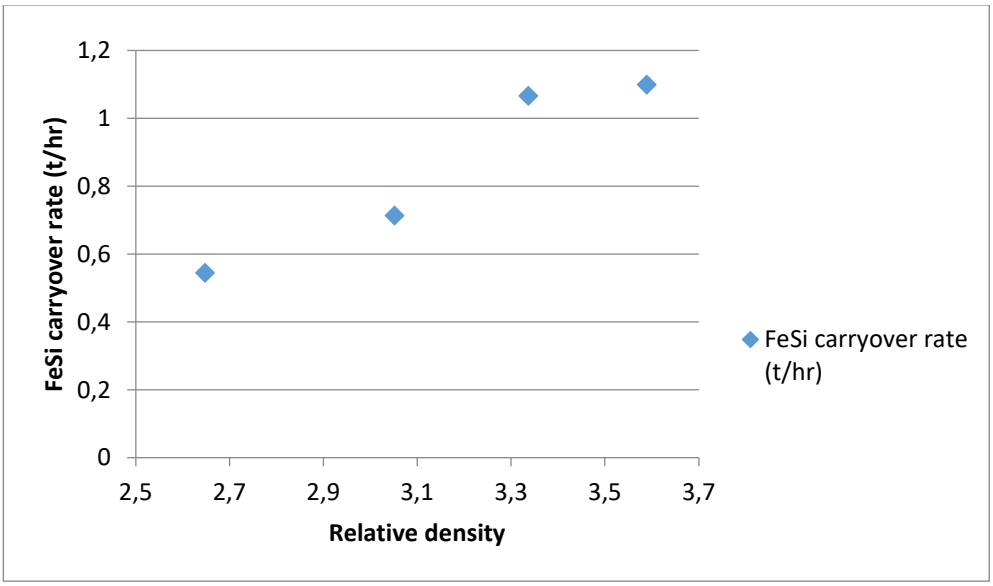

Figure 31. FeSi carryover rate over medium RD range.

With an increase in RD from 2.7 to 3.6, the FeSi carryover rate increases from 0.54 t/hr to 1.1 t/hr. Although this might be caused partly by the increase in ore transport that was observed in the previous set of data, it is not expected that the increase can be attributed entirely to the ore transport rate. As the RD of the feed increases, the rate of FeSi that is fed to the drain chamber increases with it. This is expected to result in a higher FeSi concentration in the drain chamber and therefore an increase in the rate at which FeSi is transported to the

submerged chamber from the drain chamber. If the increase in FeSi carryover rate is only a function of the increase in ore transport rate, then the FeSi concentration in the transported pulp (overflow) is expected to remain constant. It is therefore of interest to investigate the concentration of FeSi in the overflow, plotted in Figure 32.

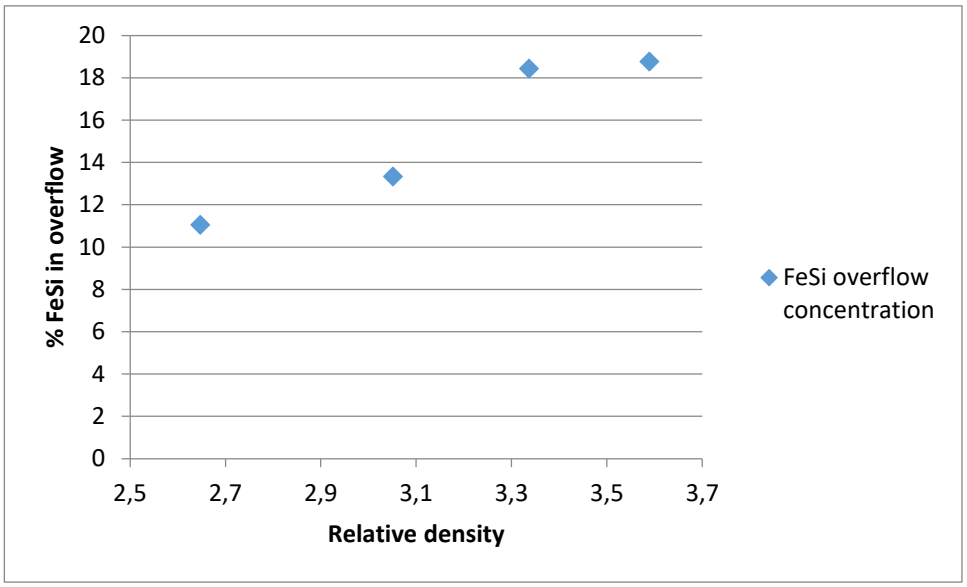

Figure 32. % FeSi in overflow over medium RD range.

Figure 32 illustrates the mass percentage of FeSi in the overflow stream. The overflow stream in this context is the total solids transported from the drain chamber to the wash chamber.

As expected, the percentage FeSi in the overflow stream increases from 11.05 % to 18.76 % with an increase in RD from 2.65 to 3.59. This confirms that the increase in FeSi carryover rate is not just a result of the slight increase in ore transport rate, but also because there is more FeSi in the drain chamber that adheres to the ore particles and is transported to the wash chamber. This result corresponds with the trends observed for medium adhesion as a function of medium RD on vibrating drain and rinse screens (Kabondo, 2018), (Napier-Munn, et al., 1995).

In addition, it is also known that an increase in moisture bypass typically leads to an increase in carryover of fines, because the water is the main mechanism of transport for fines on the screen (Gupta & Yan, 2006). As such, it is of interest to analyse the water bypass to the overflow stream next.

4.3.7. Water bypass from drain to wash chamber

The next parameter of interest is the moisture content in the overflow. Theoretically, during ideal separation, all of the medium, including water, will be drained through the apertures and only the oversized ore particles will be retained on the screen. Therefore, a measure of

inefficiency of drainage is the rate of moisture that is carried over to the submerged chamber with the oversized particles.

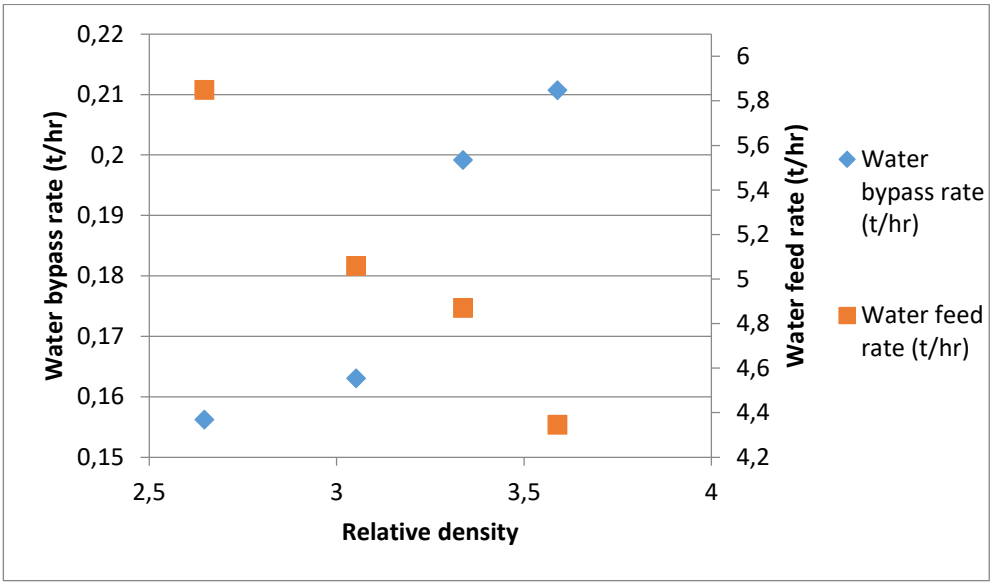

Figure 33. Water bypass rate and water feed rate over medium RD range.

Figure 33 illustrates the dependency of the water bypass rate on the relative RD of the feed to the drain chamber. On the secondary vertical axis, Figure 33 illustrates the water feed rate that was achieved at a constant pump setting over the same RD range.

The water feed rate decreases from 5.85 t/hr to 4.35 t/hr for the increase in RD from 2.7 to 3.6. Since these tests were done at a constant pump setting, but the total volumetric feed rate fluctuated in the range of 7.52 m^3/hr to 8.02 m^3/hr. The slight decrease in volumetric feed rate is due to the increase in relative density and viscosity, making the slurry more difficult to pump. With a significant increase in FeSi quantity to increase the RD from 2.7 to 3.6, the percentage water in the feed also decreases significantly from approximately 23 % to 13.86 %. As such, it is not surprising that the water flow rate should decrease with such a steep increase in FeSi quantity from 60.49 % to 71.7 %.

One might expect that a decrease in water feed rate would be accompanied by a decrease in water bypass rate from the drain chamber to the rinse chamber, as there is less water and a therefore a lower probability for water to be entrapped and carried over with the solids pulp. However, this is not the case, as the water bypass rate increases from 0.16 t/hr to 0.21 t/hr. This is due to the increase in pulp density with an increase in feed medium RD. As the pulp density increases, its ability to retain water also increases. Therefore, despite the lower water feed rate to the screen, the water entrapment rate increases. An increase in FeSi content in the

overflow stream, results in a greater solids surface area for water to cling to. This could explain the increase in water entrapment for an increase in medium RD.

4.3.8. Drainage rates

The main objective of the drain chamber is to drain the majority of the medium and water from the coarser ore particles before being transported to the rinse chamber. Water and medium that is not drained, is transported with the ore pulp to the rinse chamber. Higher drainage rates, accompanied by lower medium carryover rates and moisture bypass rates indicate better separation in the drain chamber.

In order to comment on drainage rates, it is required to discuss the mass balance over the drain chamber in detail. The next subsection will cover the mass balance and its discussion.

4.3.8.1. Drain chamber mass balance

4.3.8.1.1. Defining mass balance boundaries and streams

For the sake of the mass balance discussion, the drain chamber and the surrounding streams are defined in Figure 34 below.

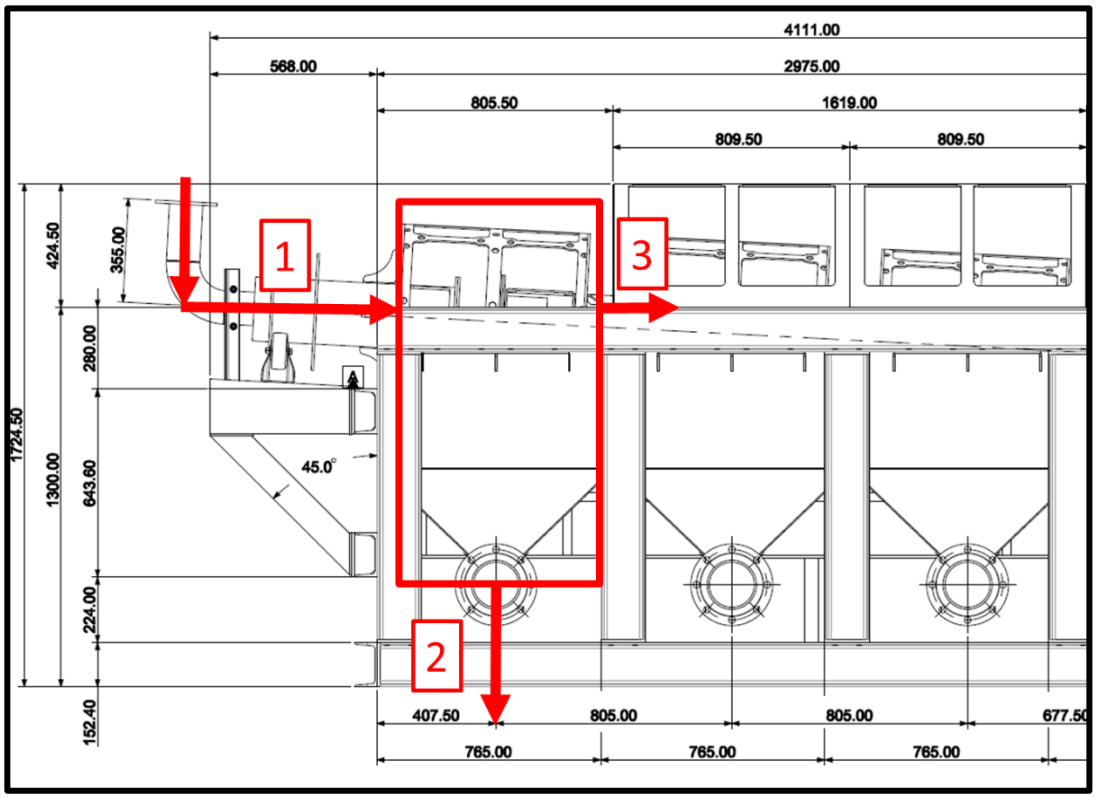

Figure 34. Illustration of boundary for mass balance over drain chamber.

The red box defines the boundaries of the drain chamber. Stream 1 is the feed. Typically, under normal operating conditions, stream 1 will consist of the slurry consisting of ore and medium from the sinks or floats of the dense medium cyclones. However, in the

approximated steady state operation for this investigation, Stream 1 only consists of water and FeSi, since ore circulation to the sump is not possible. The ore was therefore loaded into the drain chamber and transported by Stream 3 and accumulated in the next chamber, the submerged wash chamber.

Stream 2 is the drain chamber underflow stream. This stream consists of medium only (ignoring ore fines). During normal operation this stream would also contain undersized ore particles that pass through the screen apertures. In this investigation, the ore PSD was chosen such that the undersized particles were removed in order to eliminate the additional variable that undersized ore particles could be circulated with the medium via the sump, while the oversized particles were systematically removed from the system by transport and accumulation in the submerged wash chamber.

Stream 3 is the overflow stream. This stream facilitates the transport of oversized ore particles to the submerged wash chamber. As perfect separation is not attainable in the drain chamber, the ore particle pulp being transported by the overflow stream contains FeSi and moisture.

4.3.8.1.2. Mass balance results

To enable coming calculations, the mass balance around the drain chamber is completed and summarized in Table 1 to Table 3.

Table 1. Summary of ore mass balance results over drain chamber.

RD	Stream	Ore (t/hr)
3.6	1	4.53
	2	0
	3	4.53
3.3	1	4.51
	2	0
	3	4.51
3	1	4.45
	2	0
	3	4.45
2.7	1	4.19
	2	0
	3	4.19

The first important thing to note is that the ore transport rates and the ore feed rates are equal for each set of runs. It has however been stated that only the medium is circulated to approximate steady state operation, so Stream 1 is not expected to contain ore flow. This table

summarizes the expected operating parameters for the approximated steady state operation. Since the circuit is not closed and a steady ore feed rate is not maintainable, the ore was loaded in the drain chamber screen. Therefore, to estimate steady state, it was assumed that the ore transport from the screen is equal to the ore fed to the screen to satisfy the mass balance of continuous operation. The ore transport rate, and therefore the ore feed rate, increases from 4.19 t/hr at the lowest RD value of 2.7, to 4.53 t/hr at the highest RD value of 3.6. As discussed, this is a result of enhanced transport effectivity of higher density pulps.

The ore quantity in the screen was chosen at the screen capacity, to ensure that the ore transport rate is at a maximum. This was decided to accomplish one of the main objectives of the project, which is to determine the limits of operation of the Submerged DMS Trommel (Mk1) in order to enable its improvement in a new design. Operating at maximum ore transport capacity was also estimated to be the most representative of steady state operation. At the highest ore transport rate, there is excess ore that can be transported before the ore transport rate starts to decrease significantly. Conversely at lower ore quantities in the screen, the transported ore would have a bigger impact on the ore transport rate over the sampling time, because the transported ore decreases the total ore quantity in the screen, thereby decreasing the ore transport rate.

As mentioned, Stream 2 contains no ore particles as the PSD was chosen to exclude -1.5 mm particles to prevent circulation of the smaller size fraction and accumulation of the larger size fraction.

Table 2.Summary of FeSi mass balance results over drain chamber.

RD	Stream	FeSi (t/hr)
3.6	1	22.48
	2	21.38
	3	1.10
3.3	1	21.50
	2	20.43
	3	1.07
3	1	18.22
	2	17.51
	3	0.71
2.7	1	15.38
	2	14.84
	3	0.54

The FeSi feed rate increases from 15.38 t/hr to 22.48 t/hr with increase in RD from 2.7 to 3.6. This is expected as the quantity of FeSi in the system increases significantly with a similar volumetric feed rate.

The FeSi carryover rate also increases systematically from 0.54 t/hr to 1.1 t/hr with an increase in RD from 2.7 to 3.6. This is in part a result of the increase in ore transport rate, as discussed, which in turn is caused by the increase in pulp density that leads to more effective scooping and transporting of the pulp. The increase in pulp density with an increase in FeSi concentration in the pulp also further contributes to the increase in medium carryover rate.

As expected, the FeSi drainage increases from 14.84 t/hr to 21.38 t.hr with an increase in RD from 2.7 to 3.6. This shows that the system has not reached maximum FeSi drainage capability. For each increase in FeSi feed rate, the system meets it with an appropriate increase in FeSi drainage without indicating a plateau in the ability to drain more FeSi. This data will be discussed in more detail in Figure 37, in Section 4.3.8.3, which is dedicated to discussing medium drainage rate. The increase in FeSi carryover is a result of the properties of the pulp at higher densities and does not indicate failure to drain excessive amounts of FeSi.

Table 3. Summary of water mass balance results over drain chamber.

RD	Stream	Water (t/hr)
3.6	1	4.35
	2	4.14
	3	0.21
3.3	1	4.87
	2	4.67
	3	0.20
3	1	5.06
	2	4.90
	3	0.16
2.7	1	5.85
	2	5.69
	3	0.16

The drainage of water in the drain chamber is directly correlated to the rate at which water is fed to the screen. Since the water carryover rate is a function of the pulp's ability to retain water while it is being transported, all the additional water that is fed to the screen is drained. At different operating conditions, for example if the water feed rate is increased past the drain

screen's capacity, or if the screen becomes too full with ore so that the apertures become obstructed and the water is prevented from draining sufficiently, it is expected that the water bypass rate will increase as a result of water not coming into contact of the screen surface and therefore not getting a chance to drain before being transported to the following chamber. In this case, instead of draining through the screen, the water could flow over the particle bed and find its way directly to the transport scroll without being scooped by the pedals. On this specific prototype however, flow rates were limited by spillage. Increasing the flow rates to determine at which point such an extent of water bypass would occur, would lead to significant spillage by leakage and back-flow. In the available lab environment, this was unacceptable and would have to be tested at a different location.

4.3.8.2. Utilised screen area and % open area

Screen area refers to the effective area that is utilised for screening at one particular time. This is the area of the screen that the material is exposed to, to facilitate screening by coming into contact with the apertures on the screen. On a flat deck screen, this area is equal to the total area of the screen. In a trommel screen, the effective screen area is related to the quantity of the material in the screen. Figure 35 illustrates the cylindrical form of a trommel screen and an approximated bed of material filling up the screen.

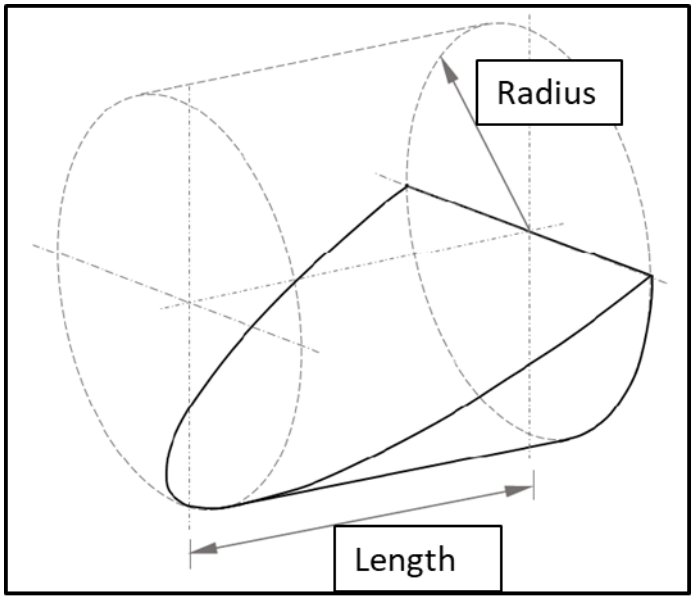

Figure 35. Illustration of assumed material distribution in a trommel to utilise a third of the total screen area.

In the context of a trommel, Multotec has used a simplified calculation derived from years of experience with trommel operation, that a third of the total surface of the cylindrical screen is exposed to the material. This is due to the extent to which a trommel screen is typically filled with material during normal operation. The area of the screen that is exposed to the material

lying on the bottom of the screen makes up a third of the total area around the cylindrical screen surface.

Due to the method of batch loading of trommel Mk1, the material distribution in the drain chamber of the trommel does not look like the assumed material distribution in a typical trommel, illustrated in Figure 35 above. Instead, the material in the drain chamber of the trommel is more evenly distributed along the length of the screen with a uniform material bed depth. The mass of ore that was loaded into the drain chamber was approximately 40 kg, which resulted in a material bed depth of approximately 200 mm. The total screen diameter of the drain chamber was 0.796 m. This means that the material bed depth was approximately 25 % of the screen diameter. A cross-sectional view of a cylinder divided into three equal parts, is illustrated in Figure 36.

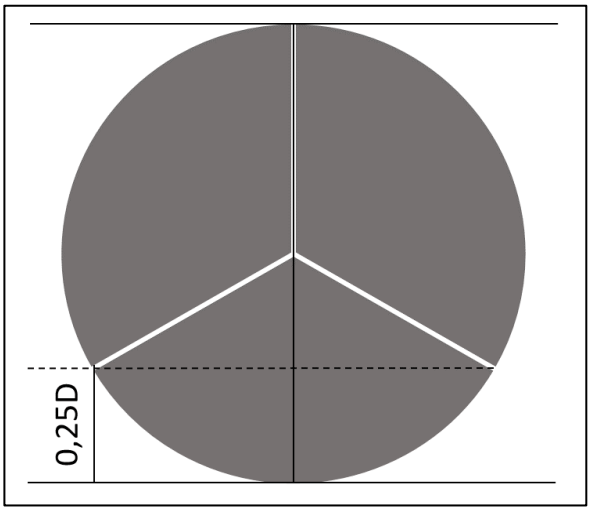

Figure 36. Cross-sectional view of cylinder divided into three equal parts.

As illustrated in Figure 36, the geometry of a circle demands that a third of the circle's circumference, positioned right at the bottom of that circle, will have a height of 25 % of the circle diameter. As such, even though the material bed in the drain chamber of trommel Mk1 does not mimic the material distribution that is assumed in industry (as illustrated in Figure 35) with a decreasing bed depth along the length of the screen, the approximation of a third of the entire screen area being exposed to the material bed still holds because a third of the screen circumference of trommel Mk1 is exposed to a uniform material bed, as illustrated in Figure 36.

Another important parameter for the comparison of drainage rates, is the % Open area of the screen media. This relates to the percentage of the screen area that the apertures make up. Increasing the number of apertures or the aperture size, increases the area through which

material can pass. The % Open area therefore refers to the percentage of the total screen area that the accumulated area of the apertures makes up.

In order to calculate the total and effective screening areas of the drain chamber of the DMS Trommel Mk1, the dimensions summarized in Table 4 are used.

Table 4. Summary of Submerged DMS Trommel Mk1 screen dimensions.

Screen radius (m)	Screen length (m)	Screen circumference (m)
0.398	0.63	2.501

As shown in Table 4, the radius of the screen is 0.398 m, resulting in a circumference of 2.501 m. The length of the screen is 0.63 m. These dimensions, with the assumption that a third of the total screen area is utilised at a particular moment during screening, is used to calculate the effective screen area in Table 5.

Table 5. Summary of screen area dimensions of Submerged DMS Trommel Mk1.

Total screen area (m^2)	Utilised screen area (m^2)	Open area %
1.58	0.53	15.04

The total screen area is based on the circumference of the screen bracket and is equal to 1.58 m^2. The calculated effective or utilised screen area is then calculated as 0.53 m^2. The % open area of the screen is calculated from the total area of the apertures as a percentage of the total area of the screen. The medium drainage rates are calculated as the underflow rate per utilised screening area. The % Open area is not used in this calculation, but is nonetheless an important parameter to consider when comparing drainage rates of different screen media.

4.3.8.3. Volumetric drainage rate

As discussed, the volumetric feed rate remains almost constant at a constant pump setting, decreasing slightly from 8 m^3/hr at RD 2.7 to 7.5 m^3/hr at RD 3.6 due to the increase in density and viscosity, making the slurry more difficult to pump. The fluctuation in the feed rate was caused mostly by fluctuation in the flow patterns in the sump. The volumetric drainage rate is plotted with the volumetric feed rate to allow direct comparison of the trends observed in both. The results are plotted in Figure 37.

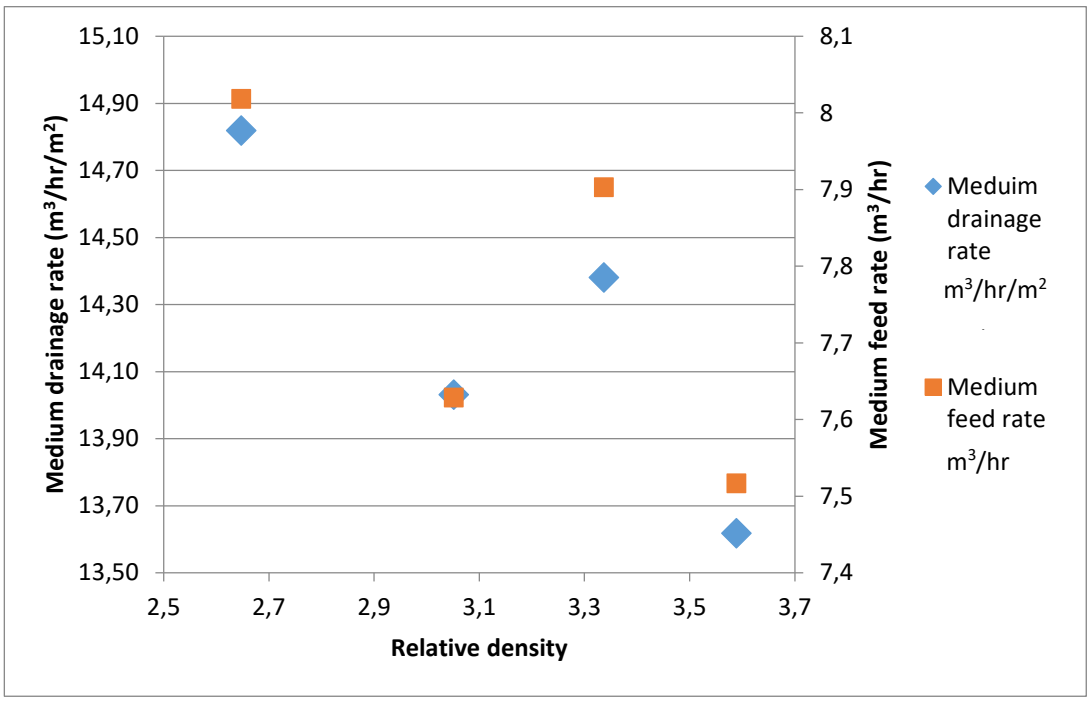

Figure 37. Plot of medium drainage rate and medium feed rate to Submerged DMS Trommel (Mk1) Drain chamber.

As illustrated in Figure 37 the drainage rate is directly related to the volumetric feed rate to the drain chamber. This is because the carryover rates of FeSi and water does not have a strong correlation with the feed rate within the parameters of this particular experiment. At every RD, what is fed to the drain chamber is drained through the screen. It can be concluded that the drainage in the drain chamber has not reached capacity and that an increase in flow rate to the drain chamber should result in greater drainage rates.

4.3.8.4. Comparison of volumetric drainage rate and mass drainage rate

It was observed that there is a strong correlation between the medium feed rate and medium drainage rate. This is best explained by considering the correlation between medium feed and carryover values. With the feed consisting mostly of FeSi, by mass, at relative densities in the range of 2.7 to 3.6 with % solids in the range of 72.45 % to 83.8 %. The FeSi feed rate and carryover rates are summarized in Table 6 over the RD range investigated:

Table 6. Summary of FeSi carryover rates and %FeSi carryover over medium RD range.

RD	FeSi feed rate (t/h)	FeSi carryover rate (t/h)	% FeSi carryover
3.6	22.48	1.10	4.89
3.3	21.50	1.07	4.96
3.0	18.22	0.71	3.91
2.7	15.38	0.54	3.54

Although there is a steady increase in FeSi carried over with an increase in FeSi fed, the increase is minor compared to the increase in the total quantity of FeSi that is fed to the screen. Of the total quantity of FeSi that is fed to the screen, the fraction that is carried over to the submerged wash chamber with the pulp transport is relatively low: between 3.54 % and 4.89 %. There is an increase in % FeSi carryover with an increase in FeSi feed rate. More significantly, however, there is an increase in FeSi drainage with an increase in FeSi feed rate and with it, an increase in total medium drainage rate. The medium drainage rate will increase with the medium feed rate until the point where the screen reaches capacity and a higher drainage rate is not achievable. This point is not reached during the set parameters for this particular investigation.

Next the volumetric medium drainage rate is plotted with the mass medium drainage rate for direct comparison in Figure 38.

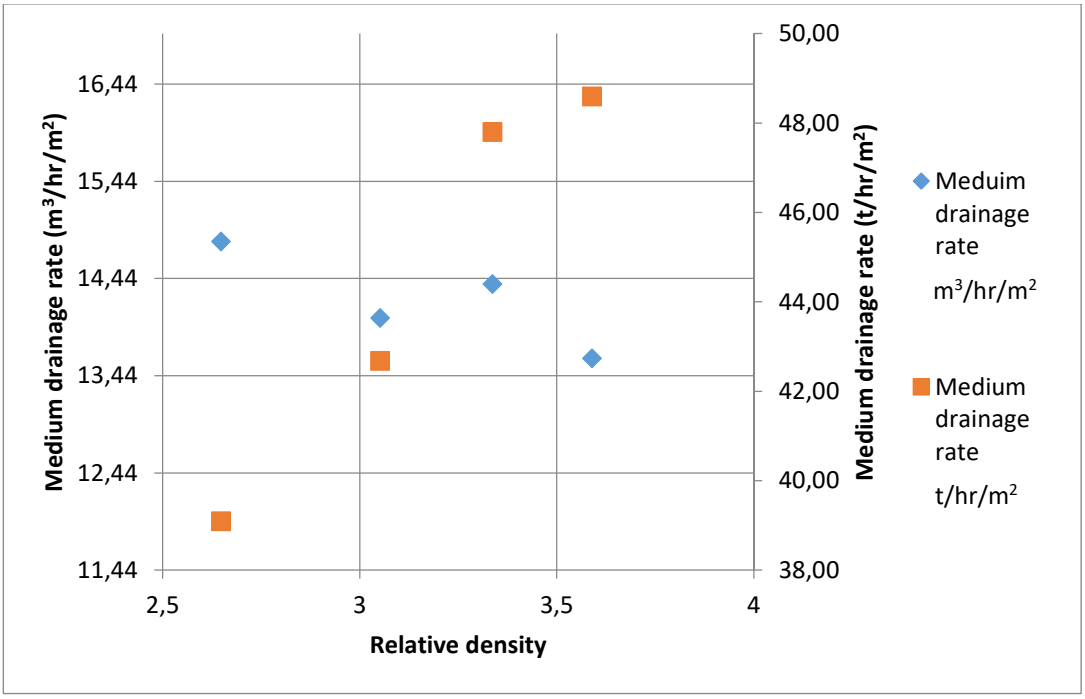

Figure 38. Plot of comparison between medium volumetric drainage rate and medium mass drainage rate (FeSi and water).

The volumetric drainage rate fluctuates about a value of approximately 14.2 $m^3/m^2/hr$ at a constant pump setting. The pump is delivering an approximate constant volumetric feed rate. Under the conditions for this experimental work, the volumetric drainage rate does not seem to depend on the medium RD. On the other hand, the mass drainage rate shows a steady increase from 39.09 $t/m^2/hr$ at RD 2.7 to 48.59 $t/m^2/hr$ at RD 3.6. This is because the relative density of the slurry is increased by adding a significant mass of FeSi to the slurry.

4.3.9. Comparison of DMS Trommel (Mk1) with Vibrating screen Drain section

The test results on the drain chamber of the DMS Trommel (Mk1) are compared to the results obtained on a vibrating drain screen performed by Kabondo, (2018). A list of operating parameters that were considered for the comparison of the vibrating screen with the drain chamber of the DMS Trommel (Mk1), follows. First the parameters that are kept constant are listed:

4.3.9.1. Parameters for consideration of comparison of screens

4.3.9.1.1. Screening area

The screening area of the vibrating screen is calculated as the total area of the flat deck screen. This is equal to 0.511 m^2. The calculated effective screening area of the trommel screen (Mk1) is 0.530 m^2. The effective screening area of the DMS Trommel (Mk1) is estimated as a third of the total screen area, according to industrial standards set by Multotec.

4.3.9.1.2. Open area

The % open area of the 1mm x 13 mm PU panels used on the vibrating screen in the study by Kabondo (2018) is equal to 12.53 %. The % open area of the Linatex mat that was developed for the test trommel (Mk1) (0.8 mm x 13 mm aperture) is 15.09%.

4.3.9.1.3. Aperture shape

Both the Linatex rubber screen mat used in the DMS Trommel (Mk1) and the PU panels in the vibrating screen had slotted apertures. The aperture dimensions on the rubber mat in the DMS Trommel (Mk1) were 0.8 mm x 13 mm. The aperture dimensions on the PU panels in vibrating screen were 1 mm x 13 mm.

4.3.9.1.4. Material

The ore that was used in both studies were supplied by Sishen iron ore mine located in Kathu.

4.3.9.1.5. Ore PSD

The iron ore PSDs for the two studies were very similar. The only major difference is that the smaller fraction (-1.5 mm) of the iron ore was removed from the ore sample for the DMS Trommel (Mk1) study. The iron ore in Kabondo's study had less than 3 wt% in the 1.5 mm size fraction, so the removal of this fraction was not expected to have a significant impact on the overall performance of the trommel. This was done because of the inability to reach steady state. Only the undersized particles that pass through the screen could be circulated while the oversized particles are accumulated in the submerged chamber after being

transported. For this reason it was decided that the circulation of all ore particles would be prevented.

Besides for these parameters that were kept close to constant between the investigations on the vibrating screen and the DMS Trommel (Mk1), there are two main operating parameters on the DMS Trommel (Mk1) that differed significantly from the investigation on the vibrating screen:

4.3.9.1.6. Feed flow rate

The volumetric feed rates that were investigated on the vibrating screen ranged from 20.4 m^3/hr to 25.1 m^3/hr. This is significantly higher than the volumetric feed rate of 7.7 m^3/hr that was investigated on the DMS trommel (Mk1). Due to shortcomings in the original design of the DMS Trommel (Mk1) causing excessive spillage at higher flow rates, the unit could not operate at higher feed rates than 7.7 m^3/hr. Only one volumetric feed rate was investigated on the DMS Trommel (Mk1).

Furthermore, it is important to consider how near to the screen capacity the operating parameters are. If a medium drain screen is saturated, it will be unable to drain any additional medium that is fed beyond saturation point. This will result in an increase in medium quantities in the overflow stream. For this reason, care must be taken when comparing overflow properties of two screens. If one is screen was operated beyond capacity while the other was not, the comparison would not be sensible. The drainage rates that were achieved by Kabondo (2018) on the vibrating screen over the feed rate range, are illustrated in Figure 39.

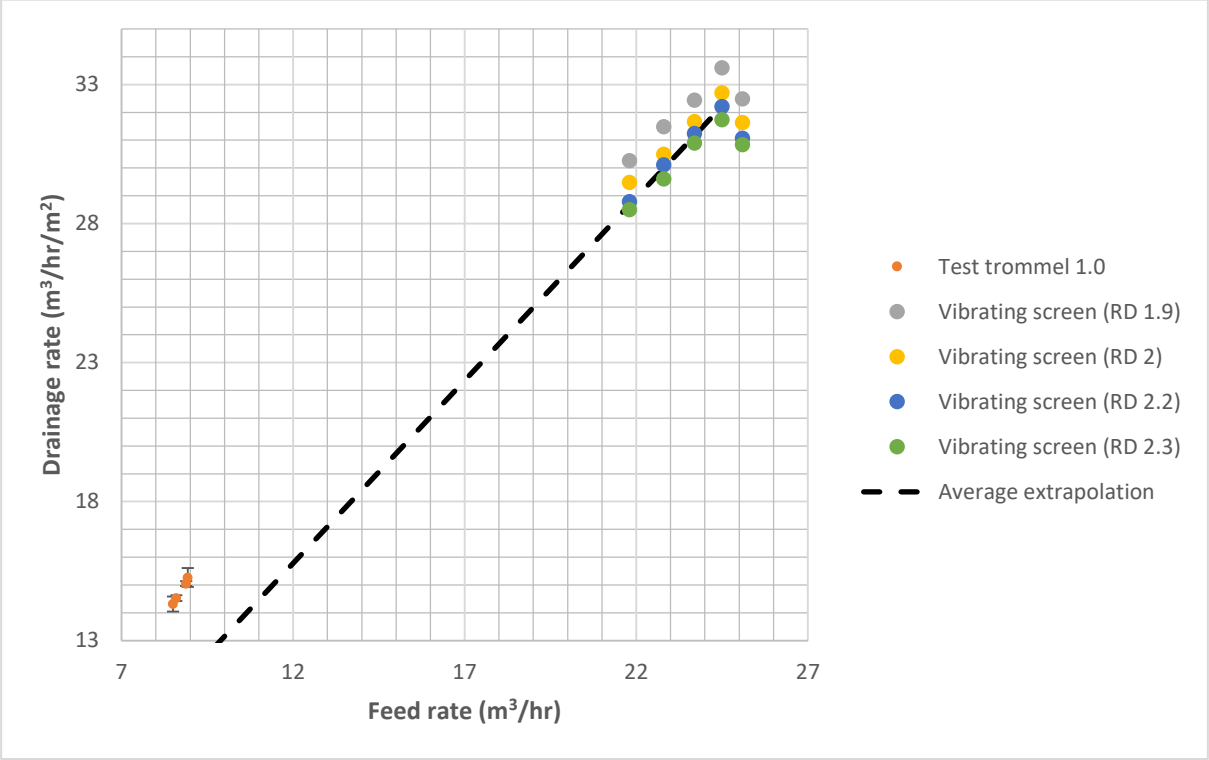

Figure 39. Plot of drainage rates achieved on Submerged DMS Trommel (Mk1) and Vibrating screen during test work performed by Kabondo (2018)

Figure 39, plotted from the experimental data produced by Kabondo (2018) from the study on drainage rates on the vibrating screen, illustrates a gradual increase in drainage rate with an increase in feed rate. This implies that feed rates under 24.5 m^3/hr were below the screen capacity. The screen was not overfed, which would result in excessive medium reporting to the overflow stream.

The linear extrapolation on Figure 39 crosses the origin of the graph because with zero feed, there will be zero drainage. The linear trend line was fitted between the origin and the average of Kabondo's data cluster in the top right of Figure 39. As the feed rate to the vibrating screen increased, there was a linear increase in drainage rate because the excess material is being drained effectively to the underflow. The linear trend of the data cluster produced by Kabondo (2018) was extrapolated to the origin to enable a comparison with the DMS trommel (Mk1).

Although the drainage rate that was accomplished in the drain section of the submerged DMS trommel (Mk1) was substantially lower than what was achieved on the vibrating screen, it still adhered to the expected trend for drainage with regards to feed rate. The slight deviation from the expected trend is likely due to a slight deviation in utilised open area from the assumed 33.3% on DMS Trommel (Mk1).

In addition, a photograph of the operation of the vibrating screen during operation by Kabondo (2018) is included in Figure 40.

Figure 40. Photograph of medium drainage region on vibrating screen during test work performed by Kabondo (2018)

As illustrated in Figure 40, the undrained medium is clearly visible near the feed end of the vibrating screen. The boundary of the area where the medium is being drained, is clearly visible. Beyond that, closer to the overflow discharge end of the screen, only ore with adhered FeSi remains on the screen. This photograph serves as further evidence that the vibrating screen was not overfed during the test work performed by Kabondo (2018).

As such, the comparison between the overflow characteristics of the DMS Trommel screen (Mk1) and vibrating screen is valid.

4.3.9.1.7. Slurry relative density

The relative density range that was investigated on the vibrating screen ranged from 1.9 to 2.7. This is much lower than typical iron ore DMS plant with medium RD ranging from 2.7 and upwards. There was concern that the test work on the DMS Trommel (Mk1) would not be applicable to industrial applications if the RD was so low that it might not be representative of actual DMS operation. In the DMS Trommel (Mk1) test work, the RD values therefore were chosen closer to the actual industrial values. The range of investigation was chosen to bridge the gap between the upper limit of the vibrating screen of 2.7, to a maximum RD of 3.6. Due to practical constraints such as the experimenter being unable to handle higher density samples, the RD range did not exceed 3.6.

The main parameters of interest that were compared between the vibrating screen and DMS Trommel (Mk1) were % moisture in overflow, % FeSi in overflow and % FeSi carryover. The first comparison is the moisture content in the overflow stream between the vibrating screen and DMS trommel (Mk1).

4.3.9.2. % Moisture in overflow as a function of RD

The % Moisture results produced on the vibrating drain and rinse screen from the study by Kabondo (2018) is plotted in comparison with the results of % Moisture on the DMS Trommel (Mk1) in Figure 41.

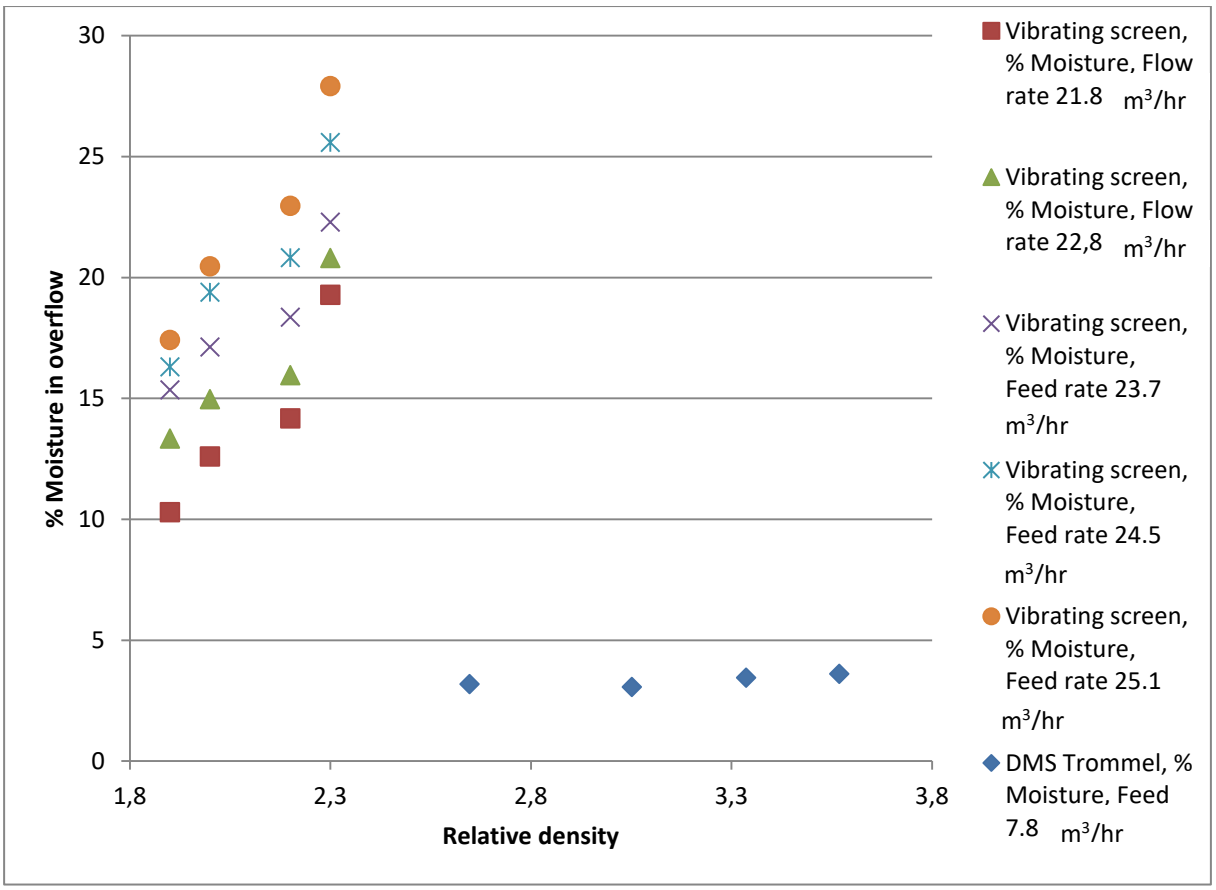

Figure 41. Comparison of % Moisture in overflow of Submerged DMS Trommel (Mk1) and vibrating screen over medium RD range.

The results for an increase in RD from 1.9 to 2.7 on the vibrating screen show a steep increase in % moisture in the overflow stream at all tested feed rates. This steep increase in moisture carryover is likely a result of the increase in density of the pulp that forms the particle bed on the screen. With an increase in pulp density, it is expected that the water experiences more resistance as it is draining through height of the particle bed on its way to the surface area.

Even though there is a steep increase in % Moisture for an increase in RD on the vibrating drain and rinse screen, the increase is expected to plateau as the FeSi mass % in the medium increases with an increase in RD.

Regardless of the increase in relative density from 2.7 to 3.6 on the DMS trommel (Mk1), illustrated in Figure 41, the % moisture in the overflow of the DMS trommel (Mk1) does not increase significantly. This does not align with the trend of increase in % moisture in the overflow on the vibrating screen.

Keep in mind that the DMS Trommel (Mk1) data was produced at a feed rate of 7.8 m^3/hr, while the vibrating screen was operated at feed rates in the range of 20.8 m^3/hr to 24.5 m^3/hr. From the comparison it is apparent that the % Moisture in the overflow of the drain chamber of the DMS Trommel (Mk1) is lower than the lowest % Moisture values that were measured on the vibrating screen over the entire RD range. This is a promising prospect for the DMS Trommel (Mk1) as it is desirable to decrease the % Moisture bypassing to the overflow stream without being drained.

One explanation could be the difference in particle beds on the flat panel and the rotating screen. On the flat panel in the vibrating screen there is a particle bed that migrates across the panel from the feed end to the overflow end. In the rotating trommel, the particle bed is continuously broken up by the rotation, causing particles to tumble over each other and rub against each other. It is possible that the rotation of the bed decreases its ability to retain water, as the bed is continuously moving, allowing water to drain from between the particles and enhancing stratification through the bed. It is possible that a particle bed on a flat panel is more able to retain moisture since the water has to migrate through the entire bed depth before draining through the screen, which hinders stratification. With a rotating screen, particles tumble over each other and the entire bed is inverted during one rotation, meaning that all of the moisture in the bed has a chance to drain from the first few layers of particles that are exposed directly to the screening area. The moisture that is carried over to the submerged chamber is therefore decreased with the bed's ability to retain water. Considering the low height of the particle bed on the vibrating screen (between 10 mm and 20 mm), it seems unlikely that the moisture in the bed would experience more obstruction to reach the screen surface than on the DMS Trommel (Mk1) with a particle bed of approximately 200 mm. It is possible that the tumbling motion of the particles in the trommel is more effective at breaking the particle-particle contact between medium and ore particles, compared to the bouncing motion of particles on a vibrating screen. If the G force that the particles experience on the vibrating screen does not break the particle-particle contact between ore and medium,

the moisture will be retained in the particle bed and report to the overflow, resulting in a greater moisture content in the overflow. The % moisture in the overflow is also likely a function of feed rate, which will be discussed in the following section.

Another possibility that could be considered would be that the moisture content in the overflow stream is lower because of the delay in sampling due to the approximated steady state. In order to approach a steady state, the trommel is rotated to allow the scrolls to fill to represent the quantity of ore that would be found in the scrolls during steady state transport. After these rotations, the transported pulp was scooped from the submerged wash chamber where it was accumulating, to scoop it back into the drain chamber screen. It could be argued that this delay to transport the ore back into the screen is enough to allow water to drain through the pulp bed while the FeSi remains adhered to the ore particles without moving during this time. This could result in a lower moisture content in the pulp because the water drains from the pulp during the down time.

This was however considered as a possibility before the test work was done. For this reason the scrolls were inspected carefully before and after rotation. It was ensured that there is no moisture leakage from either sides of the scrolls (drain and wash chamber sides) during the down time to move the transported pulp from the submerged wash chamber back to the drain chamber screen.

4.3.9.3. % Moisture in overflow as a function of Flow rate

The next set of data is % moisture as a function of feed flow rate. The compared results are illustrated in Figure 42.

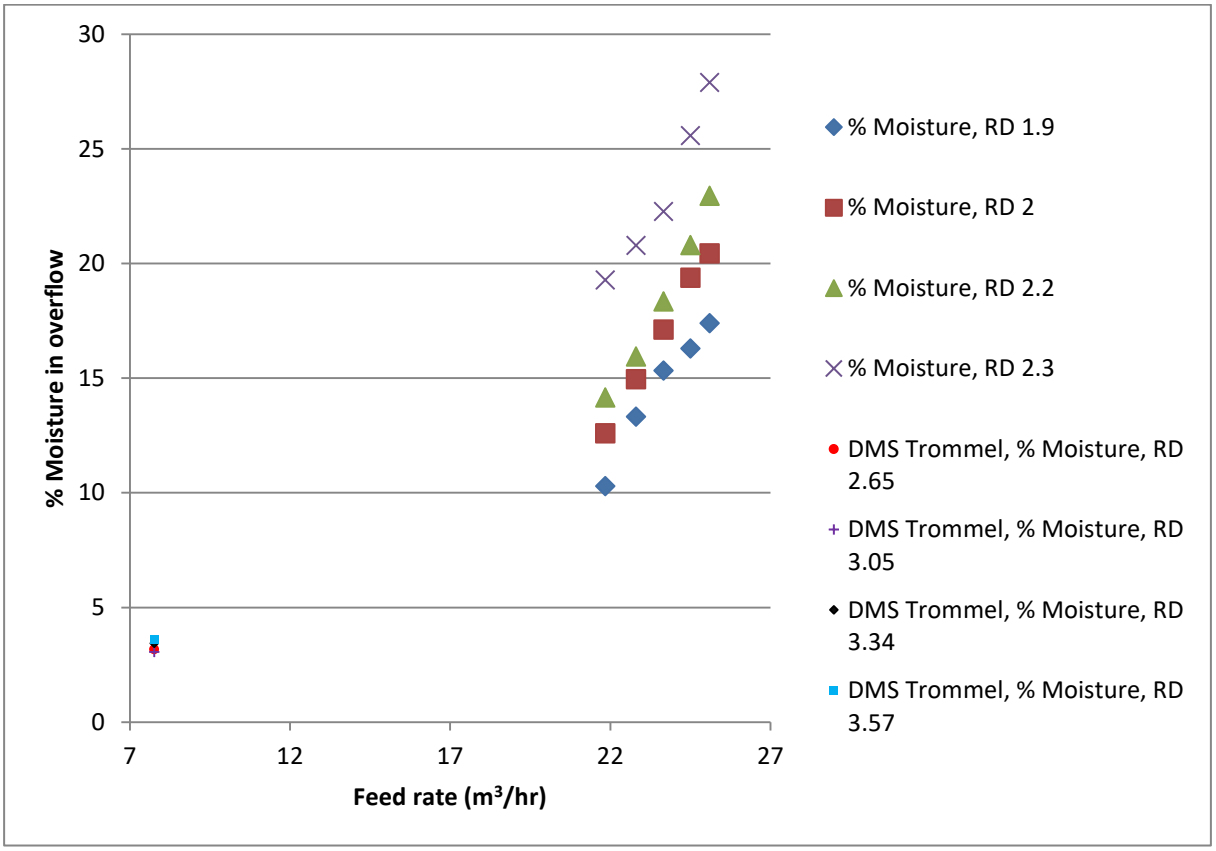

Figure 42. Comparison of % Moisture in overflow of Submerged DMS Trommel (Mk1) and vibrating screen over feed rate range.

From Figure 42 it is apparent that the % moisture is in fact a function of the feed rate to the vibrating screen at all relative densities. At the highest relative density of 2.3 on the vibrating screen, the % moisture in the overflow increases from 19.3 % to 27.9 % with an increase in feed flow rate from 21.8 m^3/hr to 25.1 m^3/hr. The % moisture trends remain similar, with a decrease in % moisture in the overflow as the relative density decreases. Finally the lowest % moisture in the overflow is achieved at the lowest relative density of 1.9, starting at 10.3 % at a flow rate of 21.8 m^3/hr and increasing so 17.4 % with an increase in flow rate to 25.1 m^3/hr.

Comparison of the DMS Trommel (Mk1) results for % moisture in the overflow with that of the vibrating screen shows that the DMS Trommel (Mk1) % moisture falls within the same range. The results for % moisture in the overflow of the DMS Trommel (Mk1) are very consistent, barely deviating from the cluster of data points. There is a very slight increase from 3.2 % to 3.6 % moisture with a relative density increase from 2.7 to 3.6. Even though the relative densities investigated on the DMS Trommel (Mk1) were significantly higher than that of the vibrating screen, the % moisture in the overflow was still reasonable for lower flow rates of the lower relative densities on the Vibrating screen. With regards to performance and separation efficiency of the DMS Trommel (Mk1), this is a promising result as a lower

moisture carryover to the submerged chamber is desirable. This implies that the pulp that is retained in the screen has a lower capacity to retain moisture in the context of a rotating, tumbling particle bed.

It is important to note at this point that the DMS Trommel (Mk1) is operating at the maximum ore transport rate. Normal feed conditions for D&R Vibrating screens from the dense medium cyclones are slurry streams with a medium to ore ratio of 5:1. Assuming that the ore transport rate from the drain chamber is equal to the feed rate of ore at the presumed steady state, a feed rate of 7.8 m^3/hr of medium corresponds with the current ore transport rate to maintain a 5:1 medium to ore ratio. This DMS Trommel (Mk1) capacity is therefore a result of the ore transport mechanism that was designed for the trommel. This limitation is not appropriate for the physical dimensions of the DMS Trommel screen (Mk1). With an improved solids transport mechanism, a trommel with similar dimensions should have a bigger capacity. This is one of the points that will be considered with improving the design of the DMS Trommel (Mk1).

4.3.9.4. % FeSi in the overflow as a function of relative density

The next major parameter of interest is the FeSi content in the overflow stream. This is determined by measuring the composition of the overflow stream. The percentage of FeSi in the overflow stream indicates the extent to which the FeSi adheres to the ore particles in the overflow stream. Figure 43 illustrates the percentage of the overflow stream that comprises of FeSi, over the investigated relative density ranges in the study performed by Kabondo (2018) on the horizontal Vibrating screen, plotted against the results from the DMS test trommel.

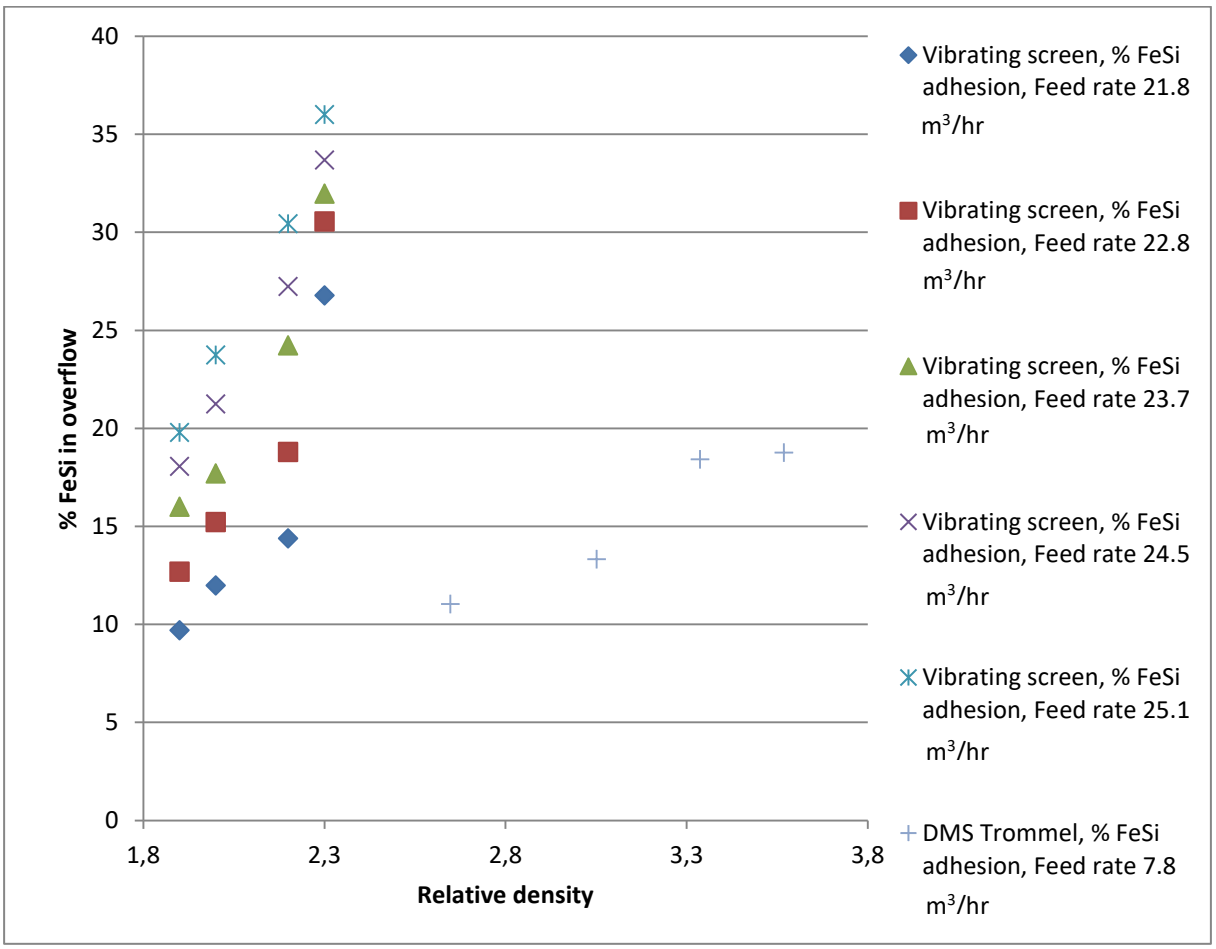

Figure 43. Comparison of % FeSi in overflow of Submerged DMS Trommel (Mk1) and vibrating screen over medium RD range.

The results illustrated in Figure 43 indicate that the FeSi adhesion in the DMS Trommel (Mk1) is lower than that achieved on the Vibrating screen, even at significantly higher RD values of ranging from 2.7 to 3.6. With an increase in RD from 1.9 to 2.3, the % FeSi composition in the overflow stream of the Vibrating screen increases steeply from 12.7 % to 26.8 % at the lowest feed rate of 21.8 m^3/hr and from 19.8 % to 36 % at the highest feed rate of 25.1 m^3/hr. The maximum measured % FeSi in the overflow on the DMS Trommel (Mk1) was 18.8 % at an RD of 3.6.

A possible explanation for this observation is the comparison between dynamics of the particle beds in a rotary screen and a flat deck screen. On a vibrating screen, the particle bed forms a layer on top of the screen surface. The vibration of the screen moves the particles upward and forward, but the bed still remains relatively intact, keeping its shape and form to some extent and covers the entire screen surface. With the vibration of the screen, all of the oversized particles move together. This causes the particle bed to bounce on top of the screen and the apertures, causing some obstruction to the drainage of medium as it has to drain through the particle bed first before reaching the screen surface.

In the DMS Trommel (Mk1), the particle bed is rotating and particles are constantly rolling and tumbling over each other. At low rotation velocity, the medium tends to drain straight downwards as a result of gravitation. With the rotation of the trommel, the material bed moves towards the direction of rotation of the trommel, which implies that the screen surface at the bottom of the trommel circumference tends to be free of a material bed. The lower material quantity on this area of the screen results in easier drainage. This implies that a fraction of medium does not necessarily have to drain through an entire particle bed to reach the screen surface and pass through the apertures. As the bed is in a constant tumbling motion, there is a greater probability that the medium comes into direct contact with the screen surface and this could possibly be the cause for a lower FeSi adhesion measured in the overflow of the DMS Trommel (Mk1), even at significantly higher slurry RD.

It is however important to keep in mind that there was a significant difference in feed rate that was investigated on the vibrating screen and the trommel (Mk1). This is expected to affect the % FeSi in the overflow, and will be discussed in the following section.

4.3.9.5. % FeSi adhesion as a function of feed rate

The next step in comparing the DMS Trommel (Mk1) with the Vibrating screen, is a comparison of the % FeSi in the overflow stream as a function of feed rate. Figure 44 illustrates the data generated on both the DMS Trommel (Mk1) and Vibrating screens.

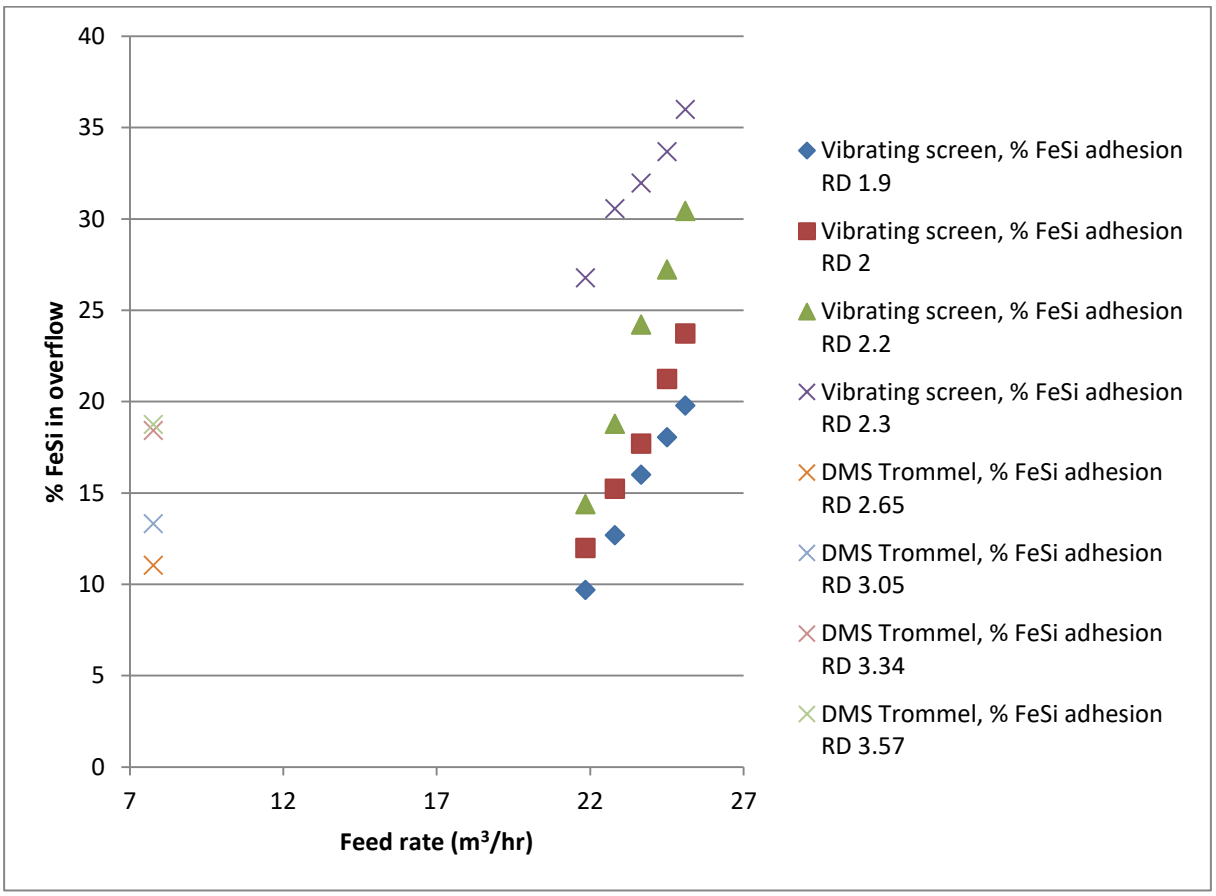

Figure 44. Comparison of % FeSi in overflow of Submerged DMS Trommel (Mk1) and vibrating screen over feed rate range.

From Figure 44 it is apparent that there is a steep decrease in % FeSi adhesion as the feed rate decreases on the Vibrating screen. At the highest RD value of 2.3, the % FeSi in the overflow stream decreases from 36 % at a feed rate of 25.1 m^3/hr to 26.8 % at a feed rate of 21.8 m^3/hr. At the lower relative densities, there are even steeper decreases in FeSi adhesion with the same decrease in feed rate. The dependency of the FeSi adhesion on feed rate at the three lower relative densities is relatively consistent with each other. At the lowest RD, the % FeSi adhesion decreases from 19.8 % to 9.7 % with a decrease in feed rate from 25.1 m^3/hr to 21.8 m^3/hr.

The DMS Trommel (Mk1) results for % FeSi in the overflow are within the same range of % FeSi adhesion than that of the vibrating screen, even though the feed rate on the DMS Trommel (Mk1) was significantly lower than on the vibrating screen.. This implies that the DMS Trommel (Mk1) drain chamber is less effective at separating the medium from the ore than the flat deck Vibrating screen is.

Even though values were achieved on the DMS Trommel (Mk1) at a significantly lower feed rate of 7.8 m^3/hr, compared to the Vibrating screen in the range of 21 m^3/hr to 25 m^3/hr, the DMS Trommel (Mk1) is not operated at the drainage capability limit, but rather at the solids

transport capacity. It is expected that an improved solids transport mechanism would allow a greater solids transport rate, which in turn would accommodate a greater feed rate. Since this investigation of the DMS Trommel (Mk1) is nowhere near its actual drainage capability, but rather limited by its solids transport capability, the feed rate could theoretically be increased significantly without drastically increasing the FeSi adhesion to the solids that are transported to the next chamber. The FeSi adhesion in the DMS Trommel (Mk1) at such low flow rates is a function of the relative density, rather than feed rate. It is expected that the dependency of FeSi in the overflow stream will only start to be influenced by the feed rate when the feed rate is increased to a point where the drainage capacity of the trommel (Mk1) is reached, or when the medium from the feed starts to bypass the screen as a result of not being drained through the screen. For this reason it is safe to assume that the FeSi adhesion values should hold at higher feed rates and is not necessarily just a result of the low feed rate used for this investigation. If this is true, the set of results on the DMS Trommel (Mk1) could be shifted to the right if the solids transport mechanism is improved to not act as a bottleneck in the capacity of the DMS Trommel (Mk1). This means that the results on the DMS Trommel (Mk1) could very well fall within the expected range of operation of the Vibrating screen, and it is not conclusive that the DMS Trommel (Mk1) is less effective at draining the medium in the drain chamber than the vibrating screen is. It is however recommended to test this theory on an improved design of the DMS Trommel (Mk1) that does not have design flaws that limit the maximum solid transport rate and maximum feed rate due to excessive spillage.

4.3.9.6. % FeSi carryover as a function of relative density

The FeSi adhesion to the ore particles is not the only measure of FeSi in the overflow stream that is of interest. It is also important to investigate which fraction of the FeSi that is fed to the screen, is carried over to the overflow stream. This value is calculated by measuring the rate at which FeSi is carried over to the overflow stream, and then calculated as a percentage of the total rate at which FeSi is fed to the screen. Figure 45 illustrates the results and comparison of both the Vibrating screen and the DMS Trommel (Mk1).

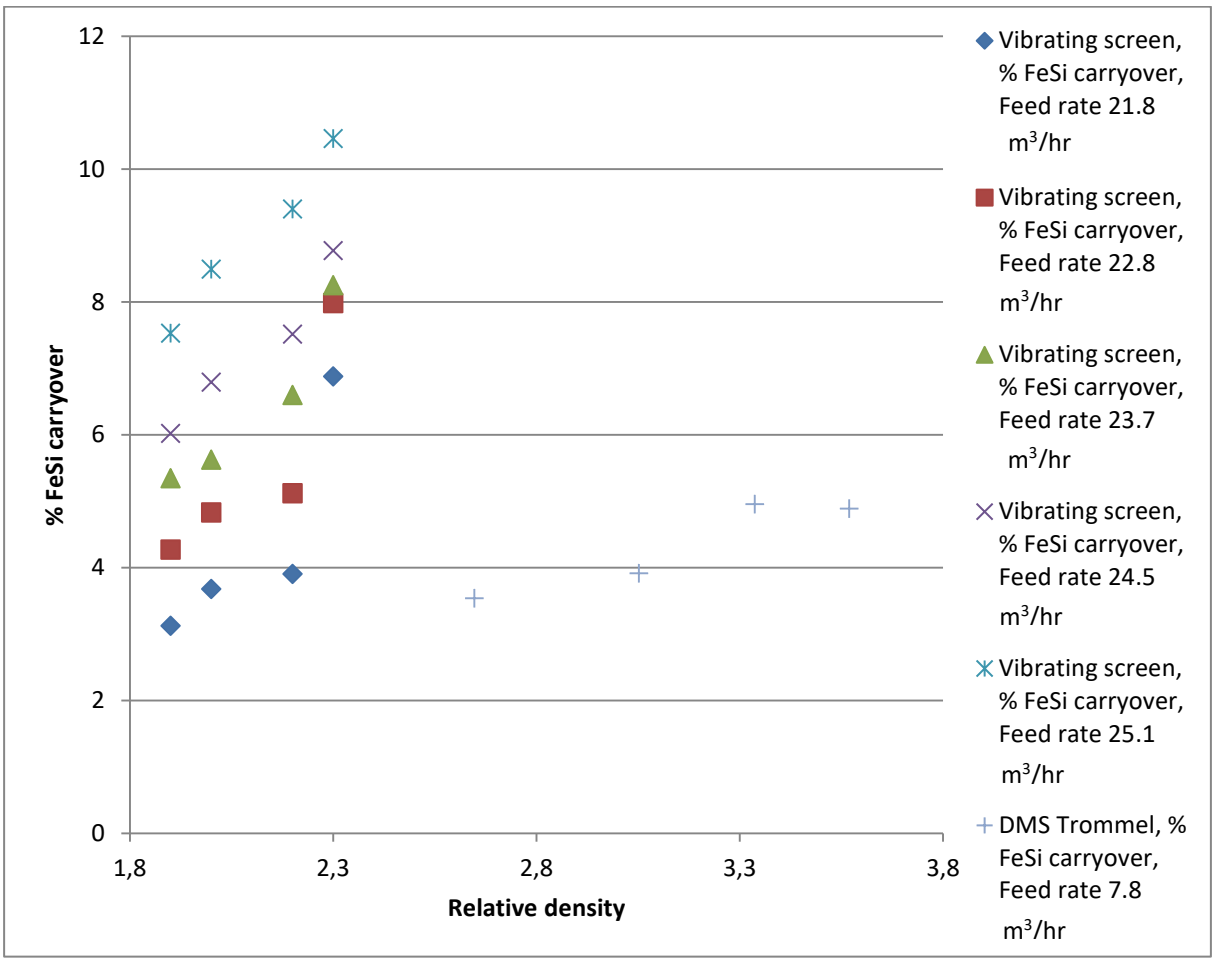

Figure 45. Comparison of % FeSi carryover of Submerged DMS Trommel (Mk1) and vibrating screen over medium RD range.

Figure 45 indicates that there is a clear correlation between % FeSi carryover and relative density on the vibrating screen. At the highest feed rate of 25.1 m^3/hr, the % FeSi carryover increases from 7.5 % to 10.5 % for a relative density increase from 1.9 to 2.3. With decreasing feed rates, the % FeSi carryover also decreases. At the lowest feed rate of 21.8 m^3/hr, the % FeSi carryover increases from 3.1 % to 6.9 % for the same relative density increase from 1.9 to 2.3.

The most obvious explanation for the increase in % FeSi carryover for an increase in feed on the vibrating screen would be that the screen was overfed and the excess medium, that could not be drained, reported straight to the overflow of the screen. However, as discussed earlier in section 4.3.9.1.6, there is ample evidence that the vibrating screen was not overfed at a feed rate of 24.5 m^3/hr and lower. It is speculated that an increase in medium RD also increases the adhesion forces between the ore and medium. At higher medium densities, the medium becomes more viscous and changes the flow properties of the pulp. This was confirmed in the first results where it was found that the ore transport rate of the pulp increased with an increase in medium RD because of this change in pulp flow properties. As the pulp on the

screen becomes more “sticky”, the pulp’s ability to retain medium also increases. If the adhesion forces between the ore and medium remained the same over the RD range, a higher medium RD would translate to a higher FeSi content in the overflow, but a constant % FeSi carryover. This is not the case. With an increase in medium RD, there also seems to be a greater volume of medium adhering to the ore particles. This is confirmed by the increase in % moisture in the overflow, which was discussed earlier. With a greater medium volume that reports to the overflow, there also seems to be slightly more FeSi being retained in the medium that is adhered to the ore particles. This corresponds to trends observed in literature (Rogers & Brame, 1985).

On the trommel (Mk1), it is more difficult to comment on a correlation between medium RD and % FeSi carryover. Considering the high variance of the data that was discussed earlier (section 4.3.4) in the results section, the correlation between medium RD and % FeSi carryover is too weak to conclude with certainty that there is a correlation, although a correlation is expected according to literature.

The % FeSi carryover that was measured during trommel (Mk1) test work was in the range of 3.54 % to 4.96 %. Considering that the trommel (Mk1) test work was conducted at a significantly higher medium RD than on the vibrating screen, the % FeSi carryover that was achieved on the trommel (Mk1) was once again a promising result for using trommels as an alternative to vibrating screens in the context of drain and rinse medium recovery for iron ore.

4.4. Wash chamber operation

4.4.1. Introduction

As with the drain chamber, the steady state is unattainable in the wash chamber following the drain chamber. Once again, steady state is approximated by loading a batch of material that would be fed to the wash chamber from the drain chamber under continuous operating conditions. As such, the drain chamber test work results were used to determine the typical characteristics of the pulp that is transported from the drain chamber to the wash chamber. The pulp was mixed in a bucket and loaded into the wash chamber as preparation for the wash chamber tests.

Due to design constraints, it is impossible to keep FeSi in suspension in the wash chambers. Insufficient agitation in the wash chambers cause the FeSi that is washed from the pulp to settle to the bottom of the wash chamber.

4.4.2. Chamber loading

4.4.2.1. Pulp loading

To test the washing capability of the wash chamber, it was decided that the tests on the wash chamber would be initiated with the highest quantity of FeSi that was found in the pulp from the drain chamber tests. The highest FeSi quantity in the transported pulp was approximately 20% and was achieved at the highest feed RD of 3.6.

At steady state, the flow rate of ore into the drain chamber is equal to the transport rate of ore out of the drain chamber to the wash chamber. Since both chambers are driven by the same motor, they both rotate at the same RPMs. With the same solids transport mechanisms, the assumption is made that the ore quantities in both chambers will be equal at steady state. Therefore the same ore quantity was chosen for the wash chamber as was used in the drain chamber.

4.4.2.2. Water loading

During typical continuous operation of the wash chambers, the pulp entering the chamber will be washed and FeSi will be washed from the ore and enter suspension in the water bath. During start-up the FeSi concentration in the water bath will increase until the rate of FeSi exiting the bath is equal to the rate of FeSi entering the chamber with the pulp. At steady state the FeSi concentration in the bath will remain constant for the duration of the steady state. It is expected that the FeSi in suspension will affect the efficiency of washing of the FeSi from the ore particles. In other words, it is expected that an increase in FeSi concentration in the water past a certain point, will start decreasing the effectiveness of washing the ore particles with the water because it is reaching saturation of FeSi in suspension.

Due to design constraints on this iteration of the DMS Trommel (Mk1) it is unable to drain FeSi from the wash chamber at the same rate as it is fed to the wash chamber with the pulp from the drain chamber. The drain at the bottom of the wash chamber is a small opening in the middle of a horizontal bottom surface. The mechanical design did not allow for the FeSi to drain to the middle of the chamber where the outlet is located. The FeSi settled too fast to the bottom of the chamber and created a horizontal bed at the bottom of the chamber. As more pulp was fed to the chamber, more FeSi was washed from the pulp and settled to the bottom of the chamber without draining, resulting in an increasing FeSi bed height at the bottom of the chamber. This bed kept increasing in height until it exceeded the height of the bottom of the screen bracket, resulting in the FeSi that was drained from the pulp to be re-mixed with the ore that it was washed from. Furthermore, the FeSi bed started to interfere with the rotation of the screen bracket as the bed depth exceeded the maximum height limit to

remain clear of the rotating screen. The only alternative to simulate the steady state FeSi concentration in suspension in the wash chamber was to keep all of the FeSi in suspension in the wash chamber so that FeSi could exit the wash chamber through the overflow weirs. Unfortunately, the mixing mechanism in the wash chamber was inadequate to keep all of the FeSi in suspension. Not only was it impossible to keep the FeSi concentration in the wash chamber at a constant value while washing to simulate the steady state, but it was also impossible to determine the FeSi concentration in the wash chamber at steady state in the first place.

As such it was not possible to perform tests in the first wash chamber that would provide representative results of the washing that occurs in the first wash chamber, even with attempting to mimic steady state in the first wash chamber. There were simply too many unknowns to claim with any certainty that the tests in the first wash chamber produced representative results of continuous operation.

Although it is not possible to estimate the operating conditions in the first wash chamber, some reasonable assumptions could however be made concerning the operating conditions in the second wash chamber. After the ore has been washed in the first wash chamber, it is expected that a smaller quantity of FeSi will remain in the pulp when it is transported to the second wash chamber. With a sufficiently high water feed rate to the second wash chamber, it is reasonable to assume that the suspended FeSi concentration in the second wash chamber should be very low, if not negligible. For this reason it was decided to investigate the operation of the second wash chamber, rather than the first one, by loading the wash chamber with clean water to investigate the washing efficiency of the chamber. As discussed before, the pulp that is loaded to the chamber is still the same concentration as the pulp coming out of the drain chamber, so it will not represent the pulp coming out of the first wash chamber that would actually enter the second wash chamber under normal operating conditions. This is done to create a “worst case scenario” in the second wash chamber for the investigation. By choosing the highest FeSi concentration in the pulp from the drain chamber, it can be claimed with confidence that the washing occurring in the second wash chamber during test work, will occur at less favourable conditions than it would under normal continuous operating conditions. By pushing the parameters of operation of the second wash chamber to the worst-case scenario, it is possible to comment on the efficiency of washing in continuous operating conditions that would in fact be more favourable than the conditions chosen for this experiment.

4.4.2.3. Wash chamber batch test results

The operating parameters for the wash chamber tests were selected to mimic the operation of the drain chamber with regards to the following parameters:

- Pulp quantity in screen (approximately 40 kg of pulp);
- Pulp composition (20 wt% FeSi, 3.6 wt% Moisture and 74.4 wt% ore);
- Rotation speed (24 RPM);
- Screen media (0.8 mm x 10 mm aperture, slot with flow);

As discussed in the experimental procedure, the intended method was to load a batch of pulp into the submerged screen, then varying the number of screen rotations to determine its effect of the washing that was achieved. The number of rotations that would be tested, was 1, 2, 3, etc. until the point was found where further rotations did not have any additional contribution to washing. Upon performing the first batch of tests with one screen rotation, it was however found that the composition of residual FeSi that remained adhered to the ore pulp after removing the pulp from the submerged chamber, was already below 0.16 wt%. It is implied that a single rotation was sufficient to wash any significant quantity of FeSi from the ore. Figure 46 illustrates the wt% FeSi in the pulp upon sampling after various number of rotations in the submerged wash chamber.

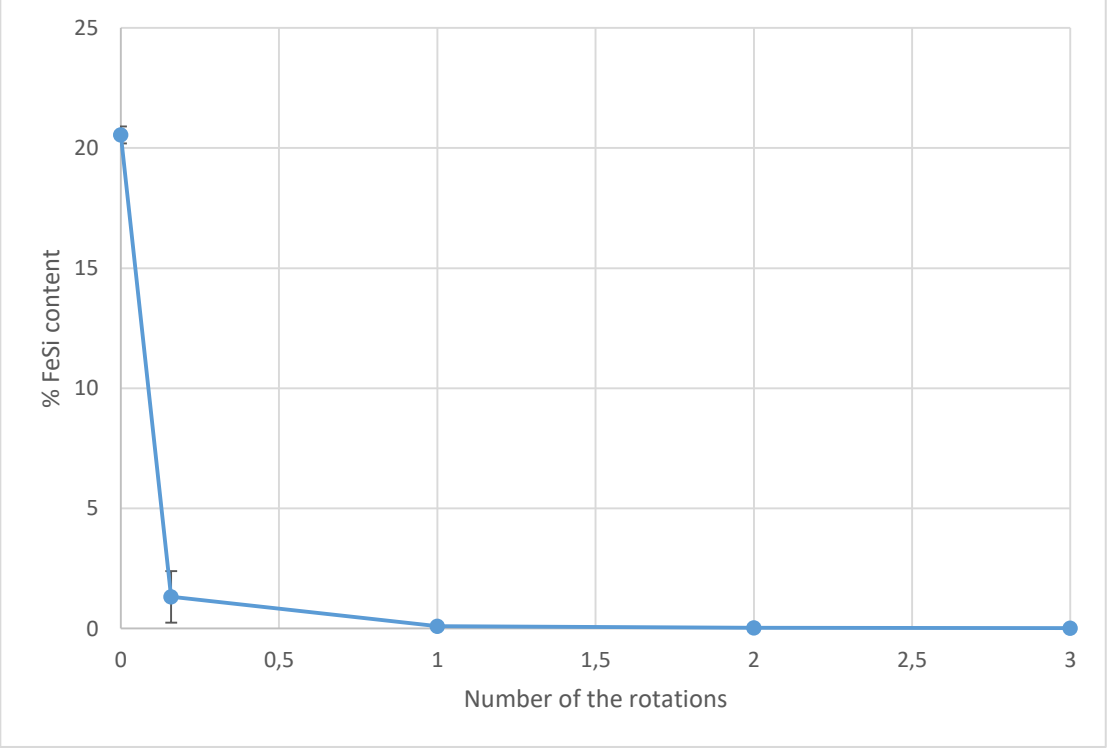

Figure 46. Illustration of % FeSi content adhering to ore after washing in wash chamber of Submerged DMS Trommel (Mk1).

In order to attempt to plot a point between zero and one rotation, where the sample still contained a significant FeSi concentration, a sample was taken from the submerged bath immediately after all of the solids were inserted into the screen. In other words, 40 kg of pulp was loaded into the screen, then upon loading the last 10 kg, the first sample was taken immediately. This sample was washed only by settling through the water to the top of the ore bed, and then being removed from the water again. Technically this sample was not exposed to any physical rotation, however in actual operation, during the time it takes for the pulp to settle to the screen surface, the screen would be rotating. In order to estimate the number of rotations that occurred during this time, it was assumed that the settling speed of the pulp after being discharged from the scroll into the submerged screen, is more or less equal to the rotation speed of the screen. This implies that the arc length of the screen that passes during the settling time, is equal to the radius of the screen. This is equal to one radian of rotation, which translates to approximately 0.1592 rotations. For this reason, the sample that was taken right after submersion was plotted at 0.1592 rotations on the x-axis of Figure 46.

For all the repeats it was found that the action of submerging the pulp in a clean water bath and then removing the ore particles from the water, without physically rotating the screen, resulted in washing approximately 96% of the FeSi mass that was in the pulp before submersion. Unfortunately, it is unclear what fraction of the washing occurred during the settling, and what fraction occurred during the action of sampling as the pulp emerged from the water. After one rotation, 99.7% of FeSi was washed from the ore bed with clean water. This indicated that submerged washing is in fact a very promising method of recovering medium from ore in the dense medium circuit.

4.5. Bench wash/rinse tests

The bench washing and rinse tests were performed to quantify and compare the concepts of submerged washing and rinsing in the context of medium recovery from iron ore pulp. As a result of the findings in the wash chamber tests, it was realised that a significant extent of washing was achieved with the settling and emerging actions of the pulp into and from the water bath. As such, two different tests were performed for the submerged washing. One set of tests was for only orbital shaking motion for 16 seconds of a pulp bed that was already submerged. These tests are called submerged wash tests (stationary) in Figure 47. For the other set of submerged washing tests, the submerged bath was stirred with orbital rotation, while the pulp got added systematically over the total duration of 16 seconds and was allowed to settle to the screen during the shaking motion. These tests are called submerged wash tests

(settling) in Figure 47. The final set of bench tests was rinse washing of the pulp bed with 3 L of water over 16 seconds.

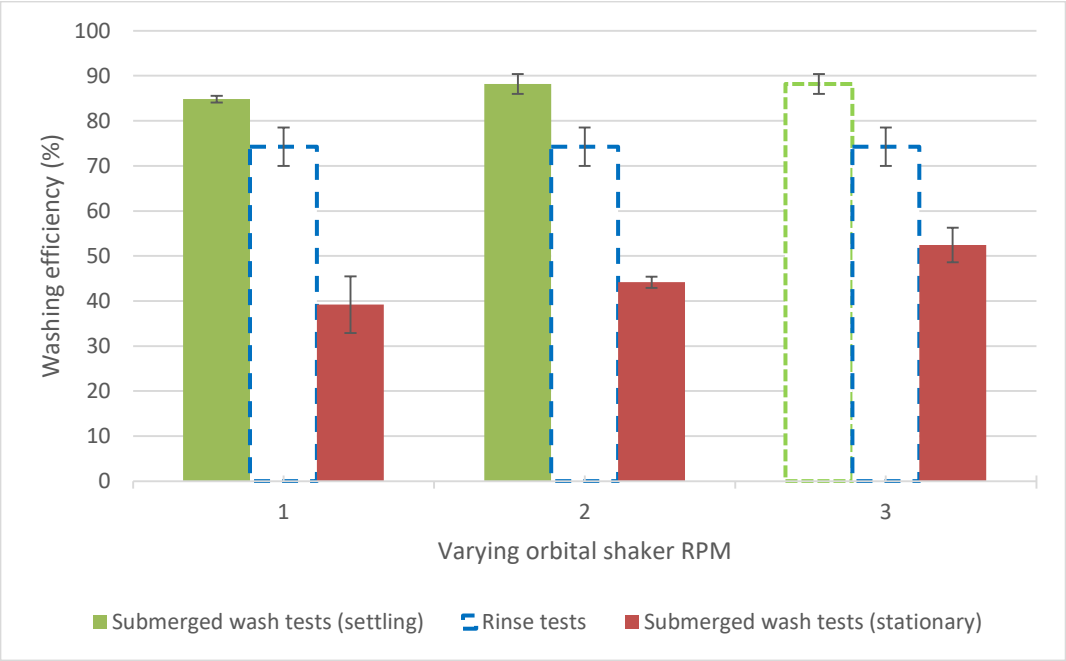

Figure 47. Washing efficiency of various bench tests,

The rinse tests results are repeated for all three orbital shaker RPMs on Figure 47 for ease of comparison. The rinse tests did not actually have a varying RPM because they were not performed on the orbital shaker. For this reason, the rinse test results are illustrated with a dotted blue line. Similarly, the submerged wash test (settling) is also illustrated with a dotted line at the highest orbital shaker setting of 105 RPM. Due to the shaking action, it was necessary to close the lid of the bucket that the tests were performed in to prevent spillage. However, for the settling submerged washing tests, the lid had to be open to drop the pulp into the water. Unfortunately, this resulted in excessive spillage, so the submerged washing test with settling could not be performed at the highest shaker RPM. For these tests, the results for 90 RPM are repeated at 105 RPM for direct comparison with the submerged washing (stationary) results at 105 RPM.

As illustrated in Figure 47, the lowest washing efficiency of 39.18% was achieved for submerged washing of a stationary bed at 75 RPM. Even though the washing efficiency increased to 52.44% with an increase in shaker speed to 105 RPM, this washing method remained the least effective. On this experimental setup, the pulp bed was shaken in an orbital motion, which caused the water to wash through the pulp bed. The FeSi particles were in suspension and ceased to adhere to the ore particles as they do when the pulp is not submerged, but the motion of the water was not sufficient to wash the FeSi particles from the

ore bed entirely. Furthermore, the fact that the ore particles remained stationary enhanced the bed's ability to retain the FeSi particles. In order to remove the medium effectively, it seems that the particle bed needs to be in motion to decrease the extent of obstruction that the stationary particles introduce to the washing and removal of the FeSi.

The second greatest and middle washing efficiency was achieved by the rinsing method. Even though the rinsing method also had a stationary particle bed, the one-directional motion of the water from top to bottom of the pulp bed enhanced the migration of particles towards the bottom of the bed. Instead of putting the FeSi particles in suspension and washing them in no particular direction for the stationary submerged washing tests, the rinsing tests continuously introduced fresh water to the top of the bed that carried the FeSi particles towards the screen surface and resulted in a greater washing efficiency of 74.24%.

The most effective washing method was submerged washing tests with settling. This method combined the benefits of having the FeSi particles in suspension to overcome the adhesive effects between the medium and ore particles, with the benefit of not having a stationary particle bed to obstruct the settling and drainage of the medium. Since the ore particles are in motion, there is more opportunity and space for the FeSi particles to exit the area of the particle bed and to drain through the screen surface and settle to the bottom of the water bed.

These submerged washing tests differ from the washing mechanism that would occur in a trommel (Mk1). It simulates the effect and proves the concept of overcoming adhesion between particles when they are in suspension, but the water and particle motion differs from the movement in a rotating drum screen. In a trommel, the particles are in constant motion and the particle bed is not stationary. From the results of these bench tests, it seems that the continuous movement of the ore particles would be beneficial to the effectiveness of submerged washing because it would continuously open up different paths through which the medium could migrate through the particle bed. Furthermore, the continuous movement of particles would expose a greater fraction of the surface area of the dirty ore particles to the washing water, thereby increasing the probability that adhering FeSi particles would enter suspension as opposed to being trapped within the particle bed. The rinsing tests indicates that it is beneficial if the washing water adhere to a downward direction through the particle bed, because FeSi particles are systematically migrated towards one side of the particle bed and ultimately gets removed from the bed without being re-introduced as a result of circular or sloshing motion of the water. As such, it is predicted that it would be ideal to combine these concepts in submerged washing, continuously feeding clean water to the top of the chamber

and having a controlled drain at the bottom of the chamber that would allow a level control of the water to ensure that the particle bed remains submerged.

5. SUMMARY AND RECOMMENDATIONS FOR SUBMERGED DMS TROMMEL 1 (Mk1)

The conclusions that were drawn from the first test campaign on the submerged DMS trommel (Mk1) are summarized below.

5.1. Drain chamber tests

5.1.1. Statistical significance of results

It was found that there was a systematic change in the system over the course of three repetitions. It was necessary to discard the first sample of each set, because the system was still in an onset phase during sampling. This implied a certain level of uncertainty in the results. As such, the results can only be used as a rough indication of screen performance, but further tests will have to be conducted to provide a higher level of confidence in the results.

5.1.2. Effect of ore mass in drain screen on clean ore transport rate

From the drainage tests in the drain chamber of the submerged DMS Trommel (Mk1), it was concluded that the ore transport rate is a function of the ore quantity in the screen. An increase in ore mass in the screen led to an increase in ore transport rate, to a maximum of approximately 0.97 kg/s for an ore mass exceeding 43 kg in the drain chamber.

5.1.3. Effect of medium RD on pulp transport rate

It was found that the introduction of medium to the ore not only resulted in medium adhesion to the ore, but that the medium also acted as an adhesive between ore particles. An increase in medium RD resulted in an increase in solids transport rate due to enhanced efficiency of the ore transport mechanism for a denser pulp. For an increase in RD from 2.7 to 3.6, the ore transport rate (clean, dried ore) increased from 1.17 kg/s to a maximum of 1.26 kg/s, where it appeared to plateau.

5.1.4. Effect of medium RD on FeSi carryover

It was found that there is a clear correlation between medium RD and FeSi carryover to the overflow stream. This result corresponds with findings of past studies (Napier-Munn, et al., 1995), (Kabondo, 2018). For an increase in medium RD from 2.7 to 3.6, the FeSi carryover rate increased from 0.54 t/hr to 1.10 t/hr and the weight % composition of FeSi in the overflow stream increased from 11.05 % to 18.76 %.

5.1.5. Effect of medium RD on moisture bypass

In addition to the increase in FeSi carryover with an increase in medium RD, the moisture carryover also increased from 0.16 t/hr to 0.21 t/hr, regardless of a slight decrease in water feed rate due to the change in medium RD. This result also corresponds with the trends

observed in literature that an increase in moisture bypass with an increase in medium RD results in an increase in FeSi carryover to the overflow, because the water is the main transport mechanism for fines in the system (Gupta & Yan, 2006).

5.1.6. Capacity limitation of drain chamber

The maximum ore transport rate that could be achieved under any circumstances from the drain chamber to the wash chamber was 1.26 kg/s. The scroll opening between the two chambers was filled entirely. This ore transport rate corresponds with a 5:1 medium to ore ratio in the screen, assuming that the ore transport rate is equal to the rate at which ore is fed at steady state. This implies that the trommel (Mk1) capacity is limited by the ore transport mechanism, because an increase in feed rate will result in an accumulation of ore in the screen, but the medium drainage rate was still well under maximum capacity under these conditions.

5.1.7. Comparison of drain chamber performance with vibrating screen performance

5.1.7.1. % Moisture in overflow

The % moisture in the overflow on the vibrating screen at a medium RD in the range of 1.9 – 2.3 was significantly higher than the % moisture in the overflow of the DMS submerged trommel (Mk1). In the vibrating screen overflow, the % moisture was in the range of 10.29 % to 27.91 %, compared to a value of approximately 3.18 % in Test Trommel Mk1 overflow. It is however important to note that the vibrating screen was operated at a much higher feed rate and the % moisture in the trommel (Mk1) overflow is also expected to increase with an increase in feed rate. The results are nonetheless promising and encourage further investigation of trommels as an alternative to vibrating drain and rinse screens.

5.1.7.2. % FeSi in overflow

The FeSi content in the DMS Trommel (Mk1) was within the same range as in the vibrating screen overflow, even though the trommel test work was performed at a significantly higher RD. The FeSi mass concentration in the vibrating screen overflow was around 9.71 % to 36.01%, compared to a maximum of 18.76 % on the DMS Trommel (Mk1). Once again, this result is greatly impacted by the higher feed rates on the vibrating screen. However, the fact that the trommel (Mk1) overflow had competitively low FeSi content in the overflow at significantly higher medium RDs is still a promising result with regards to the viability of a trommel as an alternative to vibrating drain screens.

5.1.7.3. % FeSi carryover

The % FeSi carryover on the DMS Trommel (Mk1) had a maximum value of 4.96 % at a medium RD of 3.3. Similar to the observations made for FeSi and moisture concentration in the overflow, this value fell in the lower end of the range of % FeSi carryover that was achieved on the vibrating screen. On the vibrating screen at a medium RD of 1.9, which was significantly lower than the medium RD of 3.3 on the DMS trommel (Mk1), the % FeSi carryover ranged between 3.12 % and 6.88 %.

5.1.7.4. Final conclusion: Drain chamber

Due to the variance and uncertainty associated with the DMS Trommel (Mk1) results, the tests would have to be repeated on an improved design of the DMS trommel (Mk1) to provide more certainty in the conclusions that were drawn. With that said, all the results that were produced on the DMS trommel (Mk1) indicated that the trommel is a viable alternative to the vibrating drain and rinse screen. This justifies further investigation of the trommel as a competitive alternative.

5.2. Washing tests

5.2.1. Wash chamber tests

The batch tests that were performed in the wash chamber indicated that approximately 96 % of the FeSi that was adhered to the ore being loaded into the submerged bath was washed by merely submerging and extracting the ore. After a single rotation of the screen, the washing efficiency was 99.7 %. This is a staggeringly impressive result that highly encouraged further investigation of submerged washing as a means of medium recovery.

5.2.2. Bench rinse and wash tests

The bench rinse and wash tests revealed that the lowest washing efficiency of 39.18 % was achieved for stationary submerged washing at the lowest orbital shaker speed of 75 RPM. An increase in shaker speed to 105 RPM improved the washing efficiency to 52.44 %, which was still significantly lower than the washing efficiency of 74.24 % that was achieved by rinsing of the bed. This is because submersion is not sufficient to settle FeSi from the ore bed. Flow of water from one side of the bed to the other side transports the fine FeSi particles away from the ore particles.

The highest washing efficiency of 88.18 % was achieved for submerged washing of a settling particle bed. The obstruction of FeSi settling was decreased with an ore bed that is in motion, while the benefit of complete submersion to overcome the adhesive forces between the medium and ore particles was still in effect.

5.2.2.1. Final conclusion: Washing tests

The results of the washing tests concluded that submerged washing is an immensely promising concept in the context of medium recovery. It is highly recommended to continue work to investigate this concept.

6. DESIGN CONSIDERATIONS: TROMMEL 2 (Mk2)

Due to the severe limitations imposed by the design of Test Trommel Mk1, the statistical significance of the data was low. Even though the results appeared to be promising enough to motivate the trommel as a viable alternative to the vibrating drain and rinse screen, it was necessary to increase the certainty in the results before a final conclusion could be made. The results for efficiency of submerged washing were too promising to discard as an alternative to the rinsing section of the drain and rinse vibrating screen. For these compelling reasons, it was decided to continue the investigation on an improved design of the DMS Test Trommel. Some of the most important considerations for the design of Test Trommel Mk2 are listed and discussed:

6.1. Simplification of process

One of the major problems with DMS Trommel Mk1 was the over-complication of the process. Instead of starting simple and understanding the fundamentals of the process before improving the design thereafter, the first iteration of the trommel (Mk1) was designed to fulfil a magnitude of functions including:

- Drainage of medium;
- Complex ore transport mechanism between chambers;
- Submerged washing and
- Multi-chamber continuous operation.

In an attempt to perform all of these functions, the system was over-complicated to the point where none of these functions could be investigated properly. In order to address this problem, it was decided to design a simplified drain trommel (Mk2) to perform drainage tests only. Once the drainage section of the trommel (Mk2) is understood, the other functions like submerged washing will be considered.

6.2. Ore transport limitation and inaccessibility

In DMS Trommel Mk1 the material was fed inside the screen and transported with a solids transport mechanism from inside of the same screen. This rendered the screen entirely inaccessible during operation, which led to a great deal of uncertainty about what was occurring inside of the trommel (Mk1) during operation. Furthermore, it was found that the ore transport mechanism severely limited the capacity of the trommel.

In order to address both of these problems, it was decided to design the drain section of Trommel Mk2 with an open overflow discharge. This will introduce an access point into the trommel (Mk2) from where visual inspection can be done inside the trommel during

operation. In addition, an open overflow discharge on a trommel equipped with the appropriate scroll configuration will not limit the capacity of the trommel. Instead, the capacity of the trommel (Mk2) will only be limited by the drainage capacity of the panels.

6.3. Inadequate support equipment

Another severe limitation on the experimental work was imposed by the size of the pump and the lack of a VFD on the pump during Mk1 test work. The flow rate of the medium in the first test campaign was limited to the maximum pump speed of that pump, which prevented adjustment of feed rates. In order to overcome this issue, a 4/3 pump with a VFD was motivated to accompany the design of Trommel Mk2.

6.4. Location

At Stellenbosch University, all test work had to be performed inside of the lab building. As a result of design shortcomings of Trommel Mk1, the test work was accompanied by significant spillage. Due to strict housekeeping rules and limited manpower at Stellenbosch University, many hours were lost to the never-ending battle against spillage. It was decided that the test facilities at Multotec Manufacturing, located in Spartan, Kempton Park, would be a more appropriate location to conduct the test work.

6.5. Inability to achieve steady state operation

The design of Trommel Mk1 was a series of chambers that fed each other in sequence. The inability to bypass these chambers or to operate a single chamber in isolation resulted in the inability to reach steady state operation. Immense effort was put into simulating steady state in the drain chamber, which unfortunately introduced a great deal of uncertainty in the results that were produced on Trommel Mk1. Designing a drain trommel (Mk2) that is operated separately from down-stream processes will greatly enhance the confidence in the results produced on Trommel Mk2, because steady state operation can be achieved instead of mimicked.

6.6. Sampling

One of the most important aspects of test work is to ensure accurate sampling. With the design of Trommel Mk1, the overflow steam was sampled by placing a plastic cover inside of the wash chamber (chamber 2) and collecting the ore that transported during rotation of the trommel (Mk1), as illustrated again in Figure 48:

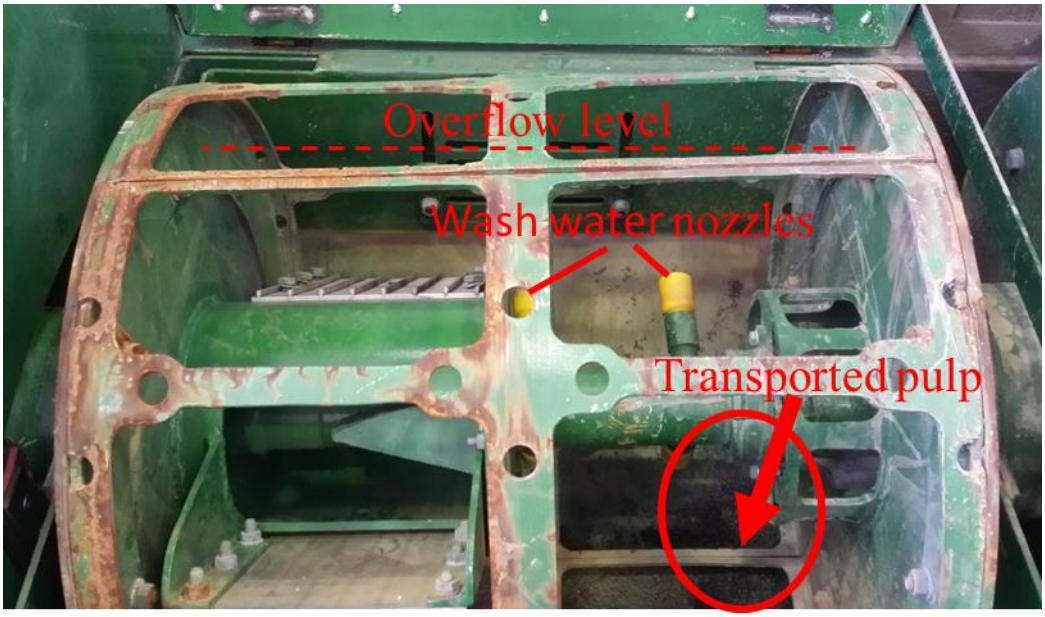

Figure 48. Photograph of location of pulp collection in wash chamber after being transported from drain chamber in Submerged DMS Trommel (Mk1).

The screen bracket in the wash chamber was an obstacle that made it extremely difficult to collect the transported pulp from the bottom of the wash chamber without spilling or contaminating the sample and thereby compromising the integrity of the work. In order to address this issue, it was decided that the best approach would be to separate the drain trommel (Mk2) from the submerged wash trommel (Mk2). The drain trommel will have an open overflow discharge so that the material can be transported freely. This would allow ease of sampling of the overflow discharge.

Furthermore, the inaccessibility of the screen combined with the fact that the screen was only equipped with a single underflow discharge, prevented the investigation of the inner workings of the trommel (Mk1). Instead, it was decided that sampling multiple underflow discharges from various positions under the screen would provide more information about what is occurring inside of the trommel (Mk2) during operation. This sampling mechanism will be discussed in more detail in the equipment description section of Trommel Mk2 following after this section.

6.7. Equipment height

Due to the density of FeSi, the material tends to settle extremely fast. As a result, settling in the system was a problem, because the equipment was not high enough to allow vertical underflow discharges. Instead, the underflow discharges were angled between 30^{o} and 40^{o} from the horizontal position. This was an insufficient angle to prevent the settling of FeSi in the pipes.

With motivation to design the trommel (Mk2) with an open overflow discharge end, as discussed before, the material will not be transported with a solids transport mechanism anymore. Instead, the solids will have to be fed to the submerged trommel by gravity. The submerged trommel will have to be high enough to allow 60^{o} angles for the water bath, to prevent excessive settling in the submerged chamber. This implies that the drain trommel (Mk2) will have to exceed this height to allow the overflow discharge to feed the submerged trommel with gravity. This is illustrated in Figure 49.

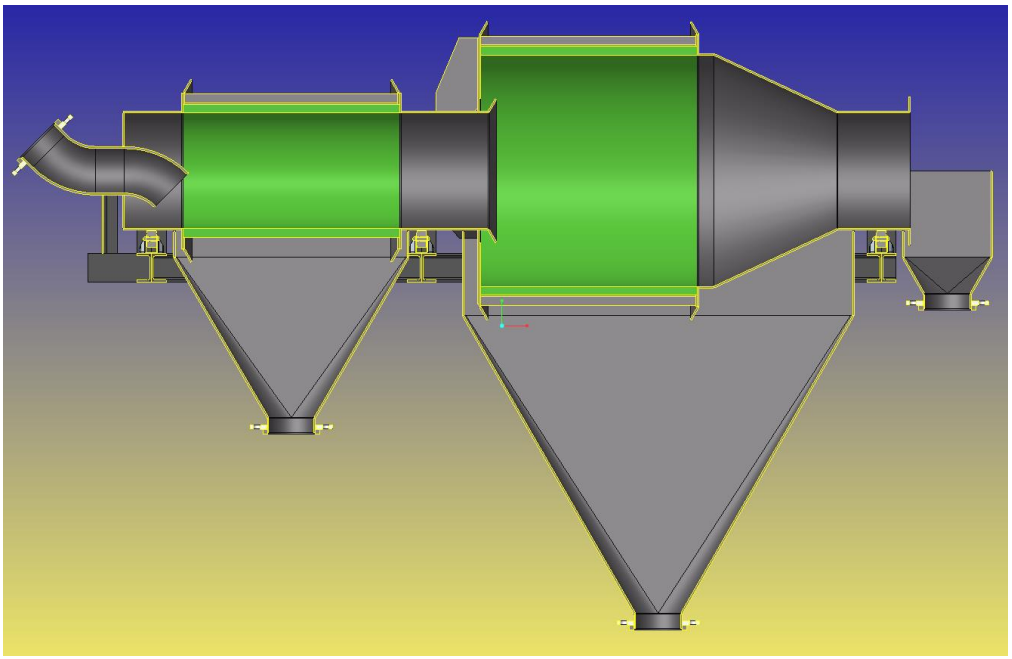

Figure 49. Conceptual drawing of Test Trommel Mk2: Drain trommel and Submerged washing trommel.

For all of these reasons, the trommel was designed to operate at a height of approximately 2.3 m.

6.8. Screen media

During the first test campaign, there was difficulty with fitting typical screen panels into the trommel (Mk1). Due to the small diameter of the trommel (Mk1), normal trommel panels could not fit in the screen brackets without rolling the panels further to match the diameter of the screen bracket. The problem with rolling the panels to such a small diameter is distortion of the apertures. Some apertures tend to open up, while others tend to get forces shut with such extreme rolling of the panels. Eventually for the first test campaign, it was decided to use a flexible rubber mat with punched apertures, however it was found that loading these mats with ore masses exceeding 30kg, the apertures also distorted due to the flexibility of the screen media. It was decided that a new specialised panel would have to be designed for the Test Trommel Mk2.

7. EXPERIMENTAL SETUP AND DESIGN: TEST TROMMEL 2 (Mk2)

7.1. Characterisation of equipment

This section consists of a brief equipment description of the second Test Trommel (Mk2) that was manufactured from the lessons that were learnt during the first test campaign on the original submerged DMS test trommel Mk1.

The approach with the second test trommel (Mk2) was to keep the equipment as simple as possible in an attempt to add value to the results by not overcomplicating the problem by attempting to accomplish too many things at once. The second test trommel (Mk2) consisted of only a single stage, drain section. The objective was to repeat the drainage test work on the second test trommel (Mk2) and to compare the results to that of the drain section of the original DMS Trommel Mk1. After quantifying and understanding the drainage of Test Trommel Mk2, the submerged stage of the trommel, which will be fed by the overflow of the drain stage of Test Trommel Mk2, will be designed and manufactured for future work on submerged washing. Figure 50 illustrates Test Trommel Mk2 after manufacturing and commissioning.

Figure 50. Photograph of Test Trommel Mk2.

In Figure 50, the slurry from the sump is pumped by the pump (5) and discharged to the trommel feed (1). The Mk2 Trommel (2) is driven by a hydraulic motor at 24 RPM. The

aperture of the screening media was selected as 0.8 mm x 13 mm and an open area of approximately 15 %, to correspond with that of the previous study. The trommel retains the coarser ore particles in the screen, which reports to the overflow stream (3) and is recirculated back to the sump. The medium is drained through the underflow discharges (4) back to the sump. The feed configuration is illustrated in Figure 51.

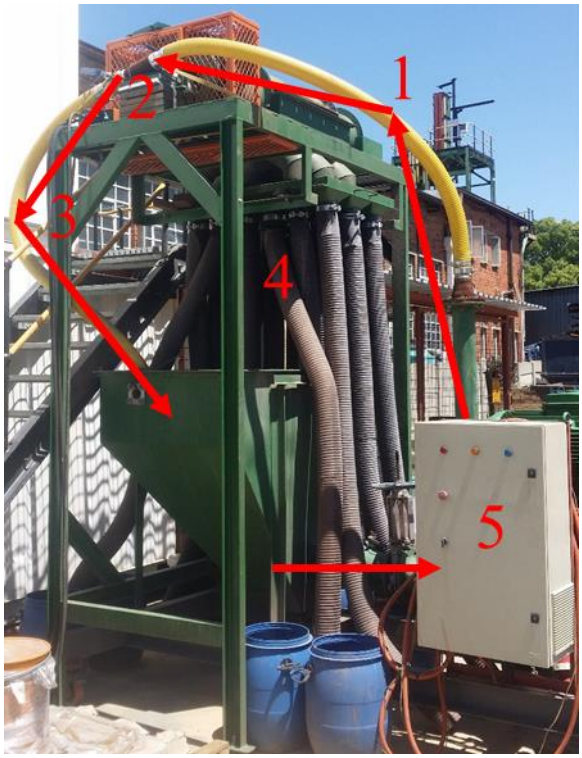

Figure 51. Photograph and illustration of Test Trommel 2 flow circuit.

The slurry is pumped by the pump at a fixed speed, set on the VSD (5), towards the feed end of the trommel. A T-piece (2) is installed at the feed end of the trommel to split the stream into a bypass stream (3) and the feed stream to the trommel. The bypass stream is required to agitate the slurry in the sump, because the underflow discharges (4) prevent the installation of an agitator in the sump.

The equipment drawing for the trommel (Mk2) frame is presented in Figure 52 to specify the dimensions.

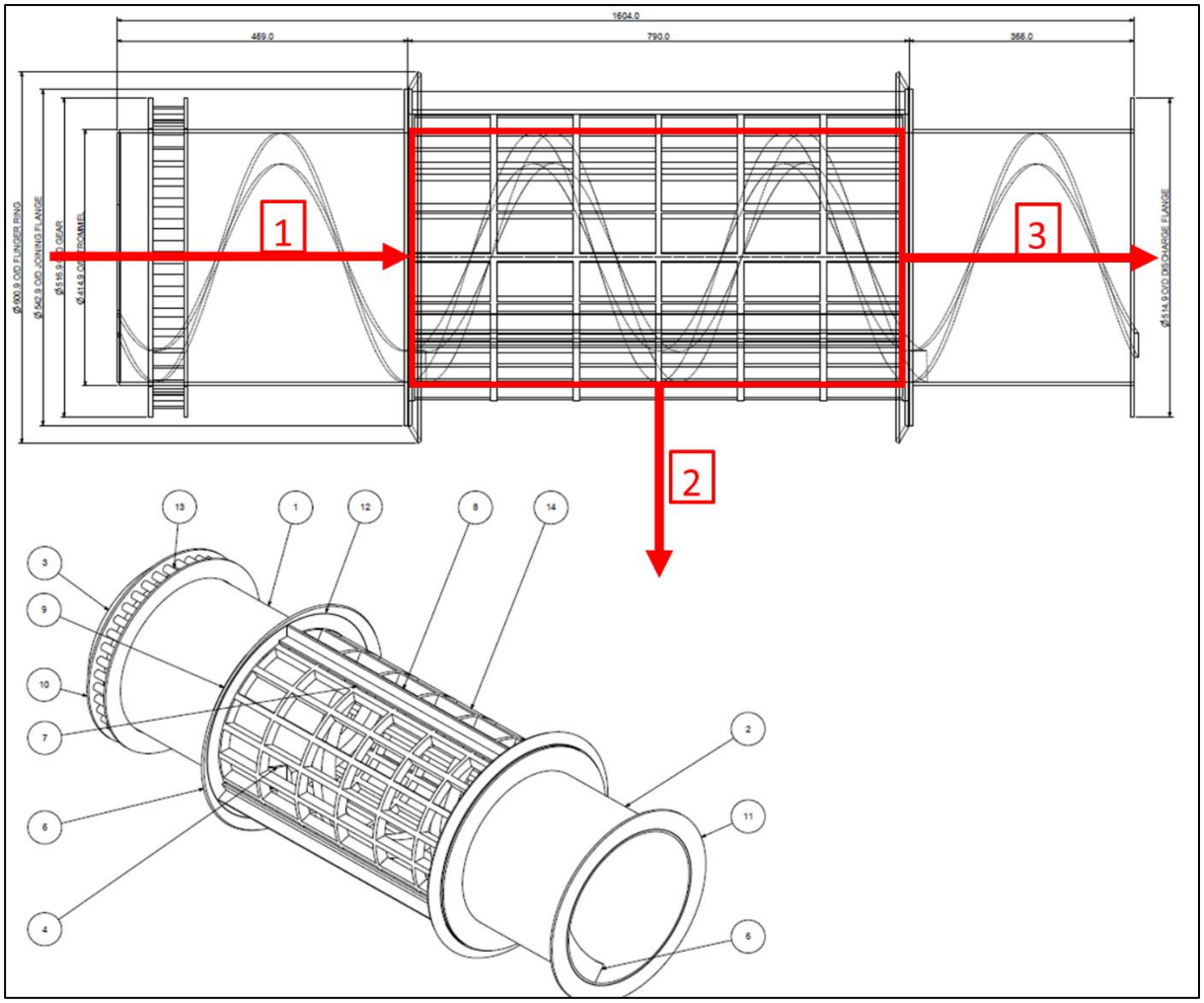

Figure 52. Equipment drawing of Test Trommel Mk2.

The feed (1) and discharge (3) ends of the trommel (Mk2) are equipped with extensions that are blanked off to allow development of flow. These sections do not have screening media and therefore no drainage occurs in these sections. The diameter of the trommel (Mk2) is 0.415 m and the length is 0.790 m. The scroll pitch is 0.395 m, resulting in a two pass, single start scroll configuration.

7.1.1. Underflow discharge notation

Due to the inaccessibility of a trommel during operation, historically it has been unknown what exactly occurs inside of a trommel during operation with regards to material distribution and drainage through various sections of the screen. Therefore the discharge chutes for this trommel (Mk2) was designed to sample sections of the trommel (Mk2) underflow at specific positions under the screen. The underflow discharge chutes were designed in a 3x3 grid under the trommel (Mk2) to sample a total of 9 underflows, which will provide insight into the

material distribution inside of the trommel (Mk2) during operation. The trommel underflow discharge layout and notation are established in Figure 53.

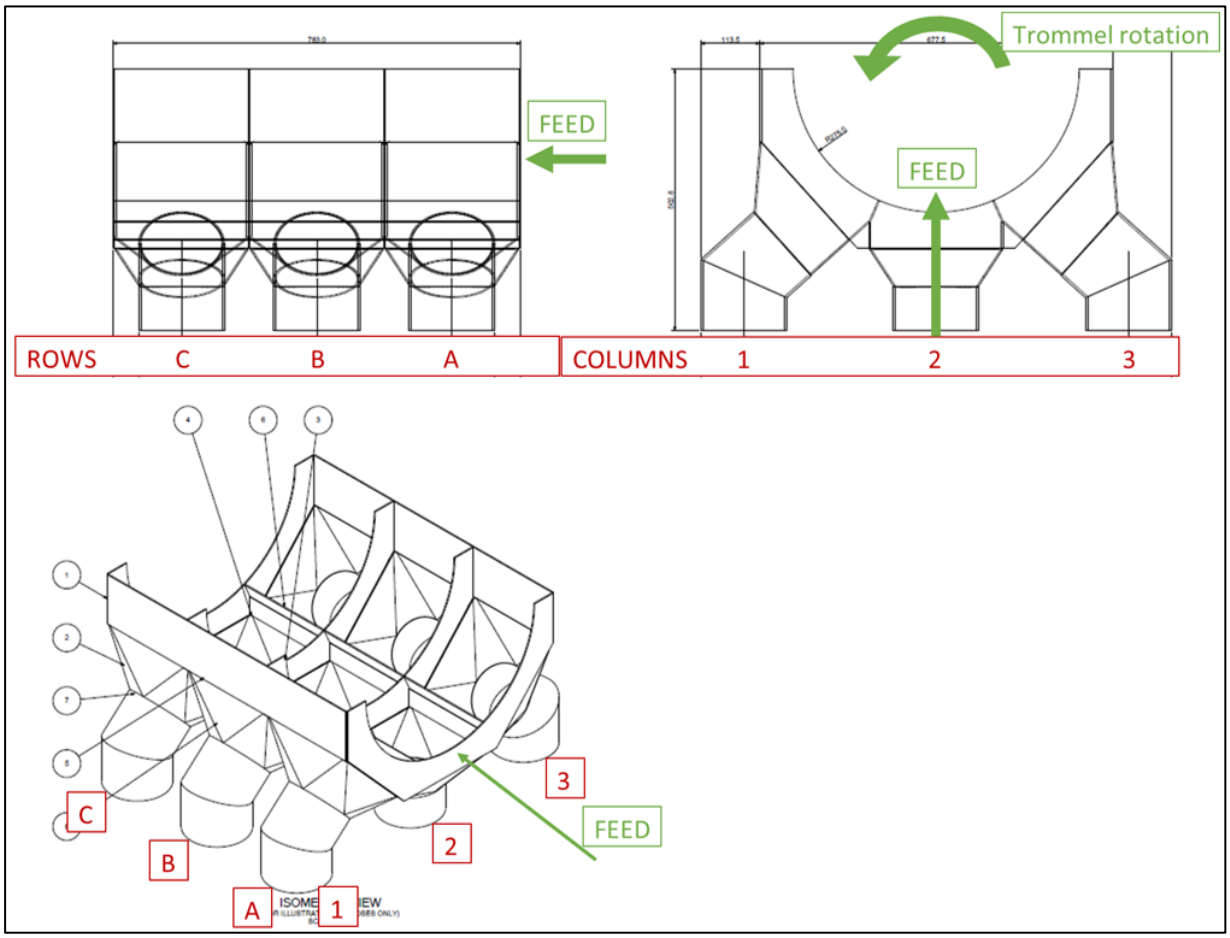

Figure 53. Notation of underflow discharges of Test Trommel Mk2.

The discharges are named with regards to their position in the grid. The grid is noted from the Mk2 trommel's feed end perspective. The first row of discharges closest to the feed end is Row A. The second row of discharges, which is the middle row of discharges, is Row B. The final row of underflow discharges right before the overflow discharge is named Row C. Similarly, the underflow discharges are named according to their position from left to right (from the feed end perspective of the Mk2 trommel). The first column on the left side of the trommel (Mk2) is Column 1. The middle row of underflow discharges is called Column 2, and the final column of discharges to the right of the trommel (Mk2) is named Column 3.

7.1.2. Underflow sampling mechanism

In order to sample 9 different underflow discharges simultaneously, it was required to develop a sampling mechanism that would facilitate that. Under the trommel (Mk2) discharge chutes, a sampling tray was installed. This tray is mounted on four wheels that allow it to be rolled from one side to the other. This tray consists of a grid of 3 x 6 discharges, with pipes

attached to each discharge. Along the length of the trommel (Mk2), from Row A to Row C, all tray discharges align with the underflow discharges. However, along the width of the trommel (Mk2), only alternating tray discharges align with the trommel (Mk2) underflow discharges. Every second row on the sampling tray is utilised at a time while the rest are inactive. During steady state operation, the tray discharges that have pipes re-circulating to the sump align with the trommel (Mk2) underflow discharges. This facilitates circulation of all material during operation. During sampling, the tray is rolled from one side to the other, aligning the other half of tray discharges with the trommel (Mk2) underflow discharges. The pipes connected to these tray discharges are placed into sampling buckets next to the sump. While the sampling discharges are aligned with the trommel (Mk2) underflow discharges, the underflow streams feed into the sampling buckets. After sampling, the sampling tray is rolled back into the re-circulating position. The sampling tray is illustrated in Figure 54.

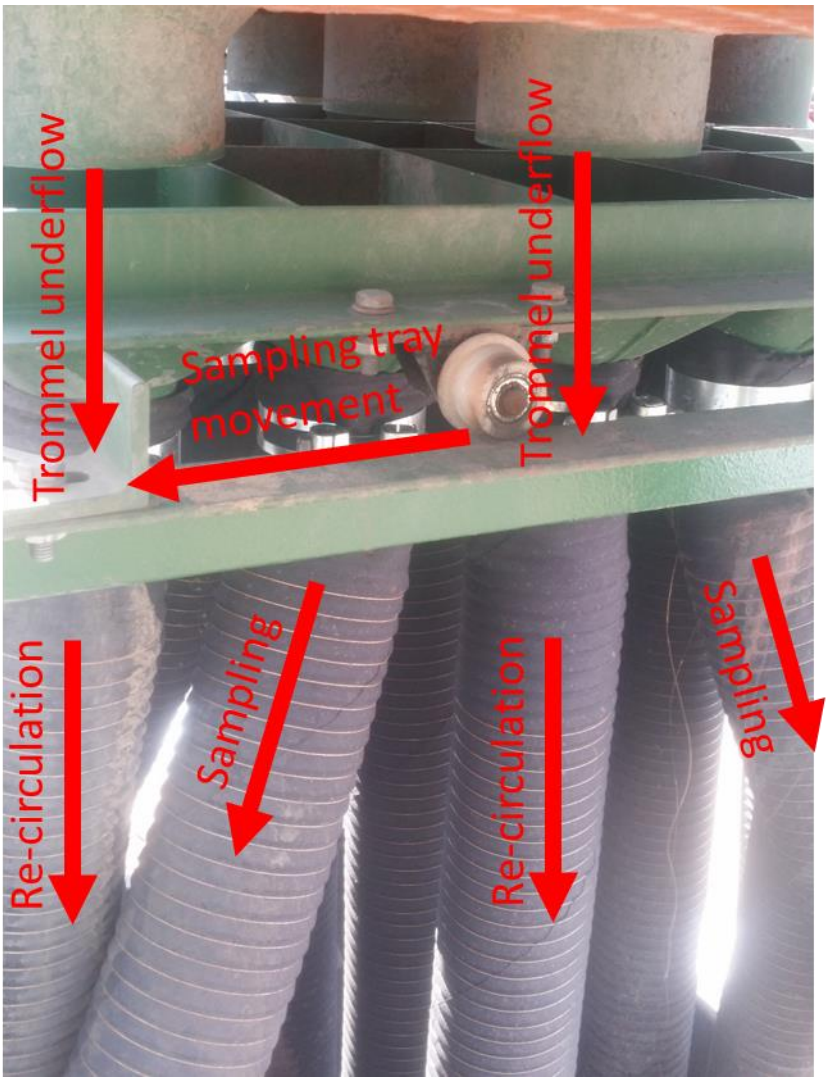

Figure 54. Photograph of Test Trommel Mk2 sampling tray and tray motion.

A detailed step-wise procedure for Test Trommel (Mk2) is provided in Appendix C.

8. RESULTS AND DISCUSSION: TEST TROMMEL 2 (Mk2)

8.1. Introduction

Due to the low statistical significance of the data that was produced on the first iteration of the DMS Trommel (Mk1), it was decided to reproduce the tests on Test Trommel Mk2 to determine whether or not the promising results of Test Trommel Mk1 are trustworthy. However, due to the improved sampling mechanism that allows the investigation of material distribution inside of Test Trommel Mk2, the feed rate was also varied to provide some insight into its effect on material distribution and underflow rates at various positions in the Mk2 trommel. These tests were performed in full at an RD of 1 (water), with three repeats of each run. Unfortunately, due to time constraints, the feed rate effect on DMS test work could not be performed with three repeats of each run. The effect of medium RD on the performance of the screen, similar to the tests that were performed on DMS Trommel Mk1, was performed with repeats to ensure statistical significance. No repeats were carried out for the variation of feed rate during the DMS work for each medium RD.

8.2. Water tests

As part of the commissioning of the new trommel (Mk2), tests were performed with water only (RD 1) at various feed rates. This was done as the first step towards understanding the operation of the new equipment. The tests were also intended to gain some insight into the limits of operation of the test trommel (Mk2).

8.2.1. Effect of feed rate on trommel operation

The feed rate was varied by adjusting the VFD on the pump. The appropriate feed rates were determined according to observations during the commissioning phase. The lowest feed rate was selected such that the majority of the water drains in the first row of discharges in the trommel (Mk2). The maximum feed rate was selected such that the trommel (Mk2) was substantially beyond saturation and there was a significant flow rate of water reporting to the overflow discharge (approximately 30% of the total feed). Two intermediate feed rates were selected between the minimum and maximum feed rates.

8.2.1.1. Row comparison: Row A

The first set of results is the comparison of flow rates through Columns 1, 2 and 3 in Row A (The first row of discharges closest to the feed end of the Mk2 trommel). The discharges in Row A that will be evaluated, are highlighted in Figure 55. The results are plotted in Figure 56 thereafter.

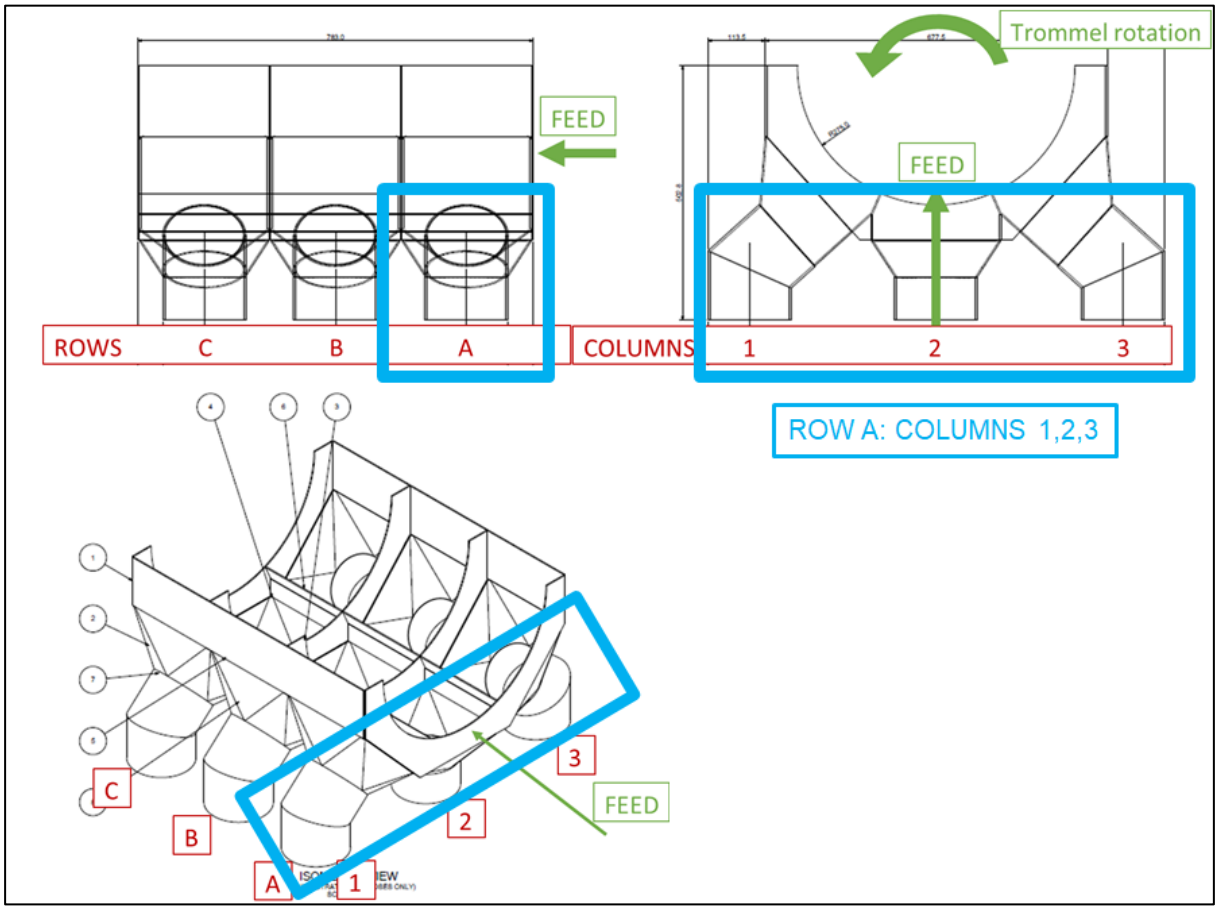

Figure 55. Illustration of discharge Row A, Columns 1, 2 and 3.

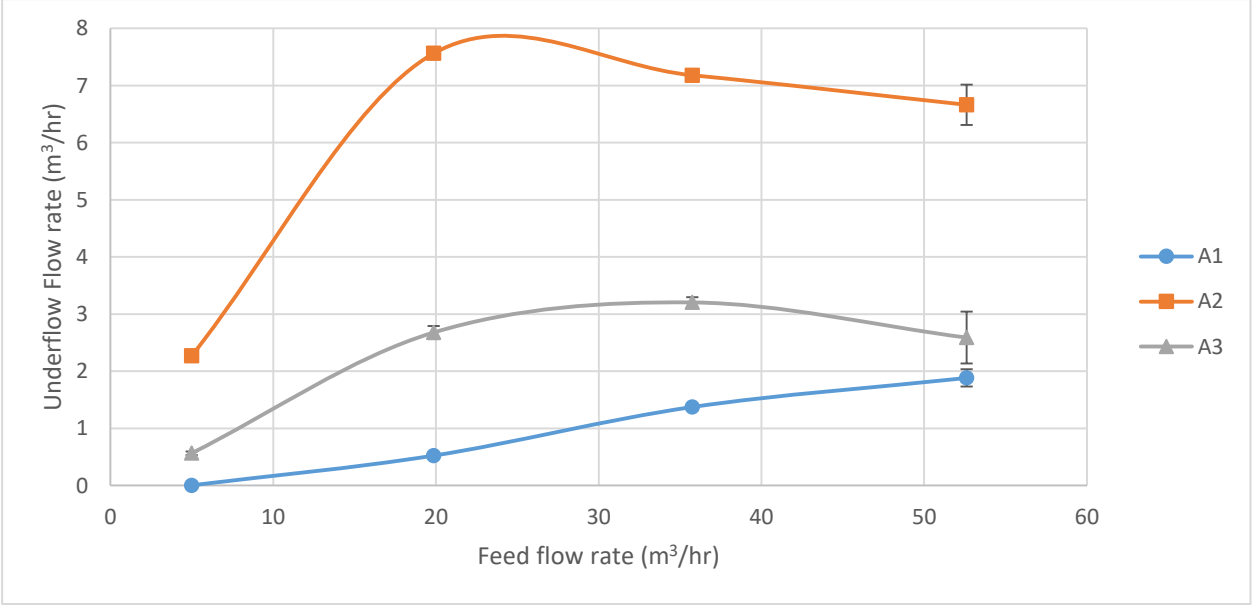

Figure 56. Water tests underflow rates for Row A over feed rate range.

The first observation from the results in Figure 61 reveals that the difference in underflow rate through the discharges in the various columns of the first row. The highest drainage was achieved through Column 2, followed by Column 3 and lastly Column 1. The majority of material in the Mk2 trommel resides in the middle of the trommel, above Column 2.

Therefore, at this feed rate, the highest drainage occurs through the middle row of discharges. More water in a particular region on the screen leads to a higher material depth which, in turn, leads to a greater hydrostatic pressure. This promotes a greater drainage rate in that particular region. Recall that the Mk2 trommel rotates in an anti-clockwise direction from the feed end perspective. This means that the direction of Mk2 trommel rotation proceeds from Column 1 to 3. As a result, the drainage in Column 3 is greater than Column 1, because the rotation of the Mk2 trommel shifts the water distribution inside the trommel slightly towards the direction of rotation.

As shown in Figure 56, there is a general increase in underflow rate for an increase in feed rate while operated under screen capacity. This is because an increase in feed rate leads to an increase in water volume inside the trommel (Mk2). An increase in water volume, in turn leads to an increase in hydrostatic pressure on the screen surface, which promotes drainage through the screen apertures. At the lowest feed rate of 5.00 m^3/hr, the underflow rate of discharge A2 starts at 2.27 m^3/hr. With an increase in feed rate to 19.86m^3/hr, the underflow rate of discharge A2 increases to 7.56 m^3/hr, after which it seems to decrease gradually for a further increase in feed rate to 52.61 m^3/hr. If this curve plateaued, it would imply that the screen surface above discharge A2 has been saturated and that excess material fed to this section of the screen would flow over to next sections of the screen. The fact that it decreases instead of plateau could be caused by experimental error, however the statistical analysis of the results showed a high repeatability, as indicated by the small range for the 95 % confidence interval. The decrease is therefore caused by a different factor that will be discussed after completion of discussion of this set of data.

Discharge A3 starts at an underflow rate of 0.57 m^3/hr for the lowest feed rate, increasing gradually to 3.21 m^3/hr with an increase in feed rate to 35.76 m^3/hr. With a further increase in feed rate, the underflow rate through discharge A3 also seem to decrease like discharge A2.

At the lowest feed rate, discharge A1's underflow rate is practically negligible at 0.004 m^3/hr. With an increase in feed rate, however, the underflow rate through discharge A1 also gradually increases to 1.88 m^3/hr, but never quite reaches the drainage that is achieved through the other two columns.

8.2.1.2. Water flow inside of Mk2 trommel during operation

In order to understand the underflow rates that were discussed in the previous section, it is necessary to evaluate the flow pattern of water inside the Mk2 trommel at different feed rates.

Figure 57 contains screen captures of videos that were recorded from the discharge end of the trommel (Mk2) during test work.

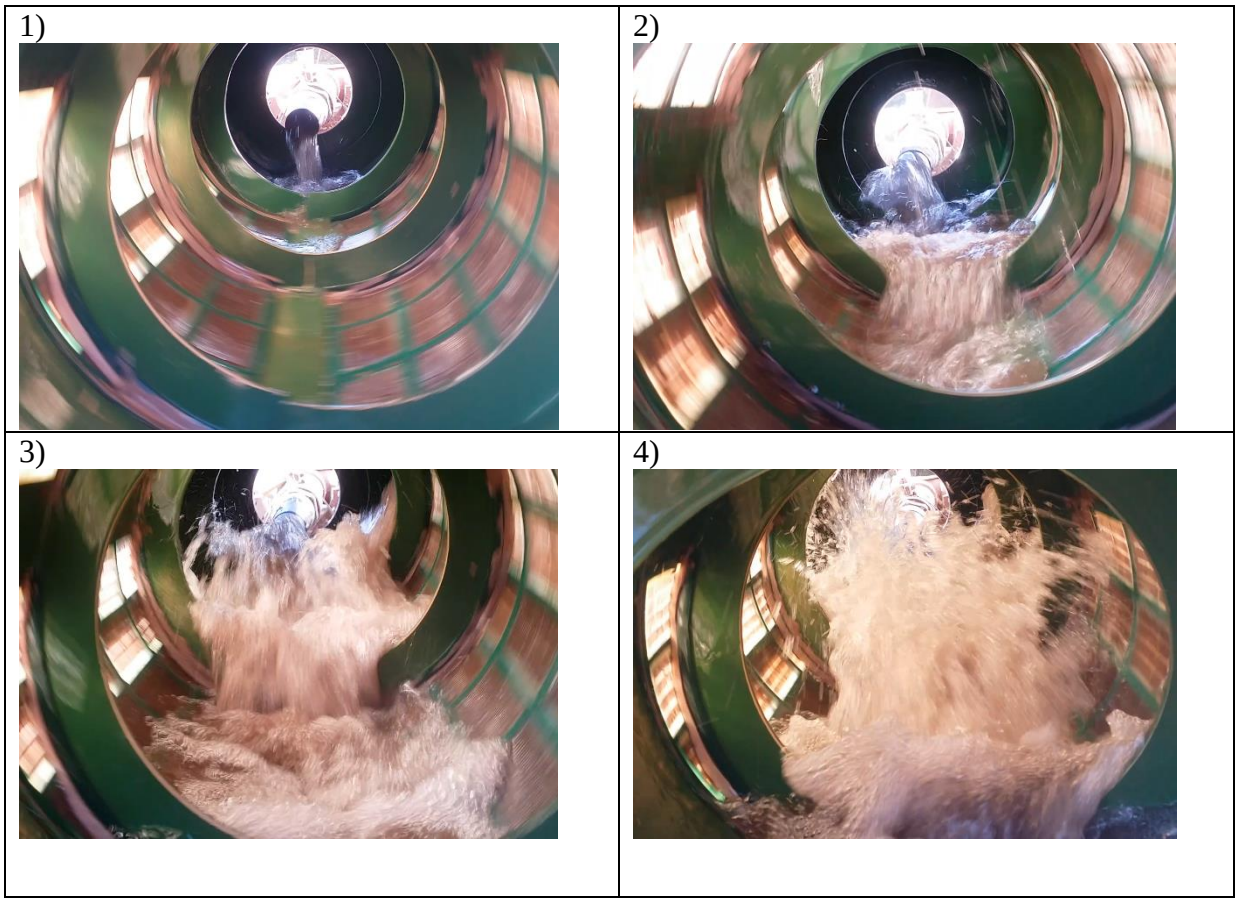

Figure 57. Photographs of water flow pattern inside Test Trommel (Mk2) during operation.

At the lower feed rates of 5.00 m^3/hr and 19.86 m^3/hr (photos number 1 and 2 in Figure 57), the flow inside of the Mk2 trommel has relatively low velocity (0.08 m/s) and low splashing. As the feed is increased to 35.76 m^3/hr (3), the flow increases in velocity (54 m/s) and splashing increases. Some water that enters the Mk2 trommel makes contact with the first scroll near the feed end and ramps slightly, causing a fraction of the water to travel along the length of the Mk2 trommel without making contact with the screen surface. At the highest feed rate of 52.61 m^3/hr, the flow inside of the Mk2 trommel has high velocity (0.8 m/s) and a large fraction of the water does not make contact with the screen surface.

The flow pattern inside of the Mk2 trommel at high feed rates provides some insight into the results for underflow rates at these feed rates. The momentum of the water and high velocity and splashing causes the water to bypass a substantial fraction of the screen area without getting any opportunity to drain through the apertures near the feed end of the Mk2 trommel. This is unideal operation of the Mk2 trommel since the screen is not being utilised to its full capacity. Such a high velocity and excessive splashing causes inefficiency of the screen if the material is allowed to bypass the screen surface. Furthermore, the high velocity and splashing

prevents the formation of a material bed, which negates the effect that hydrostatic pressure would have on enhancing drainage.

It is possible that high velocity and splashing in the Mk2 trommel could be beneficial in some applications if the flow is directed to make contact with the screen surface, as opposed to being propelled into the middle of the Mk2 trommel volume like it is in cases 3 and 4 in Figure 57. With high momentum and splashing flow, it could be possible to spread the material across a greater fraction of the total screen surface, for example the sides of the Mk2 trommel, that would not otherwise be utilised if gravity causes the material to reside exclusively in the bottom of the trommel. It is however speculation at this point and it is still unclear to what extent this would be beneficial, while the lack of hydrostatic pressure caused by a material bed would be detrimental to the total drainage that can be achieved by the screen area at the bottom of the trommel.

8.2.1.3. Row comparison: Row B

The next set of results is the comparison of the three columns in the second row of underflow discharges, Row B. First, Row B discharges are highlighted in Figure 58.The results are plotted in Figure 59 thereafter.

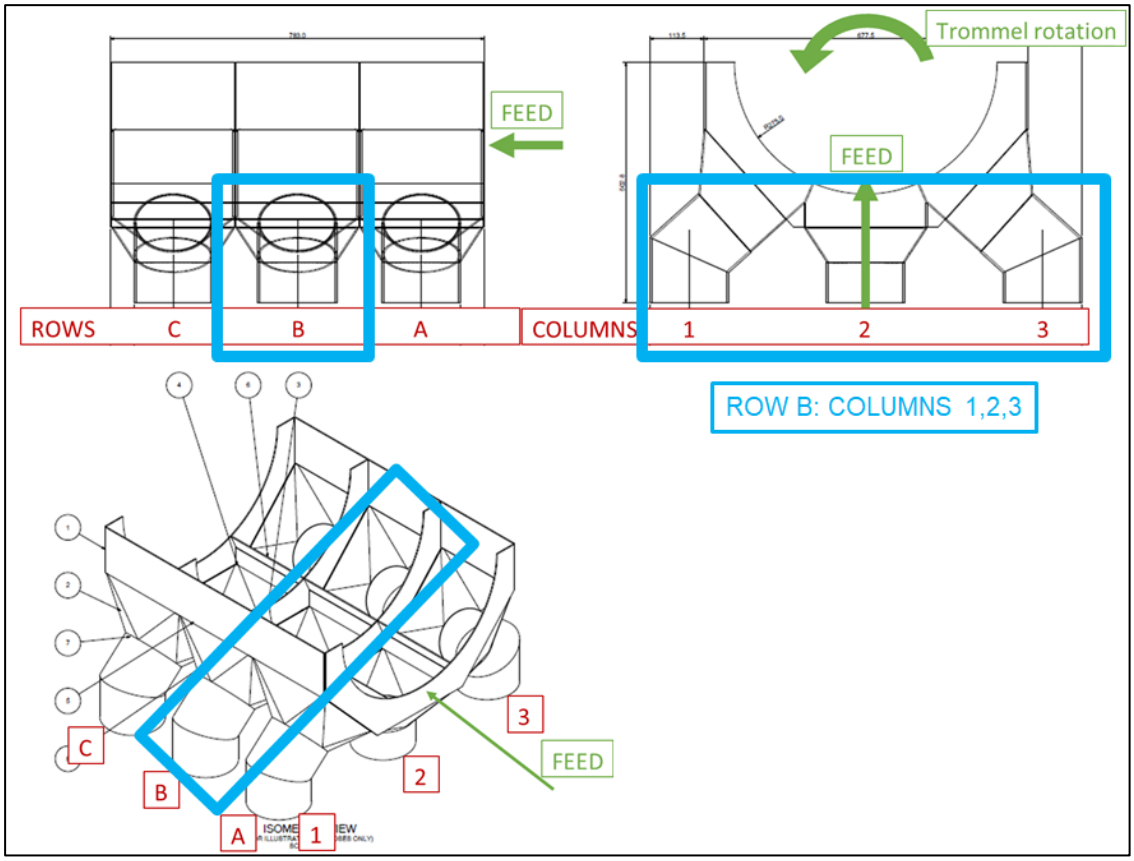

Figure 58. Illustration of discharge Row B, Columns 1, 2 and 3.

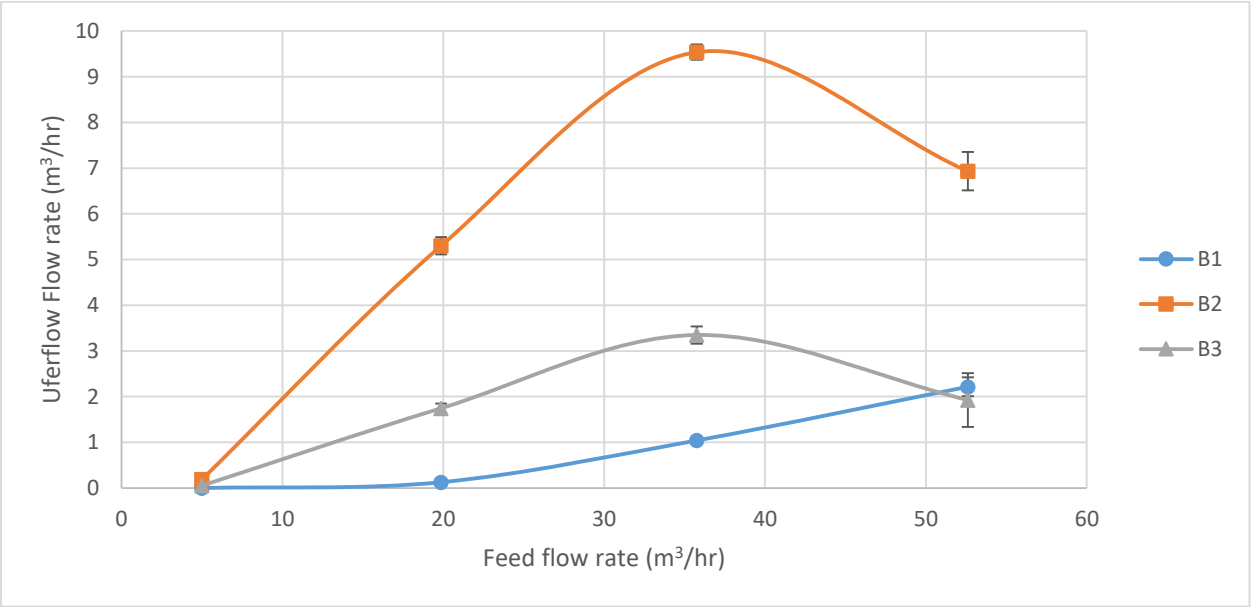

Figure 59. Water tests underflow rates for Row B over feed rate range.

A similar trend is observed with regards to the underflow rates achieved through the different columns in Row B. The highest drainage is through Column 2, followed by Column 3 which is towards the direction of rotation of the Mk2 trommel and finally the lowest drainage through Column 1.

In Row B, Column 2's underflow rate does not peak at 7.56 m^3/hr like discharge A2 did. Instead, the underflow rate of discharge B2 continued to increase to 9.54 m^3/hr for a further increase in feed rate to 35.76 m^3/hr. This indicates that the panels at discharge A2 have not been saturated and it confirms the theory that the drainage rate is limited by the high velocity and splashing of the flow in the trommel.

The underflow rates through second row of discharges all originate close to zero at the lowest feed rate. This is because the first row of panels were able to drain the entirety of material that was fed to the screen. As the feed rate increases, the underflow rate increases for all three discharges in Row B. The increasing flow velocity and splashing in the Mk2 trommel does not affect the second row of panels as soon as the first, but after increasing the feed rate beyond 35.76 m^3/hr, the drainage through discharges B2 and B3 also starts to deteriorate, while discharge B1 continues to increase.

8.2.1.4. Row comparison: Row C

The final row of discharges (Row C) is highlighted in Figure 60. The results for underflow rates through the final row of discharges are plotted in Figure 61 thereafter.

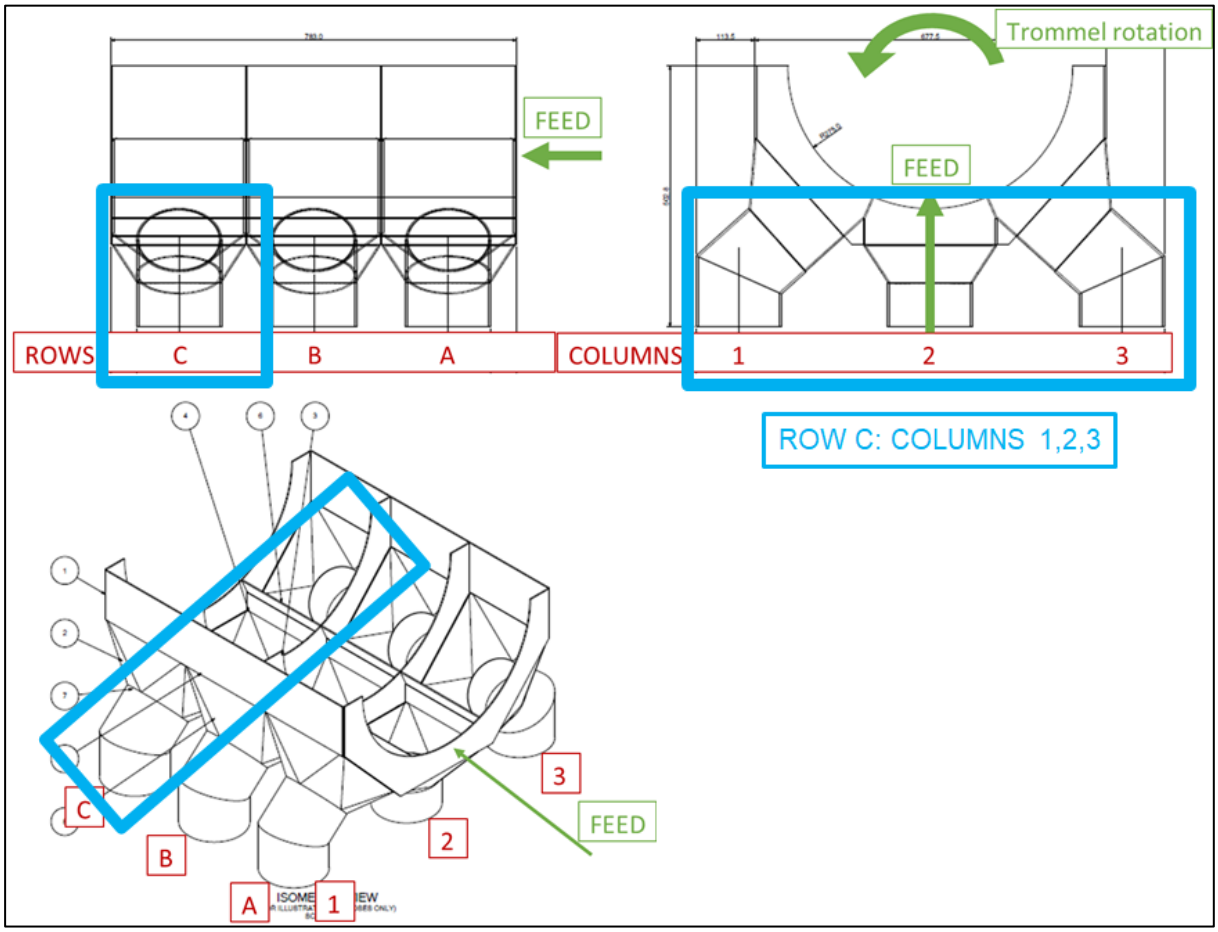

Figure 60. Illustration of discharge Row C, Columns 1, 2 and 3.

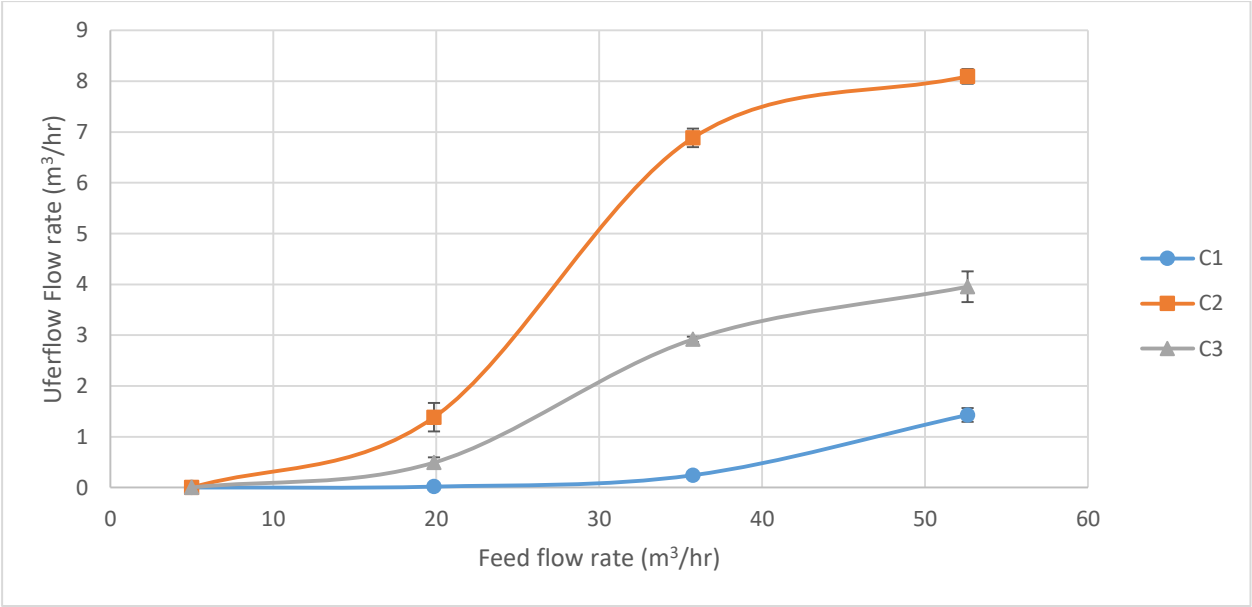

Figure 61. Water tests underflow rates for Row C over feed rate range.

Once again the impact of the rotation of the Mk2 trommel on the drainage through the three different columns can be observed. The highest underflow rate is achieved through discharge C2, increasing from zero at a feed rate of 5.00 m^3/hr to 6.89 m^3/hr at a feed rate of 35.76

m^3/hr. Beyond this feed rate, the drainage through discharge C2 seems to plateau. The underflow rate through discharge C3 gradually increases from zero to 3.95 m^3/hr for an increase in feed rate from 5.00 m^3/hr to 52.61 m^3/hr. The underflow rate through discharge C1 remains negligible until the feed rate reaches 35.76 m^3/hr, after which it starts to increase with an increase in feed rate.

8.2.1.5. Column comparison: Column 1

The next set of results is the comparison of underflow rates through the first column of discharges in Rows A, B and C. Column 1 of discharges are highlighted in Figure 62. The underflow rates for Column 1 are plotted in Figure 63 thereafter.

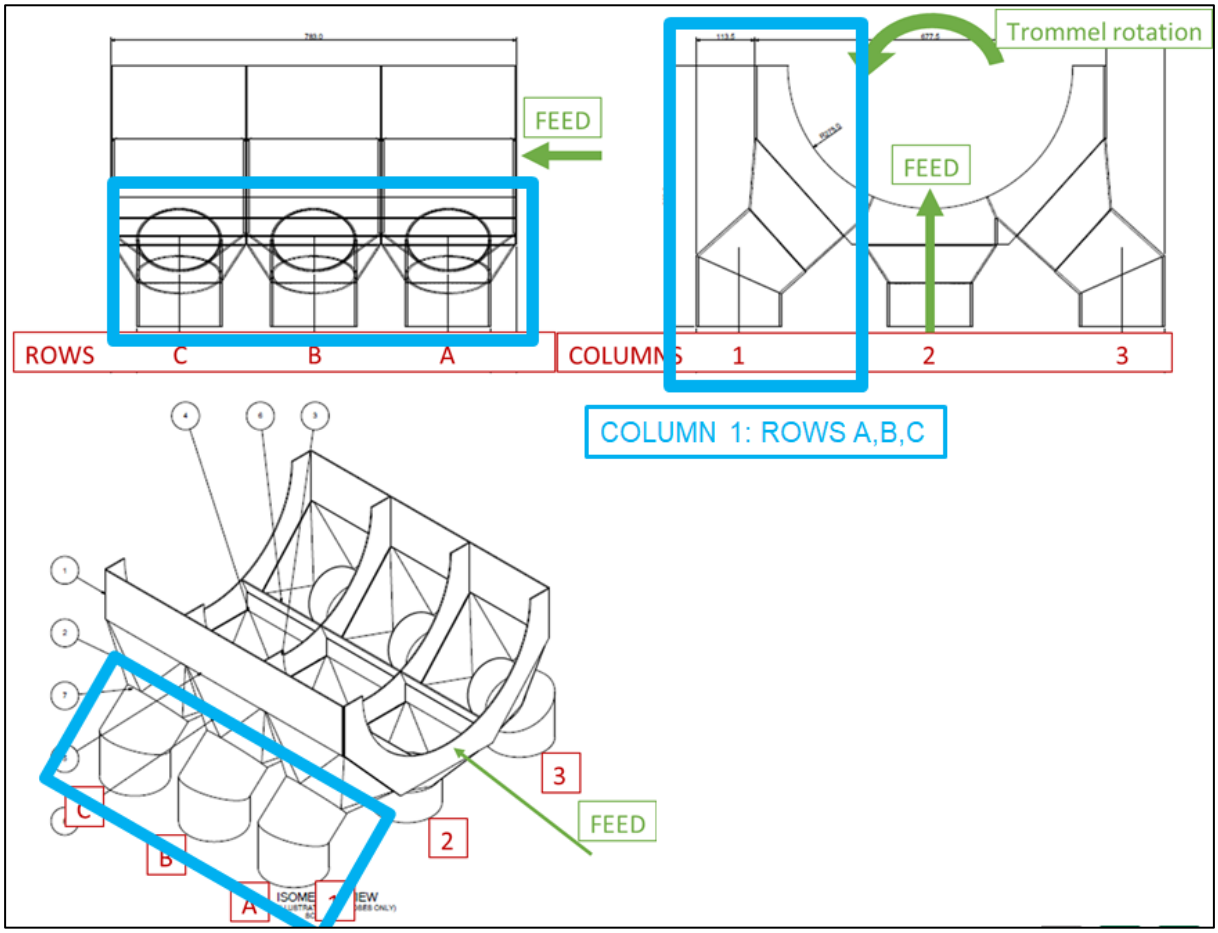

Figure 62. Illustration of discharge Column 1, Rows A, B and C.

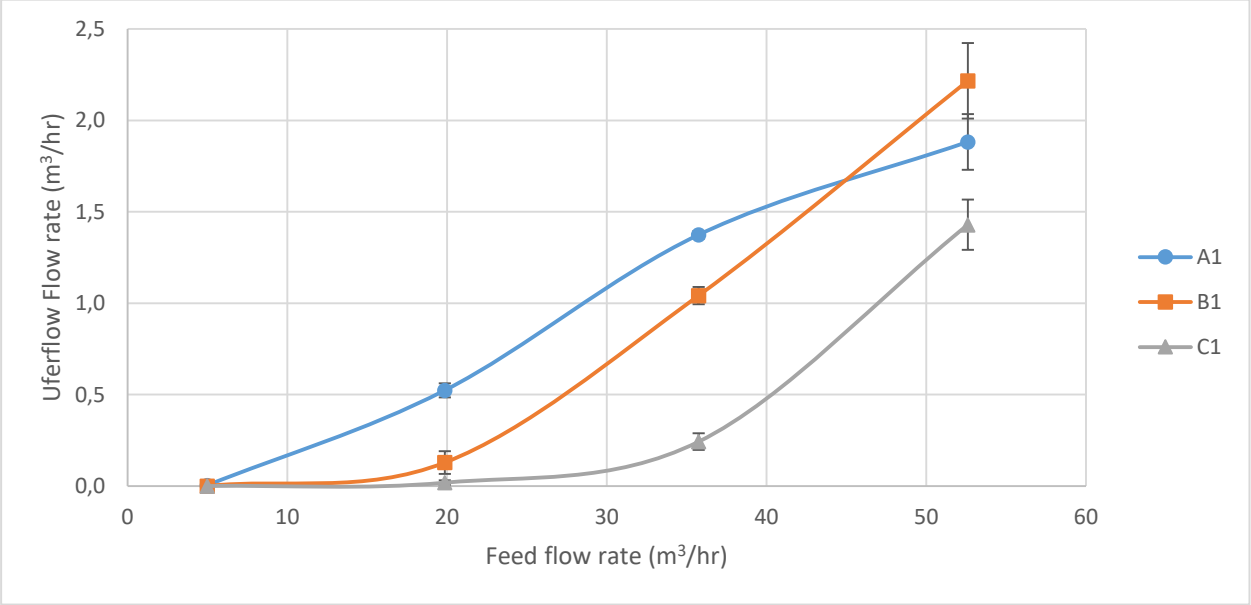

Figure 63. Water tests underflow rates for Column 1 over feed rate range.

At the lowest feed rate of 5.00 m^3/hr, all three discharges in Column 1 indicate negligible drainage. At the lowest feed rate, all material is drained through Columns 2 and 3 which is located towards the direction of trommel rotation. With an increase in feed rate, discharge A1 starts to increase first as it is closest to the feed end of the Mk2 trommel. With a further increase in feed rate to 35.76 m^3/hr, the underflow rates of discharge A1 increases to 1.37 m^3/hr, B1 to 1.04 m^3/hr and C1 to 0.24 m^3/hr. An increase in feed rate to 52.61 m^3/hr resulted in further gradual increase in underflow rates of B1 and C1 to 2.22 m^3/hr and 1.43 m^3/hr, respectively. Discharge A1 underflow rate starts to plateau at this feed rate because of the high velocity and splashing flow in the Mk2 trommel and partial bypassing of the first row of panels.

8.2.1.6. Column comparison: Column 2

The next set of results compares the underflow rates achieved through the three discharges along the length of the Mk2 trommel in the middle column (Column 2). First, Column 2 is highlighted in Figure 64. The results are plotted in Figure 65 thereafter.

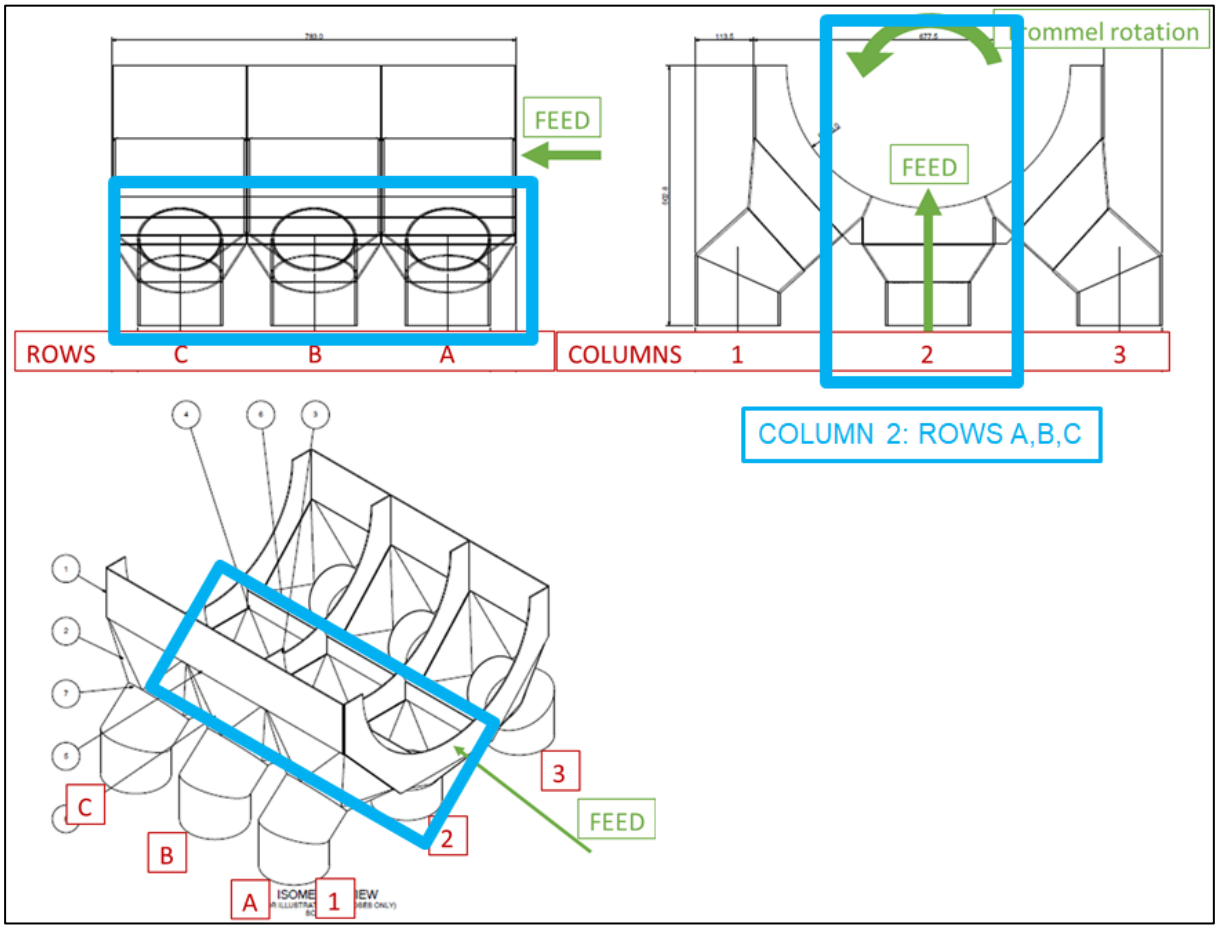

Figure 64. Illustration of discharge Column 2, Rows A, B and C.

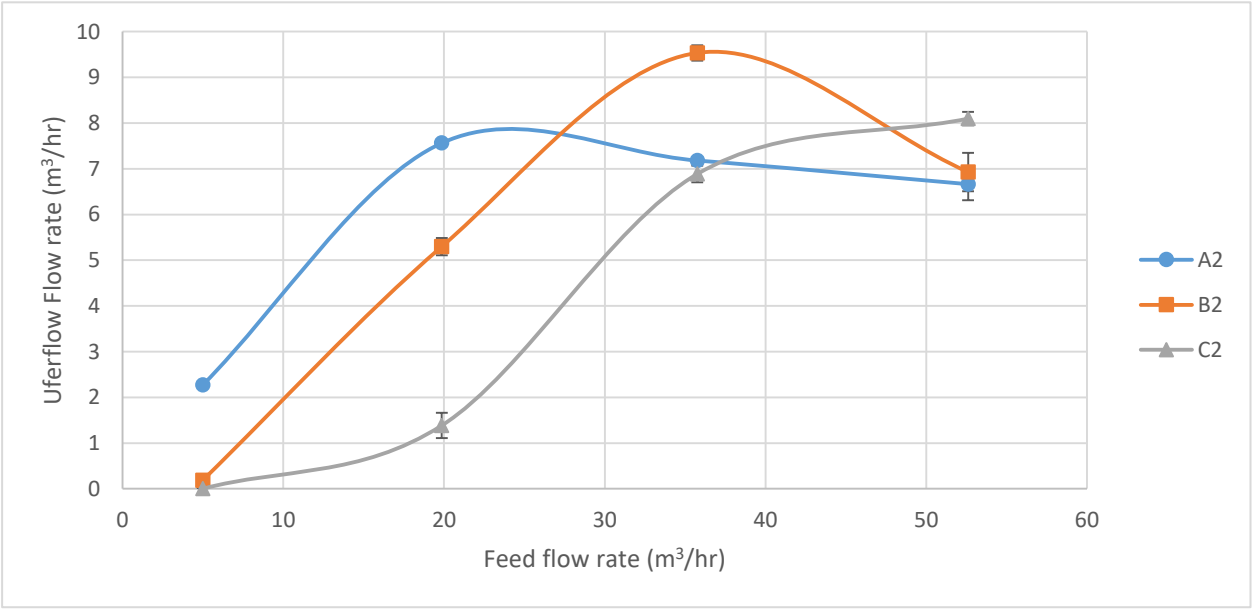

Figure 65. Water tests underflow rates for Column 2 over feed rate range.

Similar to the previous set of results, negligible drainage occurred in the second and third rows (B and C) at the lowest feed rate of 5.00 m^3/hr. This is because all the material fed to the screen was drained through the first row of panels. With an increase in feed rate, there was a

gradual increase in underflow rates through discharges A2, B2 and C2. Beyond a feed rate of 19.86 m^3/hr, the underflow rate through discharge A2 started to deteriorate first due to the high velocity and splashing flow, resulting in material bypassing the first row of panels. At this point, underflow rates through discharges B2 and C2 continued to increase for an increase in feed rate. At a feed rate of 35.76 m^3/hr, B2 underflow rate peaked at 9.54 m^3/hr, after which it also started to deteriorate for a further increase in feed rate for the same reasons. Beyond this feed rate, the underflow rate of discharge C2 started to plateau at 8.10 m^3/hr for an increase in feed rate to 52.61 m^3/hr.

8.2.1.7. Column comparison: Column 3

The final column of discharges, Column 3, is highlighted in Figure 66. The results for the final column of discharges are plotted in Figure 67 thereafter.

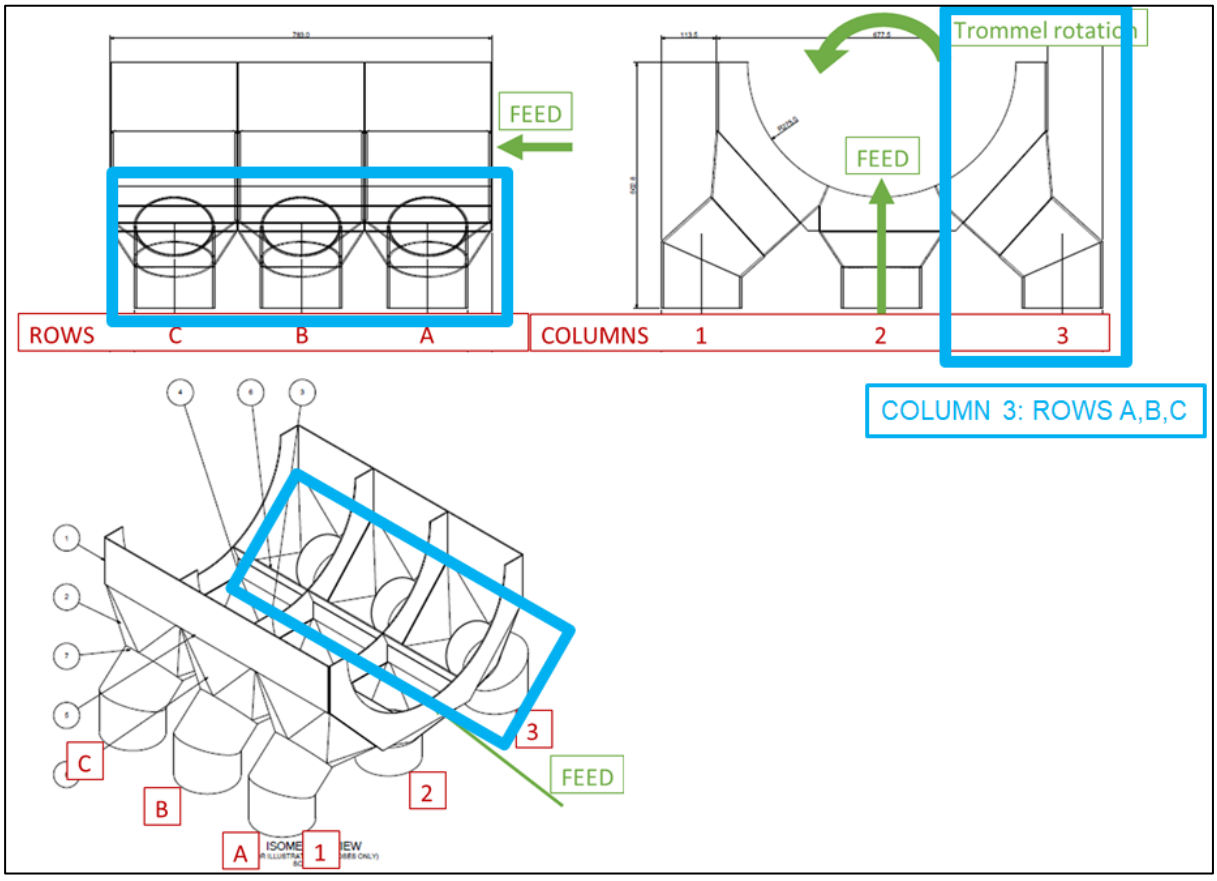

Figure 66. Illustration of discharge Column 3, Rows A, B and C.

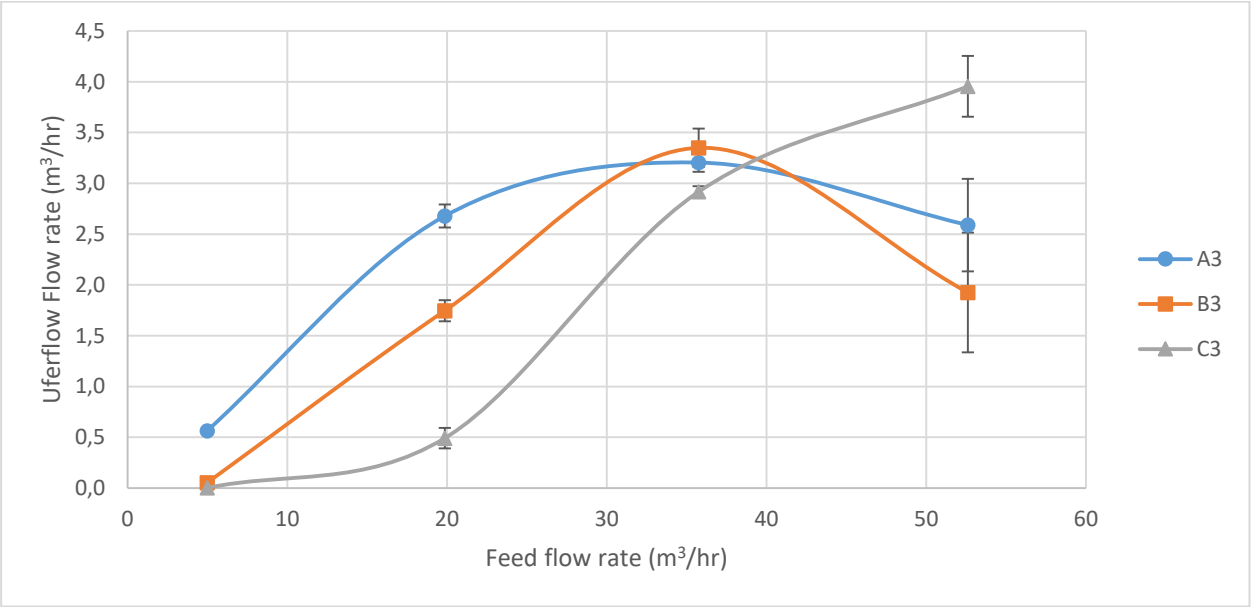

Figure 67. Water tests underflow rates for Column 3 over feed rate range.

As with the other discharge columns, all three rows in Column 3 increase for an increase in feed rate from 5.00 m^3/hr to 19.86 m^3/hr. The underflow rate through discharge A3 starts to plateau for a further increase in feed to 35.76 m^3/hr where it peaks at 3.21 m^3/hr. The underflow rate through discharge B3 also peaks at this feed rate at a maximum of 3.35 m^3/hr, which exceeds the maximum rate through discharge A3 because of the high velocity and splashing flow pattern. The underflow rate through discharge C3 continues to increase to a maximum of 3.95 m^3/hr at the maximum feed rate of 52.61 m^3/hr. As with all previous results, Row C is again the least affected by the highest velocity and splashing flow pattern in the Mk2 trommel at high feed rates. This is because the flow has time to settle down along the length of the Mk2 trommel, such that the flow does not ramp and bypass sections of the screen media closer to the end of the Mk2 trommel.

8.2.1.8. Underflow profiles

Due to the inaccessible nature of trommels during operation, historically it has been a difficult task to investigate the inner workings of a trommel and to map the material distribution. As such, it is of interest to use the information gathered from the underflow discharges from the Mk2 trommel to map the underflow profile in order to gain insight into the material distribution in the trommel. In order to do this, the assumption is made that the underflow rate through a particular discharge is directly related to the material volume over the discharge as a result of the hydrostatic pressure. At lower feed rates and turbulence, this approach should give a good estimation of the material distribution inside of the Mk2 trommel. However, this assumption becomes decreasingly accurate with an increase in turbulence of flow inside the Mk2 trommel. With splashing flow, it is expected that the angle of contact and velocity of the

material with the screen surface plays a greater role in the rate at which the material passes through the screening media.

8.2.1.8.1. Profile 1: Feed = 5.00 m^3/hr. Low velocity (0.08 m/s), low splashing.

The underflow rates through each individual discharge in the underflow discharge grid at a feed rate of 5.00 m^3/hr are plotted in Figure 68.

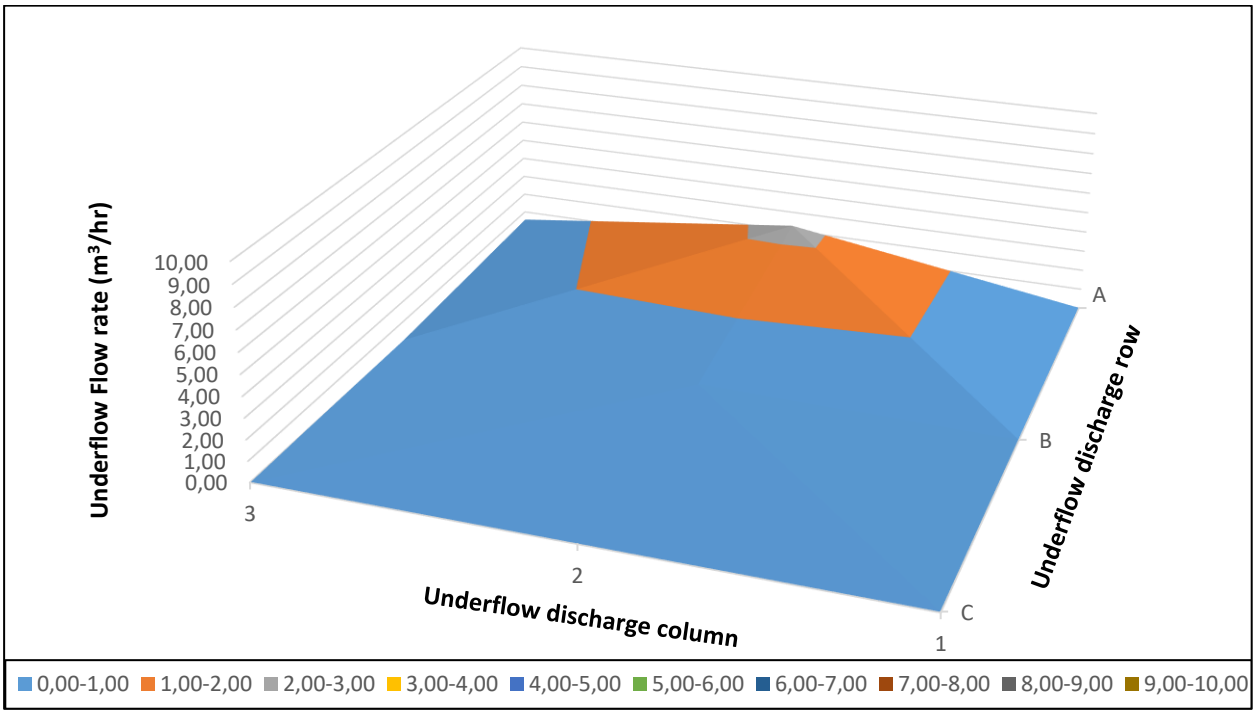

Figure 68. Underflow profile for water runs. Feed rate 5.00 m^3/hr.

As illustrated in Figure 68, a feed rate of 5.00 m^3/hr is low enough to be drained through the screen area directly in front of the feed end of the Mk2 trommel. The highest underflow rate is achieved through discharge A2 at 2.27 m^3/hr with negligible drainage along the length of the Mk2 trommel through discharges B2 and C2. A low underflow rate of 0.57 m^3/hr occurred through discharge A3 in the direction of trommel rotation.

8.2.1.8.2. Profile 2: Feed = 19.86 m^3/hr. Intermediate velocity (0.30 m/s), low splashing.

The second underflow profile is for a feed rate of 19.86, plotted in Figure 69.

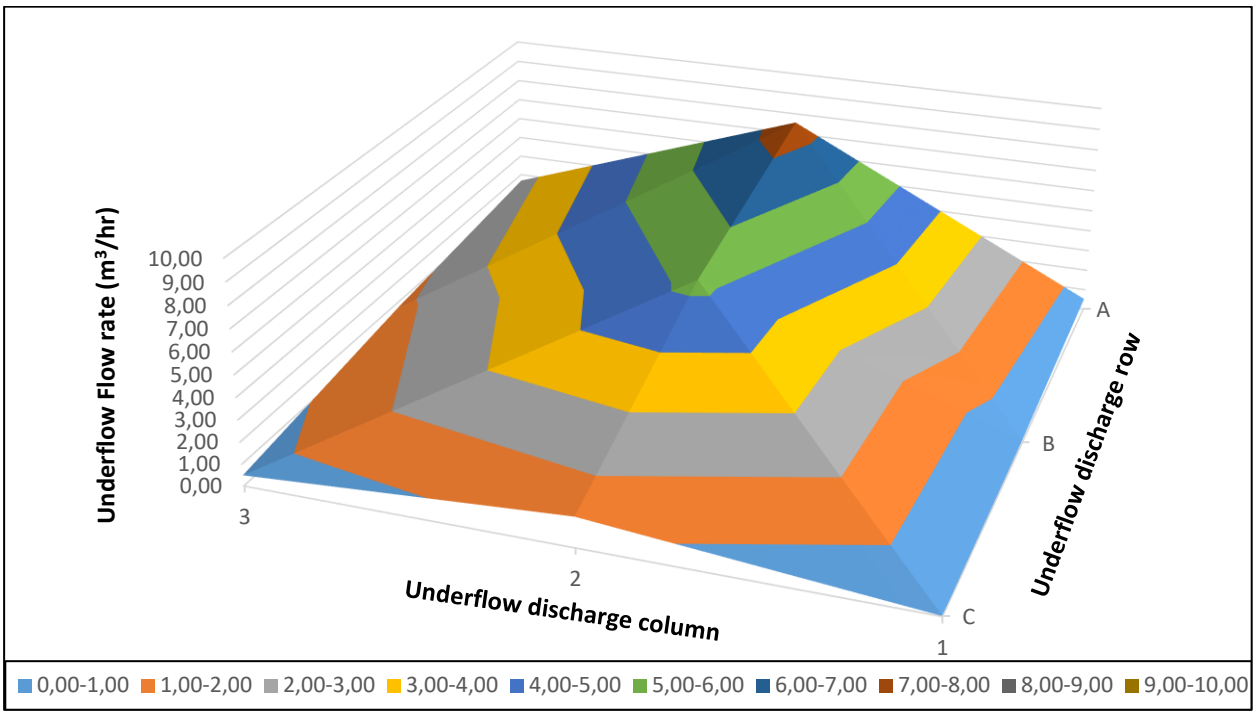

Figure 69. Underflow profile for water runs. Feed rate 19.86 m³/hr.

The increase in feed rate from 5.00 m³/hr to 19.86 m³/hr resulted in a substantially more developed profile, as illustrated in Figure 69. Column 1 underflow rates remain negligible, implying that there is a negligible material volume residing to the left side of the Mk2 trommel (from the feed end perspective). Similarly, there is very low drainage through discharge C3, because only a very small volume of water makes it all the way to the end of the Mk2 trommel without being drained.

The majority of the water slumps to the bottom of the Mk2 trommel circumference, which is located above Column 2 discharges. A steep decrease in material quantity along the length of the Mk2 trommel is observed in Column 2 as the material is drained. Figure 69 also illustrates that the material is slightly off-centre towards Column 3 as the rotation of the Mk2 trommel affects the position of the waterbed.

8.2.1.8.3. Profile 3: Feed = 35.76 m³/hr. Moderate velocity (0.54 m/s), moderate splashing.

The third profile is for a feed rate of 35.76 m³/hr, plotted in Figure 70.

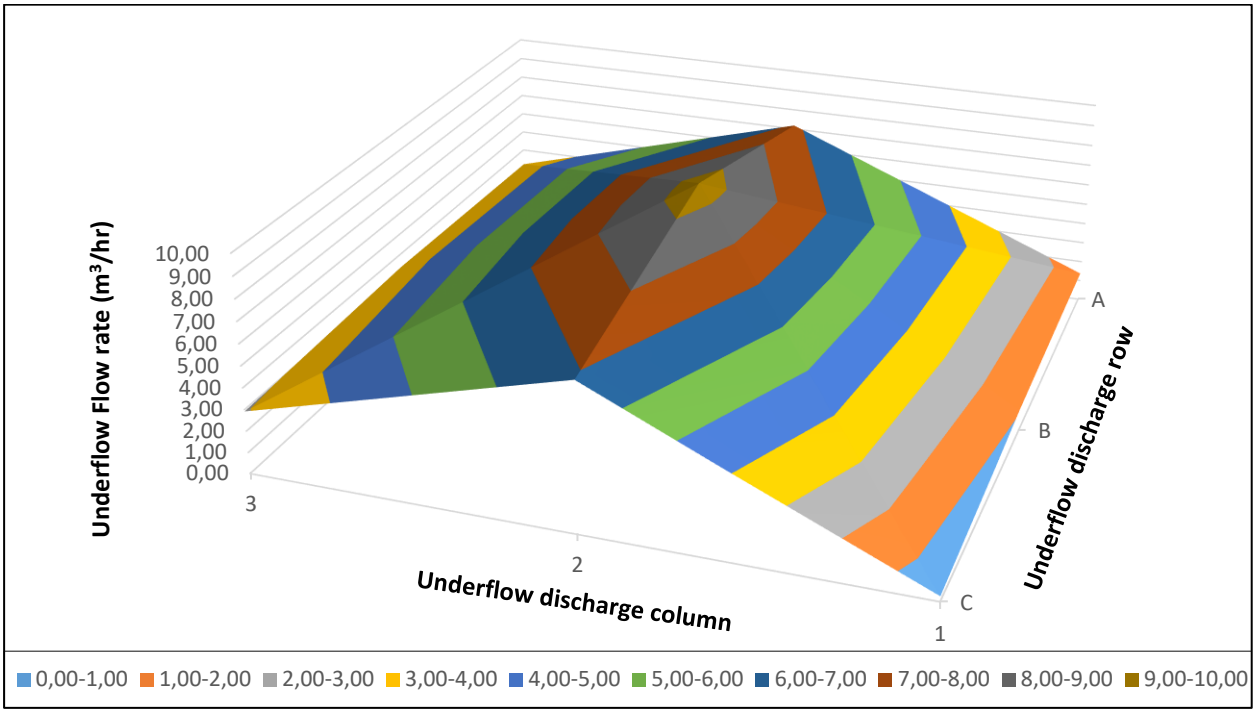

Figure 70. Underflow profile for water runs. Feed rate 35.76 m³/hr.

As the feed rate increased, the higher velocity of the flow resulted in some material being propelled over the first row of panels. As a result, the peak underflow rate at this feed rate is through discharge B2 at 9.54 m³/hr. As before, the majority of material resides in the middle of the Mk2 trommel above Column 2. The offset to the direction of rotation of the Mk2 trommel remains proportional to the offset at lower feed rates, but the underflow rate has increased for an increase in feed rate.

Note that the underflow rates of Column 3 seems to remain relatively constant at 3.2 m³/hr along the length of the Mk2 trommel at this feed rate, while the underflow rates in Column 1 gradually decrease along the length of the Mk2 trommel. This is because of the water momentum that causes the underflow rate of discharge A3 to decrease, discharge B3 to plateau and discharge C3 to continue to increase with an increase in feed rate. Column 1 is not as greatly affected by the flow pattern at this feed rate.

8.2.1.8.4. Profile 4: Feed = 52.61 m³/hr. High velocity (0.8 m/s), high splashing.

The fourth and final underflow profile for a feed rate of 52.61 m³/hr is plotted in Figure 71.

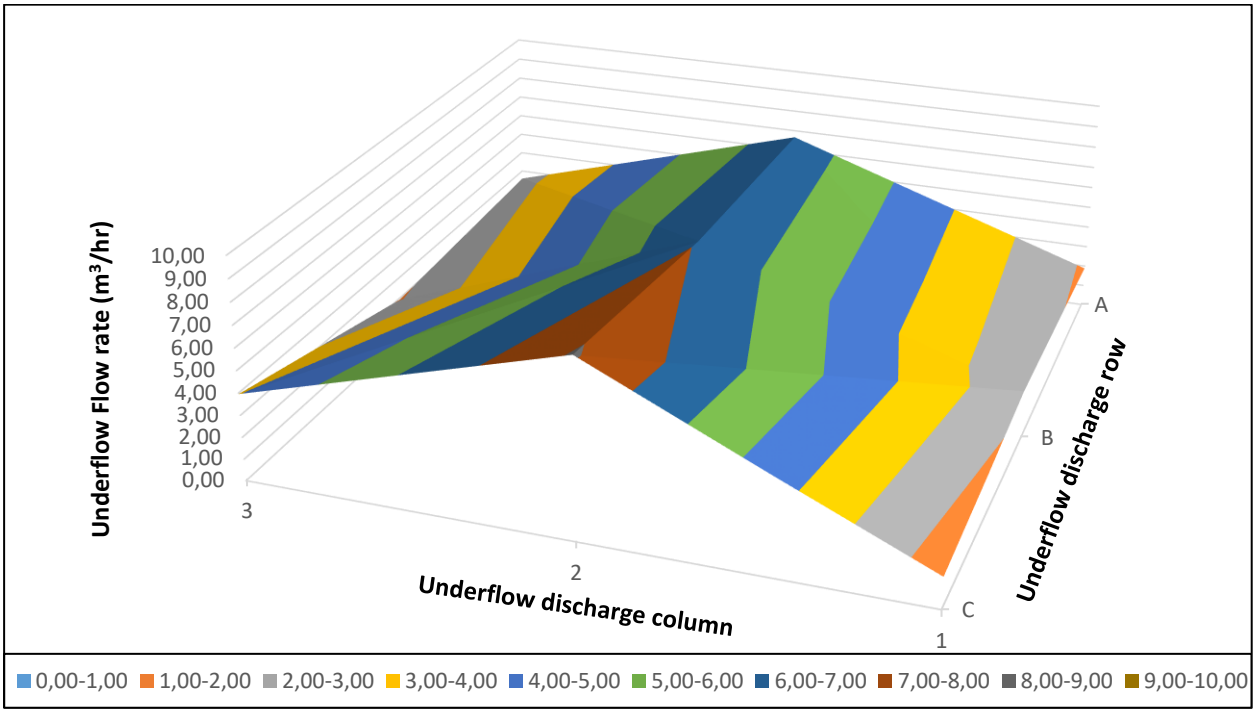

Figure 71. Underflow profile for water runs. Feed rate 52.61 m^3/hr.

This set of data illustrates to what extent the high velocity and splashing flow pattern in the Mk2 trommel affects the underflow rates. Here, the shape of the surface plot does not necessarily represent the material distribution inside of the Mk2 trommel, but rather the momentum and areas that the water makes contact with the screen surface. A substantial fraction of the water that is fed to the Mk2 trommel is propelled upwards and over the length of the Mk2 trommel, only to make contact with the screen surface near the overflow discharge. As a result, the underflow rate peak in Column 2 is in row C at a value of 8.10 m^3/hr.

Due to the angle at which the water hit the scroll in the Mk2 trommel, the water was deflected away from the area above discharge B3, resulting in a lower underflow rate through this discharge compared to the other discharges in Column 3.

As a result of near saturation of the Mk2 trommel, there is still a significant volume of water that has not been drained near the end of the Mk2 trommel (Row C). This, in turn, results in a large quantity of water being drained in Row C, which enhances the offset of water to discharge C3 from C1 due to the direction of Mk2 trommel rotation. This shows that the effect of material offset is enhanced with a greater material volume in the trommel.

8.3. DMS tests: Test Trommel Mk2

8.3.1. Measured RD (Marcy flask) vs calculated RD (dry solids mass)

After test work, all samples were processed according to the methodology that was discussed in the sample processing section. Upon analysing these results, it became apparent that there was a difference between the relative densities of the medium that was measured with a Marcy flask during test work and the relative density of the medium that was calculated with the dry and wet masses of each individual sample in the Mk2 trommel underflow. To illustrate this, the data is plotted in Figure 72:

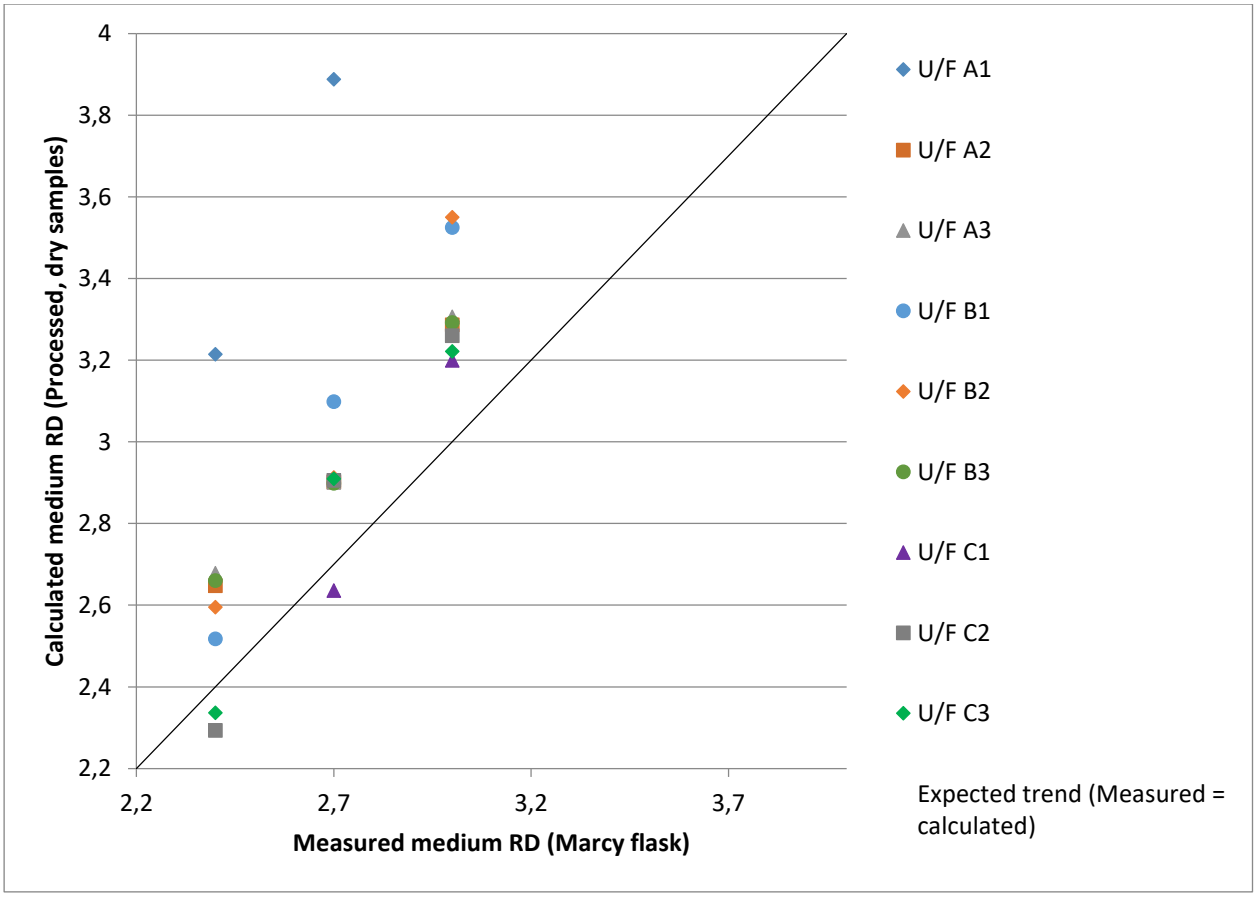

Figure 72. Comparison of measured medium RD during test work (Marcy flask) and calculation medium RD (processed, dry solids mass of samples)

All of the different underflow samples are plotted on the x-axis according to the medium RD that was measured with a Marcy flask during test work. The medium RD was measured in the stream that bypassed the Mk2 trommel and circulated back to the sump. On the y-axis, the sample RD was calculated from the wet sample mass, dry solids mass and known solids SG. Ideally the calculated RD would be equal to the measured RD during test work. This expected trend is plotted with the black trend line with the gradient of 1.

The majority of calculated sample relative densities are greater than the medium relative densities that were measured during test work. Besides for a few outliers (particularly for row

C which is the last row of discharges, as well as discharge A1) the calculated relative densities are relatively clustered around a value that is approximately 0.3 higher than the relative density measured during test work.

The tight clustering of processed sample RDs indicates reasonable accuracy of measurements. The outliers are typically only for very small samples for discharges that had the lowest flow rates that will be discussed in detail in the following section. The total wet masses of each discharge sample were measured with a big test work scale that performs optimally in the range of 1 to 40 kg sample sizes. The dried solids mass is however measured with a smaller, more accurate lab scale after the samples have been processed. This level of accuracy is not necessarily required to measure the total wet mass of the smallest samples, because they are negligible compared to the other discharge flow rates. It is however important to note that this inaccuracy did cause some outliers when calculating the relative density of each individual underflow discharge flow rate.

In order to understand the discrepancy between the measured medium RD during test work and the calculated sample RD from dried solid masses, it is important to take note of the following key factors:

- Marcy flask sampling inaccuracy;
- Stream split in T-piece at Mk2 trommel feed;
- Flow distribution in the Mk2 trommel;

The Marcy flask is a very common tool in the mineral processing industry to get a quick and convenient indication of the slurry RD. During test work the bypass stream is sampled with a Marcy flask to measure the RD. However, the high flow velocity in the bypass stream to achieve sufficient agitation in the sump, resulted in significant spillage during sampling of this stream. As a result, it was necessary to take multiple partial samples of the stream. It was attempted to take these partial samples from the entire cross section of the bypass stream at different times. This introduced some inaccuracy to the RD that was measured during test work.

As discussed in the experimental setup section, the Mk2 trommel feed is configured with a T-piece and valve system to split the discharge stream from the pump into the Mk2 trommel feed and the bypass streams. The assumption was made that the two streams exiting the T-piece configuration has the similar compositions. In reality, however, this assumption may not be entirely accurate. Solids momentum and distribution in the discharge pipe from the pump will impact the split of the stream that occurs in the T-piece configuration. For this

reason, the bypass stream and the Mk2 trommel feed stream compositions may differ slightly. It expected that this factor also contributes to the discrepancy between compositions and relative densities of the bypass and the Mk2 trommel underflow discharges.

Finally, the flow and distribution of material inside the Mk2 trommel has to be considered. In all other sections of the circuit, it can be assumed that high flow velocities in the pipes and the consequent agitation in the sump results in a uniform distribution of solids and therefore a uniform RD. This assumption is however not entirely valid inside of the Mk2 trommel, where the material is allowed to spread across the screen surface and settle out of suspension. This factor may also contribute to the discrepancy between the relative densities that was measured in the bypass stream during test work and the relative densities that was calculated from the various underflow discharges after sample processing.

Taking all of these factors into consideration, it was decided that the relative densities that were calculated after processing the samples from the individual underflow discharges is a more accurate indication of what the medium density is inside of the Mk2 trommel. Therefore, for all the following results and discussions, the calculated sample relative density is used to refer to the medium relative density in the system under specific operating conditions.

8.3.2. Effect of feed rate on Mk2 trommel operation

As discussed in the methodology section, the DMS test work was performed at a single pump setting of 20 Hz. Recall that the sump contents were agitated using the bypass stream because the underflow discharge pipes prevented installation of an agitator due to insufficient space under the Mk2 trommel. During test work it was found that the bypass stream entrapped air that got sucked into the pump if the material volume in the sump was too low. Therefore, it was necessary to load the system with a high volume of slurry to decrease the probability of entrapped air penetrating to the bottom of the sump where the pump suction pipe is located. Due to the physical labour and time required to load the system with such a substantial quantity of material (up to 670 kg FeSi and 265 kg ore for a single run), as well as the cost of large quantities of FeSi (R24 000 per ton), there was a limit the quantity of material could be loaded into the system.

It was also found that due to the change in volume of material in the system after sampling, feed rate dropped as a result of the drop in static head in the sump at a constant pump setting. Due to inaccessibility of the Mk2 trommel feed, it was necessary to calculate the feed properties by performing a mass balance on the Mk2 trommel after test work. As such, it was

only possible to calculate the total feed rate to the Mk2 trommel after the samples have been processed. Therefore it was decided to perform all runs at the same pump setting, even though the feed rate varied somewhat due to other factors in the system, because a constant pump setting was the closest guarantee to a constant feed rate during test work. After processing the samples, it was found that the first experimental run had a high feed rate at a pump setting of 20 Hz, but after removing the material of the first sample, the feed rate typically dropped significantly. With a lower feed rate, the underflow rates were also smaller, which resulted in a smaller sample for the next repeat and, in turn, a smaller reduction in the total material volume in the system. It was found that the second and third repeats in a set were clustered close together, while the first run in the set typically had a higher feed rate. For this reason it was decided to group the second and third runs in the set to calculate the average values for that set in terms of screen performance, which will be discussed in the final result section. Although the first run, which had a higher feed rate, was not included in the calculation of average values for the set, the data was not thrown out. It was found that these data points also generally conformed to the trends that was observed for various feed rates, so these data points are included in the following section.

8.3.2.1. Row comparison: Row A

The first set of results that will be discussed is the comparison of underflow rates in the first row of discharges (Row A) over the range of feed rates that were tested. These results are plotted in Figure 73.

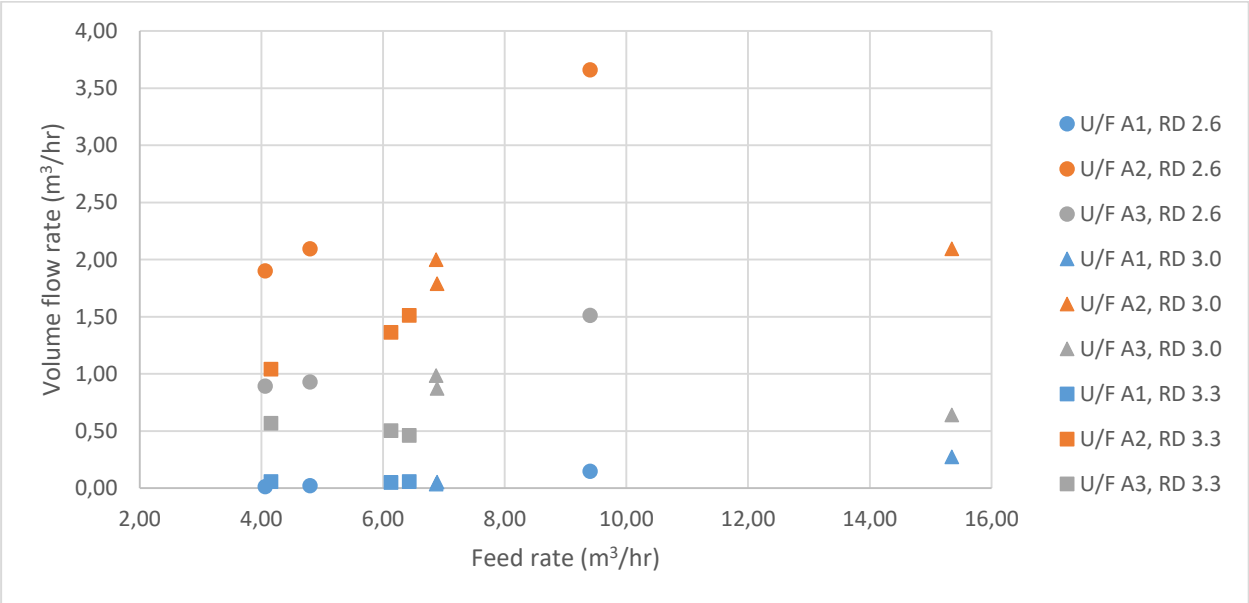

Figure 73. Underflow rates through Row A discharges over feed rate range (all medium RDs)

It was found that the underflow rates are more dependent on the feed rate to the trommel than the relative density of the medium, particularly in the region of low feed rates that do not saturate the screen. Therefore the data for three different medium RDs are plotted on the same graph to illustrate the effect of feed rate. The colour of the data points indicate the discharge column (Blue for Column 1, Orange for Column 2 and Grey for Column 3), while the shape of the data points indicate the medium RD of the tests (Circle for RD 2.6, Triangle for RD 3.0 and Square for RD 3.3).

As with the water tests, the highest underflow rate is achieved through the middle column of discharges (Column 2). Following after Column 2 was Column 3, in the direction of rotation. The lowest underflow rate through was achieved through Column 1. Regardless of the variance of the data, there were no exceptions to the rule that A2 has the highest underflow rate, followed by A3 and then A1 under specific operating conditions.

Figure 73 illustrates that there is a general increase in underflow rate for each underflow discharge for an increase in feed rate. At a medium RD of 2.6 for an increase in feed rate from 4.06 m^3/hr to 9.41 m^3/hr, underflow A2 increased from 1.90 m^3/hr to 3.66 m^3/hr while underflow A3 increased from 0.89 m^3/hr to 1.51 m^3/hr. Underflow A1 only raised from zero at the upper end of the feed rate range. At a medium RD of 3.0 for a feed rate increase from 6.87 m^3/hr to 15.35 m^3/hr, underflow A2 increased from 1.79 m^3/hr to 2.09 m^3/hr, while underflow A3 seems to have decreased slightly from 0.87 m^3/hr to 0.64 m^3/hr. Underflow A1 remained negligible until the upper end of the feed rate range. At a medium RD of 3.3 for a feed rate increase from 4.16 m^3/hr to 6.43 m^3/hr, underflow A2 increased from 1.04 m^3/hr to 1.51 m^3/hr, while underflow A3 decreased slightly from 0.56 m^3/hr to 0.46 m^3/hr. Underflow A3 remained negligible for the entire feed rate range.

The apparent plateau and slight decrease in underflow rate of discharge A2 and A3, respectively, for a significant increase in feed rate at a medium RD of 3.0 is once again attributed to the feed configuration of the Mk2 trommel. Similar to the underflow rates and flow distribution that was affected at high feed rates during the water tests, the highest feed rate of 15.35 m^3/hr did not allow sufficient time for the medium to drain through the ore bed to reach the screen surface. At lower feed rates, it was possible for the biggest fraction of medium to drain through the first row of panels. As the feed rate increased, the residence time over the first row of panels decreased and the length of the Mk2 trommel that was required for the medium to drain through the ore bed increased.

The slight apparent decrease in underflow rate of discharge A3 at a medium RD of 3.3 is accredited to experimental, sampling or sample analysis error. The two data points at feed rates 6.13 m^3/hr and 6.43 m^3/hr are very close together. These data points will be considered the same data point with relatively small variance.

A noteworthy observation is that the underflow rates at the low medium RD of 2.6 are higher than the underflow rates at higher medium RDs, even though the feed rates were lower. As a result, the lower RD data points (for all underflow discharges) seem to stand out above the general trend that is observed for the rest of the data. As mentioned in the methodology, the test parameters were selected at a medium to ore ratio of 5:1. This refers to the total quantities of the different materials loaded into the system. This implies that at lower medium RDs, there was also less iron ore in the system to maintain the appropriate medium to ore ratio. As a result, the ore quantity in the Mk2 trommel would decrease with a decrease in ore quantity in the entire system. With a lower ore quantity in the Mk2 trommel and a smaller bed depth, there is less obstruction for the medium to reach the screening surface and to pass through the apertures.

A lower medium RD also relates to a lower medium viscosity, which also contributes to more effective drainage. These results correlate with literature. Kabondo (2018) and Valine, et al. (2009) found that higher water content in a slurry, in the context of fine screening, contribute to enhanced fines transport to the underflow. A lower slurry viscosity also makes it easier for the material to drain through the coarse particle bed and screen apertures.

8.3.2.2. Row comparison: Row B

The second set of results for the DMS test work is the underflow rates through the second row of discharges (Row B) over the range of feed rates, plotted in Figure 74.

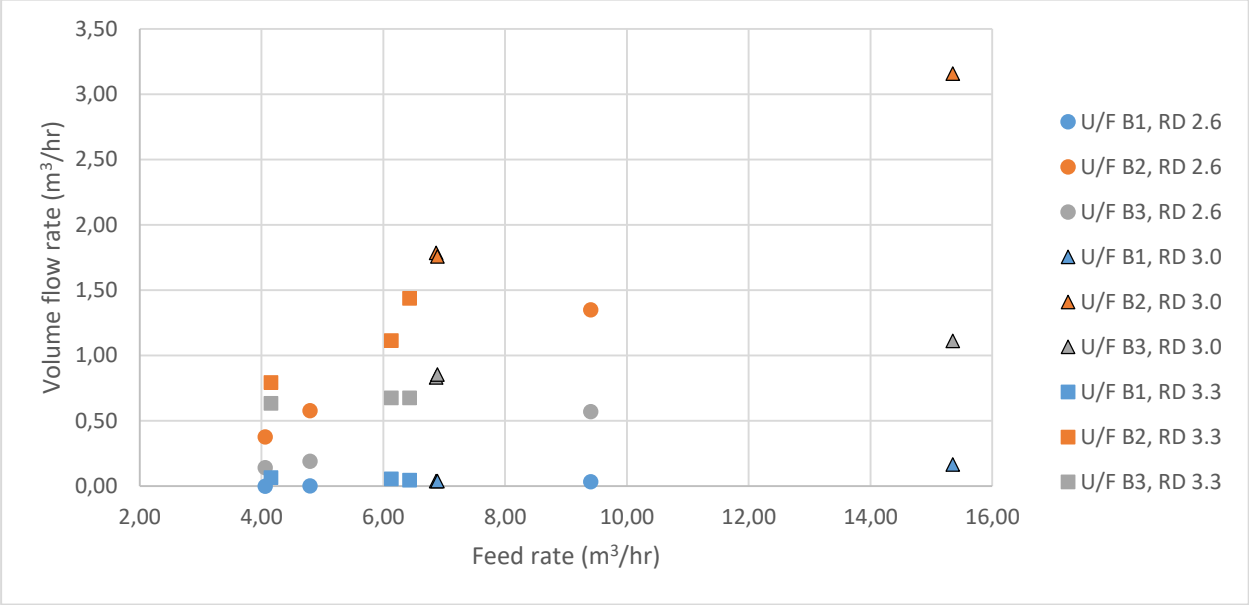

Figure 74. Underflow rates through Row B discharges over feed rate range (all medium RDs)

Once again in Row B the highest underflow rate was achieved through Column 2, followed by Column 3 and then Column 1 because of the Mk2 trommel rotation.

At a medium RD of 2.6 for an increase in feed rate from 4.06 m^3/hr to 9.41 m^3/hr, underflow B2 increased from 0.38 m^3/hr to 1.35 m^3/hr while underflow B3 increased from 0.07 m^3/hr to 0.57 m^3/hr. Underflow B1 remained at practically zero over the entire feed rate range. At a medium RD of 3.0 for a feed rate increase from 6.87 m^3/hr to 15.35 m^3/hr, underflow B2 increased from 1.79 m^3/hr to 3.16 m^3/hr, while underflow B3 increased slightly from 0.83 m^3/hr to 1.11 m^3/hr. Underflow B1 remained negligible until the upper end of the feed rate range. At a medium RD of 3.3 for a feed rate increase from 4.16 m^3/hr to 6.43 m^3/hr, underflow B2 increased from 0.79 m^3/hr to 1.44 m^3/hr, while underflow B3 plateaued at a value of 0.68 m^3/hr. Underflow A3 remained negligible for the entire feed rate range.

The apparent plateau in underflow rate of discharge B3 at medium RDs of 3.0 and 3.3 can be accredited to the higher ore quantity that accompanied the higher medium quantities to maintain the medium to ore ratio of 5:1. With a higher ore quantity, the ore bed depth in the Mk2 trommel is higher. A higher bed depth, accompanied by a higher medium viscosity at higher medium RDs, increases the difficulty for the medium to pass through the ore bed to reach the screen surface. Although an increase in feed rate would typically increase the underflow rate, this effect is counteracted by the increase in difficulty for the medium to reach the screen surface. This effect is more prominent in Column 3 than the other discharge columns, because the majority of ore resides over the third column of discharges due to the rotation of the Mk2 trommel.

Recall the previous set of results that showed a higher drainage through Row A at the lowest medium RD of 2.6, due to a lower ore quantity in the Mk2 trommel and lower viscosity of the medium. As a result of a greater drainage that occurred in Row A, specifically at a feed rate of 9.41 m^3/hr, the drainage in Row B at these conditions are lower than expected with regards to the general trend of the other data points on Figure 74. This is because the medium drainage through Row A exceeded expectation, leading to less material left in the Mk2 trommel to drain through Row B.

8.3.2.3. Row comparison: Row C

The third set of results for DMS work is the underflow rates through discharge Row C over a range of feed rates, plotted in Figure 75.

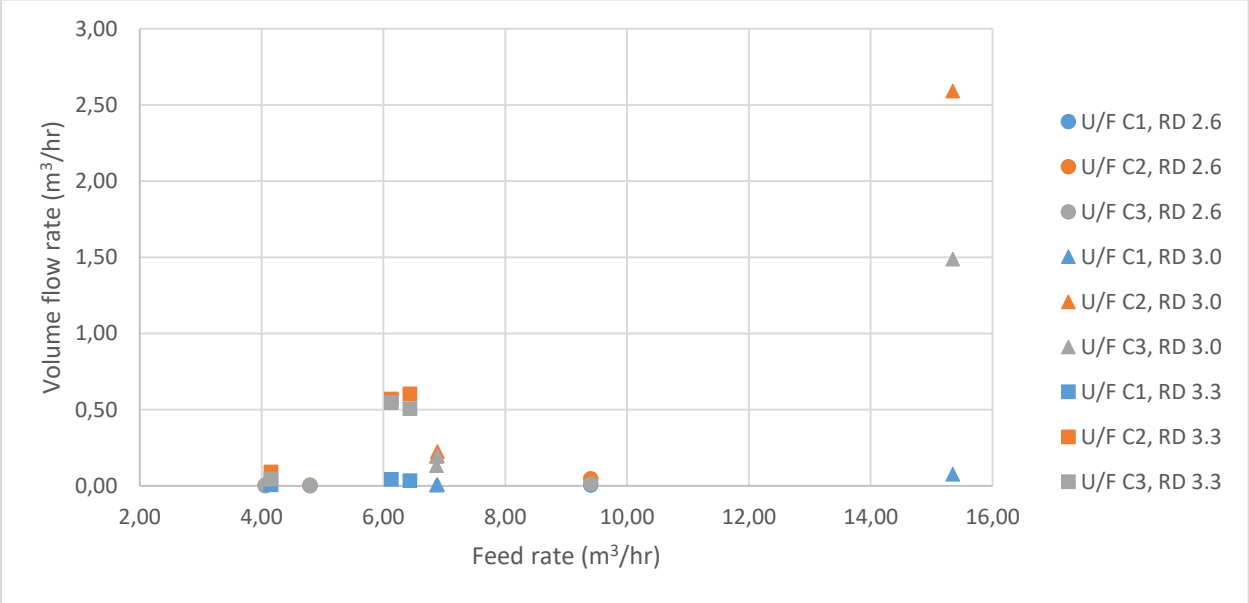

Figure 75. Underflow rates through Row C discharges over feed rate range (all medium RDs)

Of all the row comparisons that have been done for the DMS test work, the comparison of Row C illustrates the smallest distinction in underflow rates between the three columns caused by the rotation of the Mk2 trommel. This is because Row C, the final row before the overflow discharge, was not utilised fully in terms of drainage. The range of feed rates that was investigated did not saturate the Mk2 trommel, which means that the majority of the material was able to drain through Rows A and B. At a medium RD of 3.0 and lower, only the highest feed rate of 15.35 m^3/hr required the final row of discharges to a significant extent, to drain all of the medium. At a feed rate of 6.87 m^3/hr, the same medium RD of 3.0 only achieved approximately 0.13 m^3/hr underflow rates through discharges C2 and C3. The only exception was at the highest medium RD of 3.3, where the underflow rates of discharges C2 and C3 were in the range of 0.5 m^3/hr to 0.6 m^3/hr at a feed rate of approximately 6.1

m^3/hr to 6.43 m^3/hr. This is due to the high medium RD. With a high medium RD, the ore bed is deeper and the medium viscosity is higher, which increases the difficulty for the medium to drain through the ore bed and reach the screen surface. Therefore under these operating conditions a longer length of screen surface was utilised to drain the medium, resulting in a higher underflow rate in Row C than for lower medium RDs.

8.3.2.4. Column comparison: Column 1

The next set of results compares the underflow rates achieved through the first column of discharges, located in the opposite direction of rotation of the Mk2 trommel. The results are plotted in Figure 76.

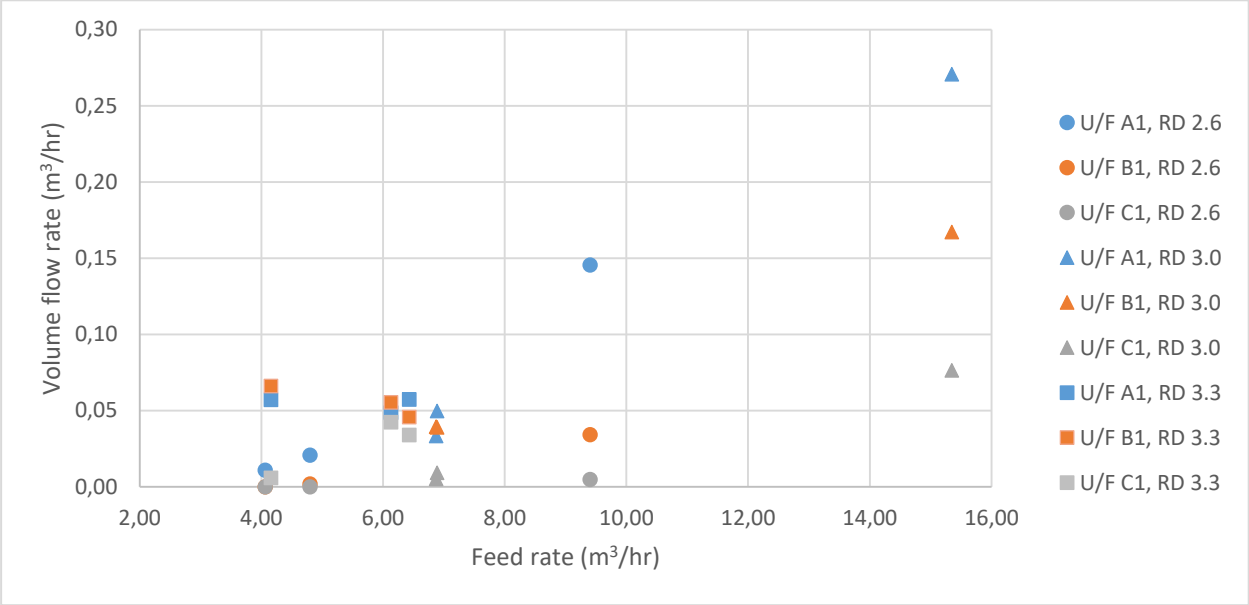

Figure 76. Underflow rates through Column 1 discharges over feed rate range (all medium RDs)

At a medium RD of 2.6 for an increase in feed rate from 4.06 m^3/hr to 9.41 m^3/hr, underflow A1 increased from 0.01 m^3/hr to 0.15 m^3/hr while underflow B1 increased slightly from zero m^3/hr to 0.07 m^3/hr. Underflow C1 remained at practically zero over the entire feed rate range. At a medium RD of 3.0 for a feed rate increase from 6.87 m^3/hr to 15.35 m^3/hr, underflow A1 increased from 0.03 m^3/hr to 0.27 m^3/hr, while underflow B1 increased from 0.04 m^3/hr to 0.17 m^3/hr and underflow C1 increased from 0.01 m^3/hr to 0.08 m^3/hr. At a medium RD of 3.3 for a feed rate increase from 4.16 m^3/hr to 6.43 m^3/hr, underflow A1 fluctuated about a value of approximately 0.06 m^3/hr, while underflow B1 decreased from 0.07 m^3/hr to 0.05 m^3/hr. Underflow C1 increased slightly from 0.01 m^3/hr to 0.03 m^3/hr.

Due to the fact that Column 1 is located to the opposite side of rotation of the Mk2 trommel, all underflow rates through this column is very low compared to the drainage in the rest of the Mk2 trommel. As such, these values are very sensitive to experimental, sampling and sample

processing inaccuracies. For this reason one must be careful of reading into some of the smaller trends observed, for example the decrease in underflow rate for an increase in feed rate through discharge C1 at a medium RD of 3.3. There is more confidence in the trends observed for a bigger increase in feed rate, indicating an increase in underflow rate for the majority of discharges. There also seems to be a decrease in underflow rate along the length of the Mk2 trommel, which is intuitive because the underflow rate decreases with the material volume in the Mk2 trommel. The material volume in the Mk2 trommel decreases along the length of the Mk2 trommel as the material is getting drained through the screen apertures.

8.3.2.5. Column comparison: Column 2

The next set of results is the comparison of the underflow rates achieved through discharge Column 2, plotted in Figure 77.

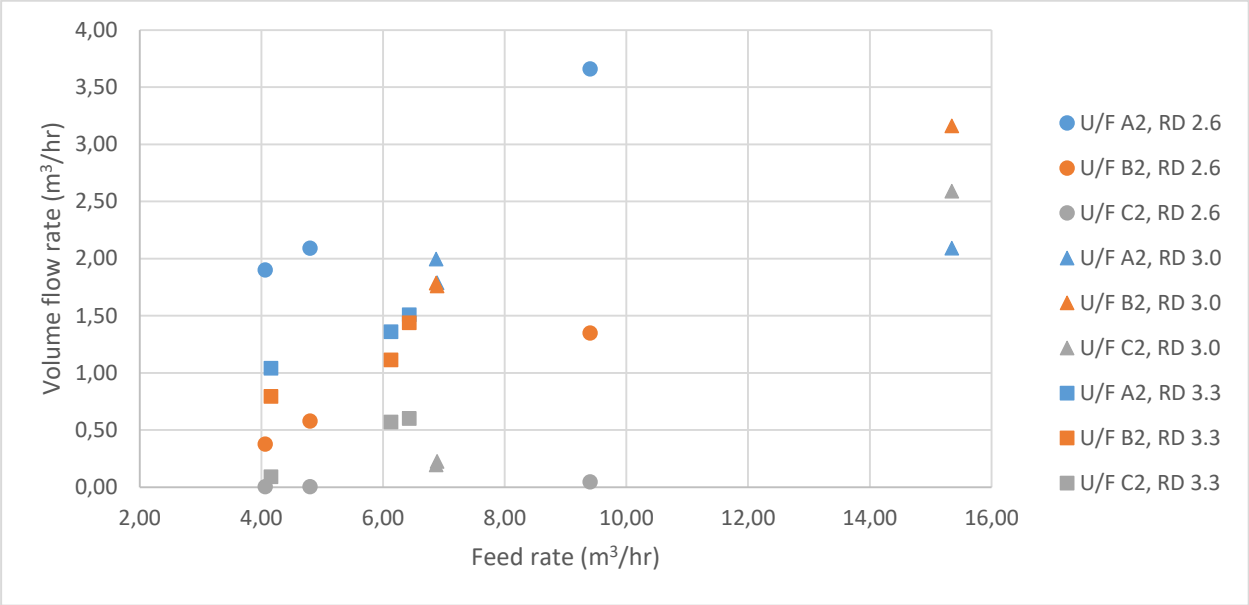

Figure 77. Underflow rates through Column 2 discharges over feed rate range (all medium RDs)

At a medium RD of 2.6 for an increase in feed rate from 4.06 m^3/hr to 9.41 m^3/hr, underflow A2 increased from 1.90 m^3/hr to 3.66 m^3/hr while underflow B2 increased from 0.38 m^3/hr to 1.35 m^3/hr. Underflow C1 remained at practically zero over the entire feed rate range. At a medium RD of 3.0 for a feed rate increase from 6.87 m^3/hr to 15.35 m^3/hr, underflow A2 increased slightly from 1.79 m^3/hr to 2.09 m^3/hr and plateaued for a further increase in feed rate, while underflow B2 increased from 1.79 m^3/hr to 3.16 m^3/hr and underflow C2 increased from 0.19 m^3/hr to 2.59 m^3/hr. At a medium RD of 3.3 for a feed rate increase from 4.16 m^3/hr to 6.43 m^3/hr, underflow A2 increased from 1.04 m^3/hr to 1.51 m^3/hr, while underflow B2 decreased from 0.79 m^3/hr to 1.44 m^3/hr. Underflow C2 increased from 0.09 m^3/hr to 0.60 m^3/hr.

The general trend that is observed in Figure 77 is an increase in underflow rate for each discharge in Column 2 for an increase in feed rate, with decreasing underflow rates along the length of the Mk2 trommel. The only exception was at a high feed rate of 15.35 m^3/hr at a medium RD of 3.0, where the underflow rate through discharge A2 started to deteriorate for an increase in feed rate. This resulted in the underflow rates through discharges B2 and C2 exceeding the underflow rate through discharge A2. This phenomenon of a plateau and even a slight decrease in underflow rate through discharge A2 seems to indicate that the drainage capacity of the panel above discharge A2 has been reached. This is however misleading. The underflow rates through discharges B2 and C2 at a feed rate of 15.35 m^3/hr indicate that the panels are in fact capable of draining a greater quantity than what discharge A2 achieved under these exacts conditions.

One contributing factor to this effect is the feed and scroll configuration. Figure 78 illustrates the material behaviour inside of the Mk2 trommel during operation at 15.35 m^3/hr and a medium RD of 3.0.

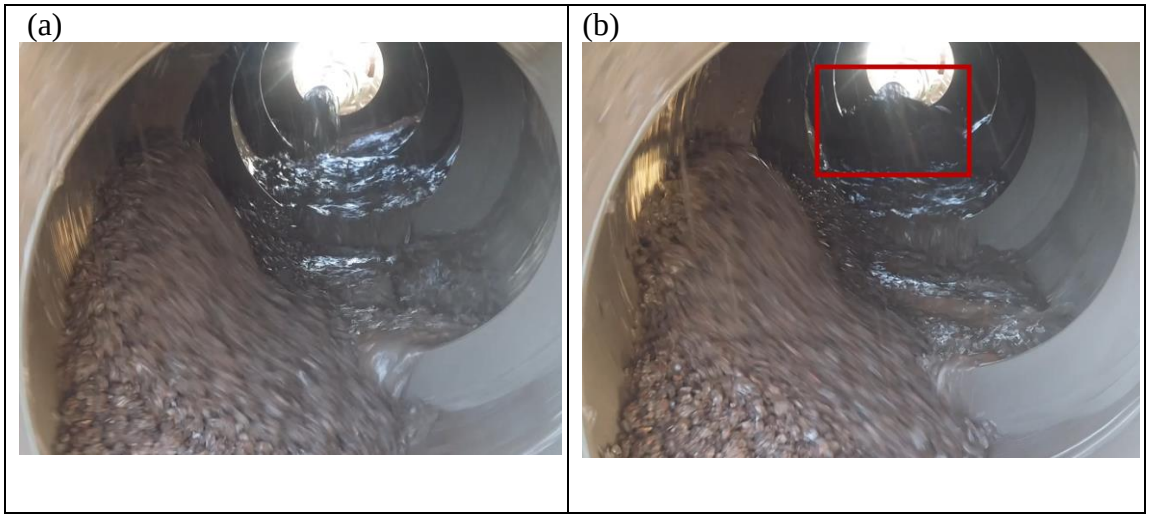

Figure 78. Photograph of material distribution inside Mk2 trommel during DMS work, illustrating slurry momentum as a result of collision with scroll.

At a high feed rate, the material that is fed to the Mk2 trommel collides directly with the scrolls near the feed end at a specific position of the Mk2 trommel's rotation. The Figure 78(a) on the left, illustrates the feed when the Mk2 trommel's position is such that the scroll position is clear of the feed stream. Figure 78(b) to the right, illustrates the feed when the Mk2 trommel position is such that the scroll is directly under the feed, causing the material to hit the scroll directly and get propelled over the scroll along the length of the Mk2 trommel. This effect causes the drainage through the first row of panels to be lower because some of the material bypasses Row A and falls directly onto Row B's region in the Mk2 trommel. As

the material pools up above Row B, the drainage is enhanced relatively to Row A, because there is a greater volume of material residing over this region of the screen.

Furthermore, Figure 78 illustrates another important factor to understand the trends observed for underflow rates in Figure 77. One can observe that the slurry close to the feed end of the Mk2 trommel tends to slump to the bottom of the Mk2 trommel, which is the lowest point on the Mk2 trommel circumference. As the medium is drained from the slurry, the remaining pulp becomes more resistant to flow. Closer to the end of the Mk2 trommel, the majority of medium has been drained from the slurry and only a pulp consisting of mostly iron ore with residual FeSi and water remains in the screen. This pulp seems to stick to the screen surface more than the slurry, causing cataract motion of particles as opposed to a slumping motion. As more medium is being drained from the screen, the position of the remaining ore bed shifts in the direction of Mk2 trommel rotation, causing it to reside over Column 3, where the slurry tends to slump over Column 2 in the middle of the Mk2 trommel. The position of the ore bed is expected to affect the drainage in different regions of the Mk2 trommel, because the ore particles obstruct the path for medium to reach the screen surface. Near the feed end of the Mk2 trommel, more apertures are obstructed by the ore particles, decreasing the effective open area of the panels. As the material moves along the length of the Mk2 trommel, the rotation of the Mk2 trommel moves the ore particles away from Column 2, clearing the obstruction and allowing a greater underflow rate through Row B. As the medium in the Mk2 trommel is drained, the material volume decreases and therefore the medium drainage starts to decrease along the length of the Mk2 trommel towards Row C.

8.3.2.6. Column comparison: Column 3

The final comparison is between the underflow rates that were achieved in the third column of discharges over the range of feed rates, plotted in Figure 79.

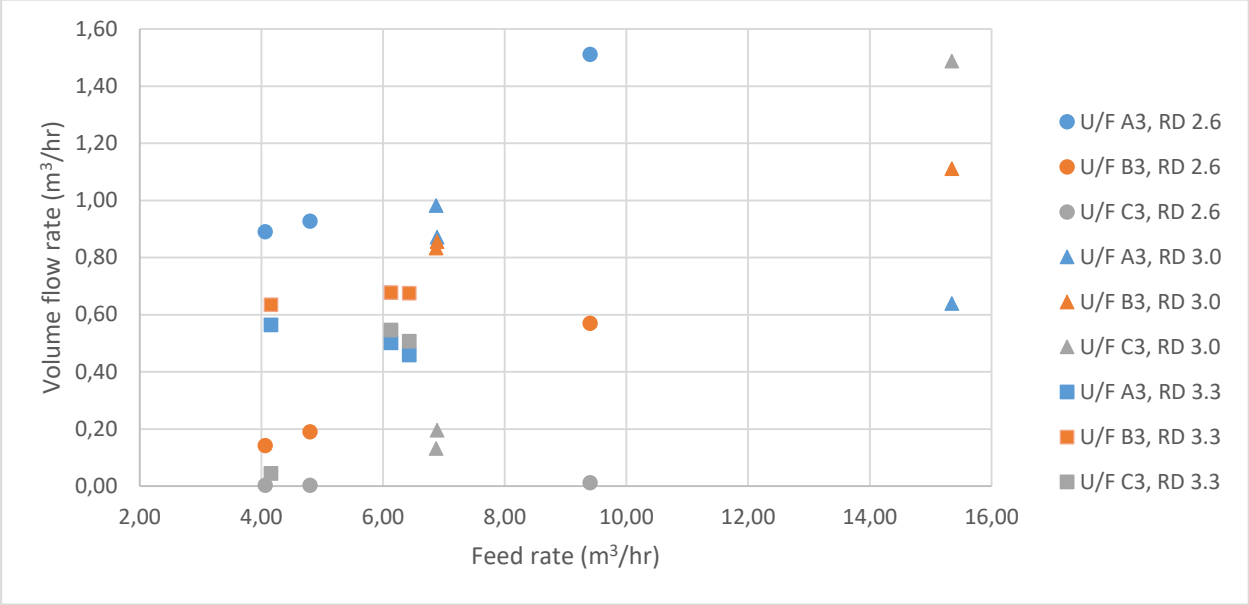

Figure 79. Underflow rates through Column 3 discharges over feed rate range (all medium RDs)

At a medium RD of 2.6 for an increase in feed rate from 4.06 m^3/hr to 9.41 m^3/hr, underflow A3 increased from 0.89 m^3/hr to 1.51 m^3/hr while underflow B3 increased from 0.14 m^3/hr to 0.57 m^3/hr. Underflow C1 remained at practically zero over the entire feed rate range. At a medium RD of 3.0 for a feed rate increase from 6.87 m^3/hr to 15.35 m^3/hr, underflow A3 decreased from approximately 0.90 m^3/hr to 0.64 m^3/hr, while underflow B3 increased from 0.83 m^3/hr to 1.11 m^3/hr and underflow C3 increased from 0.13 m^3/hr to 1.49 m^3/hr. At a medium RD of 3.3 for a feed rate increase from 4.16 m^3/hr to 6.43 m^3/hr, underflow A3 decreased from 0.56 m^3/hr to 0.46 m^3/hr, while underflow B3 increased from 0.64 m^3/hr to 0.68 m^3/hr. Underflow C3 increased from 0.04 m^3/hr to 0.51 m^3/hr.

On first glance, the data for Column 3 seems to have the most exceptions to the expected trend of an increase in underflow rate for an increase in feed rate, as well as a decrease in underflow rate long the length of the Mk2 trommel. The first exception is the decrease in underflow rate through discharge A3 for an increase in feed rate at a medium RD of 3.3. This is once again due to the feed configuration and the momentum of the slurry that hits the scrolls as it is fed to the screen. The feed configuration limits the formation of a bed of material on the first row of panels, which in turn limits the drainage that can be achieved through these panels.

The second exception that can be observed is the apparent increase in underflow rates along the length of the Mk2 trommel at the highest feed rate of 15.35 m^3/hr. The highest underflow rate of 1.49 m^3/hr is achieved in Row C, followed by Row B at 1.11 m^3/hr and the lowest for A3 at 0.64 m^3/hr. The assumption that the underflow rate should decrease along the length of

the Mk2 trommel is derived from the fact that the material volume in the screen decreases along the length of the screen as the material is being drained systematically. It is however important to keep the discussion of slurry slumping and pulp cataract motion in mind. As the material progresses along the length of the Mk2 trommel, the slurry develops into a pulp as the medium is being drained. The pulp then tends to migrate more towards the direction of Mk2 trommel rotation, above discharge Column 3. The underflow rate of medium in this column therefore increases as a function of the volume of material that resides over the column.

The third exception is that the underflow rate through discharge B3 exceeded that of A3 over the entire feed rate range at a medium RD of 3.3. The effect is similar to what was discussed in section 8.3.2.5, with the properties of the pulp changing as the medium is removed, which affects the position of the pulp in the Mk2 trommel and in turn affects the drainage through a specific row of panels. As the volume of the medium decreases, the underflow rate also decreases from Row B to Row C. The small apparent decrease in underflow rate for an increase in feed rate under these conditions is considered to be variance introduced by experimental, sampling or sample processing inaccuracy.

8.3.2.7. Underflow profiles: DMS work

As before, the underflow profiles for the DMS work are plotted to correlate the data with the material distribution inside of the Mk2 trommel.

8.3.2.7.1. Profile 1: Feed = 4.16 m^3/hr. (Medium RD = 3.3)

The first underflow profile is for the lowest feed rate of 4.16 m^3/hr at a medium RD of 3.3. The underflow profile plotted as a surface plot in Figure 80.

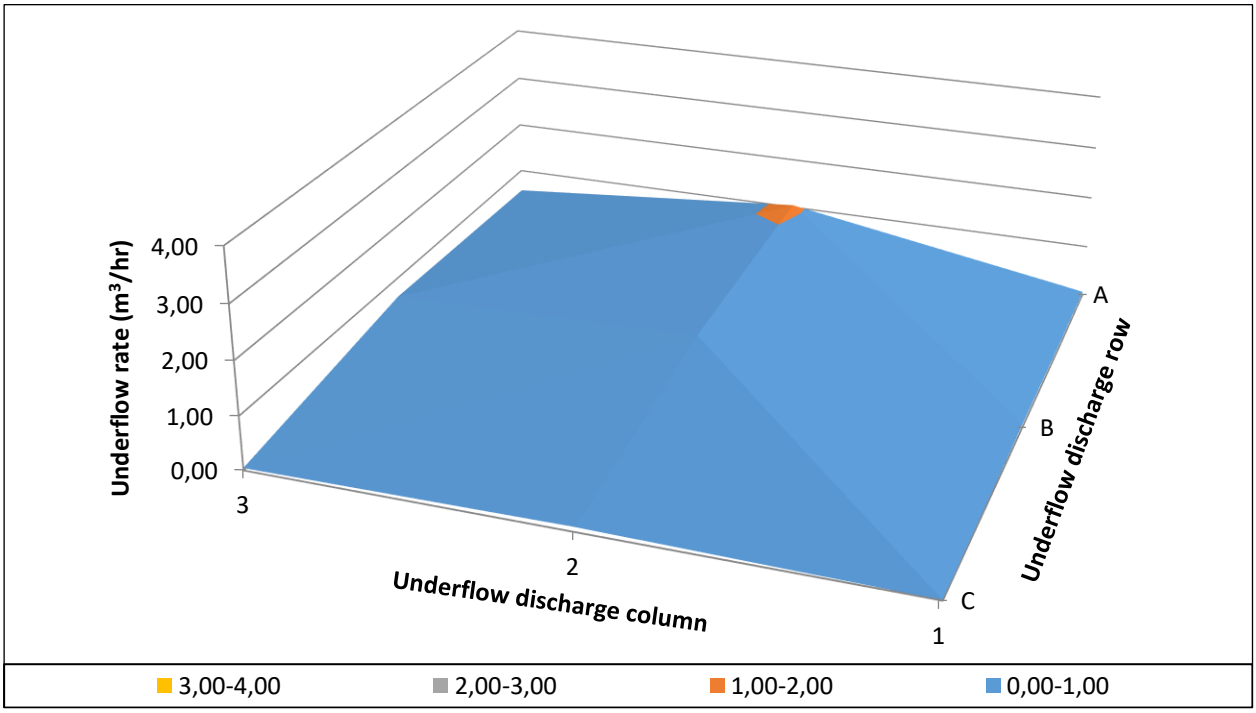

Figure 80. Underflow profile for DMS tests. Feed rate 4.16 m³/hr.

At the lowest feed rate of 4.16 m³/hr, the majority of medium is drained through discharge A2 and B2, with underflow rates of 1.04 m³/hr and 0.79 m³/hr, respectively. Discharge A3 with an underflow rate of 0.56 m³/hr is exceeded by discharge B3 with an underflow rate of 0.64 m³/hr. As discussed before, the increase in underflow rate from discharge A3 to B3 is likely due to the change in pulp properties, which affects the location of the pulp in the Mk2 trommel. As a larger fraction of the pulp begins to reside over Column 3 in Row B, the rate at which the medium passes through the screen media in that location increases. Beyond Row B, the medium decreases to such an extent that the underflow rate drops to negligible for all discharges in Row C. All discharges in Column 1 has negligible underflow rate at this low feed rate.

8.3.2.7.2. Profile 2: Feed = 6.43 m³/hr. (Medium RD = 3.3)

The second underflow profile is for a feed rate of 6.43 m³/hr at a medium RD of 3.3. This underflow profile is plotted in Figure 81.

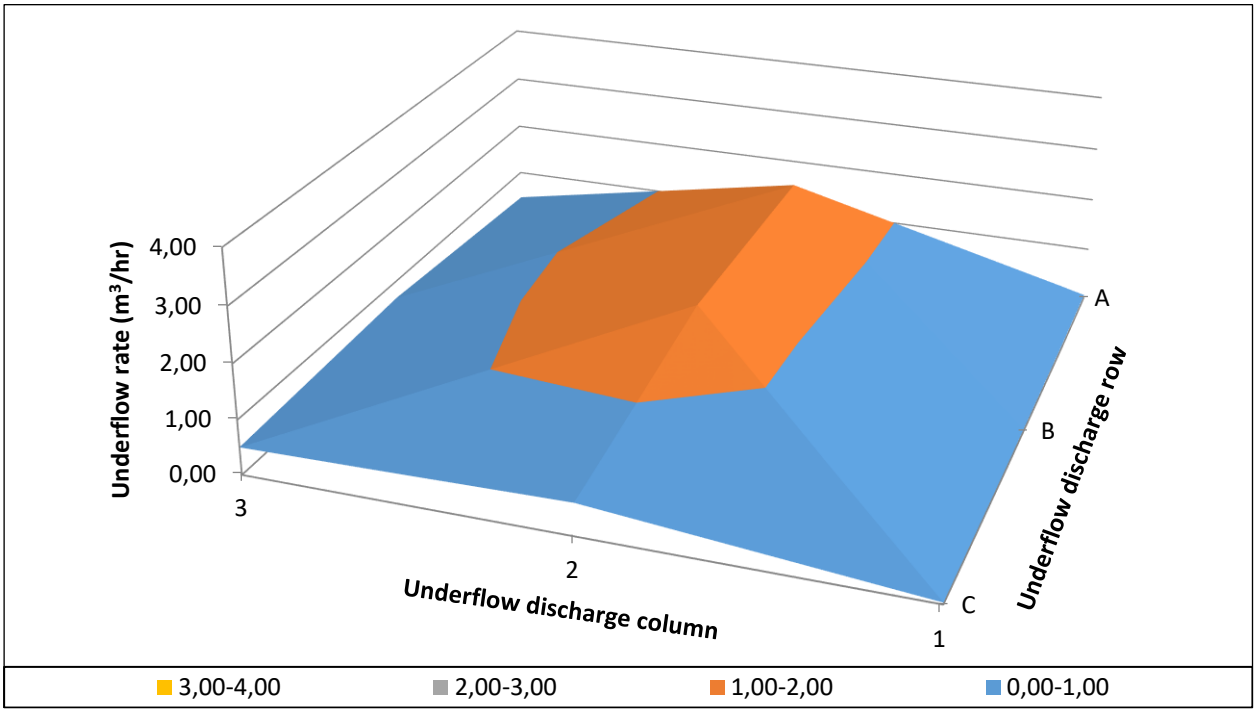

Figure 81. Underflow profile for DMS tests. Feed rate 6.43 m³/hr.

Figure 81 illustrates a more developed underflow profile for an increase in feed rate to 6.43 m^3/hr. Once again, the greatest underflow rate of 1.51 m^3/hr was achieved through discharge A2, followed closely by discharge B2 with an underflow rate of 1.44 m^3/hr. At this higher feed rate, there was still some medium left in the Mk2 trommel at discharge Row C, resulting in a small underflow rate of 0.60 m^3/hr. Similar to before, discharge B3 underflow rate of 0.68 m^3/hr exceeds that of discharge A3 with an underflow rate of 0.46 m^3/hr. With the greater feed rate, there is also some medium left in the pulp over Column 3 beyond Row B, resulting in an underflow rate of 0.51 m^3/hr through discharge C3. As before, the underflow rates through discharge Column 1 remains negligible along the entire length of the Mk2 trommel.

8.3.2.7.3. Profile 3: Feed = 15.35 m^3/hr. (Medium RD = 3.0)

The third underflow profile is for a high feed rate of 15.35 m^3/hr at a medium RD of 3.0, plotted in Figure 82.

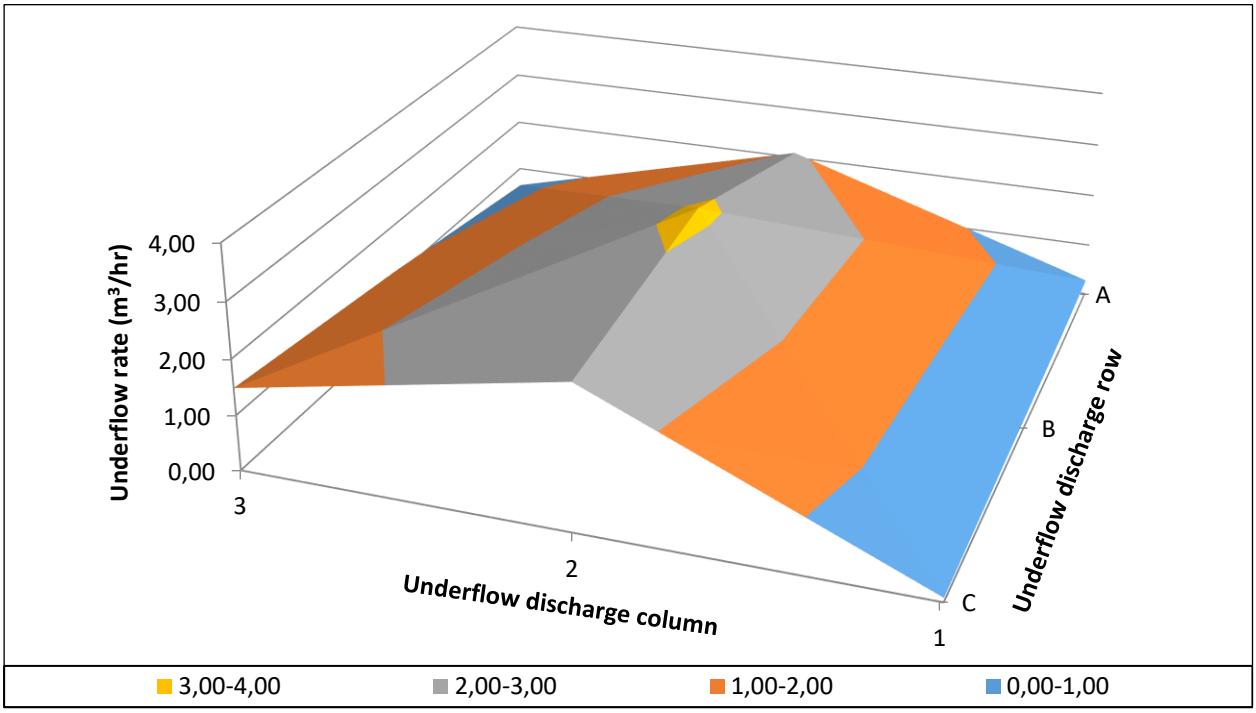

Figure 82. Underflow profile for DMS tests. Feed rate 15.35 m³/hr.

At a feed rate of 15.35 m³/hr, the underflow rate through discharge A2 of 2.09 m³/hr was exceeded by that of discharge B2 with an underflow rate of 3.16 m³/hr. As discussed, this is caused by a combination of the way the feed stream collides with the scrolls, as well as the location of the ore bed that shifts as its properties change with a decrease in medium content. As more of the medium was being drained from the Mk2 trommel, the underflow rate in Column 2 proceeded to decrease to 2.59 m³/hr by Row C. Along the length of the Mk2 trommel, the pulp tends to reside more towards Column 3 discharges, resulting in a steady increase in underflow rate from 0.64 m³/hr in Row A, to 1.11 m³/hr in Row B and ultimately to 1.49 m³/hr in Row C. The underflow rates through discharge A1 has increased slightly to a value of 0.27 m³/hr for this significant increase in feed, while the underflow rates through Rows B and C in Column 1 remained negligible.

8.3.3. Drainage rate comparison

In order to comment on the viability of a trommel as an alternative to vibrating screens for the purpose of medium recovery in a dense medium circuit, arguably one of the most crucial parameters to compare is the drainage rate. This is because capacity is a very important specification for most mining equipment.

Working under the assumption that approximately 33% of a trommel's screen area is effectively being utilised at a time, Test Trommel Mk2 has an effective screen area of 0.34 m², which is significantly smaller than the screen areas of Test Trommel Mk1 and the test Vibrating screen, with screen areas of 0.53 m² and 0.51 m², respectively. As such, it was not

possible to compare the drainage rates achieved on the screens directly over the range of feed rates, because the different screens have different appropriate feed rates. Drainage rate per screen area ($m^3/hr/m^2$) is a parameter that normalises underflow rate for a screen area to enable the comparison of underflow rates on different size screens. Similarly, in order to compare feed rates to different size screens, the feed rate can be normalised by dividing the total feed rate by the utilised screen area. This unit of measurement will be called "Normalised feed" and has a unit of measurement of $m^3/hr/m^2$. The drainage rate is plotted over the range of feed to screen area ratios in Figure 83.

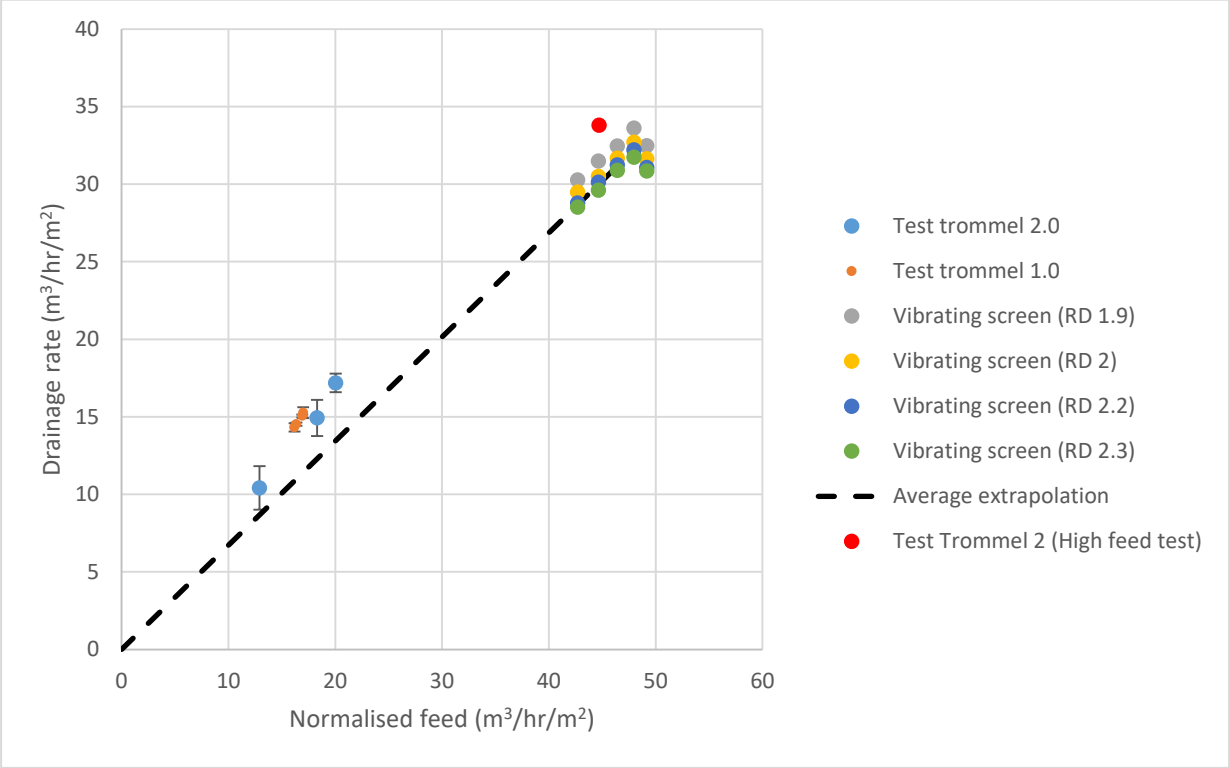

Figure 83. Comparison between drainage rates of Test Trommel Mk1, Test Trommel Mk2 and Vibrating screen during test work performed by Kabondo (2018)

Due to equipment constraints on Test Trommel Mk1, the feed rate was limited. Test parameters for Test Trommel Mk2 was selected to allow direct comparison with Test Trommel Mk1 in terms of overflow properties and medium recovery. In order to compare the overflow properties of Test Trommel Mk2 with Test Trommel Mk1, it was decided to use similar Feed to screen area ratios for the two trommel test campaigns. The feed to screen area ratios tested on the trommels, in the range of 12.9 $m^3/hr/m^2$ to 20 $m^3/hr/m^2$, are significantly lower than for the test work on the vibrating screen by Kabondo (2018), which was performed in the range of 42.7 $m^3/hr/m^2$ to 49.2 $m^3/hr/m^2$.

It is intuitive that drainage rate will increase with an increase in feed rate, as long as the screen is operated under its maximum capacity. Furthermore, it is also known that the

drainage rate will be equal to zero if there is no feed to the screen. The data in Figure 83 appears to conform to a linear relationship between drainage rate and normalised feed, with a gradient of 0.66. This is because any additional feed gets drained to the underflow, so long as the screen is operated under capacity. From this information one might expect a gradient of 1, but it is important to remember that the feed also consists of oversized ore particles, which reports to the overflow stream.

A single test run was performed on Test Trommel Mk2 at a high feed rate, which is comparable to the normalised feeds that the vibrating screen was operated at. Although this is just a single data point with no statistical backing, it still provides value by proving that Test Trommel Mk2 can compete with the vibrating screen in terms of drainage rate. Due to the fact that this point does not have any repetitions, it was not included in the calculations and comparison of Test Trommel Mk1 and Test Trommel Mk2 overflow properties, however it was decided that this data point still adds value to the comparison of drainage rates because it conforms entirely to the trend that is observed for a magnitude of data points in Figure 83.

All drainage rates for Trommel Mk1 and Trommel Mk2 fall above the expected trend with a gradient of 0.66, imposed by the data on the Vibrating screen. This is likely due to a slightly higher medium to ore ratio in the trommel tests. A higher medium to ore ratio implies that a greater fraction of the feed reports to the underflow, while a smaller fraction of oversized ore particles reports to the overflow stream. This was a result of the difficulty of predicting the quantity of ore that would reside in the Mk2 trommel at any particular moment. If the slurry in the sump is made up at a 5:1 medium to ore ratio by calculating the masses of each component that is required to achieve that ratio, the ore retention in the Mk2 trommel affects the medium to ore ratio in the rest of the system, and therefore, in turn, the feed to the Mk2 trommel as well. The quantity of ore that resides in the Mk2 trommel depends on the feed rate, ore composition of the feed, Mk2 trommel rotation speed and scroll configuration in the Mk2 trommel. As such, it is extremely difficult to guarantee a medium to ore ratio of 5:1 during test work. The approach to attempt to achieve a 5:1 medium to ore ratio in the Mk2 trommel feed, was to calculate the masses required to achieve a 4:1 medium to ore ratio in the sump, assuming that the ore retention in the Mk2 trommel will increase the medium to ore ratio in the feed to approximately 5:1. From these results, it appears that the mass of ore that resided in the Mk2 trommel was slightly overestimated, resulting in a slightly greater material split to the underflow and, in turn, a slightly higher drainage rate associated with a particular feed.

Under the assumption that a third of the total screen area is being utilised, these results illustrate that, in the context of medium recovery, a trommel is a competitive alternative to the drain section of a horizontal vibrating screen.

8.3.4. Evaluation of utilised screen area

The assumption that a third of the total trommel screen area is utilised at one particular moment, is a rule of thumb that is accepted within Multotec based on years of industrial experience. Utilised screen area of a trommel is however not a constant parameter. It depends on operating parameters of the trommel, such as feed rate, drainage capability of the screen media, and all other parameters that contribute to the drainage capacity of the screen, including but not limited to (Wills & Napier-Munn, 2006):

- Application (type of commodity and composition of feed);
- Solids PSD;
- Feed RD;
- Screen media (aperture size, shape, %Open area);

One of the motivations for designing the 3 x 3 underflow discharge sample grid was to investigate and evaluate the assumed industry standard of trommels utilising a third of the total screen area. It is known that the rule of thumb does not hold for all applications at all operating parameters, and must therefore be tested. In order to evaluate this, the fraction of the total underflow rate that occurred through each individual discharge, was calculated. These fractions were then accumulated for each underflow discharge starting from the feed end of the Mk2 trommel to the overflow discharge end. Since the trommel (Mk2) is rotating in an anti-clockwise direction, very low drainage was achieved through Column 1 of discharges. As such, Columns 2 and 3 were accumulated first to determine the total area required to drain 98 % of the total underflow rate that was achieved. The accumulated screen area, starting from Row A towards the direction of row C, up to the discharge where 98 % of the total underflow rate was achieved, was then calculated as the utilised screen area. The total utilised screen area was then used to calculate the percentage of the total screen area that was utilised for drainage. In cases where significant drainage (greater than 2% of the total drainage) was achieved through Column 1, this Column's screen area was also added to the total accumulated screen area from Row A to C. The results are illustrated in Figure 84.

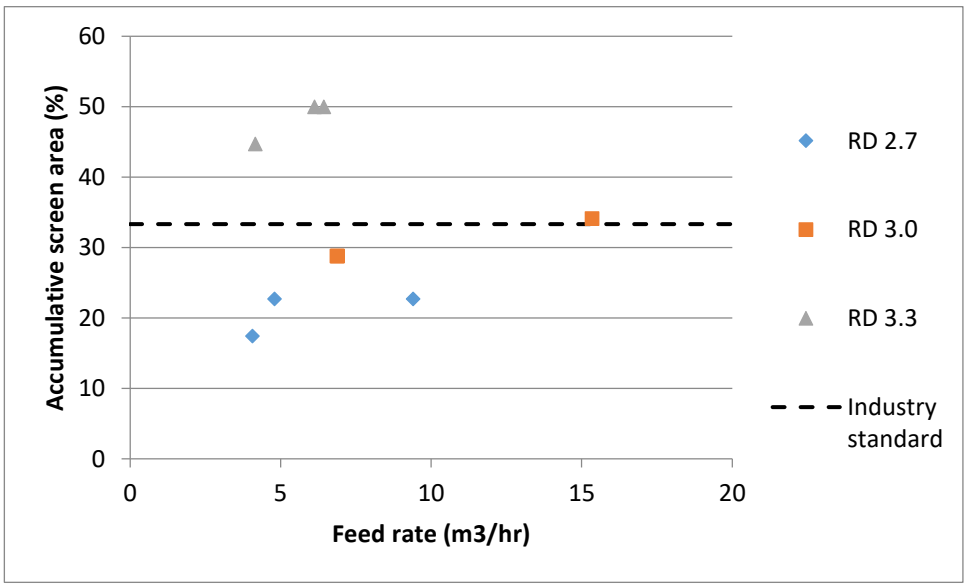

Figure 84. Calculated utilised screen area of Test Trommel Mk2 over feed rate range.

As Illustrated in Figure 84, the first observation is that there is typically an increase in utilised screen area with an increase in feed rate for all densities. This is intuitive because an increase in feed rate leads to a higher material quantity that needs to be drained. With a finite drainage capacity for each panel, more panels need to be utilised to achieve complete drainage.

The maximum utilised screen area that was calculated, is 50% for a medium RD of 3.3 feed rates of 6.13 m^3/hr and 6.43 m^3/hr. The maximum is 50%, because the other half of the Mk2 trommel screen area is facing upwards and drainage does not occur through the upper half of the screen. At lower feed RDs, all of the medium could be drained through a third or less of the total screen area, which is approximately 66% of the length of the screen. As the medium RD decreases, the viscosity of the slurry decreases with it, which makes the slurry easier to drain. In addition, a higher medium RD translates to a higher ore quantity in the feed at a constant medium to ore ratio of approximately 5:1. An increase in ore bed depth and width, increases the screen area that is obstructed by the ore bed, which would lead to a lower drainage rate through these panels and a larger screen area requirement to achieve complete drainage of the medium.

At a medium RD of 3.0, the calculated utilised screen area was 28.8 % at a feed rate of 6.87 m^3/hr and increased to approximately 34.14 % at a feed rate of 15.35 m^3/hr. These results are the closest to the assumed industry standard of 33.33 % utilised screen area of a trommel. It can be concluded that the assumed industry standard of 33.33 % is relatively accurate as a rule of thumb for simplified design and sizing of trommels, however this specification is a function of application and other operating parameters such as feed rate and feed properties.

8.4. Performance comparison to DMS Trommel (Mk1)

The final step in the data analysis was to compare the results that were produced on the second Test Trommel (Mk2) with that which was produced on the first DMS Test Trommel (Mk1). Since an in depth comparison with the vibrating screen performance was already completed in the first study, all of the results will not be plotted again in the figures in this section. The focus of this comparison is to discuss the difference between results on the first and second test trommels. The comparison with the vibrating screen results will only be mentioned briefly to recap the comparison with the vibrating screen.

8.4.1. Moisture concentration in the overflow

As before, the first overflow parameter to quantify the screening efficiency and medium recovery of the Test trommel (Mk2) is the moisture content. The results for the % Moisture over the relative density range are illustrated in Figure 85.

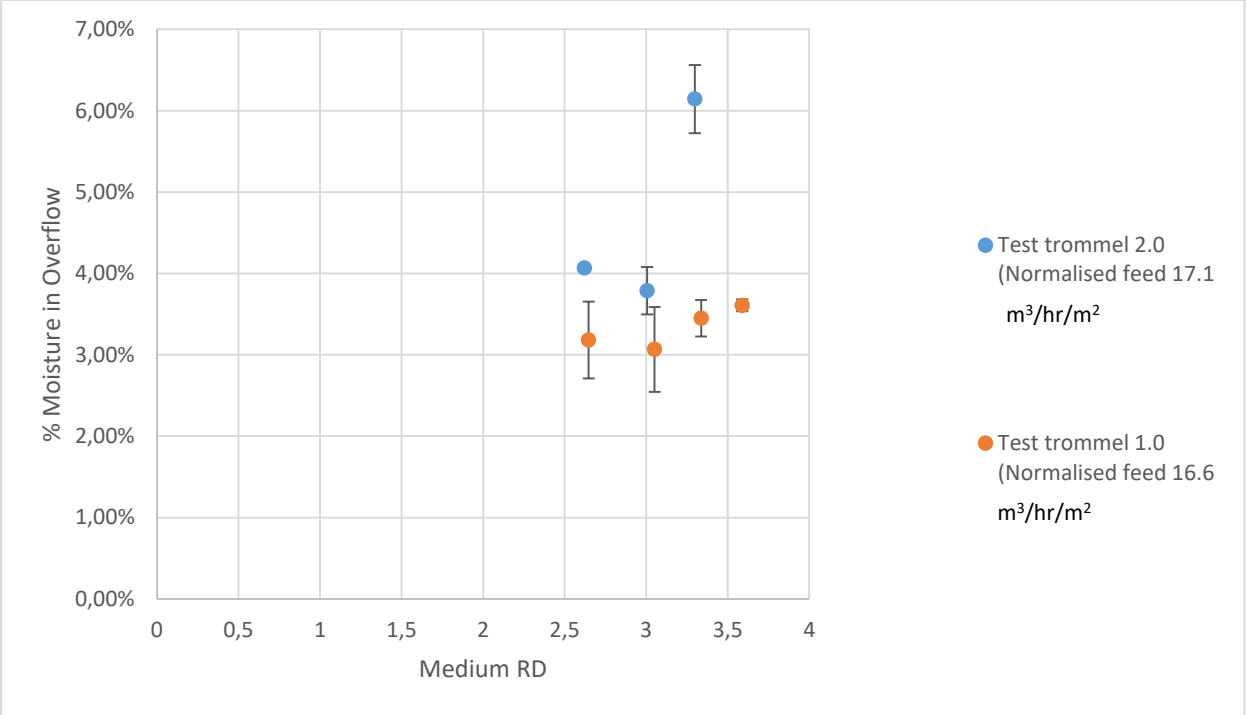

Figure 85. Comparison of % Moisture in overflow between Test Trommel (Mk1) and Test Trommel (Mk2) over medium RD range.

Due to the setup of the second Test Trommel (Mk2) with nine different underflow discharge pipes re-circulating back into the sump, it was physically impossible to install an agitator in the sump of the second Test Trommel (Mk2). It was found that the bypass stream was insufficient to keep the contents of the sump agitated at medium RDs above 3.3. Above this medium RD, the solids started to settle and stall the system. As such, the medium RD was limited to a maximum of 3.3.

The results for % Moisture in the overflow that were produced on Test Trommel (Mk2) closely represented the results that were produced on Test Trommel (Mk1), with the exception of a moisture concentration of 6.14 % in the overflow at a medium RD of 3.3. Originally during the first test campaign, there was a possibility that the % Moisture in the overflow stream remained constant and that the apparent trend was just experimental variance, due to a weak correlation and high experimental variance. However, with the results from Trommel (Mk2), the percentage moisture seems to follow the same trend. With an increase in medium RD from 2.6 to 3.3, there appears to have been an increase in % Moisture in the overflow stream from 4.07 % to 6.14 %. Although the moisture content in the overflow of Trommel Mk2 were consistently higher than that in the overflow of Trommel Mk1, the results are very close. Since neither of the trommels were overfed, the moisture content in the overflow stream indicates the ability of the pulp to retain moisture while being transported through the trommel. With an increase in FeSi content, there is a greater surface area of solids that the moisture adheres to. This is likely the cause for the increase in percentage moisture for an increase in medium RD. Interestingly there seemed to have been a drop in % Moisture in the overflow stream at a medium RD of 3 for both test campaigns on the two different trommels. However, the variance of these values indicates that there is no statistical significance to this observation.

These values fall well under the range of moisture contents that were obtained in the overflow of the vibrating screen, ranging from 10.29 % at a medium RD of 1.9, up to 27.91 % at a medium RD of 2.3. It has to be noted however that the vibrating screen was operated at a normalised feed of approximately 46 $m^3/hr/m^2$, while the trommels were operated at a normalised feed between 16 $m^3/hr/m^2$ and 17 $m^3/hr/m^2$. It is expected that increasing the normalised feed to the trommels beyond saturation of the trommel would result in significant increases in water content in the overflow.

8.4.2. FeSi concentration in the overflow

The second overflow parameter of interest the FeSi content in the overflow stream. The result comparison between Trommel Mk1 and Trommel Mk2 are illustrated in Figure 86.

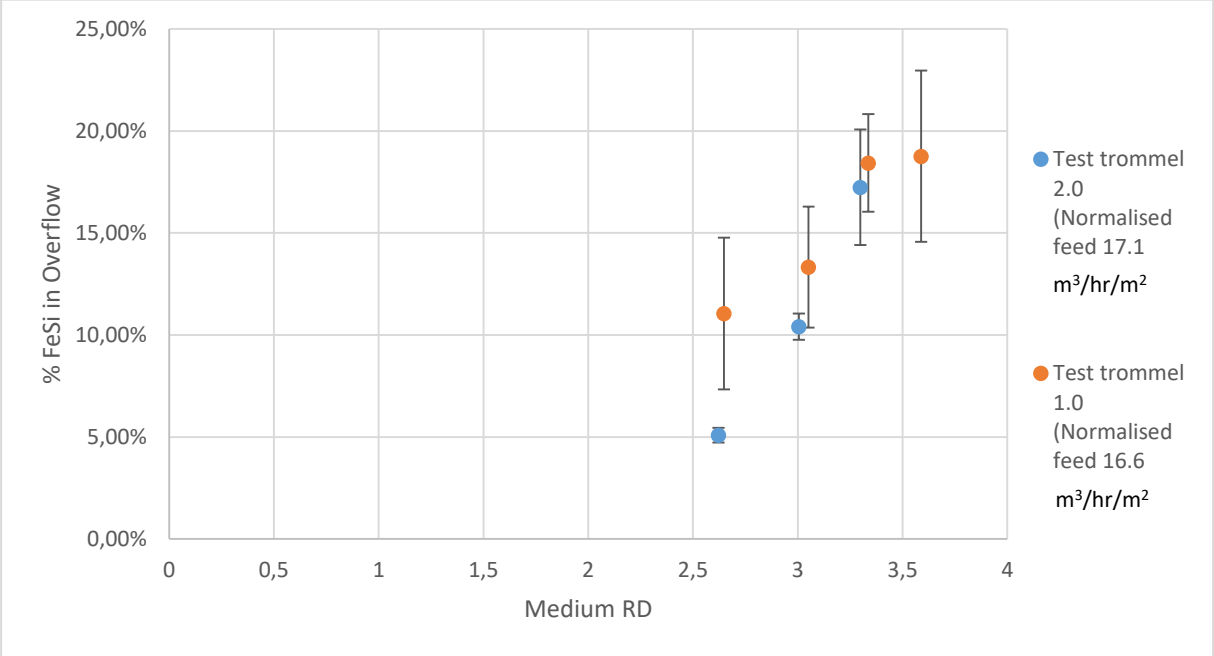

Figure 86. Comparison of % FeSi in overflow between Test Trommel Mk1 and Test Trommel Mk2 over medium RD range.

The most noteworthy observation for this comparison is arguably the improvement in repeatability of the experimental work. 95 % Confidence intervals were calculated in both studies by assuming a normal distribution and performing a two-tailed test with one degree of freedom (since one of the three samples had to be thrown out due to the system changing due to sampling). The 95 % confidence intervals in Figure 86 illustrates the drastic improvement in statistical significance of the results after the improved design of drain Trommel Mk2, which was a result of the learnings of the first experimental campaign. Although there was still a significant variance for FeSi content in the overflow at the highest medium RD of 3.3, the repeats of the lower two densities were near perfect repetitions with a very small confidence interval. These results contributed significantly to the overall confidence in the conclusions drawn from the experimental work, as opposed to a high level of uncertainty that still had to be cleared up after the first campaign on DMS Trommel Mk1.

As illustrated in Figure 86, the results obtained on Trommel Mk2 once again closely resembled the results obtained on Trommel Mk1. For an increase in medium RD from 2.6 to 3.3, there was a steep increase in FeSi concentration in the overflow discharge from 5.09 % to 17.24 %. The FeSi concentration in the overflow stream of Trommel Mk2 was consistently lower than that of Trommel Mk1, but was very close to the result obtained on Trommel Mk1 at a medium RD of 3.3. This is likely due to the difference between the ore transport mechanisms between the two Trommels. In Trommel Mk1, the ore was loaded into the screen in batch, after which the medium was circulated over the particle bed during screen rotation.

The paddles that were attached to the shaft, rotated with the Mk1 trommel and scooped the pulp into the scroll opening. With this setup, the screen length was 0.63 m, and the paddles were located approximately in the middle of the screen. As a result, the feed inlet was located very close to the pulp transport mechanism, implying that the medium had a relatively short screen length to drain before being transported to the wash chamber. The fact that vision into the Mk1 trommel was completely obstructed when the screen was installed means that analysis of the inner workings of Trommel Mk1 was limited to speculation. It is speculated that some FeSi that was fed to the Mk1trommel did not have the opportunity to drain through the pulp bed and screen media before being scooped up into the solids scroll. This may have resulted in a slightly inflated FeSi content in the overflow stream of Trommel Mk1.

In Trommel Mk2, the ore transport mechanism was simplified to a scroll on the screen surface. As a result, there is a smaller probability that some of the material that is fed to the screen will bypass the screen surface and report directly to the overflow stream (as long as the screen is operated under capacity). As such, the medium that reports to the overflow stream is purely a function of medium adhesion to the ore particles, which results in a smaller FeSi concentration in the overflow stream.

For the FeSi percentage in the overflow stream, the data is plotted for direct comparison in Figure 87.

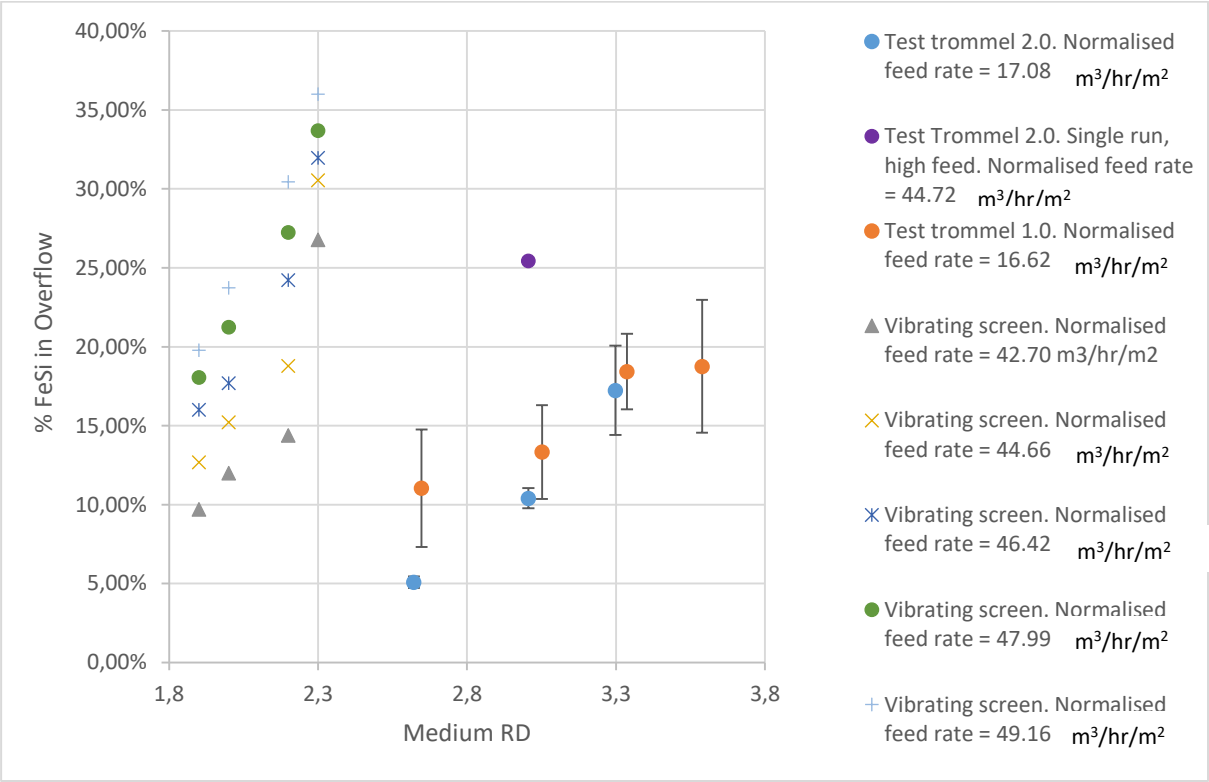

Figure 87. Comparison of % FeSi in overflow between Test Trommel Mk1, Test Trommel Mk2, and vibrating screen (from Kabondo (2018)) over medium RD range.

The study on the vibrating screen by Kabondo (2018) at a normalised feed rate range of 42.70 $m^3/hr/m^2$ to 49.16 $m^3/hr/m^2$ and an RD range of 1.9 to 2.3, the FeSi concentration in the overflow was in the range of 9.71 % to 36.01 %. Even though the medium RD during the trommel test work was significantly higher, in the range of 2.7 to 3.3 for Trommel 2 and up to 3.6 for Trommel Mk1, the FeSi concentration in the overflow was in the range of 5.09 % to 17.24 % for Trommel Mk1 and 11.05 % to 18.76 % for Trommel Mk1. This is substantially lower than the FeSi concentrations that were obtained on the vibrating screen. It can be argued that the higher feed rate to screen area ratio would contribute to the higher FeSi content in the overflow stream. A single test was performed on Trommel Mk2, with a normalised feed rate of 44.72 $m^3/hr/m^2$, which falls right in the normalised feed range on the vibrating screen. Typically, this result would not be included in the discussion because of the low statistical significance, however it is believed that this data point still provides value and insight into the operation of Trommel Mk2. At a normalised feed rate of 44.72 $m^3/hr/m^2$, the overflow consisted of 25.44 % FeSi. This illustrates that an increase in feed does in fact increase the FeSi concentration in the overflow stream, as expected. However, even though there is a significant increase in FeSi concentration in the overflow, it was still within the range of FeSi concentrations in the overflow that were achieved on the vibrating screen.

Considering that this data point was produced at a medium RD of 3.0, the result is very promising with regards to FeSi recovery compared to a vibrating screen.

8.4.3. Percentage FeSi carryover

The third and final quantification of screening efficiency that will be compared between Test Trommels Mk1 and Mk2, is the percentage of FeSi that was fed to the screen, reporting to the overflow. In other words, this refers to the percentage of FeSi that did not get drained in the drain section of the drain and rinse process. The results for the percentage FeSi carryover on Trommels Mk1 and Mk2 are illustrated in Figure 88.

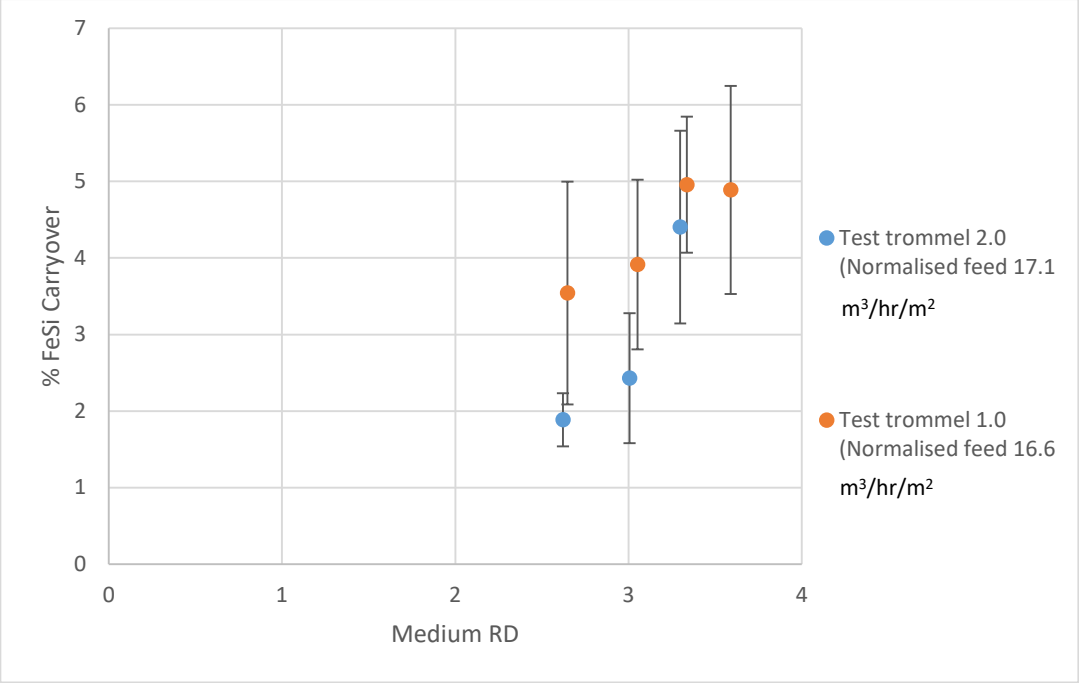

Figure 88. Comparison of % FeSi carryover between Test Trommel Mk1 and Test Trommel Mk2 over medium RD range.

The data for percentage carryover of FeSi to the overflow in Figure 88 illustrates a correlation with medium RD. On Trommel Mk2, an increase in medium RD from 2.6 to 3.3 resulted in an increase in % FeSi carryover from 1.88 % to 4.40 %. After completing the test work on the improved design of the Mk 2trommel, this correlation became clearer than for the original test work performed on Trommel Mk1. The 95% confidence interval on Trommel Mk2 is still relatively large compared to the change in % FeSi carryover for an increase in medium RD, so the correlation is not particularly strong compared to the variance of the data. On Trommel Mk1, this correlation was unclear due to the large variance in the data and the weak correlation. However on Trommel Mk2, the decreased variance provided more confidence in the data and the correlation.

The increase % FeSi carryover with an increase in medium RD is not as intuitive as the increase in percentage FeSi in the overflow with an increase in RD that was discussed before. With an increase in medium RD, there is a greater concentration of FeSi in the feed and the medium that adheres to the ore particles contains more FeSi. However, if this was the only factor that increased the FeSi concentration in the overflow stream, it would be expected that the % FeSi carryover would remain constant as a constant fraction of the medium (with various concentrations) adheres to the ore particles. The increase in % FeSi carryover means that a greater fraction of the FeSi adheres to the ore particles. It is hypothesised that the increase in medium RD also results in a slightly greater volume of medium adhering to the ore particles. Not only does the increase in medium RD imply a greater quantity of FeSi particles in the medium that adheres to the ore particles, but also a slightly larger volume of medium, leading to even more FeSi particles adhering to the ore. This is confirmed by the increase in % moisture in the overflow with an increase in medium RD. These results correspond with past studies that found that an increase in feed slurry density led to lower screen performance and an increase in fines reporting to the overflow (Rogers & Brame, 1985).

The separation efficiency results of the second test trommel resembled the results that were achieved on the first test trommel, As such, the results for overflow composition and therefore separation efficiency of test trommel Mk2 provided further confidence in the results that were obtained on the Test Trommel Mk1. In addition, the higher repeatability of the experimental work on trommel Mk2 resulted in smaller 95% confidence intervals and also more confidence in the results.

The % FeSi carryover of Test Trommels Mk1 and Mk2, ranging from 3.54% to 4.96 % and from 1.88 % to 4.40%, respectively, were significantly lower than what was achieved on the vibrating screen in the range of 6.88 % to 10.46 % at a medium RD of 2.3. This is a very promising result that encourages further investigation of trommels as an alternative to vibrating drain and rinse screens.

9. SUMMARY FOR TEST TROMMEL 2 (Mk2)

The final conclusions from the second campaign on Test Trommel Mk2 are summarized and discussed:

9.1. Water tests

9.1.1. Underflow analysis for varying feed rate

The highest drainage occurs through the middle column of the Mk2 trommel, because the majority of water resides at the bottom of the Mk2 trommel circumference above Column 2.

The water location in the Mk2 trommel was slightly off-centre because of the rotation of the Mk2 trommel. As a result, the second highest drainage occurred through the middle discharge Column 2.

Discharge Column 3, which is on the opposite direction of Mk2 trommel rotation, had low underflow rates for the entire feed rate range investigated.

9.1.1.1. Low to intermediate velocity flow (<0.30 m/s) and splashing

Low to intermediate velocity and splashing was maintained in the trommel (Mk2) at feed rates below 19.86 m^3/hr.

Throughout the entire trommel (Mk2), the water drainage increased with an increase in feed rate, while the trommel (Mk2) was operated under its capacity and the flow in the Mk2 trommel had low to intermediate velocity and splashing.

The underflow rate through a single discharge (A2) peaked at 7.56 m^3/hr at a feed rate of 19.6 m^3/hr. The underflow rate decreased along the length of the trommel (Mk2) to 5.30 m^3/hr through discharge B2 and 1.39 m^3/hr through discharge C2 at this feed rate.

As the water volume on the screen decreased, there is a decrease in hydrostatic pressure that drives drainage through the screen apertures. Therefore there was a decrease in underflow rate along the length of the trommel (Mk2).

9.1.1.2. Moderate to high velocity flow (>0.54 m/s) and splashing

As the feed rate increased beyond 19.86 m^3/hr, the flow in the Mk2 trommel increased in velocity and splashing. At high feed rates, the water was being propelled over the screen surface of Row A after colliding with the scroll close to the feed end of the trommel (Mk2). A peak underflow rate of 9.54 m^3/hr at a feed rate of 35.76 m^3/hr through underflow discharge B2 was measured. The turbulent flow pattern in the screen caused the peak of underflow through discharge B2 exceed that of discharge A2. With a further increase in feed rate,

underflow rates through the first rows of panels started to decrease due to water bypass of the screen surface. This had a detrimental effect on the drainage performance of the panels.

9.1.1.3. Underflow profiles

The underflow profiles for low to intermediate velocity flow and splashing in the trommel (Mk2) indicate material distribution inside of the trommel because the underflow rates are related to the hydrostatic pressure and therefore the water depth at that location in the trommel.

The underflow profiles for moderate to high velocity flow and splashing in the trommel (Mk2) indicate material velocity and collision with screen surfaces after being airborne. This results in more uneven underflow profiles than for low to intermediate velocity flow.

9.2. DMS tests

The high feed rate required to achieve sufficient agitation of the sump contents resulted in inaccurate RD measurements using a Marcy flask. It was necessary to calculate medium RD by processing the underflow samples for dry solids mass.

9.2.1. Underflow analysis

9.2.1.1. Effect of feed rate on underflow rate

The screen was operated under its maximum capacity, so an increase in feed rate resulted in an increase in underflow rate.

9.2.1.2. Underflow distribution in the Mk2 trommel

Similar to the trends observed during the water tests, the majority of drainage occurs through the middle of the trommel (Mk2) at the bottom of the circumference. The rest of the drainage occurs through Column 3 (the area above the direction of rotation), while drainage through Column 1 was practically negligible for all tests.

The highest feed rate of 15.35 m^3/hr at a medium RD of 3.0 resulted in some screen area being bypassed because of the angle of collision with the scroll near the feed end. At high feed rates, this resulted in a greater drainage through the second row of discharge than the first.

9.2.1.3. Effect of medium RD on drainage rate

Lower slurry RD resulted in more effective drainage. Higher water content in a slurry, in the context of fine screening, enhances the transport of fines to the underflow. Lower viscosity also leads to easier drainage of slurry through the particle bed and through the screen apertures.

9.2.1.4. Change in material motion as a result of medium drainage

Near the feed end of the trommel (Mk2), the slurry slumps to the bottom of the screen because of the flow properties of the entire feed slurry. As the medium drained from the screen, the remaining ore pulp became dryer. The pulp became more resistant to flow and the friction coefficient between the pulp and the screen surface increases. Along the length of the trommel with a decrease in medium, the remaining pulp migrated to the direction of trommel rotation and follows a cascading motion as opposed to the slumping motion of the slurry near the feed end. As the pulp moved away from the middle of the trommel, the screen area in the middle of the trommel had less obstruction for medium drainage. With more material residing over Column 3, the drainage through this Column also increased because the medium drained straight downward from the pulp residing over that area of the screen.

9.2.2. Screen performance

9.2.2.1. Drainage rate

The highest feed rate of 15.35 $m^3/hr/m^2$ at a medium RD of 3.0 on Test Trommel Mk2 accomplished a drainage rate of 33.79 $m^3/hr/m^2$, which was approximately equal to the maximum drainage rate of 33.61 $m^3/hr/m^2$ that was achieved in the study by Kabondo (2018) at significantly lower medium RD of 1.9. This indicates that the trommel is competitive with regards to screen capacity in the context of medium recovery.

9.2.2.2. Utilised screen area

The industry standard that a third of a trommel's screen surface is being utilised at a time, is a relatively accurate rule of thumb. However it was found that the utilised screen area depends on the application of the screen and is a function of parameters that affect drainage of a screen, including but not limited to:

- Feed rate;
- Solids PSD;
- Feed RD;
- Aperture shape, size and % Open area of the screen.

9.2.2.3. Comparison of Trommel Mk2 results with Trommel Mk1 results

The most notable observation in the comparison of results from the first and second test trommels, was an improvement in confidence of the results. Not only did the data from Test Trommel Mk2 have a higher statistical significance, the results also mimicked the results that were obtained during the first test campaign, which further improves the confidence in these results.

9.2.2.3.1. Effect of medium RD on % moisture in the overflow

Results from Test Trommel Mk2 confirmed an increase in % moisture with an increase in medium RD, a correlation that was unclear from the work on Test Trommel Mk1. This corresponds with the results obtained by Kabondo (2018). The results were very similar to the results produced on test trommel Mk1, which further improves confidence in the data. The results ranged between 3.79 % and 6.14 % moisture, which are significantly lower than the results produced on the vibrating screen in the range of 10.29 % to 27.91%. It has to be noted, however, that the feed rate for these tests was still significantly lower than the feed rate range on the vibrating screen.

9.2.2.3.2. Effect of medium RD on % FeSi in the overflow

The FeSi concentration in the overflow of Test Trommel Mk2 also closely resembled the results that were obtained on Test Trommel Mk1. For an increase in medium RD from 2.6 to 3.3, there was a steep increase in FeSi concentration in the overflow discharge from 5.09 % to 17.24 %.

A high feed rate result of Test Trommel Mk2, with a similar normalised feed to that of the vibrating screen study of 44.72 $m^3/hr/m^2$ was added to the comparison with the vibrating screen. Even at a high RD of 3.0 compared to the maximum RD of 2.3 on the vibrating screen, the % FeSi in the overflow of Test Trommel Mk2 was 25.44 %, which was comparable to the results obtained on the vibrating screen. This is a very promising result that encourages further investigation of trommels as an alternative to vibrating drain and rinse screens.

9.2.2.3.3. Effect of medium RD on % FeSi carryover

The % FeSi carryover of Test Trommels Mk1 and Mk2, ranging from 3.54% to 4.96 % and from 1.88 % to 4.40%, respectively, were significantly lower than what was achieved on the vibrating screen in the range of 6.88 % to 10.46 % at a medium RD of 2.3. This is a very promising result that encourages further investigation of trommels as an alternative to vibrating drain and rinse screens. There is an increase in fines bypassing to the overflow stream with an increase in medium RD in the context of wet screening.

Once again, the second test campaign on Test Trommel Mk2 enhanced confidence in the results that were obtained on Test Trommel Mk1, because they were closely related.

10. CONCLUSIONS

This section contains a brief summary of the findings and conclusions that have been made over the entire study, including the first and second test campaign.

10.1. First test campaign on Mk1 Trommel

First, a brief summary of the findings on Trommel Mk1 follows.

10.1.1. Drain chamber tests

An increase in medium RD resulted in an increase in pulp transport rate due to pulp adhesion and flow properties.

Secondly, an increase in medium RD resulted in an increase in FeSi carryover to the wash chamber, as well as FeSi content in the overflow stream. This correlates with literature findings.

Lastly, an increase in medium RD resulted in an increase in moisture bypass to the overflow stream of the drain chamber.

An increase in medium RD decreases the screen performance with regards to separation efficiency.

It was found that the capacity limiting mechanism of the DMS Trommel (Mk1) was ore transport rate from the drain chamber.

10.1.1.1. Comparison with vibrating screen results

Comparison of Mk1 trommel results with results produced on a vibrating screen by Kabondo (2018) revealed that there was a significantly lower % moisture in the overflow of Trommel Mk1 than what was achieved on a vibrating screen.

Secondly there was a significantly lower % FeSi in the overflow of Trommel Mk1 than what was achieved on a vibrating screen, even though Trommel Mk1 was operated in a significantly higher medium RD range.

Finally, Trommel Mk1's % FeSi carryover fell in the lower range of % FeSi carryover that was achieved on the vibrating screen by Kabondo (2018), regardless of a significantly higher medium RD on the Mk1 Test Trommel.

10.1.2. Washing tests

Submerged washing was investigated and quantified, producing the following results:

10.1.2.1. Wash chamber tests

Extremely efficient washing was achieved in the wash chamber. A 96% washing efficiency was achieved after just submersion and emersion of pulp in clean water. After a single rotation of Trommel Mk1 submerged wash chamber, 99.7% washing efficiency was achieved.

10.1.2.2. Bench tests

The bench washing and rinsing tests revealed that the lowest washing efficiency was achieved by submerged washing of a stationary bed (maximum of 52.44 %). Intermediate washing efficiency was achieved by rinsing tests (74.24 %). Finally, the highest washing efficiency achieved by submerged washing of a stationary, settling bed (88.18 %). This showed that submerged washing is a very promising alternative to rinse washing in the context of media recovery, if done correctly. A submerged trommel should be designed to allow a mechanism for transport of FeSi particles from the ore bed.

10.1.3. Mark1 campaign conclusion

Due to systematic change in the results over multiple sequential repeat tests, the confidence in the results on Test Trommel Mk1 was limited. The fact that the comparisons of the drainage and washing results with vibrating drain and rinse screens were extremely promising, motivated the continuation of test work on an improved design (Test Trommel Mk2). Therefore Mk2 of the test trommel was designed with the purpose of replicating promising results and improve the statistical significance of the results.

10.2. Second test campaign on Mk2 Trommel

In addition to repeating the tests from Test Trommel Mk1, the design of Test Trommel Mk2 also allowed the investigation of material distribution inside of the trommel and underflow rates as a function of location inside the trommel.

10.2.1. Water tests (Mk2)

As the majority of material tends to reside over the lowest point of the trommel's circumference, maximum drainage occurs through the middle column of discharges (Column 2). Column 3 (in the direction of trommel rotation) achieved the second greatest drainage. Practically negligible drainage occurs through Column 1, which is in the opposite direction of rotation of the trommel.

The water tests also revealed that an increase in feed rate during operation under Mk2 capacity resulted in an increase in drainage rates. At a lower velocity feed, the drainage decreased along the length of the trommel (Mk2), while at higher velocity feeds, splashing

caused the material to be propelled over the first row of discharges, resulting in higher drainage in subsequent underflow discharges.

10.2.2. DMS tests (Mk2)

During operation under the screen capacity, an increase in feed rate resulted in an increase in drainage rate.

The maximum drainage that was achieved on Mk2 Trommel was 33.79 $m^3/hr/m^2$, which is practically equal to the maximum drainage rate of 33.61 $m^3/hr/m^2$ achieved on a vibrating screen by Kabondo (2018) at similar normalised feed rates.

The industry standard for estimation of utilised screen area of 33.3 % proved to be fairly accurate, but is subject to factors affecting drainage rate, such as:

- Feed rate;
- Solids PSD;
- Feed RD;
- Aperture shape, size and % Open area of the screen.

An increase in medium RD resulted in a decrease in drainage in Trommel Mk2. This correlates with literature.

Secondly, an increase in medium RD increased FeSi carryover to wash chamber, as well as FeSi content in the overflow stream. This correlates to literature findings.

Finally, an increase in medium RD resulted in an increase in moisture bypass to the overflow stream of Trommel Mk2.

10.2.2.1. Observations from comparison of Mk2 trommel results with Mk1 trommel results

The results on the Mk2 Trommel had a greater repeatability and statistical significance, proving that the improved design of Mk2 trommel produced results that inspires greater confidence in their accuracy.

The results from the second test campaign on Mk2 Trommel correlated very well with the results from the first test campaign on Mk1 Trommel, providing further confidence in the performance that was measured on both trommels.

10.2.2.2. Comparison of trommel results with vibrating screen results

Trommels are competitive alternatives to vibrating drain and rinse screens in terms of drainage capacity and separation performance in the context of media recovery.

Although the majority of DMS tests on Mk2 Trommel was at a significantly lower feed rate than the tests performed on a vibrating screen, the results indicated that the Mk2 Trommel can compete with drainage rates of the vibrating screen at a similar normalised feed of approximately 45 $m^3/hr/m^2$. The % FeSi in the overflow of Trommel Mk2 was still in the lower region of the range of %FeSi in the overflow of the vibrating screen at this feed rate, regardless of the fact that the medium RD on Trommel Mk2 of 3.3 was significantly higher than the value of 2.3 on the vibrating screen.

The % FeSi carryover on Trommel Mk2 was also significantly lower than what was achieved on the vibrating screen by Kabondo (2018).

11. RECOMMENDATIONS AND FUTURE WORK

After proving that statistically sound test work can be performed on Test Trommel Mk2, the continuation of DMS work is recommended to fully understand the parameters that govern the operation and performance of a trommel for medium recovery at maximum throughput. These parameters are: Feed rate; RD, PSD and particle shape; Material flowability; Aperture size, shape, orientation and percent open area; Panel perforated thickness; Scroll configuration; and Screen rotation velocity. This information can then be used to design a submerged washing section that will be operated in series with the drain section. Design considerations for the submerged washing trommel are discussed in Appendix D. The development and optimisation of such a unit would revolutionise the DMS plant designs.

DEM and CFD coupled modelling are being recommended to predict trommel operation and to enable efficient and accurate sizing of trommel screens for any application. It is however required to obtain empirical data to verify and calibrate these models.

References

Alter, H., Gavis, J. & Renard, M. L., 1981. Design models of trommels for resource recovery processing. *Resources and Conservation*, Volume 6, pp. 223-240.

Bevilacqua, P. & Ferrara, G., 1994. Carry-Over of Water and Suspension of Fines by Coarser Particulate Solids - its Influence on the Design of DMS Regeneration Circuits. *Minerals Engineering*, 7(7), pp. 943-949.

Bosman, J., 2014. The art and science of dense medium selection.. *Journal of the Southern African Institute of Mining and Metallurgy*, Volume 114, pp. 529-536.

Burke, T. & Craig, E., 2005. Getting the most out of your screening operations.. *Minerals Engineering*, 1(5), pp. 25-30.

Chen, Y. et al., 2010. Size Separation of Particulates in a Trommel Screen System. *Chemical Engineering and Processing: Process Intensification*, Volume 49.

Collins, B., Napier-Munn, T. & Sciarone, M., 1974. The Production, Properties, and Selection of Ferrosilicon Powders for Heavy-Medium Separation. *Journal of the South African Institute of Mining and Metallurgy*, 75(5), pp. 103-119.

Dong, K. & Yu, A., 2009. DEM simulation of particle flow on a multi-deck banana screen. *Minderals Engineering*, 22(11), pp. 910-920.

Feller, R., 1976. Screening duration and size distribution effects on sizing efficiency.. *Journal of Agricultural Engineering Research*, Volume 21, pp. 347-353.

Ferrera, G., Preti, U. & Schena, G., 1988. Modelling of Screening Operations. *International Journal of Mineral Processing*, Volume 22, pp. 193-222.

Gaudin, A., 1939. *Principles of Mineral Dressing.* New York: McGraw-Hill.

Glaub, J., Jones, D. & Savage, G., 1982. *The Design and Use of Trommel Screens for Processing Municipal Solid Waste.* New York, American Society of Mechanical Engineers.

Grobler, J., Sandenbergh, R. & Pistorius, P., 2002. The stability of ferrosilicon dense medium suspensions.. *The south african Institute of Mining and Metallurgy*, Issue March, pp. 83-86.

Guerreiro, F., Gedraite, R. & Ataide, C., 2015. Residual moisture content and separation efficiency optimization in pilot-scale vibrating screen.. *Powder Technology*, Volume 287, pp. 301-307.

Gupta, A. & Yan, D., 2006. Introduction to mineral processing design and operation.. In: *Mineral processing design and operation.* s.l.:s.n., pp. 293-353.

Hudson, R. & Jansen, M. L. P., 1969. Batch sieving of deep particulate beds on a vibratory sieve. *Powder Technology,* 2(4), pp. 229-240.

Kabondo, L., 2018. *Determination of medium drainage rates for different vibrating screen slot sizes,* Stellenbosch: s.n.

Kelly, J., 2007. Flight Design in Rotary Dryers. *Drying Technology: An International Journal,* 10(4), pp. 979-993.

Liu, K., 2009. Some factors affecting sieving performance and efficiency.. *Powder Technology,* 193(2), pp. 208-213.

Marsh, C., 1945. *Heavy media separation process for assorting solids.*. United states, Patent No. US-2,496,590 A, 1.

Mellmann, J., 2001. The Traverse Motion of Solids in Rotating Cylinders - Forms of Motion and Transition Behaviour. *Powder Technology,* Volume 118, pp. 251-270.

Napier-Munn, T., Kojovic, T. & Scott, I., 1995. Some causes of medium loss in dense medium plants. *Minerals Engineering,* 8(6), pp. 659-678.

Napier-Munn, T., Morrell, S., Morrison, R. & Kojovic, T., 1999. *Mineral Comminution Circuits. Their Operation and Optimisation.* 2 ed. Indooroopilly: Julius Kruttschnitt Mineral Research Centre.

Napier-Munn, T. & Scott, I., 1990. The effect of demagnetisation and ore contamination on the viscosity of the meduim in a dense medium cyclone plant. *Minerals Engineering,* 3(6), pp. 607-613.

Orrino, J. & Khakhar, D., 2000. Mixing and segregation of granular materials. *Annu. Rev. Fluid mechanics,* p. 32.

Rogers, R. & Brame, K., 1985. An Analysis of the High-Frequency Screening of Fine Slurries. *Powder Technology,* pp. 297-304.

Sabusanghe, G., Schaap, W. & Kelly, E., 1989. Modelling the screening process : A probabilistic approach.. *Powder Technology,* Volume 59, pp. 37-44.

Sawant, A., Mohan, M. & Ashok, S., 2016. Study and Analysis of Deck Inclination Angle on Efficiency of Vibration Screen. *International Journal of Engineering Development and Research*, 4(1), pp. 631-635.

Soldinger, M., 1999. Interrelation of stratification and passage in the screening process.. *Minerals Engineering*, 12(5), pp. 497-516.

Sripriya, R., Bapat, J. & Singh, N., 2003. Development of an alternative to magnetite for use as heavy media in coal washeries.. *Mineral Processing*, 71(1-4), pp. 55-71.

Sripriya, R., Dutta, A. & Narasimha, M., 2006. An analysis of medium losses in coal washing plants.. *Mineral Processing*, Volume 80, pp. 177-188.

Standish, N., Bharadwaj, A. & Hairi-Akbari, G., 1986. A study of the effect of operating variables on the efficiency of a vibrating screen.. *Powder Technology*, 48(2), pp. 161-172.

Stessel, R. & Cole, K., 1996. Laboratory Investigation of a New TRommel Model. *Journal of the Air & Waste Management Association*, 46(6), pp. 558-568.

Stessel, R. I. & Kranc, S., 1992. Particle Motion in Rotary Screen. *Journal of Engineering Mechanics*, 118(3).

Sucher, R., 1969. *Sieving - Theoretical and Experimental Investigations.*, Kansas: ProQuest Dissertations Publishing.

Sullivan, J., 2013. *Screening theory and practice.* Dallas, Triple/S dynamics services, inc.

Trumic, M. & Magdalinovic, N., 2011. New model of screening kinetics.. *Minerals Engineering*, 24(1), pp. 42-49.

Valine, S., Wheeler, J. & Albuquerque, L., 2009. Fine Sizing with the Derrick Stack Sizer Screen. In: *Recent Advances in Mineral Processing Plant Design.* Littleton: Society for Mining, Metallurgy & Exploration, pp. 433-443.

Vesilind, P. & Rimer, A., 1981. *Unit Operations in Resource Recovery Engineering.* Eaglewood Cliffs, New Jersey: Prentice-Hall, Inc.

Wills, B. & Finch, J., 2016. *Wills' Mineral Processing Technology: An Introduction To The Practical Aspects Of Ore Treatment And Mineral Recovery*. Eighth ed. Oxford: Elsevier Ltd.

Wills, B. & Napier-Munn, T., 2006. *Mineral processing technology-An introduction to the practical aspects of ore treatment and mineral processing.* 7th ed. s.l.:Elsevier Science & Technology Books.

Zhou, Z., Li, J., Zhou, J. & Li, S. F. J., 2016. Enhancing Mixing of Cohesive Particles by Baffles in a Rotary Drum. *Particuology*, Volume 25, pp. 104-110.

APPENDIX A

Submerged DMS Trommel (Mk1) modifications and commissioning

An equipment drawing of the submerged test trommel is provided in Figure 89.

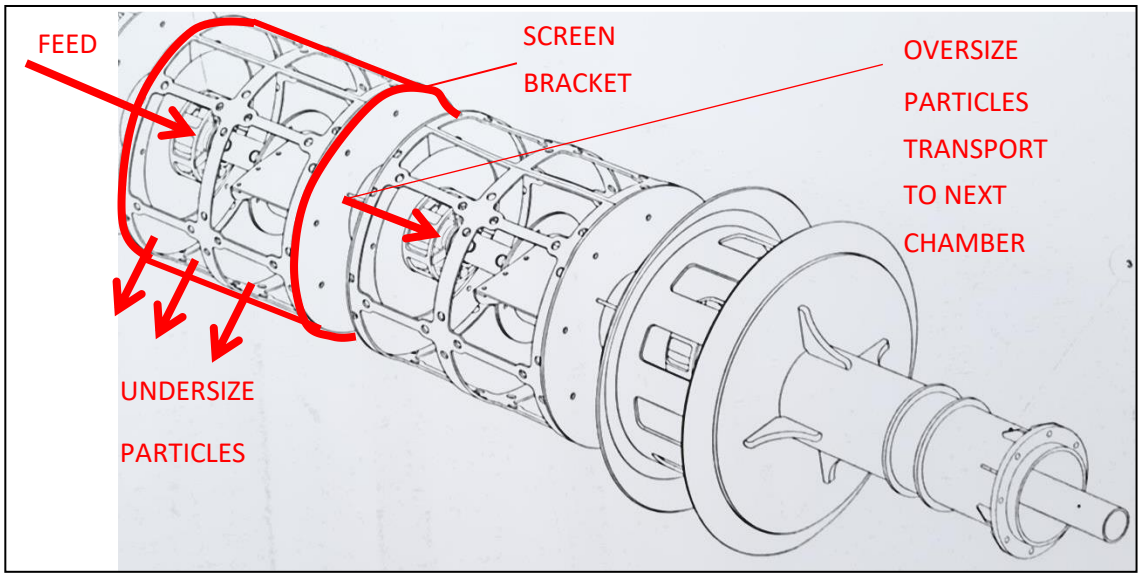

Figure 89. Equipment drawing of DMS Trommel (Mk1).

The discharge from the dense medium cyclone consisting of ore and medium is fed into the drain chamber screen, which is the first chamber of the DMS Trommel (Mk1). The majority of medium is drained through the drain chamber screen while the oversized ore particles with adhering medium is retained in the screen. The pulp is transported to the subsequent submerged wash chamber. Here the adhered medium is washed from the ore and drained to the underflow of the wash chamber. The clean ore particles are transported along the length of the trommel and discharged at the solids discharge end of the trommel.

1. Select and prepare location for pilot plant

The first step to commission the trommel screen (Mk1) was to select an appropriate location and to plan the preparation of the location and necessary support units to operate the equipment, such as a slurry pump and sump. With little knowledge on the working of the new submerged trommel screen (Mk1), it was decided that the commissioning of the pilot plant would start roughly and temporary in order to enable preliminary testing to gain some understanding in the working of the trommel screen (Mk1). As the understanding of the trommel screen (Mk1) was developed, the pilot plant was adjusted to suit the needs that were unknown initially.

As with typical mineral processing plants, it was expected that the operation of the trommel screen (Mk1) would result in some slurry spillage and splatter. For this reason the location of

the unit was chosen near the mineral processing pilot plant bunding area in the big lab of the Department of Process engineering of the Stellenbosch University. The convenience of extending the bunding area and the availability of three phase power were the main drives behind this decision for location.

2. Select and install additional units required for operation

An old tank with a volume of approximately 250 L was available and selected for an initial sump. Similarly an old slurry pump was available. The pump has a pulley system that can control the pump speed. After testing the pump, the sump and the pump were positioned under the trommel (Mk1) and power was supplied to the pump and the trommel screen (Mk1).

Building of the bunding wall required special permission and would have an unknown time delay. A temporary solution was devised by placing the sump tank and the pump on top of a wide steel plate with obstructions to contain spillage. It was unknown if the pilot plant location would be approved or if it would have to be re-positioned, so the temporary solution was convenient for the initial testing.

3. Test trommel (Mk1) motors

After providing the trommel screen (Mk1) motor with power, it was tested. The motor fan was damaged during transportation and had to be removed and re-shaped to avoid obstruction of the fan. Further it was discovered that the motor does not rotate true on its axis. There is a vertical oscillation of the shaft. This caused the motor chain to make contact with the mesh of the motor casing. The chain was grinding against the mesh. Eventually the motor chain jumped off of its gear and the motor stopped. The motor had to be opened and repaired. It was determined that the small sprocket in the motor came loose for unknown reasons. It was decided that the mesh over the motor chain had to be grinded open to prevent contact with the moving chain of the motor. The sprocket was tightened and the motor problems were solved.

4. Manufacture and install trommel (Mk1) covers

The trommel screen (Mk1) was deemed unsafe for operation with open moving parts. It was decided that custom covers had to be made for the uncovered trommel (Mk1) chambers to ensure safe operation. These covers would also provide cover to minimize splashing from the machine. The cover lids were constructed of steel and coated with corrosive protective paint. In order to allow visual observation of the inside of the trommel (Mk1) during operation, the cover sheets were made of polycarbonate, which is flexible and transparent.

5. Initial investigation of trommel screen (Mk1) operation

After the trommel screen (Mk1) was deemed safe for operation, initial tests were conducted to develop an understanding of the workings of the equipment. It was discovered that the direction of rotation of the motor corresponded with the direction that the pedals scoop the solids into the shaft opening, as expected, however the direction of the scroll conveyors was in the opposite direction and transported solids back from the second chamber to the first. This was a design flaw, because if the motor direction was inverted, the pedals would scoop in the wrong direction. It was decided that it is easier to reverse the motor direction and the pedal direction, than it is to reverse the scrolls. In order to reverse the scrolls, it would be necessary to strip the entire screen bracket and shaft of each chamber, remove the scroll flights, design and construct new ones, weld the new scrolls into the shaft and then re-assemble all of the parts. The reversal of the motor just required swapping two of the three live wires in the three phase cable and grinding the pedals off, create a new pedal bracket, weld it to the old one and then re-attach the pedal plates. It was decided that the corrections will first be applied to the draining chamber to see if it is effective, before it is applied to the other chambers as well. Figure 90 shows the pedals and shaft opening for ore transport from the drainage chamber to the rinse chamber.

Figure 90. Photograph of ore transport pedals after adjustment to correspond with direction of screw.

Some test runs were conducted with andalasite to attempt to gain a better understanding of the inner workings of the trommel (Mk1). Only the first chamber, the drain chamber, was utilized with screens. It was discovered that there was significant build-up in the pedal openings. This

resulted in a significant decrease in the “scooping area”, or the opening in the shaft into which the retained solids are scooped for transport to the next chamber. Figure 91 illustrates the material build-up before the improvements.

Figure 91. Ore buildup due to inefficient transport by screw.

A literature study on screw conveyors revealed that most screw conveyors are fed mid-screw to avoid the “entry area” where solids are scooped and then forced into the screw before transportation occurs. In an attempt to solve the build-up problem by imitating the screw designs in literature, “extended screws” were designed to extend past the opening in order to ensure that solids being scooped into the opening are immediately exposed to conveyance by the screw. This design also included a plate on the opposite side of the opening facing down, to prevent solids falling straight through the shaft opening down at the bottom without coming into contact with the screw. Figure 92 illustrates the adjustments made to the screws to improve ore transport.

Figure 92. Improvement to screws by extension.

2.1. Quantify flow rates and mass balances

It is desired to quantify the flow rate and transport rate through the trommel (Mk1) screen and perform mass balances over every chamber. The first step is to perform mass balances over the drain chamber at various operating parameters. At least the feed and drain streams need to be quantified to perform a mass balance. A complication was encountered in the sump with settling solids. The initial strategy was to attempt to quantify the settling solids in order to determine if the particle bed always formed in the same way. If this was the case, the solids could be added to the sump until the particle bed stabilized, after which additional solids would enter circulation. This was not the case, for the following reasons:

- The sump flow pattern was completely dependent on the position and flow rate from the drain chamber outlet. During sampling, the flexi pipe has to be adjusted using the bucket and stopwatch method and the flow is interrupted. The change in flow pattern in the sump disturbed settled particles and upset the bed, causing more solids to enter circulation momentarily.
- Over time, the larger particles tended to settle out more, while the smaller particles were more likely to remain in suspension and therefore remain in circulation through the trommel (Mk1).

These factors contributed to near impossibility of characterizing a constant feed.

It was deemed necessary to implement an agitator in the sump in order to prevent settling of solids. In an attempt to save time, an old agitator in storage was utilized. The motor is powered by three phases. Spare cables and a switch were collected and the motor was installed. A spare impeller was used for mixing.

2.2. Installation of agitator

Upon installation of agitator, it was discovered that the flow pattern in the sump hindered the flow to the pump. A low pressure area formed in the vortex in front of the sump outlet to the pump. This caused the pump to suck air and achieve much lower flow rates than before. Further the dripping from the gland packing increased significantly such that it was a constant stream flowing from the gland instead of periodic dripping. In an attempt to tighten the gland, it was determined that the gland packing has aged significantly and could not be tightened further. The gland packing had to be replaced.

The next step was to replace the agitator impeller with a less aggressive impeller. A smaller impeller with three blades instead of four was used. The individual blade area was also smaller than the first impeller, while the blade angles were also decreased to decrease the aggression of the impeller.

2.3. Feed characterization after installation of agitator

The feed flow in the draining chamber crashed into the opposing flat surface and burst into the trommel (Mk1) covers. The fluid penetrated all crevices and leaked out of the chamber down onto the ground. The splashing was also aggressive enough to escape the drain chamber cover on the feed side. Figure 93 and Figure 94 show the result of splashing that occurred.

Figure 93. Photograph of slurry splashing.

Figure 94. Photograph of slurry splashing.

In an attempt to stop the splashing, the pump speed was decreased but the splashing persisted. The splashing is not a major issue with the screens inserted in the drain chamber. The screens prevent splashing by containing the splashing material and only letting the fluid out by draining out of the bottom of the screens. This is not a suitable solution to the splashing problem, because the screens have to be removed in order to characterize the feed.

In order to characterize the feed and to develop a pump calibration curve, the screens have to be removed and the material must be circulated through the draining chamber. As soon as the screens are inserted, it is not possible to characterize the feed, because the flow is altered by passing through the screen. The feed inlet is inside of the screens and it is therefore not accessible when the screens are inserted.

The splashing problem was solved by building a deflector to direct the flow from the feed straight to the outlet of the drain chamber. The deflector is removable because the flow must only be directed straight towards the outlet during feed characterization runs. After the deflector was inserted, the flow did not splash inside of the chamber anymore, however the fed material built up inside of the feed opening to the drain chamber. The inner feed pipe is positioned inside of an outer pipe which rotates around the feed pipe without the feed pipe having to rotate. The inner feed pipe is not precisely in the middle of the rotating pipe around it. For this reason the existing seal between the inner and outer pipe is not completely effective. The buildup of material between these two pipes resulted in extreme leakage from the feed opening when the pump was switched on. This problem was solved by cutting a sponge material and sealing the inlet leaks temporarily for the feed characterization runs.

The flow director, shown in Figure 95, must be inserted over the feed opening to direct the flow straight to the outlet, instead of splashing against the default flow distributor.

Figure 95. Flow director for feed characterization procedures.

In order to prevent back-flow out of the feed end of the trommel (Mk1) due to the obstruction of flow by the flow director, additional seals must be inserted into the outer pipe of the feed opening. This seal is shown in Figure 96.

Figure 96. Seal inserted into feed opening to prevent back-flow.

Figure 97 shows the seal after being inserted into the feed opening:

Figure 97. Seals inside of feed opening to prevent back-flow during feed characterization runs.

After the seals are inserted, the flow director is inserted onto the feed opening in the drain chamber. This is illustrated in Figure 98. A wooden wedge is used to secure the flow director in place to prevent it being displaced by the slurry flow.

Figure 98. Flow director inserted onto feed opening in drain chamber.

2.4. Y-piece valve installation for sampling

After the leakage problems were solved it was determined that the flow pattern inside of the sump is not constant as the drain chamber outlet has a large effect on the flow pattern. Each time that the outlet pipe is adjusted for sampling, the flow pattern in the sump changes. Sometimes a vortex forms above the agitator impeller which allows the pump to suck air. Then the pump chamber is filled with air, the pump ceases to displace fluid until the chamber is filled with material. In this time, the flow through the drain chamber stops and the sump fills up to the maximum level.

The method of sampling directly from the flexi outlet of the drain chamber also caused the additional problem of extreme spillage from the sump and sampling bucket. The repeated movement of the flexi pipe with relatively high material flow velocities through it not only upset the flow in the sump, but was also extremely difficult to control and maintain a safe and clean working environment due to excessive spillage.

The best solution for both of these problems was to design a Y-piece valve on the drainage chamber outlet pipe. This valve is showed in Figure 99. The first outlet of the Y-piece valve recycles to the sump. This ensures that the material flow into the sump remains in a fixed position, thereby ensuring that the flow pattern in the sump does not fluctuate as heavily as it would with constant adjustment of the position of the pipe.

The second outlet of the valve goes to the sampling bucket. This allows the operator to sample the outlet of the drain chamber while all pipes remain in a fixed position. This

decreases the spillage during sampling significantly as the pipes do not have to be moved between the sump and sampling bucket while there is high material flow through them.

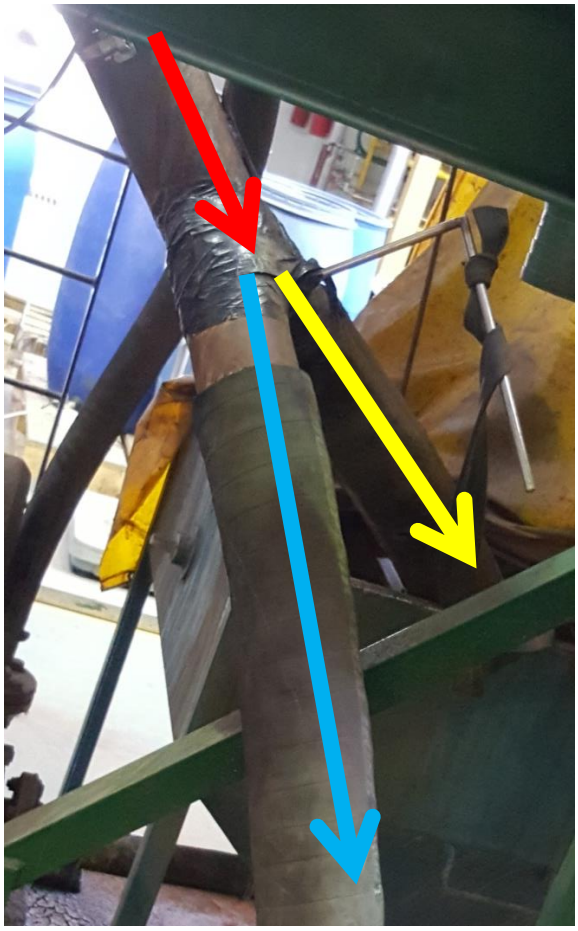

Figure 99. Y-piece valve for sampling. Inlet (red arrow) from drainage chamber outlet. Outlet 1 (yellow arrow) recycle stream back to sump. Outlet 2 (blue arrow) sample stream to sampling bucket.

2.10 Sampling bracket

Sampling at higher flow rates and slurry densities introduced an additional problem that is the physical transport of heavy samples. Due to fluctuations in flow rate, it is desired to sample at least for three seconds to increase the accuracy of estimation of flow rates with the bucket and stopwatch method. The downside of large samples is the difficulty of handling these heavy samples, often reaching a mass of 30 kg. In order to decrease the sample size without compromising the accuracy by decreasing the sampling time, a bracket was built for the sampling bucket, as shown in Figure 100. This bucket swivels about an axis, which allows one to pour the sample into smaller, more manageable sample sizes to pour back into the sump one at a time. This bracket was covered with anti-corrosive paint to prolong its lifetime, considering its constant exposure to water. This bracket also allows one to sample into a large container, which decreases splashing compared to sampling into a smaller container.

Figure 100. Photograph of sampling bracket.

2.11 Mass balancing and steady state

The trommel screen (Mk1) with all of the available chambers (1 drain chamber and 2 rinse chambers) is a very complex system and it is not possible to investigate the operation of all chambers simultaneously. Operation of each chamber individually, however prevents one from reaching steady state as the course particles are transported to the following chamber and not back to the sump. This gives rise to the problem that steady state is not reachable with the operation of individual chambers. During strategic discussion with the developers and investors (Multotec and partners) it was determined that the objective that takes priority is to investigate how the particle bed that forms in the drainage chamber screen, affects the drainage rate of water and FeSi in this chamber. Therefore it was decided that the experimental procedure should change. Instead of adding ore and FeSi into the sump and simulating a mixed slurry that would typically be found in the dense medium circuit, the ore particles should rather be added in known quantities to the drain chamber screen while the slurry that is circulated consists only of FeSi and water.

Where a mixture of ore, FeSi and water would normally be fed to the trommel screen (Mk1), this experimental approach mimics the accumulation of ore particles in the screen by adding them in known quantities and investigating its effect on the drainage rate. To accomplish this, it is necessary to prevent the transport of retained ore particles to the following chamber by

closing the shaft openings and preventing the ore particles to come into contact with the transport scrolls inside of the shaft. Figure 101 illustrates the plates that were installed to close the ore transport openings off to ensure that the ore is retained within the screen in the drain chamber.

Figure 101. Photograph of closed ore transport opening.

2.12 Improvement of screen panels

The default screen panels that were used to perform initial testing of the trommel screen (Mk1) were large, semi-circular wedge wire screen panels that fit over the screen brackets. These screen panels were relatively heavy and unmanageable, implying that the installation procedure is an energy and time intensive activity for at least two people. This is not desirable and it was deemed necessary to find a more practical alternative.

The first alternative that was investigated was the modular polyurethane screen panels manufactured by Multotec. These screen panels are very common in the industry and were also used on the vibrating screen that the trommel screen (Mk1) will be compared to. These panels can be used in industrial scale trommel screens where the screen diameter is great enough that the panels (normally manufactured as a flat panel) can fit into the round trommel by bending it slightly. For application on a pilot plant scale trommel screen on the other hand, the installation of these panels were not as simple as the diameter of the screen is much smaller. This implies that the panels had to be bent farther than they normally would in the industry. The panels were rolled to meet the specifications of the trommel screen (Mk1), however it was found that rolling these panels to fit such a small diameter caused the apertures to warp in shape and opening size. This is not acceptable as it would have a significant impact on the screening capabilities of these panels.

The next attempt to fit these modular panels into the trommel screen (Mk1) was to cast the panels with the required curve instead of rolling them after casting. This ensured that the size and shape of the apertures in the panels meet the specifications, however the task of installing these panels in the trommel screen (Mk1) brackets proved to be an unrealistic task. The panels are designed to have a very tight fit to prevent leakage, but due to the design of the trommel screen (Mk1), the screen brackets are not particularly accessible. In order to make these panels fit into the brackets it is necessary to apply significant force to the panels to keep them in place while using a hammer to hit them into their final position. This procedure was not viable in the context of the trommel screen (Mk1) as it was not designed with sufficient space to swing a hammer onto the area where the panels are located.

Finally it was decided that a new type of screen technology will be best for investigation of the trommel screen (Mk1). These new screen panels are mats made of rubber. The mat is 2mm thick and the apertures are punched into the mat after casting. Installation and maintenance of these screen mats are much more practical and manageable for one person. Figure 102 illustrates the screen mat while wrapped around the screen brackets in the drain chamber of the trommel (Mk1).

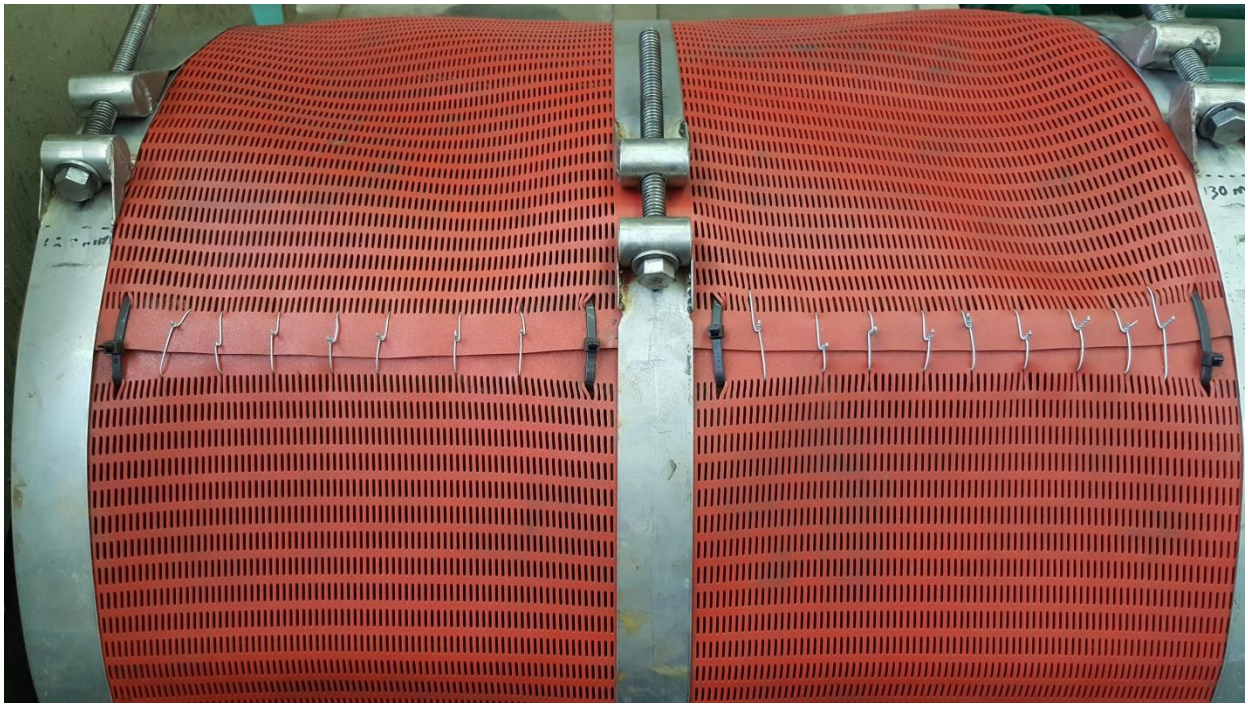

Figure 102. Photograph of rubber Linatex screen mat. Secured with straps and stitched with wire to prevent leakage in DMS Trommel (Mk1).

The mat is wrapped around the screen bracket and held in place with metal straps that are tightened around the bracket. In order to prevent leakage through the edges where the two sides of the mat meet, it is stitched closed with wire.

Due to the flexibility of the mat, tightening the straps causes the mat to bend with the straps. Particularly in the area where the bolt is located that is used to tighten the straps, the mat bends and leaves small openings between the mat and the bracket, as shown in Figure 103.

Figure 103. Photograph of screen mat bending under strap that secures it on screen bracket. Bend leaves small openings that cause leakage.

These gaps are not acceptable because it allows leakage of ore into the underflow of the screen. Some of the ore is therefore allowed to bypass the screen, which directly lowers the screening efficiency. It was decided that these gaps must be filled with silicon upon installation of the mats to prevent leakage of ore into the drainage outlet with FeSi into the sump.

APPENDIX B

STEP-WISE EXPERIMENTAL PROCEDURES

Submerged DMS Trommel (Mk1): Drain chamber

A step-wise procedure for experimental work on drain chamber of DMS Test Trommel (Mk1):

1. Ensure unit is clean to prevent contamination;
2. Clean screening media (Linatex screen mat);
3. Secure screening media to drain chamber bracket, but leave an opening to insert ore into trommel (Mk1);
4. Begin to load weighed and clean ore into drain trommel (Mk1). Ensure that ore is spread evenly over screen media to mimic a bed at steady state. Load approximately 40 kg of ore to ensure maximum ore transport from drain chamber; Record mass added.
5. After loading required ore mass, secure Linatex screening mat completely with screen braces, cable ties and wire stiches;
6. Add appropriate volume of water to sump;
7. Switch on sump agitator;
8. Load required mass of dense medium (FeSi) to sump while agitating;
9. Check slurry RD;
10. Continue to load FeSi until desired medium RD is achieved;
11. Perform a triplicate RD test to ensure that RD remains constant at desired value;
12. Switch on pump to begin feeding medium to drain chamber;
13. Switch on Trommel (Mk1) to begin rotation and mixing of medium with ore;
14. Rotate trommel (Mk1) for approximately 4 minutes to ensure proper mixing of ore and medium, then switch off trommel (Mk1).
15. Switch off pump to cease circulation of medium through trommel (Mk1) drain chamber;
16. Collect pulp that was transported to submerged chamber;
17. Open up drain chamber screen media slightly. Be careful of opening too wide and cause spillage of ore from drain chamber to underflow discharge.
18. Reload transported pulp that was collected from submerged chamber back into drain chamber.
19. Close drain chamber screen media to prevent any spillage during rotation of trommel (Mk1);
20. Insert plastic sheet into submerged chamber (overflow discharge of drain chamber) to collect pulp that will be transported during trommel (Mk1) rotation;

21. Switch on pump to continue circulation of medium through drain chamber of trommel (Mk1).
22. Switch off agitator;
23. Switch on trommel (Mk1) immediately after switching off agitator and begin time on stopwatch;
24. Allow trommel (Mk1) to rotate between 9 and 10 seconds (4 rotations). Sample drain chamber underflow during trommel (Mk1) rotation;
25. Stop trommel (Mk1) rotation, underflow sampling and stopwatch simultaneously.
26. Switch off pump to cease medium circulation through drain chamber of trommel (Mk1);
27. Switch on agitator immediately to prevent settling of solids.
28. Measure and record underflow sample (drained medium) mass and volume;
29. Collect overflow pulp that was transported and collected in submerged chamber during trommel (Mk1) rotation. Ensure no spillage;
30. Measure and record total wet mass of transported pulp (overflow);
31. Add clean ore to drain chamber to replace the ore that was removed with the previous sample by repeating steps 4 to 19;
32. Repeat steps 19 to 30 to perform the next experimental run (repeat);

Continue until 3 repetitions are completed for the set of experimental parameters.

Sample processing

Samples are processed differently based on their composition. The samples either consist of medium only (FeSi and water) or medium and ore.

Medium only sample processing

1. Immediately after taking the sample, weigh and record mass;
2. Ensure that pressure filter is clean;
3. Weigh pressure filter paper on a 3 decimal scale and record paper mass;
4. Insert filter paper into pressure filter and secure container to ensure no leakage will occur;
5. Pour sample into pressure filter container carefully;
6. Use small volume of water to wash entire sample out of sample container and into pressure filter container;
7. Close lid on filter pressure and open air flow;
8. Continue air flow until no more liquid is being discharged from bottom of pressure filter;
9. Close air flow;
10. Open filter pressure lid and remove pressure filter container;
11. Carefully remove filter paper with moist FeSi and place into oven tray. Label sample clearly;
12. Insert sample into oven at approximately 80 ^{o}C for three to four hours, depending how long it takes to dry the sample completely (inspect by mixing the solids up. Return sample to oven if any moisture is left);
13. Dry sample overnight to ensure no moisture is left in sample;
14. Remove sample from oven using oven mitts;
15. Weigh dry mass of solids and record;
16. Perform mass balance to calculate composition of FeSi and water in the original wet sample;

Medium and ore sample processing

1. Immediately after taking the sample, weigh and record total wet mass;
2. Clean a 1mm aperture sieve;
3. Scoop a handful of sample onto the sieve over a clean sample bucket;
4. Use clean water to wash FeSi from ore bed until only wet ore is left on the sieve.
5. Oven dry clean, wet ore samples at 80 ^{o}C for three to four hours, depending how long it takes to dry the sample completely (inspect by mixing the solids up. Return sample to oven if any moisture is left);

6. For the dilute medium that is collected from washing the ore particles, Repeat steps 1 to 16 in the procedure for *Medium only sample processing* in section 0;
7. Weigh dry masses of all dried components in the original wet sample and record;
8. Perform a mass balance to calculate the composition of iron ore and medium in the original wet sample.

Submerged DMS Trommel (Mk1): Wash chamber step-wise experimental procedure

A step-wise procedure for experimental work on wash chamber of the Submerged DMS Trommel (Mk1) is as follows:

1. Ensure unit is clean to prevent contamination;
2. Clean screening media (Linatex screen mat);
3. Secure screening media to wash chamber bracket, but leave an opening to insert ore into trommel (Mk1);
4. Fill wash chamber with clean water until water level reaches overflow level;
5. Prepare dirty pulp with appropriate quantity of iron ore, FeSi and moisture to simulate discharge of drain chamber at various medium RD's.
6. Begin to load weighed and dirty pulp into wash chamber of DMS Test Trommel (Mk1). Ensure that ore is spread evenly over screen media to mimic a bed at steady state. Load approximately 40 kg of ore to mimic steady state operation, assuming that the ore quantity in the drain chamber and wash chambers will be equal. Record mass added.
7. After loading required pulp mass, secure Linatex screening mat completely with screen braces, cable ties and wire stiches, as with drain chamber;
8. Switch on trommel (Mk1) to rotate for appropriate number of rotations (No rotations, one rotation and two rotations);
9. Stop trommel (Mk1) rotation and lock out equipment for safety purposes;
10. Open securing mechanisms of screen and open screen slightly to remove washed ore from submerged screen;
11. When all of the ore particles are removed from the screen, perform sample processing procedure discussed in Section 0 to determine composition of sample;
12. Drain and wash system after use.

APPENDIX C

Step-wise experimental procedure: Trommel Mk2

A step-wise procedure for experimental work on Test Trommel (Mk2) (Drain section) follows:

1. Fill sump with approximately 250 L of water;
2. Ensure that both valves 1 and 2 (Trommel (Mk2) feed and bypass, respectively) are open, as illustrated in Figure 104:

Figure 104. Photograph of Test Trommel (Mk2) T-piece feed configuration.

3. Set VFD to 20 Hz;
4. Check hydraulic motor piping and ensure that all connections are secured;
5. Switch on trommel (Mk2) hydraulic motor to commence trommel rotation;
6. Check that trommel (Mk2) is rotating at correct speed (24 RPM);
7. Ensure that trommel (Mk2) sampling tray is in correct position (underflow discharges aligned with re-circulating pipes);
8. Switch on pump to circulate water through trommel (Mk2) and bypass;
9. Check for excessive leakage and fix if necessary;
10. Place 50 L drums in appropriate positions and place trommel (Mk2) underflow discharge pipes into drums to collect possible spillage, as illustrated in Figure 105:

Figure 105. Photograph of sampling buckets for Test Trommel (Mk2) underflow discharges.

11. Begin to add FeSi to raise medium RD. Ensure adequate mixing with bypass stream;
12. Check medium RD from bypass stream. Continue adding FeSi until appropriate medium RD is reached;
13. Repeat triplicate RD tests to ensure correct RD and steady state operation;
14. Record video of steady state operation for record;
15. Switch sampling pipes from spillage collection buckets to sampling buckets in preparation for sampling;
16. Sample by pulling sampling tray towards operator. Time with stopwatch; Sample overflow discharge simultaneously;
17. After sampling, move sampling tray back into re-circulating position and stop stopwatch;
18. Remove sampling pipes from sampling buckets as quickly as possible and place pipes back into spillage collection buckets;
19. Weigh wet mass of 9 underflow samples and 1 overflow sample and record masses;
20. Perform triplicate RD tests to ensure steady state operation;
21. Repeat steps 14 to 19 three times for three repetitions;
22. Drain system and recover medium and ore.
23. Switch off equipment;

APPENDIX D

Submerged Section Design Considerations

1) Dual hydraulic power pack

Very little information is known about submerged washing in the context of dense medium separation. As such, it is still unclear how factors such as rotation speed of the submerged trommel will affect washing efficiency. For this reason, a dual hydraulic power pack was acquired as the drain Trommel Mk2 was manufactured. This will allow separate drives for the drain trommel (Mk2) and the submerged trommel, which enables the variation of rotation speed of both trommels independently.

2) Submerged trommel feed configuration

From the submerged washing test work that was conducted, it was found that a very large extent of the washing occurs during the submersion action of the pulp. This indicates the requirement that the pulp should be discharged into bath where the water level exceeds the bed height, to ensure that the particle is dropped into and allowed to settle in relatively clean water.

3) Water circulation

From the submerged washing work, it was also found that a constant flow of water from one side of the pulp bed to the other side, enhances washing. Instead of having stagnant water that sloshes around through the pulp bed, it is important to have a constant flow of fresh water to transport the FeSi from the bed, through the screen media and away from the ore. As such the submerged bath should have a fresh water feed, preferably at the discharge end of the submerged trommel, to perform a final wash of the ore emerging from the bath with clean water before it exits the trommel. An outlet will be located at the bottom of the submerged bath, where the dilute medium will be removed from the bath. This outlet should have a valve that will allow control of the water flow rate from the bath to maintain the water level and ensure submersion of the trommel.

4) Transparent section in submerged tank for visual accessibility

It is important to know what is occurring inside of the submerged tank during operation. For this reason, a window of sorts will be installed into the submerged tank so that the operator can determine the depth of the FeSi bed that is settling at the bottom of the submerged tank.

5) Steep bath angles to promote settling to a single point

During test work on Trommel Mk1, it was found that FeSi settles very easily. FeSi will settle at any angle less than 60^{o} from the horizontal, which would lead to accumulation of FeSi in the submerged bath during operation. For this reason, it is important to design the bath to be relatively deep, with all angles exceeding 60^{o}, as illustrated in Figure 106:

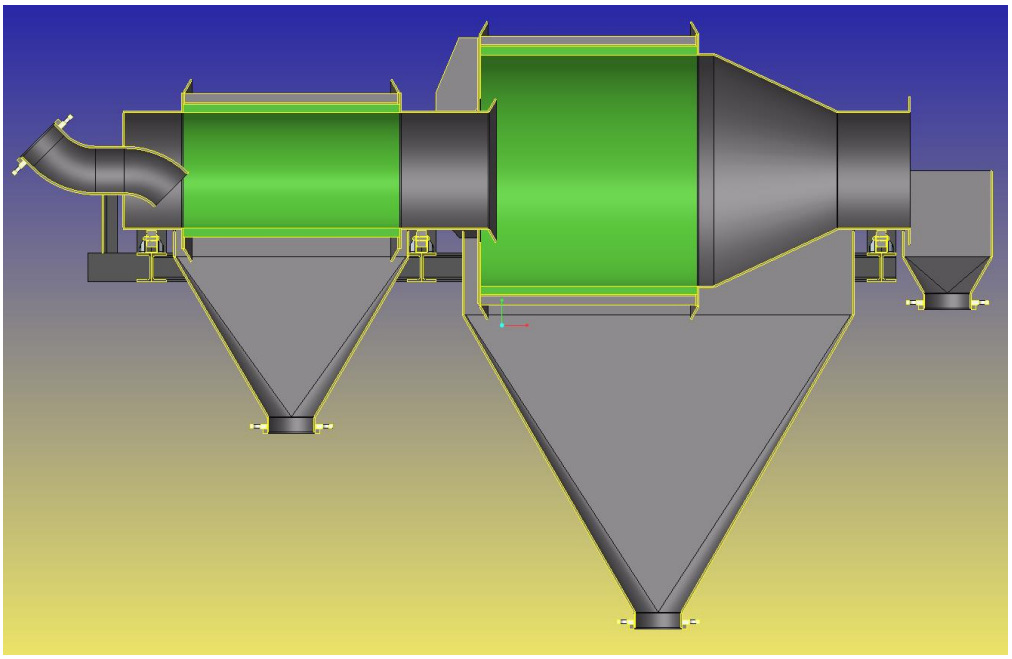

Figure 106. Conceptual drawing of Test Trommel Mk2: Drain section and Submerged washing section.

This will ensure that all of the FeSi settles towards the outlet of the bath and will not accumulate in the tank.

6) Mobility and adjustability of equipment

During test work on Trommel Mk1, the importance of equipment adjustability was realized. The limitations that were imposed on the investigation by the fact that the entire series of chambers in the trommel were inseparable, were immense. As such, it is considered good practice to allow for adjustability of the equipment, to allow the submerged section and the drain section to be fully detachable and mobile as separate units.

7) Magnetic separator

With circulation of water and removal of the dilute medium at the bottom of the submerged bath, it will be necessary to use a magnetic separator to concentrate and recycle the medium. A Low Intensity Magnetic Separator (LIMS) will be considered for this task. Prior to the final design of the submerged trommel, a test work campaign will be conducted to understand the crucial operating parameters and limits of the LIMS. This information will be used to assist with the final sizing of the submerged trommel.

8) Mesh scroll for ore transport

As with the drain trommel (Mk2), a scroll will be required to transport the ore from the feed end to the overflow discharge end of the submerged trommel. It is important that these scrolls do not entrap FeSi with the ore and transport it with the clean ore, because that will decrease washing efficiency. The scrolls must allow washed FeSi to pass through and to be drained. Therefore, these scrolls will be manufactured with a screening material, such as wedge wire or perhaps a polyurethane scroll with apertures that resembles a panel.

APPENDIX E

Sample calculations

1. **Calculate flow rate from recorded mass and time**

$$\dot{m} = \frac{mass\ (kg)}{time\ (s)}$$

$$\dot{m} = \frac{10.63\ kg}{7.72\ s}$$

$$\dot{m} = 1.377\,\frac{kg}{s}$$

2. **Calculate wt% solids of a slurry**

$$wt\%\ solids = \frac{Dried\ solids\ mass\ (kg)}{Total\ wet\ mass\ (kg)}.100\%$$

$$wt\%\ solids = \frac{7.612\ kg}{10.63\ kg}.100\%$$

$$wt\%\ solids = \frac{7.612\ kg}{10.63\ kg}.100\%$$

$$wt\%\ solids = 71.61\%$$

3. **Calculate medium density from solids wt%**

$$\rho_m = \frac{100}{\frac{c_w(\%)}{\rho_s\left(\frac{kg}{m^3}\right)} + \frac{100 - c_w(\%)}{\rho_l\left(\frac{kg}{m^3}\right)}}$$

$$\rho_m = \frac{100}{\frac{71.61(\%)}{7200\left(\frac{kg}{m^3}\right)} + \frac{100 - 71.61(\%)}{1000\left(\frac{kg}{m^3}\right)}}$$

$$\rho_m = 2608\,\frac{kg}{m^3}$$

4. **Calculate volumetric flow rate from mass flow rate**

$$\dot{V} = \frac{\dot{m}\left(\frac{kg}{s}\right)}{\rho_m\left(\frac{kg}{L}\right)}$$

$$\dot{V} = \frac{1.38\left(\frac{kg}{s}\right)}{2.608\left(\frac{kg}{L}\right)}$$

$$\dot{V} = 0.53\left(\frac{L}{s}\right)$$

5. Calculate overflow FeSi concentration

$$FeSi\ wt\% = \frac{Dried\ FeSi\ mass\ (kg)}{Total\ wet\ mass\ (kg)}.100\%$$

$$FeSi\ wt\% = \frac{0.2292\ (kg)}{4.72\ (kg)}.100\%$$

$$FeSi\ wt\% = 4.88\ \%$$

6. Calculate %FeSi carryover

$$\%FeSi\ carryover = \frac{FeSi\ mass\ reporting\ to\ overflow\ \left(\frac{t}{hr}\right)}{FeSi\ mass\ in\ feed\ \left(\frac{t}{hr}\right)}$$

$$\%FeSi\ carryover = \frac{0.11\ \left(\frac{t}{hr}\right)}{6.26\ \left(\frac{t}{hr}\right)}$$

$$\%FeSi\ carryover = 1.76\ \%$$

7. Calculate drainage rate per single discharge A2

$$Drainage\ rate = \frac{Volumetric\ underflow\ rate\ \left(\frac{m^3}{hr}\right)}{Discharge\ area\ (m^2)}$$

$$Drainage\ rate = \frac{1.90\ \left(\frac{m^3}{hr}\right)}{0.057\ (m^2)}$$

$$Drainage\ rate = \frac{33.22\ \left(\frac{m^3}{hr}\right)}{(m^2)}$$

8. Calculate 95% confidence interval of %FeSi in overflow

$$95\%\ CI\ of\ \%FeSi\ in\ overflow = mean \pm z\frac{Standard\ deviation\ (sample)}{\sqrt{number\ of\ samples}}$$

$$95\%\ CI\ of\ \%FeSi\ in\ overflow = 5.09\% \pm (1.96)\frac{0.26\%}{\sqrt{2}}$$

$$95\%\ CI\ of\ \%FeSi\ in\ overflow = 5.09\% \pm 0.37\%$$

9. Calculate flow velocity in pipe

$$v = \frac{\dot{V}\left(\frac{m^3}{hr}\right)}{Pipe\ area(m^2)}$$

$$v = \frac{5{,}078\left(\frac{m^3}{hr}\right)}{0.0182(m^2)}$$

$$v = 273.38\left(\frac{m^3}{hr}\right)$$

$$v = 0.08\left(\frac{m}{s}\right)$$